Causes and consequences of population fluctuations in spatial ecological systems

Tarik Claude Gouhier

Department of Biology, Faculty of Science

McGill University
Montreal, Quebec, Canada
January 2010

A thesis submitted to McGill University in partial fulfillment of the requirements of the degree of Doctor of Philosophy

ABSTRACT

Assessing the relative influence of biotic (i.e. species interactions) and abiotic (i.e. the environment) processes on the distribution of population abundance is a fundamental but controversial issue in ecology. Scale-dependent frameworks predict that the influence of biotic processes is confined to local populations, whereas abiotic processes control regional patterns of abundance. In this thesis, I show that the relative influence of local biotic and regional abiotic processes does not depend on their respective spatial scales but rather on the properties of dispersal.

I develop and validate a theory of marine metacommunities that demonstrates that local biotic processes (succession, predation) interact with limited dispersal to control the distribution of population abundance in space (1,800 km) and time (6 years) of the mussel *M. californianus* and the barnacle *B. glandula* along the West coast of the United States, despite strong environmental forcing by regional abiotic processes. This interaction between local biotic processes and limited dispersal leads to patterns of connectivity at spatial scales (~450 km) that are much larger than the scale of dispersal (~100 km).

I then investigate the implications of this theory for the design of marine reserve networks. I show that the application of current marine reserve theory, which advocates the use of the scale of dispersal as the distance between reserves in order to maintain connectivity, leads to a reduction in both mean abundance and persistence in these systems because it limits natural patterns of connectivity. However, using the scale of connectivity imposed by the interaction between local

processes and limited dispersal maximizes mean abundance and persistence inside and outside of reserves, thus simultaneously satisfying conservation and fishery goals.

In more complex spatial food webs, I show that the rate of dispersal controls the destabilizing effect of abiotic processes: low rates of dispersal facilitate abiotic destabilization, whereas high rates of dispersal limit environmental destabilization. Irrespective of dispersal rate, food webs undergo dynamic shifts in the relative importance of biotic and abiotic processes.

RÉSUMÉ

Le contrôle relatif qu'exercent les facteurs biotiques (interactions entre espèces) et abiotiques (l'environnement) sur la distribution des populations est une question fondamentale et controversée en écologie. Les théories hiérarchiques postulent que l'influence des processus biotiques est limitée aux petites échelles spatiales, tandis que les processus abiotiques contrôlent la distribution des populations à l'échelle régionale. Dans cette thèse, je montre que l'influence relative des processus abiotiques et biotiques dépend non pas de leur échelle spatiale, mais des caractéristiques de la dispersion des organismes.

Je développe et valide une théorie des méta communautés marines qui démontre que les processus biotiques locaux (succession, prédation) interagissent avec la dispersion locale afin de contrôler la distribution de l'abondance des populations de moule (*M. californianus*) et de balane (*B. glandula*) à l'échelle continentale (1 800 km) sur une période de 6 ans. Les processus biotiques maintiennent ce contrôle malgré l'action des processus abiotiques à l'échelle régionale. Cette interaction synergétique entre les processus biotiques locaux et la

dispersion locale génère des patrons de connectivité à des échelles spatiales (~ 450 km) qui excédent largement l'échelle de dispersion (~ 100 km).

Cette interaction a des implications fondamentales pour la conception des réserves marines. En effet, la théorie actuelle préconise de séparer les réserves marines par l'échelle de dispersion afin de maintenir la connectivité entre les réserves. Je montre que cette conception des réserves marines réduit l'abondance moyenne et la persistance des populations parce qu'elle limite la formation de patrons de connectivité à grande échelle. Lorsque la distance entre les réserves est basée sur l'échelle des patrons de connectivité, les réserves marines maximisent l'abondance et la persistance des populations qui se trouvent à l'intérieur et à l'extérieur des réserves. Ainsi, ce type de réserve marine peut être utilisé pour conserver les espèces et gérer la pêche simultanément.

Je montre que dans des systèmes écologiques plus complexes comme les chaînes alimentaires, le taux de dispersion contrôle l'effet déstabilisant des processus abiotiques: un faible taux de dispersion facilite la déstabilisation alors qu'un fort taux de dispersion limite la déstabilisation. Je montre aussi que peu importe le taux de dispersion, l'influence relative des processus biotiques et abiotiques sur les chaines alimentaires varie dans le temps.

TABLE OF CONTENTS

LIST OF TABLES

Chapter 1

Chapter 2

Chapter 3

Chapter 4

LIST OF FIGURES

Chapter 1

Figure S2: Time series of the correlation between the annual *M. californianus* cover and the multi-year average environment at 48 sites located along the West coast of the United States.

Figure S3: The spatial structure of both the environment and the correlation between the environment and the annual *M. californianus* cover time series at 48 sites located along the West coast of the United States.

Figure S4: Spatial synchrony of annual mussel cover in the predator-prey model for metapopulations undergoing different environmental and dispersal treatments.

Figure S5: Using model selection to detect nonlinear spatial synchrony patterns in the mussel cover time series of metapopulation models.

Figure S6: The occurrence of nonlinear spatial synchrony patterns in the mussel cover time series of the predator-prey metapopulation model.

Figure S7: The time series of the mussel cover from the successional model with sample spatial synchrony analyses for a metapopulation undergoing limited dispersal and no environmental variability.

Figure S8: The time series of the mussel cover from the successional model with sample spatial synchrony analyses for a metapopulation undergoing limited dispersal and spatiotemporal environmental variability.

Figure S9: The time series of the mussel cover from the successional model with sample spatial synchrony analyses for a metapopulation undergoing regional dispersal and no environmental variability.

Figure S10: The time series of the mussel cover from the successional model with sample spatial synchrony analyses for a metapopulation undergoing regional dispersal and spatiotemporal environmental variability.

Chapter 2

Chapter 3

Chapter 4

Movie A2: The abundance time series of predator *P*, consumer C_1 and consumer C_2 in a metacommunity with high dispersal and constant environmental conditions.

Movie A3: Local consumer correlation for metacommunities with low dispersal experiencing constant environmental conditions, mildly disruptive or strongly disruptive correlated environmental fluctuations.

Movie A4: Local consumer correlation for metacommunities with high dispersal experiencing constant environmental conditions, mildly disruptive or strongly disruptive correlated environmental fluctuations.

Figure B1: The effect of dispersal on global stability, global mean abundance, global temporal variance, intraspecific synchrony and global consumer correlation in metacommunities experiencing constant environmental conditions and chaotic dynamics.

Figure B2: The effect of environmental fluctuations on global stability for predator *P*, consumer C_1, consumer C_2 and global consumer correlation for metacommunities experiencing chaotic dynamics and either high or low dispersal.

Figure B3: The effect of positively correlated and negatively correlated environmental fluctuations on intraspecific synchrony and global consumer correlation, global temporal variance, global mean abundance and global stability for metacommunities experiencing chaotic dynamics and either high or low dispersal.

Figure B4: The effect of autocorrelated environmental fluctuations on global stability for predator *P*, consumer C_1, consumer C_2 and global consumer correlation for metacommunities with high and low dispersal.

Figure B5: The effect of positively cross-correlated and negatively cross-correlated autocorrelated environmental fluctuations on intraspecific synchrony and global

consumer correlation, global temporal variance, global mean abundance and global stability for metacommunities with high and low dispersal.

Figure B6: The effect of additive demographic noise on global stability for predator P, consumer C_1, consumer C_2 and global consumer correlation for metacommunities with high and low dispersal.

Figure B7: The effect of positively correlated and negatively correlated environmental fluctuations on intraspecific synchrony and global consumer correlation, global temporal variance, global mean abundance and global stability for metacommunities with high and low dispersal.

PREFACE

Acknowledgements

I wish to thank my supervisor, Frédéric Guichard, for his invaluable guidance during the past four years. I am also grateful to my friends and family for their unwavering support. Last but not least, I would like to thank the following 'Guichardians' for their assistance, advice and friendship: Filip Petrovic, Pradeep Pillai, Oscar Puebla, Kecia Kerr, Cesar Largaespada, Anaïs Lacoursière-Roussel, Eric Pedersen, Alana Domingo, Aline Fouard, Tri Nguyen Quang, Nicolas Le Corre, Philippe Girard and Julian Xue.

Contributions of authors

T. Gouhier developed and organized all of the chapters presented in this thesis. Specifically, T. Gouhier coded all of the models, analyzed all of the data and wrote all of the chapters. F. Guichard contributed to the development of the thesis and co-

wrote all of the chapters, and B. Menge and A. Gonzalez co-wrote parts of chapters 1, 2 and 4.

Note on the structure of the thesis

This is a manuscript-based thesis; I have used connecting statements to provide logical bridges between each chapter. Since each chapter contains a review of the literature, the general introduction that follows presents the overarching theme of the thesis and some background material on my main study system, the intertidal ecosystem of the West coast of the United States.

Novelty and impact of thesis research

In this thesis, I present and validate a novel framework to elucidate the processes that govern the spatiotemporal distribution of population abundance in model and natural systems.

In chapter 1, I apply spatial synchrony analysis to simple models and survey data to show that local biotic processes affecting population abundance interact with limited dispersal to control the distribution of population abundance at the continental scale despite regional environmental forcing. To my knowledge, this is the first study to show that the properties of spatial synchrony can be used to infer both the scale of dispersal and the relative importance of biotic and abiotic factors for the distribution of mussel population abundance along the West coast of the United States. Using a series of models, I show that these results are general and apply to any spatial ecological system undergoing local population fluctuations and limited dispersal. These results highlight the importance of including cross-scale

interactions between local processes and dispersal to understand the distribution of population abundance at the continental scale and predict the effects of global climate change.

In chapter 2, I extend the model and analyses developed in chapter 1 to understand the relationship between population abundance, recruitment and the environment in intertidal systems along the West coast of the United States. I show that limited dispersal generates a persistent match between patterns of recruitment and the environment and an intermittent mismatch between patterns of population abundance and recruitment. To my knowledge, this is the first study that explains the paradoxical mismatch between patterns of population abundance and recruitment observed in intertidal systems along the coasts of the Western United States and Chile. This work shows that even perfect knowledge about recruitment (or its environmental correlates) cannot be used to successfully predict the distribution of population abundance when dispersal is limited. Overall, this study emphasizes the importance of adopting a balanced approach that integrates processes affecting adult abundance and recruitment to better understand intertidal systems.

In chapter 3, I show that the results of chapters 1-2 have important implications for the design of marine reserve networks. I show that by neglecting to account for population dynamics, current marine reserve networks can lead to reduced mean abundance and persistence in both protected and unprotected areas. However, when they account for the consequences of population dynamics, marine reserve networks can maximize mean abundance and persistence in both protected and unprotected areas, and thus satisfy both fishery and conservation goals. To my knowledge, this is the first study that demonstrates the conditions under which the

consequences of population dynamics must be considered in order to design effective marine reserve networks.

In chapter 4, I show how local population dynamics, dispersal and regional environmental variability interact to control the stability of spatial food webs. To my knowledge, this is the first study to demonstrate that dispersal mediates the destabilizing effect of regional environmental variability by controlling the dynamics of food webs at local and regional scales. This study highlights how two components of environmental change (low dispersal due to habitat fragmentation and environmental variability) can interact synergistically to reduce food web stability in natural systems.

GENERAL INTRODUCTION

Determining the relative influence of biotic (i.e. species interactions) and abiotic (i.e. the environment) factors on the distribution of population abundance and community structure is a fundamental but controversial issue in ecology (Andrewartha and Birch 1954, Nicholson 1957, Ricklefs 2008). This controversy has been rehashed several times since its inception, and each iteration has introduced new terminology to emphasize a different perspective (density-dependent vs. density-independent: Andrewartha and Birch 1954, Nicholson 1957, intrinsic vs. extrinsic: Grenfell et al. 1998, stabilizing vs. equalizing: Chesson 2000, deterministic vs. stochastic: Coulson et al. 2004, endogenous vs. exogenous: Melbourne and Hastings 2009). Overall, proponents of the biotic regulation perspective emphasize negative feedbacks that buffer population fluctuations and thus promote persistence, whereas proponents of the abiotic limitation perspective contend that negative feedbacks are

weak or inexistent and that populations essentially undergo (extremely slow) random walks to extinction (Murdoch 1994). Hence, resolving this debate has fundamental implications for both our perception and the preservation of natural systems. Indeed, if ecological systems are governed mainly by abiotic limitation, they may be extremely vulnerable to environmental variability induced by global climate change (Walther et al. 2002).

Current frameworks addressing this debate advocate a scale-dependent or hierarchical approach, whereby the effects of biotic processes are circumscribed to local spatial scales whereas abiotic processes dominate at regional spatial scales (Turner et al. 2001, Willis and Whittaker 2002, Pearson and Dawson 2003). A similar scale-dependent approach has been proposed to explain the distribution of population abundance and community structure in my main model system, the rocky intertidal.

THE RELATIVE IMPORTANCE OF BIOTIC REGULATION AND ABIOTIC LIMITATION IN THE ROCKY INTERTIDAL: A SCALE-DEPENDENT APPROACH

At the local scale

The rocky intertidal is well represented globally and has been studied extensively in Europe (Connell 1961a, b), North America (Paine 1966, 1984), Australia (Underwood 2000), Chile (Navarrete et al. 2005, Lagos et al. 2007, Lagos et al. 2008, Navarrete et al. 2008) and New Zealand (Menge et al. 2003). Early studies identified consistencies in the spatial distribution of population abundance and community structure across rocky intertidal zones in the United Kingdom and the West coast of

the United States (Connell 1961a, b, Paine 1966, Connell 1970, Dayton 1971, Paine 1984). These regular and consistent spatial patterns were attributed to the joint effects of biotic and abiotic processes: the distribution of species abundance is limited by predation (Connell 1961a, Paine 1966) in the lower intertidal and desiccation stress in the upper intertidal (Connell 1961b). Within this zone, biotic processes in the form of competition (Connell 1961b, a, Dayton 1971, Paine 1984) and keystone predation (Paine 1966) largely govern the distribution of population abundance and community structure.

However, other studies found no evidence of these consistent spatial patterns within the rocky intertidal (Underwood 1978, Underwood et al. 1983, Underwood et al. 2000). Instead, these studies discovered that patterns of population abundance, community structure and species interactions were highly variable and dependent upon recruitment[1] (Underwood 1978, Underwood et al. 1983, Underwood et al. 2000). Since many intertidal species possess a sessile adult stage and a planktonic larval stage (Grantham et al. 2003), this finding led to a shift in focus from local biotic processes affecting adults to regional abiotic processes controlling the recruitment of larvae to explain patterns of population abundance and community structure (Underwood 1978, Underwood et al. 1983, Underwood et al. 2000).

[1] Recruitment is defined as the arrival of propagules in a location.

At the regional scale

Early work attempting to predict patterns of population abundance and community structure at the regional scale assumed that populations were open: large-scale larval dispersal[2] was assumed to decouple local recruitment from adult dynamics (Roughgarden et al. 1985, Iwasa and Roughgarden 1986, Johnson 2005). By decoupling recruitment from adult population dynamics, open system theory relies entirely on abiotic processes affecting recruitment to explain the regional spatiotemporal patterns of variability observed in intertidal systems (Gouhier and Guichard 2007). Indeed, in order to accommodate the variable patterns of recruitment and adult abundance observed in natural systems, early models were modified to allow variable recruitment in time and space in response to abiotic processes such as nearshore oceanographic regimes (Lewin 1986, Roughgarden et al. 1987, Roughgarden et al. 1988, Alexander and Roughgarden 1996). However, these models can neither generate nor explain the persistent mismatch between patterns of recruitment and patterns of abundance observed in natural systems (Menge et al. 2009).

A synthesis integrating the effects of local biotic and regional abiotic processes

Recently, a synthesis integrating local biotic processes and regional abiotic processes was proposed in order to address the mismatch between patterns of recruitment and

[2] Dispersal is defined as the movement of propagules from their birthplace to a different location.

patterns of abundance. Using the West coast of the United States as a model system, Roughgarden et al. (1988) proposed that oceanographic processes controlling recruitment determine the relative importance of regional abiotic and local biotic processes. Specifically, a strong and persistent latitudinal gradient in oceanographic conditions is hypothesized to determine the distribution of population abundance and community structure by controlling larval recruitment (Roughgarden et al. 1988, Connolly and Roughgarden 1998, 1999, Connolly et al. 2001).

In California, strong and persistent upwelling currents transport intertidal larvae offshore. Only during brief and infrequent relaxation events do offshore currents subside and return larvae to the shore where they can settle onto the intertidal and metamorphose into adults (Roughgarden et al. 1988, Connolly and Roughgarden 1998, 1999, Connolly et al. 2001). Using closed (no dispersal of larvae from one population to another) competition and predator-prey models, Connolly and Roughgarden (1998, 1999) predicted that by limiting recruitment, oceanographic conditions in California lead to low abundance and weak species interactions (Roughgarden et al. 1988, Connolly and Roughgarden 1998, 1999, Connolly et al. 2001). In the Pacific northwest, relaxation events are much more frequent and lead to a large supply of recruits. Using the same closed models, Connolly and Roughgarden (1998, 1999) predicted that large larval supply leads to higher abundance and stronger species interactions (Roughgarden et al. 1988, Connolly and Roughgarden 1998, 1999, Connolly et al. 2001).

Hence, this theory predicts that the importance of local biotic processes (species interactions) depends entirely on the effects of regional abiotic processes (upwelling currents) on larval supply: when abiotic processes limit larval supply, adult

abundance and community structure are more likely to reflect patterns of recruitment; when abiotic processes do not limit larval supply, patterns of adult abundance and community structure are more likely to reflect the effects of local biotic processes (Connolly and Roughgarden 1998, 1999). However, experimental tests have failed to find the predicted latitudinal gradient in the strength of biotic interactions (Menge et al. 2004). The mismatch between patterns of recruitment and adult abundance thus remains unresolved (Lagos et al. 2007, Broitman et al. 2008).

BUILDING AN ALTERNATIVE FRAMEWORK: COUPLING ADULT POPULATIONS AND RECRUITMENT IN SPACE AND TIME

So far, all attempts to predict spatiotemporal variability in population abundance and community structure have relied almost entirely on variability in abiotic processes affecting recruitment (Roughgarden et al. 1987, Roughgarden et al. 1988, Connolly and Roughgarden 1998, 1999, Connolly et al. 2001). Hence, these efforts will always predict a match between the regional abiotic processes affecting patterns of recruitment and population abundance. We need to integrate another source of variability in order to explain the observed mismatch between patterns of recruitment and adult abundance in space and time.

One source of variability that has not been integrated into these models is the potential effect of biotic processes on the dynamics of adult populations at regional scales. Indeed, when coupled with limited dispersal, these biotic processes (Connell 1961a, b, Paine 1966, Paine and Levin 1981, Paine 1984) have been shown to generate complex regional patterns of abundance in space and time (Jansen and de

Roos 2000, Guichard et al. 2004, Guichard 2005, Gouhier and Guichard 2007). However, this source of variability remains largely untapped because classical models assume that populations are either demographically open (no coupling between recruitment and adult abundance) or closed (no coupling between populations). Hence, local biotic processes cannot generate variability in time and space in these systems. Only if we relax the assumption of demographic openness can we turn to local biotic processes as an alternative (or supplementary) source of regional variability in recruitment and adult abundance.

So, how valid is the assumption of demographic openness in marine systems? A recent meta-analysis of 300 studies has shown that pelagic larval duration, the main justification for the assumption of demographic openness, is a poor predictor of the scale of dispersal and connectivity[3] in marine populations (Weersing and Toonen 2009). Hence, long pelagic larval durations do not necessarily lead to dispersal and connectivity over large spatial scales, let alone demographic openness. Consistent with this finding, tagging experiments (Jones et al. 1999, Jones et al. 2005) and genetic analyses (Palumbi 2003, Taylor and Hellberg 2003, Puebla et al. 2009) have shown large local retention of larvae and strong spatial genetic structure in coral reef fishes despite their long (> 3 week) pelagic larval durations (Cowen et al. 2000). Local retention of larvae (Becker et al. 2007) and strong genetic differentiation at small scales (25-42 km) (Gilg and Hilbish 2003) have also been documented in marine invertebrates despite their long pelagic larval duration. It thus appears that

[3] Connectivity is defined as the level of demographic coupling between segregated populations due to the exchange of propagules via dispersal.

effective dispersal distances may well be limited in marine systems despite the potential for large-scale dispersal afforded by strong currents and long pelagic larval durations.

Based on this evidence, I relax the assumption of demographic openness and build an alternative framework that explores the joint effects of biotic and abiotic processes on regional patterns of population abundance, recruitment and community structure. Using this framework, I demonstrate that dispersal controls the relative importance of local biotic and regional abiotic processes in spatial ecological systems (Fig 1).

DESCRIPTION OF THE SURVEYS OF POPULATION ABUNDANCE AND RECRUITMENT USED TO VALIDATE MODEL PREDICTIONS

In order to test and validate the model predictions generated in chapters 1-2, I used spatially-explicit survey data on the recruitment and adult abundance (percent cover) of mussels (*M. californianus*) and barnacles (*B. glandula*) collected by the Partnership for Interdisciplinary Studies of Coastal Oceans (PISCO). The adult abundance surveys were conducted once a year between 1999-2004 for 48 sites located along a 1850 km stretch of the West coast of the United States. At each site and for each species, the mean annual abundance was determined by averaging the percent cover found within thirty 0.25 m^2 quadrats placed randomly along three 50 m transects located in the mid-intertidal zone (i.e. 10 random quadrats per transect).

Annual larval recruitment of barnacles and mussels was measured from 1997 to 2005 at 30 sites along a 1320 km stretch of the West coast of the United States

using standard procedures. Mussel recruitment was quantified using standardized plastic mesh collectors and barnacle recruitment was quantified using 10x10 cm plexiglass or PVC plates covered with tape. These materials were used because they emulate the characteristics of the preferred settlement substrate for barnacle and mussel larvae. Recruits from 5-8 replicates were counted in the laboratory and standardized to the number of individuals per plate (100 cm^2) for barnacles and the number of individuals per collector (~100 cm^3) for mussels. Recruitment was measured on a monthly basis and the results were subsequently averaged to provide annual estimates of barnacle and mussel recruitment for each site.

The data from these annual adult abundance and recruitment surveys have been thoroughly vetted for accuracy by the PISCO staff and have been the subject of numerous scientific publications. In chapter 1-2, I use these datasets to validate novel model predictions regarding the relative contribution of biotic and abiotic factors to spatiotemporal patterns of population abundance and recruitment in intertidal communities along the West coast of the United States.

SUMMARY OF CHAPTERS

In chapter 1, I develop and validate a theory of marine metapopulations that demonstrates that dispersal is critical for predicting the distribution of population abundance of the dominant mussel *M. californianus* along the West coast of the United States (Fig 1). Using dynamic metapopulation models and survey data, I show that local fluctuations generated by biotic processes (succession, predation) interact with limited dispersal to govern the distribution of mussel abundance in space (1,800 km) and time (6 years), despite strong environmental forcing by regional abiotic

processes. By comparing the spatial patterns of abundance generated by the models and the survey data, I estimate that the mean scale of dispersal of *M. californianus* is approximately 100 km (~6% of the spatial extent of the survey data). The cross-scale interaction between local biotic processes and limited dispersal shows the limitations of the scale-dependent approach (Turner et al. 2001, Willis and Whittaker 2002, Pearson and Dawson 2003) and the importance of dispersal (Connolly and Roughgarden 1998, 1999) for predicting the distribution of abundance of the mussel *M. californianus* along the West coast of the United States.

In chapter 2, I extend the theory developed in chapter 1 from populations to communities and determine the relative importance of local biotic processes and regional abiotic processes for patterns of recruitment (8 years, 1,330 km) and abundance in the mussel *M. californianus* and the barnacle *B. glandula* along the West coast of the United States (Fig 1). I show that despite strong environmental forcing by regional abiotic processes, the interaction between local biotic processes and limited dispersal controls the distribution of population abundance and recruitment in natural mussel and barnacle populations. Furthermore, I show that patterns of recruitment invariably match the environment, whether populations are controlled by regional abiotic processes or the interaction between local biotic processes and limited dispersal. Since these patterns of recruitment are universal, they cannot be used to assess the relative importance of biotic and abiotic processes for the distribution of adult population abundance. This could explain why establishing a link between patterns of recruitment and abundance has proven so difficult (Lagos et al. 2007, Broitman et al. 2008, Lagos et al. 2008, Navarrete et al. 2008).

In chapter 3, I focus on the implications of chapter 1 and 2 for the design of effective marine reserve networks (Fig 1). Current marine reserve theory emphasizes the importance of maintaining connectivity by using the scale of dispersal as the distance between individual reserves (Botsford et al. 2001, Botsford et al. 2003, Gerber et al. 2003, Shanks et al. 2003, Sale et al. 2005, Halpern et al. 2006). However, chapters 1 and 2 show that local biotic processes interact with dispersal and generate patterns of connectivity at spatial scales that are much larger than that of dispersal. Under these conditions, I show that using the scale of dispersal as the size and spacing of marine reserves reduces mean abundance and persistence by compromising natural patterns of connectivity. However, using the scale of natural patterns of connectivity as the size and spacing of reserves maximizes mean abundance and persistence inside and outside of reserves. Hence, such marine reserve networks can simultaneously satisfy conservation and fishery goals (Hastings and Botsford 2003). Overall, this chapter emphasizes the distinction between the scale of dispersal (potential connectivity) and the scale of connectivity (realized connectivity) and strongly advocates the use of the latter for the size and spacing of marine reserves.

In chapter 4, I extend the theory developed in the first three chapters to investigate the role of dispersal for the maintenance of stability in spatial 'keystone' food webs (one generalist predator, two consumers, one resource; Fig 1). In this keystone food web, the predator preferentially consumes the superior competitor and, in doing so, generates asynchronous fluctuations among competitors (compensatory dynamics) that maintain food web persistence (McCann et al. 1998, Vasseur and Fox 2007, Gouhier et al. 2010). Here, I show that the stabilizing effect

of these compensatory dynamics depends on the rate of dispersal. Low rates of dispersal dampen and desynchronize fluctuations among food webs, thus facilitating environmental destabilization. However, high rates of dispersal induce synchronized fluctuations among food webs that mitigate environmental destabilization (Gouhier et al. 2010). Regardless of dispersal, I show that abiotic and biotic processes interact to govern food web dynamics: food webs alternate between periods of biotic regulation and periods of abiotic limitation (Gouhier et al. 2010). These dynamic switches in the dominance of abiotic limitation and biotic regulation have important implications for assessing their relative importance in natural systems (Houlahan et al. 2007).

LITERATURE CITED

Alexander, S. E. and J. Roughgarden. 1996. Larval transport and population dynamics of intertidal barnacles: A coupled benthic/oceanic model. Ecological Monographs **66**:259-275.

Andrewartha, H. and L. Birch. 1954. The distribution and abundance of animals. University of Chicago Press, Chicago.

Becker, B. J., L. A. Levin, F. J. Fodrie, and P. A. McMillan. 2007. Complex larval connectivity patterns among marine invertebrate populations. PNAS **104**:3267-3272.

Botsford, L. W., A. Hastings, and S. D. Gaines. 2001. Dependence of sustainability on the configuration of marine reserves and larval dispersal distance. Ecology Letters **4**:144-150.

Botsford, L. W., F. Micheli, and A. Hastings. 2003. Principles for the design of marine reserves. Ecological Applications **13**:S25-S31.

Broitman, B. R., C. A. Blanchette, B. A. Menge, J. Lubchenco, C. Krenz, M. Foley, P. T. Raimondi, D. Lohse, and S. D. Gaines. 2008. Spatial and temporal patterns of invertebrate recruitment along the west coast of the United States. Ecological Monographs **78**:403-421.

Chesson, P. 2000. Mechanisms of maintenance of species diversity. Annual Review of Ecology and Systematics **31**:343-366.

Connell, J. H. 1961a. Effects of Competition, Predation by Thais Lapillus, and Other Factors on Natural Populations of Barnacle Balanus Balanoides. Ecological Monographs **31**:61-104.

Connell, J. H. 1961b. The Influence of Interspecific Competition and Other Factors on Distribution of Barnacle Chthamalus Stellatus. Ecology **42**:710-723.

Connell, J. H. 1970. A Predator-Prey System in Marine Intertidal Region .1. Balanus-Glandula and Several Predatory Species of Thais. Ecological Monographs **40**:49-78.

Connolly, S. R., B. A. Menge, and J. Roughgarden. 2001. A latitudinal gradient in recruitment of intertidal invertebrates in the northeast Pacific Ocean. Ecology **82**:1799-1813.

Connolly, S. R. and J. Roughgarden. 1998. A latitudinal gradient in northeast Pacific intertidal community structure: Evidence for an oceanographically based synthesis of marine community theory. American Naturalist **151**:311-326.

Connolly, S. R. and J. Roughgarden. 1999. Theory of marine communities: Competition, predation, and recruitment-dependent interaction strength. Ecological Monographs **69**:277-296.

Coulson, T., P. Rohani, and M. Pascual. 2004. Skeletons, noise and population growth: the end of an old debate? Trends in Ecology & Evolution **19**:359-364.

Cowen, R. K., K. M. M. Lwiza, S. Sponaugle, C. B. Paris, and D. B. Olson. 2000. Connectivity of marine populations: Open or closed? Science **287**:857-859.

Dayton, P. K. 1971. Competition, Disturbance, and Community Organization - Provision and Subsequent Utilization of Space in a Rocky Intertidal Community. Ecological Monographs **41**:351-389.

Gerber, L. R., L. W. Botsford, A. Hastings, H. P. Possingham, S. D. Gaines, S. R. Palumbi, and S. Andelman. 2003. Population models for marine reserve design: A retrospective and prospective synthesis. Ecological Applications **13**:S47-S64.

Gilg, M. R. and T. J. Hilbish. 2003. The geography of marine larval dispersal: coupling genetics with fine-scale physical oceanography. Ecology **84**:2989-2998.

Gouhier, T. C. and F. Guichard. 2007. Local disturbance cycles and the maintenance of spatial heterogeneity across scales in marine metapopulations. Ecology **88**:647-657.

Gouhier, T. C., F. Guichard, and A. Gonzalez. 2010. Synchrony and Stability of Food Webs in Metacommunities. The American Naturalist **175**:E16-E34.

Grantham, B. A., G. L. Eckert, and A. L. Shanks. 2003. Dispersal potential of marine invertebrates in diverse habitats. Ecological Applications **13**:S108-S116.

Grenfell, B. T., K. Wilson, B. F. Finkenstadt, T. N. Coulson, S. Murray, S. D. Albon, J. M. Pemberton, T. H. Clutton-Brock, and M. J. Crawley. 1998. Noise and determinism in synchronized sheep dynamics. Nature **394**:674-677.

Guichard, F. 2005. Interaction strength and extinction risk in a metacommunity. Proceedings of the Royal Society of London B **272**:1571-1576.

Guichard, F., S. A. Levin, A. Hastings, and D. Siegel. 2004. Toward a dynamic metacommunity approach to marine reserve theory. Bioscience **54**:1003-1011.

Halpern, B. S., H. M. Regan, H. P. Possingham, and M. A. McCarthy. 2006. Accounting for uncertainty in marine reserve design. Ecology Letters **9**:2-11.

Hastings, A. and L. W. Botsford. 2003. Comparing designs of marine reserves for fisheries and for biodiversity. Ecological Applications **13**:S65-S70.

Houlahan, J. E., D. J. Currie, K. Cottenie, G. S. Cumming, S. K. M. Ernest, C. S. Findlay, S. D. Fuhlendorf, U. Gaedke, P. Legendre, J. J. Magnuson, B. H.

McArdle, E. H. Muldavin, D. Noble, R. Russell, R. D. Stevens, T. J. Willis, I. P. Woiwod, and S. M. Wondzell. 2007. Compensatory dynamics are rare in natural ecological communities. Proceedings of the National Academy of Sciences **104**:3273-3277.

Iwasa, Y. and J. Roughgarden. 1986. Interspecific Competition among Metapopulations with Space-Limited Subpopulations. Theoretical Population Biology **30**:194-214.

Jansen, V. and A. de Roos. 2000. The role of space in reducing predator-prey cycles. Pages 183–201 *in* U. Dieckmann, R. Law, and J. A. J. Metz, editors. The geometry of ecological interactions: simplifying spatial complexity. Cambridge University Press, Cambridge, U.K.

Johnson, M. P. 2005. Is there confusion over what is meant by 'open population'? Hydrobiologia **544**:333-338.

Jones, G. P., M. J. Milicich, M. J. Emslie, and C. Lunow. 1999. Self-recruitment in a coral reef fish population. Nature **402**:802-804.

Jones, G. P., S. Planes, and S. R. Thorrold. 2005. Coral Reef Fish Larvae Settle Close to Home. Current Biology **15**:1314-1318.

Lagos, N. A., J. C. Castilla, and B. R. Broitman. 2008. Spatial environmental correlates of intertidal recruitment: A test using barnacles in northern Chile. Ecological Monographs **78**:245-261.

Lagos, N. A., F. J. Tapia, S. A. Navarrete, and J. C. Castilla. 2007. Spatial synchrony in the recruitment of intertidal invertebrates along the coast of central Chile. Marine Ecology-Progress Series **350**:29-39.

Lewin, R. 1986. Supply-Side Ecology. Science **234**:25-27.

McCann, K., A. Hastings, and G. R. Huxel. 1998. Weak trophic interactions and the balance of nature. Nature **395**:794-798.

Melbourne, B. A. and A. Hastings. 2009. Highly Variable Spread Rates in Replicated Biological Invasions: Fundamental Limits to Predictability. Science **325**:1536-1539.

Menge, B. A., C. Blanchette, P. Raimondi, T. Freidenburg, S. Gaines, J. Lubchenco, D. Lohse, G. Hudson, M. Foley, and J. Pamplin. 2004. Species interaction strength: Testing model predictions along an upwelling gradient. Ecological Monographs **74**:663-684.

Menge, B. A., F. Chan, K. J. Nielsen, E. D. Lorenzo, and J. Lubchenco. 2009. Climatic variation alters supply-side ecology: impact of climate patterns on phytoplankton and mussel recruitment. Ecological Monographs **79**:379-395.

Menge, B. A., J. Lubchenco, M. E. S. Bracken, F. Chan, M. M. Foley, T. L. Freidenburg, S. D. Gaines, G. Hudson, C. Krenz, H. Leslie, D. N. L. Menge, R. Russell, and M. S. Webster. 2003. Coastal oceanography sets the pace of rocky intertidal community dynamics. Proceedings of the National Academy of Sciences of the United States of America **100**:12229-12234.

Murdoch, W. W. 1994. Population Regulation in Theory and Practice - the Robert-H-Macarthur-Award-Lecture Presented August 1991 in San-Antonio, Texas, USA. Ecology **75**:271-287.

Navarrete, S. A., B. R. Broitman, and B. A. Menge. 2008. Interhemispheric comparison of recruitment to intertidal communities: Pattern persistence and scales of variation. Ecology **89**:1308-1322.

Navarrete, S. A., E. A. Wieters, B. R. Broitman, and J. C. Castilla. 2005. Scales of benthic-pelagic coupling and the intensity of species interactions: From recruitment limitation to top-down control. Proceedings of the National Academy of Sciences of the United States of America **102**:18046-18051.

Nicholson, A. J. 1957. The Self-Adjustment of Populations to Change. Cold Spring Harbor Symposia on Quantitative Biology **22**:153-173.

Paine, R. T. 1966. Food Web Complexity and Species Diversity. American Naturalist **100**:65-75.

Paine, R. T. 1984. Ecological Determinism in the Competition for Space. Ecology **65**:1339-1348.

Paine, R. T. and S. A. Levin. 1981. Inter-Tidal Landscapes - Disturbance and the Dynamics of Pattern. Ecological Monographs **51**:145-178.

Palumbi, S. R. 2003. Population genetics, demographic connectivity, and the design of marine reserves. Ecological Applications **13**:S146-S158.

Pearson, R. G. and T. P. Dawson. 2003. Predicting the impacts of climate change on the distribution of species: are bioclimate envelope models useful? Global Ecology and Biogeography **12**:361-371.

Puebla, O., E. Bermingham, and F. Guichard. 2009. Estimating dispersal from genetic isolation by distance in a coral reef fish (Hypoplectrus puella). Ecology **90**:3087-3098.

Ricklefs, R. E. 2008. Disintegration of the Ecological Community. American Naturalist **172**:741-750.

Roughgarden, J., S. Gaines, and H. Possingham. 1988. Recruitment Dynamics in Complex Life-Cycles. Science **241**:1460-1466.

Roughgarden, J., S. D. Gaines, and S. W. Pacala. 1987. Supply-side ecology: the role of physical transport processes. Blackwell Scientific Publications, London.

Roughgarden, J., Y. Iwasa, and C. Baxter. 1985. Demographic-theory for an open marine population with space-limited recruitment. Ecology **66**:54-67.

Sale, P. F., R. K. Cowen, B. S. Danilowicz, G. P. Jones, J. P. Kritzer, K. C. Lindeman, S. Planes, N. V. C. Polunin, G. R. Russ, Y. J. Sadovy, and R. S. Steneck. 2005. Critical science gaps impede use of no-take fishery reserves. Trends in Ecology & Evolution **20**:74-80.

Shanks, A. L., B. A. Grantham, and M. H. Carr. 2003. Propagule dispersal distance and the size and spacing of marine reserves. Ecological Applications **13**:S159-S169.

Taylor, M. S. and M. E. Hellberg. 2003. Genetic evidence for local retention of pelagic larvae in a Caribbean reef fish. Science **299**:107-109.

Turner, M., R. Gardner, and R. O'Neill. 2001. Landscape ecology in theory and practice: pattern and process. Springer-Verlag, New York.

Underwood, A. J. 1978. Refutation of Critical Tidal Levels as Determinants of Structure of Inter-Tidal Communities on British Shores. Journal of Experimental Marine Biology and Ecology **33**:261-276.

Underwood, A. J. 2000. Experimental ecology of rocky intertidal habitats: what are we learning? Journal of Experimental Marine Biology and Ecology **250**:51-76.

Underwood, A. J., M. G. Chapman, and S. D. Connell. 2000. Observations in ecology: you can't make progress on processes without understanding the patterns. Journal of Experimental Marine Biology and Ecology **250**:97-115.

Underwood, A. J., E. J. Denley, and M. J. Moran. 1983. Experimental Analyses of the Structure and Dynamics of Mid-Shore Rocky Intertidal Communities in New-South-Wales. Oecologia **56**:202-219.

Vasseur, D. A. and J. W. Fox. 2007. Environmental fluctuations can stabilize food web dynamics by increasing synchrony. Ecology Letters **10**:1066-1074.

Walther, G.-R., E. Post, P. Convey, A. Menzel, C. Parmesan, T. J. C. Beebee, J.-M. Fromentin, O. Hoegh-Guldberg, and F. Bairlein. 2002. Ecological responses to recent climate change. Nature **416**:389-395.

Weersing, K. and R. Toonen. 2009. Population genetics, larval dispersal, and connectivity in marine systems. Marine Ecology Progress Series **393**:1-12.

Willis, K. J. and R. J. Whittaker. 2002. Ecology - Species diversity - Scale matters. Science **295**:1245-1248.

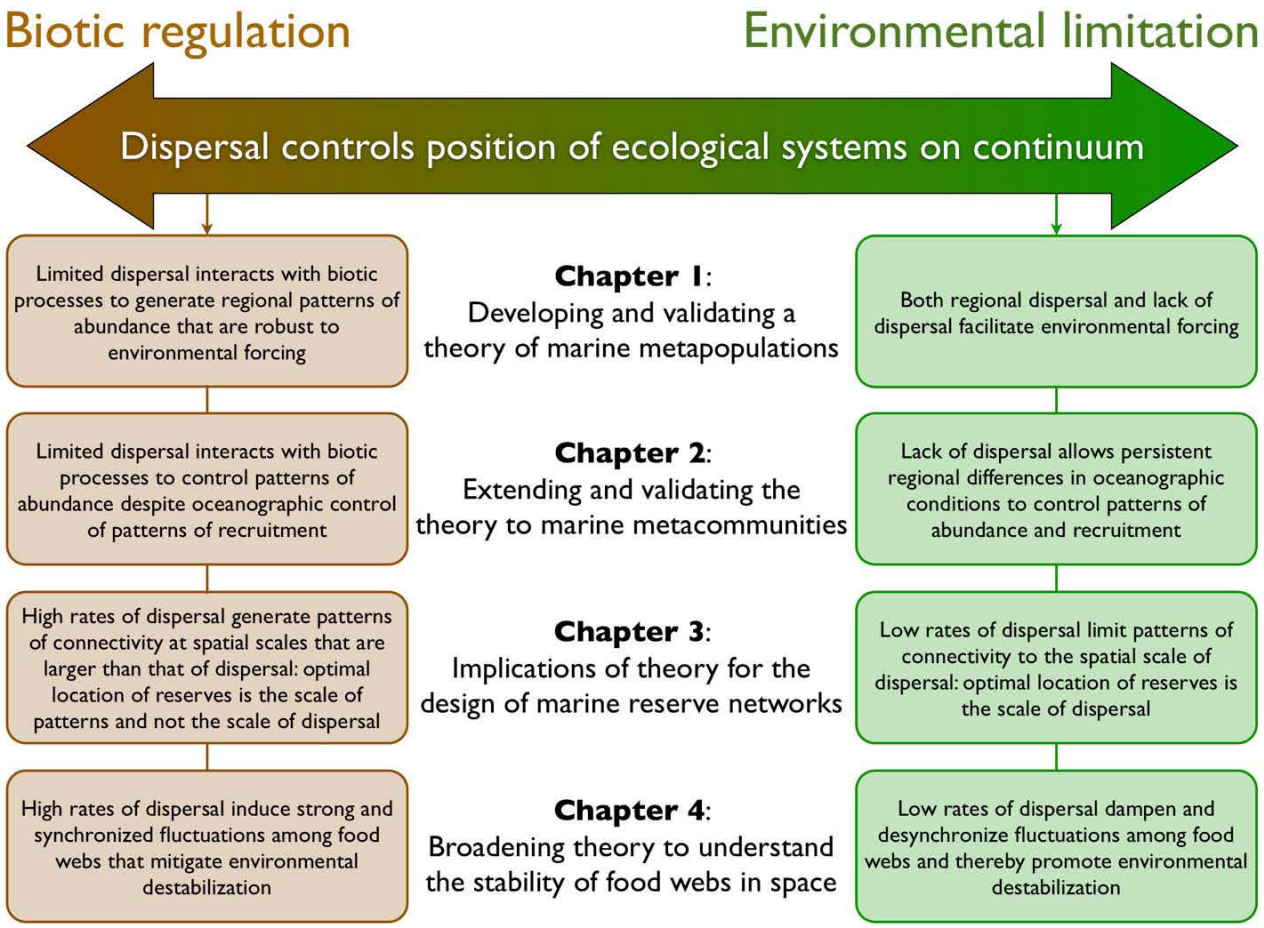

Figure 1: Overarching theme of the thesis and main results.

CHAPTER 1: ECOLOGICAL PROCESSES CAN SYNCHRONIZE MARINE POPULATION DYNAMICS OVER CONTINENTAL SCALES

Tarik C. Gouhier [1,*], Frédéric Guichard [1] and Bruce A. Menge [2]

[*] Corresponding author: tarik.gouhier@gmail.com | Phone (514) 398-4120 | Fax: (514) 398-5069

[1] Department of Biology, McGill University, 1205 Avenue Docteur Penfield, Montréal, Québec, H3A 1B1, Canada

[2] Department of Zoology, 3029 Cordley Hall, Oregon State University, Corvallis, OR 97331, USA

Keywords: synchrony, environmental variability, dispersal, metapopulation

Status: Proceedings of the National Academy of Sciences (*in press*)

ABSTRACT

Determining the relative importance of local and regional processes for the distribution of population abundance is a fundamental but contentious issue in ecology. In marine systems, classical theory holds that the influence of demographic processes and dispersal is confined to local populations whereas the environment controls regional patterns of abundance. Here, we use spatial synchrony to compare the distribution of population abundance of the dominant mussel *M. californianus* observed along the West coast of the United States to that predicted by dynamical models undergoing different dispersal and environmental treatments in order to infer the relative influence of local and regional processes. We reveal synchronized fluctuations in the abundance of mussel populations across a whole continent despite limited larval dispersal and strong environmental forcing. We show that dispersal among neighboring populations interacts with local demographic processes to generate characteristic patterns of spatial synchrony that can govern the dynamic distribution of mussel abundance over 1,800 km of coastline. Our study emphasizes the importance of dispersal and local dynamics for the distribution of abundance at the continental scale. It further highlights potential limits to the use of 'climate envelope' models for predicting the response of large-scale ecosystems to global climate change.

INTRODUCTION

Synchronized fluctuations in abundance among spatially-segregated populations are common in nature and can be used to quantify and understand the distribution of abundance in space and time (*1*). Synchrony can be induced by local intrinsic

processes such as dispersal among populations and strong interactions with mobile predators, or regional extrinsic processes such as spatially-correlated environmental variability (*1*). Although these processes are well known, identifying their relative contribution to patterns of synchrony remains a challenge (*1*). Recent work has shown that when the processes that contribute to synchrony can be studied in isolation, be it via natural barriers to dispersal among populations (*2, 3*) or experimental manipulation (*4*), synchrony patterns can be ascribed to their underlying cause. However, when intrinsic and extrinsic causes of synchrony co-occur, as is the case in most systems, assigning synchrony patterns to any specific causal process becomes onerous (*1*). Here, we show that in marine populations experiencing both intrinsic and extrinsic sources of synchrony, the shape of spatial synchrony patterns can be used to infer the cause of synchrony and explain the regional distribution of abundance.

Marine population theory has relied mostly on the environment to explain the regional (>1,000km) dynamics of populations. This focus is motivated by the lengthy pelagic larval stage commonly found in marine organisms, during which the larvae can be transported over large distances by strong nearshore currents (*5*). The potential for large-scale transport, along with the difficulties associated with measuring larval dispersal, has prompted many studies to assume either completely closed (no exportation of larvae to other populations) or completely open (no coupling between larval production and recruitment) demography (5, 6, but see 7, 8). This assumption, typically associated with equilibrium dynamics at the local scale, has emphasized the effect of large-scale heterogeneity in nearshore environmental conditions on recruitment (i.e. supply-side theory) to explain the regional dynamics

of marine populations (6, 9). However, recent progress on the quantification of larval dispersal distance has motivated the relaxation of demographic openness in several marine species (10-12). In light of these recent developments, we relax the assumptions of demographic openness and local equilibrium dynamics and compare the distribution of population abundance predicted by dynamical metapopulation models undergoing different dispersal and environmental treatments to that of the dominant mussel *Mytilus californianus* observed along the West coast of the United States in order to assess the relative importance of nearshore environmental heterogeneity and dispersal.

RESULTS AND DISCUSSION

The role of the environment in natural mussel populations

We first focus on the role of environmental heterogeneity by quantifying the strength and the consistency of the relationship between nearshore environmental conditions and the abundance (% cover) of *M. californianus*. Although nearshore environmental conditions have a strong effect on patterns of recruitment (13, 14), that effect seems lost on the regional distribution of *M. californianus* cover (15) (Fig 1A). Indeed, the spatial correlation between the environmental conditions and the mean annual *M. californianus* cover is relatively weak and inconsistent through time (Fig 1A), regardless of the temporal lag used (Fig S1), the temporal scale over which the environment is averaged (Fig S2) or whether the analysis explicitly accounts for the spatial heterogeneity observed in nearshore conditions (Fig S3). This weak spatial correlation reflects the mismatch between the persistent spatial gradient in the environment and the spatiotemporal variability in the cover of *M. californianus* (Fig

S3). This mismatch leads to local correlations whose strength and sign vary in space and time (Fig S3). Once spatially averaged, these highly variable local correlations lead to weak and inconsistent spatial correlations at the regional scale (Fig 1A, S2). Spatial synchrony, which measures the correlation in the time series of pairs of sites as a function of the lag distance that separates them (see Materials and Methods), more succinctly reveals the same discrepancy between the persistent spatial gradient in nearshore environmental conditions and the more complex spatiotemporal patterns in the cover of *M. californianus* (Fig 1B). All environmental variables undergo a slow and statistically significant linear decrease in synchrony with increasing lag distance (Fig 1B, see Materials and Methods and table 1 for statistical details). However, the cover of *M. californianus* shows a statistically significant nonlinear pattern, oscillating between synchrony and asynchrony with increasing lag distance (Fig 1B, table 1). This discrepancy suggests that intrinsic processes (i.e. dispersal and species interactions) rather than local nearshore environmental conditions may control the spatial synchrony patterns exhibited by *M. californianus*.

The effect of dispersal and species interactions on natural and model mussel populations

To elucidate how dispersal and species interactions can generate the complex spatial synchrony patterns observed in natural *M. californianus* populations, we develop metapopulation models that describe disturbance-succession (16, 17) and predator-prey (18-20) dynamics in a network of mussel populations connected by dispersal. Dispersal was implemented as a symmetrical kernel in the successional model (see Materials and Methods) and as a symmetrical and uniform nearest-neighbor process

in the predator-prey model (see Supporting Information). We subjected these metapopulation models to environmental variability treatments based on the nearshore environmental conditions observed along the West coast of the United States by varying mussel fecundity (21) according to a linear spatial gradient (i.e. spatial environmental variability) and a linear spatial gradient with normally-distributed white noise (i.e. spatiotemporal environmental variability; see Materials and Methods). We now perform a factorial experiment on the metapopulation models by using different dispersal and environmental treatments in order to assess the relative importance of dispersal and environmental variability for generating nonlinear spatial synchrony patterns of abundance that are compatible with those observed in natural mussel populations.

When there is no dispersal (i.e. full local retention of larvae), regional mussel dynamics is strictly controlled by environmental heterogeneity. Under this scenario, the model metapopulations experiencing either spatial or spatiotemporal environmental variability predict a weak and inconsistent spatial correlation between the mussel cover and the 1-year lagged environmental conditions (Fig 2A,B). This weak and inconsistent relationship is compatible with the results from our survey data (Fig 1A) and previously published accounts (15). However, model metapopulations predict that environmental variability induces a rapid decay in the spatial synchrony pattern of the mussel cover that is incompatible with the nonlinear spatial synchrony pattern observed in natural populations of *M. californianus* (Fig 2C,D). We now introduce dispersal among populations and vary the environment and the scale of dispersal to determine their relative contribution to spatial synchrony.

When dispersal is limited to neighboring populations (herein *limited dispersal*; 8.6% of the spatial domain for results in Fig 3-4), model metapopulations undergoing either spatial or spatiotemporal environmental variability predict a weak and inconsistent relationship between mussel cover and 1-year lagged environmental conditions (Fig 3A,C) that is similar to the one observed in the survey data (Fig 1A). However, regional dispersal (44% of the spatial domain in Fig 3-4) leads to a strong and dynamical relationship between the mussel cover and the environment (Fig 3B,D) that is inconsistent with the weak spatial correlation observed between populations of *M. californianus* and nearshore environmental conditions (Fig 1A). This suggests that limited dispersal between fluctuating populations might be an important driver of abundance in natural populations of *M. californianus*. Indeed, this role of limited dispersal is made more evident through the analysis of spatial synchrony.

In metapopulations experiencing limited dispersal, both the successional model (Fig 4A,C,E) and the predator-prey model (Fig S4A,C,E) accurately predict the nonlinear spatial synchrony pattern observed in natural populations of *M. californianus*, regardless of environmental variability. In contrast, in metapopulations undergoing regional dispersal, both the successional model (Fig 4B,D,F) and the predator-prey model (Fig S4A,C,E) predict that the spatial synchrony pattern displayed by mussels will match the quasi-linear decay displayed by the environment, despite the strong but inconsistent spatial correlation between the environment and mussel cover (Fig 3B,D). Hence, in successional and predator-prey metapopulation models, limited dispersal is critical for the emergence of nonlinear spatial synchrony patterns that are compatible with those observed in natural populations of *M.*

californianus. Nonlinear spatial synchrony patterns arise because limited dispersal (Fig. S5) couples neighboring populations and thus allows local fluctuations (Fig. S6) to scale-up and generate complex, non-stationary spatiotemporal patterns at the regional scale (Fig S7,S8) that are robust to environmental forcing (Fig 4B,D,F; Fig S4B,D,F). This cross-scale interaction between local population dynamics and limited dispersal is a general property of metapopulations (Fig 4,S4) that merely requires that local populations undergo sustained fluctuations (Fig S6) and that the average dispersal distance represents 3-10% of the spatial domain (Fig S5). Regional dispersal prevents these cross-scale interactions by spatially synchronizing population fluctuations across the entire metapopulation and thus generating regular regional oscillations characterized by stationary and quasi-linear spatial synchrony patterns (Fig 4B,D,F, Fig S4B,D,F, Fig S9-S10).

The shape of spatial synchrony can thus be used to determine the relative influence of cross-scale interactions and environmental forcing on the distribution of abundance in space and time. This can be achieved by fitting nonlinear and linear statistical models representing respectively cross-scale interactions and environmental forcing to the observed spatial synchrony patterns, and then comparing their performance using model selection (see Data analysis and Fig S5).

Using spatial synchrony to quantify the scale of dispersal in natural populations

Our metapopulation models show that the shape of nonlinear spatial synchrony patterns can be used to quantify the scale of dispersal. Indeed, the spatial range, defined as the lag distance at which synchrony first reaches zero (22), is

systematically associated with the average dispersal distance in both our successional model (Fig 4A,C,E) and our predator-prey model (Fig S4A,C,E) when dispersal is limited. Applying this result to our survey data, we estimate that the scale of dispersal of *M. californianus* is approximately 100 km (i.e. 6% of the domain). This estimate falls within the 95% confidence interval of dispersal distances documented for other bivalve species (72-220 km, see (11)) and is very similar to the scale of dispersal (97-115 km) of more closely related *Mytilus* species in other systems (11). Our estimate is based on the number of recruits that survive to the adult stage and is smaller than the 250 km estimate derived empirically by measuring the density of settlers in the same system (23). This is because spatial synchrony estimates integrate post-settlement processes that can limit the effective scale of dispersal.

Spatial synchrony reveals the relative influence of intrinsic and extrinsic processes on the distribution of population abundance

Theory has shown that local dynamics and limited dispersal can lead to complex spatial (24, 25) or spatiotemporal (26, 27) patterns at the regional scale that can promote coexistence (28), stability (27, 29), persistence (26, 29, 30) and functioning (24, 25) in spatial ecological systems. Similar complex spatiotemporal patterns have also been used to describe insect (31) and epidemic (32) outbreaks at regional and continental scales. However, linking local dynamics and limited dispersal to regional patterns has typically required extensive time series and characteristic spatial signatures such as Turing structures (24, 25), travelling waves (26, 31) or power laws (33). Here, we extend these theories by showing that in systems lacking these

characteristic spatial signatures, the shape of spatial synchrony patterns can be used to infer the joint effect of local dynamics and dispersal on the regional distribution of abundance. Hence, our framework moves away from the use of correlations between abundance and the environment to infer the causal effect of abiotic processes on biological patterns. Instead, by partitioning long non-stationary time series into smaller quasi-stationary time series and applying spatial synchrony analysis, we show that the spatial and temporal properties of spatial synchrony patterns can be used to determine the relative influence of intrinsic and extrinsic factors on the regional distribution of abundance in natural systems: limited dispersal interacts with local intrinsic fluctuations to generate nonlinear and non-stationary spatial synchrony patterns that are robust to environmental forcing, whereas regional dispersal facilitates environmental forcing and leads to stationary and linear spatial synchrony patterns.

Our results have important implications for identifying the processes that control the distribution of species abundance in natural systems and for predicting their response to global climate change. A popular approach for understanding and predicting species abundance distributions is to build species' 'climate envelopes' by either mapping the current species distribution to climate variables via correlation techniques or by determining the physiological tolerances of individual species (see review in 34). This climate envelope can then be used to predict the future distribution of species under various climate change scenarios (34). However, climate envelope models have been criticized because they do not integrate the effects of species interactions and dispersal on the distribution of population abundance (35-38). A recent synthesis proposes integrating the effects of dispersal and species

interactions into climate envelopes by adopting a hierarchical modeling framework (34). According to this hierarchical framework, species interactions and dispersal control the distribution of species abundance at smaller spatial scales (<200 km) whereas climate dominates at larger spatial scales (>200 km) (34). Here, we have shown that despite strong regional environmental forcing, local dynamics interact with limited dispersal to control the distribution of population abundance at scales that are much larger (>1,000 km) than that of dispersal (~100 km). Hence, our work suggests that processes occurring at small spatial scales can interact synergistically to control the distribution of population abundance at large spatial scales. Such cross-scale interactions demonstrate the limitations of adopting climate envelope models based on hierarchical frameworks to understand the distribution of species abundance and predict the effects of global climate change.

Overall, by applying spatial synchrony analysis to a large dataset of mussel populations along the West Coast of the United States, our study provides the first evidence that limited connectivity among local populations affects the dynamic distribution of abundance over >1,000 km. Our work supports the suggested shift toward a more dynamical approach to regional conservation, one that emphasizes patterns and processes across scales instead of those limited to the scale of the environment or dispersal.

MATERIALS AND METHODS

Data collection

Abundance (percent cover) of *M. californianus* was quantified annually from 1999 to 2004 at 48 sites located along the West coast of the United States and stretching

from southern California to northern Washington (40) (32.7 °N to 48.4 °N). For each site, the cover of *M. californianus* was surveyed in 10 randomly placed 0.25 m^2 quadrats for each of three 50 m transects located within the mid-intertidal zone. Mean annual sea surface temperature (SST, in °C), chlorophyll-a concentration (chl-a, in mg/m^3) and upwelling index (in $m^3/s/100$ m of coastline) data from 1997 to 2003 occurring within a 0.2 degree radius (1 degree radius for upwelling) of each of the 48 sites were obtained respectively from the Advanced Very High Resolution Radiometer (NOAA), the Sea-viewing Wide Field-of-view Sensor (NASA) and sea level pressure maps (Pacific Fisheries Environmental Laboratory). These environmental data series were validated by comparing them to *in situ* buoy measurements (see Data validation in Supporting Information).

Data analysis

Prior to conducting spatial synchrony analysis, all variables were detrended by subtracting the global mean time series from each site's time series in order to remove any bias caused by common large-scale trends (41). The distances between all pairs of sites were then computed and used to group the detrended time series data into equally-spaced distance bins (66 km wide). The coefficient of synchrony for each bin was calculated by computing the correlation coefficient between the time series of all pairs of sites within the bin. The extent of the spatial synchrony analysis was restricted to half of the spatial domain in order to avoid large discrepancies in the number of pairs of sites within each bin (22). Statistical significance was determined by using a one-tailed test (α=0.05) on 10,000 Monte Carlo randomizations (22). Specifically, for each bin, the p-value was calculated by

shuffling the data pairs within the bin 10,000 times, computing the coefficient of synchrony for each randomization and then calculating the proportion of randomizations with a coefficient of synchrony greater than or equal to that obtained with the original data. The same one-tailed randomization technique was used to assess the statistical significance of the correlation between the annual cover of *M. californianus* at year *i* and each environmental variable at year *i-1* (1-year lag). We used a 1-year lag because it corresponds to the temporal scale at which the correlation between the annual cover of *M. californianus* and each nearshore environmental variable is statistically significant (Fig S1).

We used model selection to detect linear and nonlinear spatial synchrony patterns in the environmental (SST, chl-a, upwelling index) and *M. californianus* datasets. For each dataset, we fit a linear statistical model $m|_{\text{linear}}$ and a nonlinear statistical model $m|_{\text{nonlinear}}$ to the spatial synchrony pattern:

$$m|_{\text{linear}} = a \cdot l + b \qquad (1)$$

$$m|_{\text{nonlinear}} = a \cdot \cos\left(\frac{l}{\max(l)} \cdot 3\pi \right) + b \qquad (2)$$

where l is the lag distance vector, a, b represent fitted coefficients and $\frac{l}{\max(l)} \cdot 3\pi$ is the normalized lag distance vector scaled to the domain $[0, 3\pi]$. This scaling of the lag distance vector allows the cosine function in the nonlinear model $m|_{\text{nonlinear}}$ to fit modal patterns of spatial synchrony over the spatial domain. For each statistical model, we calculated the Akaike Information Criterion corrected for small samples (42):

$$\mathrm{AIC_c} = -2\log(L) + 2K + \frac{2K(K+1)}{n-K-1} \qquad (3)$$

where L represents the maximum likelihood, $K = 3$ represents the number of parameters in each statistical model and n represents the number of samples. The statistical model with the smallest $\mathrm{AIC_c}$ value was selected for each dataset (42).

The successional model

The successional model describes local disturbance and recovery dynamics in a network of mussel populations that are connected by dispersal (17). Within populations, the successional dynamics observed in natural intertidal systems (16, 43) are represented as a mean-field implementation of a spatial process affecting the proportional abundance of (i) the dominant mussel (m), (ii) the wave disturbance (w) and (iii) the empty substrate (s) (44). A maximum fraction $\alpha_0 = 1$ of the proportional abundance of the dominant mussel species (m) can be displaced by wave disturbances (w). A proportion $(1-\delta_0)$ of disturbances displaces mussels through a density-dependent contact process with aggregation (Moore neighborhood, $q = 8$), while a proportion $\delta_0 = 10^{-3}$ of disturbances is density-independent. This disturbance dynamic is based on the assumption that wave disturbances destroy the byssal thread attachments of mussels around the edges of disturbed areas, thus making them temporarily more susceptible to further disturbance (44, 45). Hence, newly disturbed areas allow the local propagation of wave disturbances to adjacent mussel beds. Once the disturbance has propagated away from the newly disturbed area, the area transitions from the 'wave disturbed' state to the 'empty substrate' state. Similarly to disturbance, a maximum fraction

$\alpha_2 = 0.65$ of the empty substrate (s) can be colonized by mussels. A proportion $\delta_2 = 0.1$ of colonization occurs through a density-independent process, while the remaining colonization is density-dependent $(1-\delta_2)$. Mussel colonization also depends on the production and recruitment of larvae. Within populations x, larval production is a function of local mussel proportional abundance m_x and fecundity f_x $\left(\overline{f} = 5.25\right)$. The recruitment rate C_x^t is described by a Poisson process (46) $C_x^t = 1 - e^{-\beta_x^t}$, where β_x^t integrates (i) the total number of larvae produced and retained in populations x at time t and (ii) the total number of larvae produced in other populations y and dispersed to populations x at time t. The dynamics of the model are represented by the following integro-difference equation system for populations x in a metapopulation consisting of $n = 256$ populations:

$$\begin{aligned} w_x^{t+1} &= \alpha_0 m_x^t \left(\delta_0 + (1-\delta_0)\left(1-\left(1-w_x^t\right)^q\right)\right) \\ s_x^{t+1} &= w_x^t + s_x^t - \alpha_2 C_x^t s_x^t \left(\delta_2 + m_x^t (1-\delta_2)\right) \\ m_x^{t+1} &= 1 - w_x^t - s_x^t \end{aligned} \qquad (4)$$

with:

$$\begin{aligned} C_x^t &= 1 - e^{\beta_x^t} \\ \beta_x^t &= m_x^t f_x (1-d) + \int m_y^t f_y \, dD(|x-y|)\,\mathrm{d}y \\ D(|x-y|) &= \frac{3|x-y|^2}{2} e^{-|x-y|^3} \\ x &= u\left(\frac{2}{n}\mathbf{L} - 1\right) \\ \mathbf{L} &= [0,\ldots,n-1] \end{aligned} \qquad (5)$$

where D is the symmetrical mussel dispersal kernel resulting from larval transport at a constant speed and with a time-dependent settlement rate (double Weibull distribution (47)), d represents the proportion of larvae being dispersed, u represents the scale of dispersal and **L** represents a zero-based vector of population locations. We vary dispersal by manipulating d, the proportion of larvae being dispersed ($d = 0$ means that all larvae are retained locally, whereas $d = 1$ means that all larvae are dispersed), and u, the scale of dispersal ($u = 2$ corresponds to regional dispersal and $u = 10$ corresponds to limited dispersal). We assumed periodic boundary conditions for all simulations and set the dispersal rate to $d = 1$ (i.e. no local retention) unless otherwise specified (i.e. Fig 2 where $d = 0$). All successional model simulations were performed for 256 populations and the results were analyzed over 2000 post-transient time steps. Because our goal was to test the importance of local ecological processes and dispersal, all parameter values detailed above were selected to be representative of the broad parameter space characterized by spatiotemporal heterogeneity (17, 39). Here, we further assess the model's sensitivity to dispersal distance and to fecundity *f* as a means to determine the role of environmental variability in marine metapopulations.

Environmental variability can have a significant impact on the productivity of intertidal populations (21, 48). Here, we implement this effect by varying mussel fecundity spatially and spatiotemporally. Specifically, the spatial environmental treatment consists of varying the mussel fecundity *f* linearly from 3 to 7.5 over the entire spatial range $\left(\overline{f} = 5.25\right)$. We generate the spatiotemporal environmental treatment by adding normally-distributed white noise with zero mean and variance

$\sigma^2 = 2.7$ to the previously described spatial variation in fecundity $\left(\overline{f} = 5.25\right)$. The spatial and spatiotemporal environmental treatments thus preserve the same mean fecundity as the successional model undergoing no environmental variability. These spatial and spatiotemporal treatments were chosen to roughly mimic the spatial and spatiotemporal properties of the environment along the West coast of the United States. Applying the same spatial and spatiotemporal treatments to the mussel growth rate α_2 yields qualitatively similar results.

Model analysis

We applied the spatial synchrony and model selection methods (see Data analysis) used on the survey data to the post-transient time series of the successional and the predator-prey (see Supporting Information) models in order to assess their ability to generate nonlinear spatial synchrony patterns that are compatible with those observed in natural populations of *M. californianus*. Specifically, the model time series (2000 post-transient time steps) was split into 10-time step windows and spatial synchrony analysis was conducted over each window. We chose 10-time step windows in order to approximate the temporal extent of our intertidal survey data. However, our results are robust to window size (Fig S5B,D,F). For each time window, we fit the same linear $\left(m|_{\text{linear}}\right)$ and nonlinear $\left(m|_{\text{nonlinear}}\right)$ statistical models described in the Data analysis section to the spatial synchrony patterns generated by the metapopulation models. For each time window, the nonlinear statistical model was selected if $\text{AIC}_c|_{\text{nonlinear}} < \text{AIC}_c|_{\text{linear}}$ (42). The model spatial synchrony patterns presented in all figures were computed by averaging the spatial synchrony patterns

from all 10-time step windows in which the nonlinear statistical model was selected. When no compatible synchrony pattern exists for the entire model time series (i.e. for the regional dispersal treatment), the spatial synchrony patterns from *n* randomly selected time windows are computed and averaged (where *n* corresponds to the number of compatible synchrony patterns for the limited dispersal treatment). This allows for unbiased comparisons across dispersal treatments.

ACKNOWLEDGEMENTS

We thank G. Fussmann, B. Cazelles and J. van de Koppel for providing insightful comments on a previous version of the manuscript. T.C.G. was supported by a McGill Majors fellowship; F.G. was supported by a grant from the James S. McDonnell foundation; B.A.M was supported by grants from the David and Lucile Packard Foundation, the Gordon and Betty Moore Foundation, the Wayne and Gladys Valley Foundation, the Andrew W. Mellon Foundation, and the US National Science Foundation. This is publication number 360 from the Partnership for Interdisciplinary Studies of Coastal Oceans (PISCO), a large-scale, long-term consortium primarily funded by the David and Lucile Packard Foundation and the Gordon and Betty Moore Foundation.

REFERENCES

1. Liebhold A, Koenig WD, & Bjornstad ON (2004) Spatial synchrony in population dynamics. *Annu. Rev. Ecol. Evol. Syst.* 35:467-490.
2. Post E & Forchhammer MC (2002) Synchronization of animal population dynamics by large-scale climate. *Nature* 420(6912):168-171.
3. Grenfell BT*, et al.* (1998) Noise and determinism in synchronized sheep dynamics. *Nature* 394(6694):674-677.
4. Vasseur DA & Fox JW (2009) Phase-locking and environmental fluctuations generate synchrony in a predator-prey community. *Nature* 460(7258):1007-1010.
5. Roughgarden J, Iwasa Y, & Baxter C (1985) Demographic-theory for an open marine population with space-limited recruitment. *Ecology* 66(1):54-67.
6. Connolly SR & Roughgarden J (1999) Theory of marine communities: Competition, predation, and recruitment-dependent interaction strength. *Ecological Monographs* 69(3):277-296.
7. Hastings A & Higgins K (1994) Persistence of Transients in Spatially Structured Ecological Models. *Science* 263(5150):1133-1136.
8. Alexander SE & Roughgarden J (1996) Larval transport and population dynamics of intertidal barnacles: A coupled benthic/oceanic model. *Ecological Monographs* 66(3):259-275.
9. Roughgarden J, Gaines SD, & Pacala SW (1987) *Supply-side ecology: the role of physical transport processes* (Blackwell Scientific Publications, London) pp 491–495.
10. Swearer SE*, et al.* (2002) Evidence of self-recruitment in demersal marine populations. *B Mar Sci* 70:251-271.
11. Kinlan BP & Gaines SD (2003) Propagule dispersal in marine and terrestrial environments: a community perspective. *Ecology* 84:2007-2020.
12. Gilg MR & Hilbish TJ (2003) The geography of marine larval dispersal: coupling genetics with fine-scale physical oceanography. *Ecology* 84(11):2989-2998.
13. Connolly SR, Menge BA, & Roughgarden J (2001) A latitudinal gradient in recruitment of intertidal invertebrates in the northeast Pacific Ocean. *Ecology* 82(7):1799-1813.
14. Connolly SR & Roughgarden J (1998) A latitudinal gradient in northeast Pacific intertidal community structure: Evidence for an oceanographically based synthesis of marine community theory. *American Naturalist* 151(4):311-326.
15. Menge BA, Chan F, Nielsen KJ, Lorenzo ED, & Lubchenco J (2009) Climatic variation alters supply-side ecology: impact of climate patterns on phytoplankton and mussel recruitment. *Ecological Monographs* 79(3):379-395.
16. Paine RT & Levin SA (1981) Inter-Tidal Landscapes - Disturbance and the Dynamics of Pattern. *Ecological Monographs* 51(2):145-178.
17. Guichard F (2005) Interaction strength and extinction risk in a metacommunity. *Proceedings of the Royal Society of London B* 272:1571-1576.

18. Paine RT (1966) Food Web Complexity and Species Diversity. *American Naturalist* 100(910):65-75.
19. Rosenzweig ML & MacArthur RH (1963) Graphical Representation and Stability Conditions of Predator-Prey Interactions. *American Naturalist* 97(895):209-223.
20. Holland MD & Hastings A (2008) Strong effect of dispersal network structure on ecological dynamics. *Nature* 456(7223):792-794.
21. Leslie HM, Breck EN, Chan F, Lubchenco J, & Menge BA (2005) Barnacle reproductive hotspots linked to nearshore ocean conditions. *Proceedings of the National Academy of Sciences of the United States of America* 102(30):10534-10539.
22. Fortin M & Dale M (2005) *Spatial Analysis: A Guide for Ecologists* (Cambridge University Press).
23. Navarrete SA, Broitman BR, & Menge BA (2008) Interhemispheric comparison of recruitment to intertidal communities: Pattern persistence and scales of variation. *Ecology* 89(5):1308-1322.
24. Rietkerk M & van de Koppel J (2008) Regular pattern formation in real ecosystems. *Trends in Ecology & Evolution* 23(3):169-175.
25. van de Koppel J*, et al.* (2008) Experimental Evidence for Spatial Self-Organization and Its Emergent Effects in Mussel Bed Ecosystems. *Science* 322(5902):739-742.
26. Blasius B, Huppert A, & Stone L (1999) Complex dynamics and phase synchronization in spatially extended ecological systems. *Nature* 399(6734):354-359.
27. Jansen V & de Roos A (2000) The role of space in reducing predator-prey cycles. *The geometry of ecological interactions: simplifying spatial complexity*, eds Dieckmann U, Law R, & Metz JAJ (Cambridge University Press, Cambridge, U.K.), pp 183–201.
28. Hassell MP, Comins HN, & May RM (1994) Species Coexistence and Self-Organizing Spatial Dynamics. *Nature* 370(6487):290-292.
29. Briggs CJ & Hoopes MF (2004) Stabilizing effects in spatial parasitoid-host and predator-prey models: a review. *Theoretical Population Biology* 65(3):299-315.
30. Hassell MP, Comins HN, & May RM (1991) Spatial structure and chaos in insect population dynamics. *Science* 353:255-258.
31. Bjornstad ON, Peltonen M, Liebhold AM, & Baltensweiler W (2002) Waves of larch budmoth outbreaks in the European Alps. *Science* 298(5595):1020-1023.
32. Viboud C*, et al.* (2006) Synchrony, Waves, and Spatial Hierarchies in the Spread of Influenza. *Science* 312(5772):447-451.
33. Solé R & Bascompte J (2006) *Self-organization in complex ecosystems* (Princeton University Press, Princeton, New Jersey).
34. Pearson RG & Dawson TP (2003) Predicting the impacts of climate change on the distribution of species: are bioclimate envelope models useful? *Global Ecol Biogeogr* 12(5):361-371.
35. Suttle KB, Thomsen MA, & Power ME (2007) Species Interactions Reverse Grassland Responses to Changing Climate. *Science* 315(5812):640-642.
36. Gill JA*, et al.* (2001) The buffer effect and large-scale population regulation in migratory birds. *Nature* 412(6845):436-438.

37. Davis AJ, Jenkinson LS, Lawton JH, Shorrocks B, & Wood S (1998) Making mistakes when predicting shifts in species range in response to global warming. *Nature* 391(6669):783-786.
38. Davis AJ, Lawton JH, Shorrocks B, & Jenkinson LS (1998) Individualistic species responses invalidate simple physiological models of community dynamics under global environmental change. *Journal of Animal Ecology* 67(4):600-612.
39. Guichard F & Steenweg R (2008) Intrinsic and extrinsic causes of spatial variability across scales in a metacommunity. *J. Theor. Biol.* 250(1):113-124.
40. Schoch GC*, et al.* (2006) Fifteen degrees of separation: Latitudinal gradients of rocky intertidal biota along the California Current. *Limnol. Oceanogr.* 51(6):2564-2585.
41. Koenig WD (1999) Spatial autocorrelation of ecological phenomena. *Trends in Ecology & Evolution* 14(1):22-26.
42. Burnham K & Anderson D (2002) *Model Selection and Multimodel Inference: A Practical Information-theoretic Approach* (Springer, New York).
43. Paine RT (1984) Ecological Determinism in the Competition for Space. *Ecology* 65(5):1339-1348.
44. Guichard F, Halpin PM, Allison GW, Lubchenco J, & Menge BA (2003) Mussel disturbance dynamics: signatures of oceanographic forcing from local interactions. *The American Naturalist* 161(6):889-904.
45. Denny MW (1987) Lift as a mechanism of patch initiation in mussel beds. *Journal of Experimental Marine Biology and Ecology* 113:231-245.
46. Caswell H & Etter R (1999) Cellular automaton models for competition in patchy environments: Facilitation, inhibition, and tolerance. *Bulletin of Mathematical Biology* 61(4):625-649.
47. Neubert MG, Kot M, & Lewis MA (1995) Dispersal and Pattern-Formation in a Discrete-Time Predator-Prey Model. *Theoretical Population Biology* 48(1):7-43.
48. Menge BA, Daley BA, Wheeler PA, & Strub PT (1997) Rocky intertidal oceanography: An association between community structure and nearshore phytoplankton concentration. *Limnol. Oceanogr.* 42(1):57-66.

FIGURE LEGENDS

Figure 1: The dynamics of *M. californianus* cover and the environment along the West coast of the United States. (A) The correlation between the mean annual *M. californianus* cover and the 1-year lagged mean annual (i) sea surface temperature (SST, dark blue squares), (ii) chl-a concentration (chl-a, green diamonds), (iii) upwelling index (light blue triangles) and (iv) the first axis of the principal component analysis of all three environmental variables (PCA axis 1, red circles) at each site. (B) Spatial

synchrony of the mean annual (i) *M. californianus* cover (red circles), SST (dark blue squares), chl-a (green diamonds) and upwelling index (light blue triangles). The curves correspond to nonlinear (*M. californianus*) and linear (chl-a, SST, upwelling index) statistical models fitted to each dataset (see Materials and Methods). Full circles indicate statistical significance (α=0.05).

Figure 2: The dynamics of the annual mussel cover in successional model metapopulations undergoing no dispersal and environmental variability. (A, B) The correlation between the model mussel cover and the 1-year lagged environment at each site during a randomly selected 100-time step window. (C,D) The coefficient of synchrony of the model (i) mussel cover (blue solid curve, mean±S.E) and the (ii) 1-year lagged environment (green dashed curve, mean±S.E). The spatial synchrony of the annual *M. californianus* cover from the West coast of the United States is also depicted to facilitate comparisons (red circles). (A) and (C) correspond to spatial environmental variability whereas (B) and (D) correspond to spatiotemporal environmental variability. Full circles indicate statistical significance (α=0.05).

Figure 3: Time series of the correlation between the annual mussel cover in the successional model and the 1-year lagged environment at each site. (A, B) The correlation time series for metapopulations undergoing spatial environmental variability and (A) limited (8.6% of the domain) or (B) regional (44% of the domain) dispersal. (C, D) Correlation time series for metapopulations undergoing spatiotemporal environmental variability and (C) limited or (D) regional dispersal. Full circles indicate statistical significance (α=0.05).

Figure 4: Spatial synchrony of annual mussel cover in the successional model for metapopulations undergoing different environmental and dispersal treatments. (A, B)

No environmental variability and either (A) limited or (B) regional dispersal. (C, D) Spatial environmental variability and either (C) limited or (D) regional dispersal. (E, F) Spatiotemporal environmental variability and either (E) limited or (F) regional dispersal. The spatial synchrony of the mussel cover in the successional model is represented in blue solid curves (mean±S.E) while that of the 1-year lagged environment is represented in green dashed curves (mean±S.E). The spatial synchrony of annual *M. californianus* cover from the West coast of the United States is also depicted to facilitate comparisons (red circles). The scale of dispersal is represented by the blue vertical dotted line. The spatial extent of the limited dispersal treatment corresponds to 8.6% of the domain while that of the regional dispersal treatment corresponds to 44% of the domain. Full circles indicate statistical significance (α=0.05).

TABLES AND FIGURES

Table 1: Fitting linear and nonlinear statistical models to the spatial synchrony patterns observed in the survey datasets.

	Linear statistical model				Nonlinear statistical model			
Dataset	*n*	p-value	R^2	AIC_c	*n*	p-value	R^2	AIC_c
chl-a	14	0.007	0.420	0.07	14	0.54	0.033	8.34
SST	14	$8.6*10^{-6}$	0.82	-10.48	14	0.77	0.007	13.36
Upwelling	14	$7.3*10^{-7}$	0.88	1.26	14	0.48	0.043	30.26
M. californianus	14	0.58	0.03	5.11	14	$3.7*10^{-4}$	0.67	-9.89

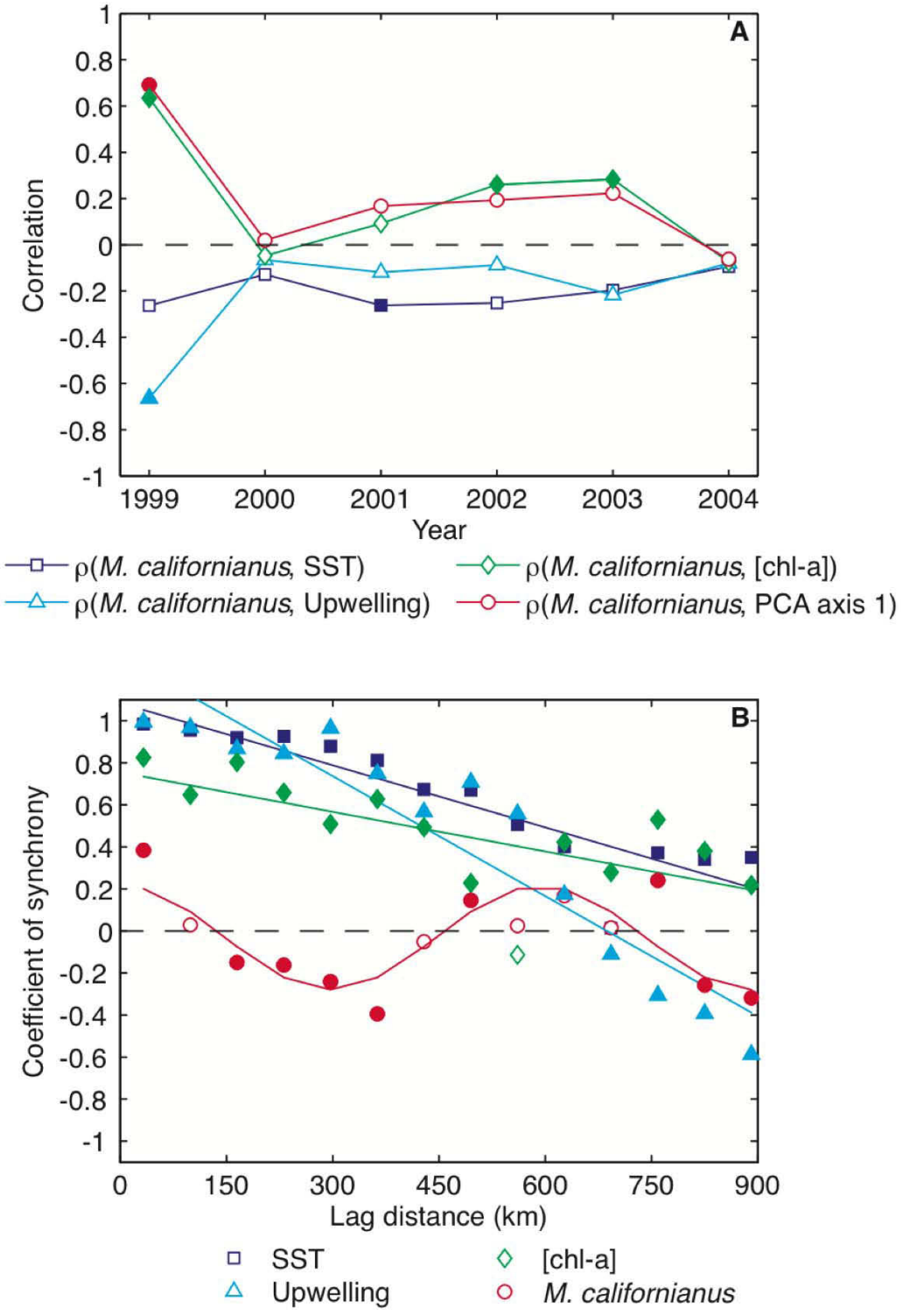
A
Correlation
Year
1999
2000
2001
2002
2003
2004
ρ(M. californianus, SST)
ρ(M. californianus, [chl-a])
ρ(M. californianus, Upwelling)
ρ(M. californianus, PCA axis 1)
B
Coefficient of synchrony
Lag distance (km)
SST
[chl-a]
Upwelling
M. californianus

Figure 1

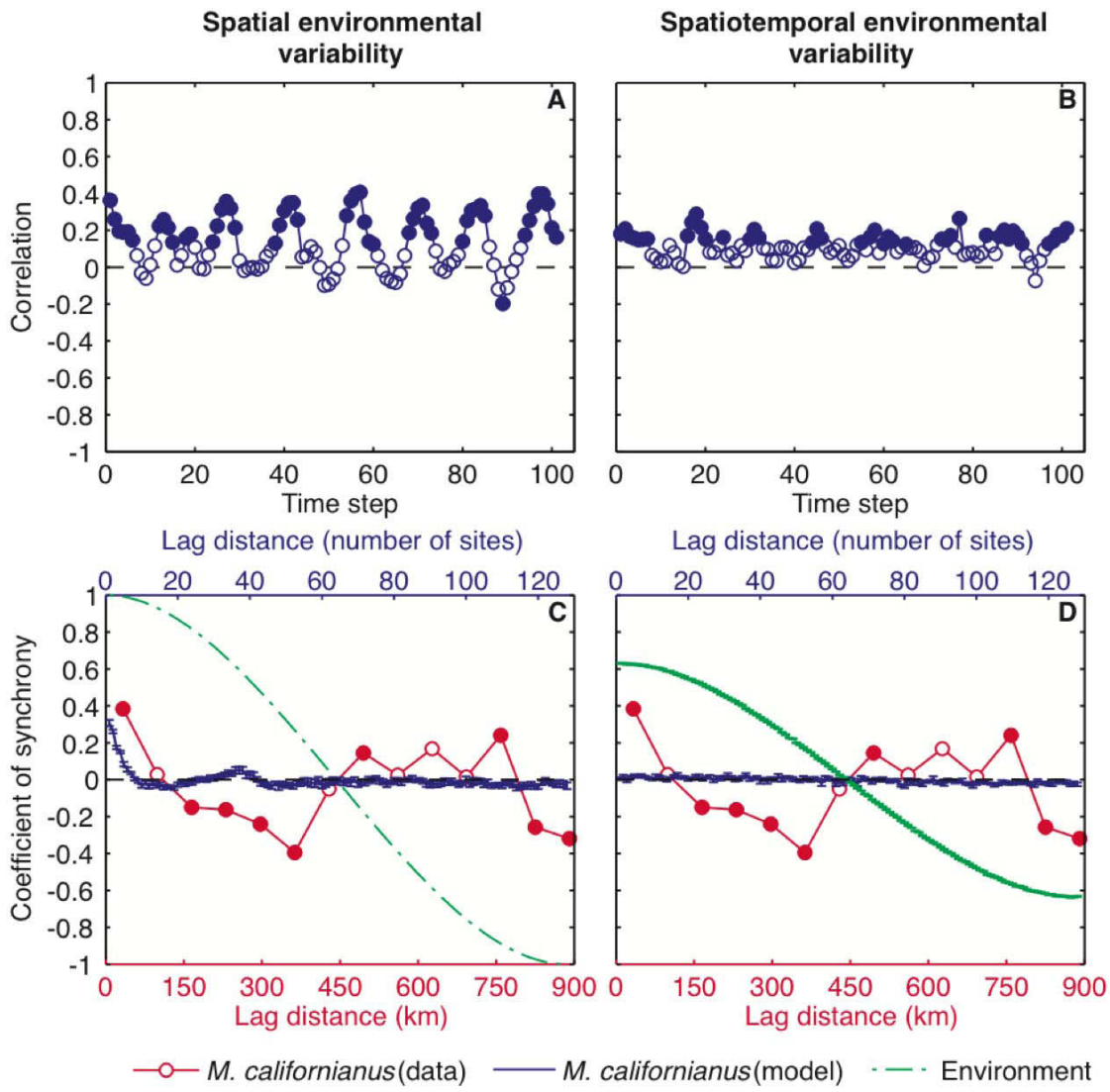
Spatial environmental variability
Spatiotemporal environmental variability
A
B
Correlation
Time step
Lag distance (number of sites)
C
D
Coefficient of synchrony
Lag distance (km)
M. californianus(data)
M. californianus(model)
Environment

Figure 2

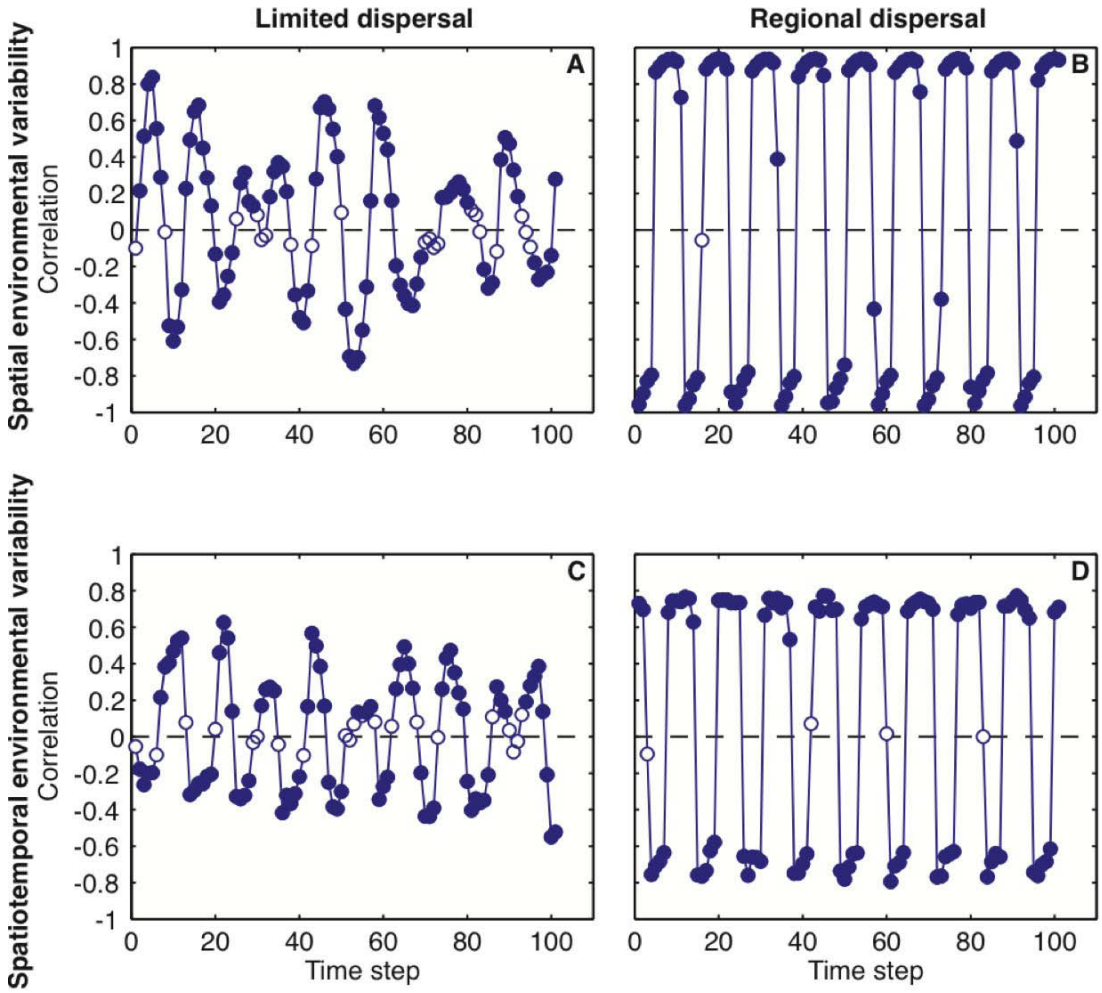
Limited dispersal
Regional dispersal
Spatial environmental variability
Spatiotemporal environmental variability
Correlation
A
B
C
D
1
0.8
0.6
0.4
0.2
0
-0.2
-0.4
-0.6
-0.8
-1
0
20
40
60
80
100
Time step

Figure 3

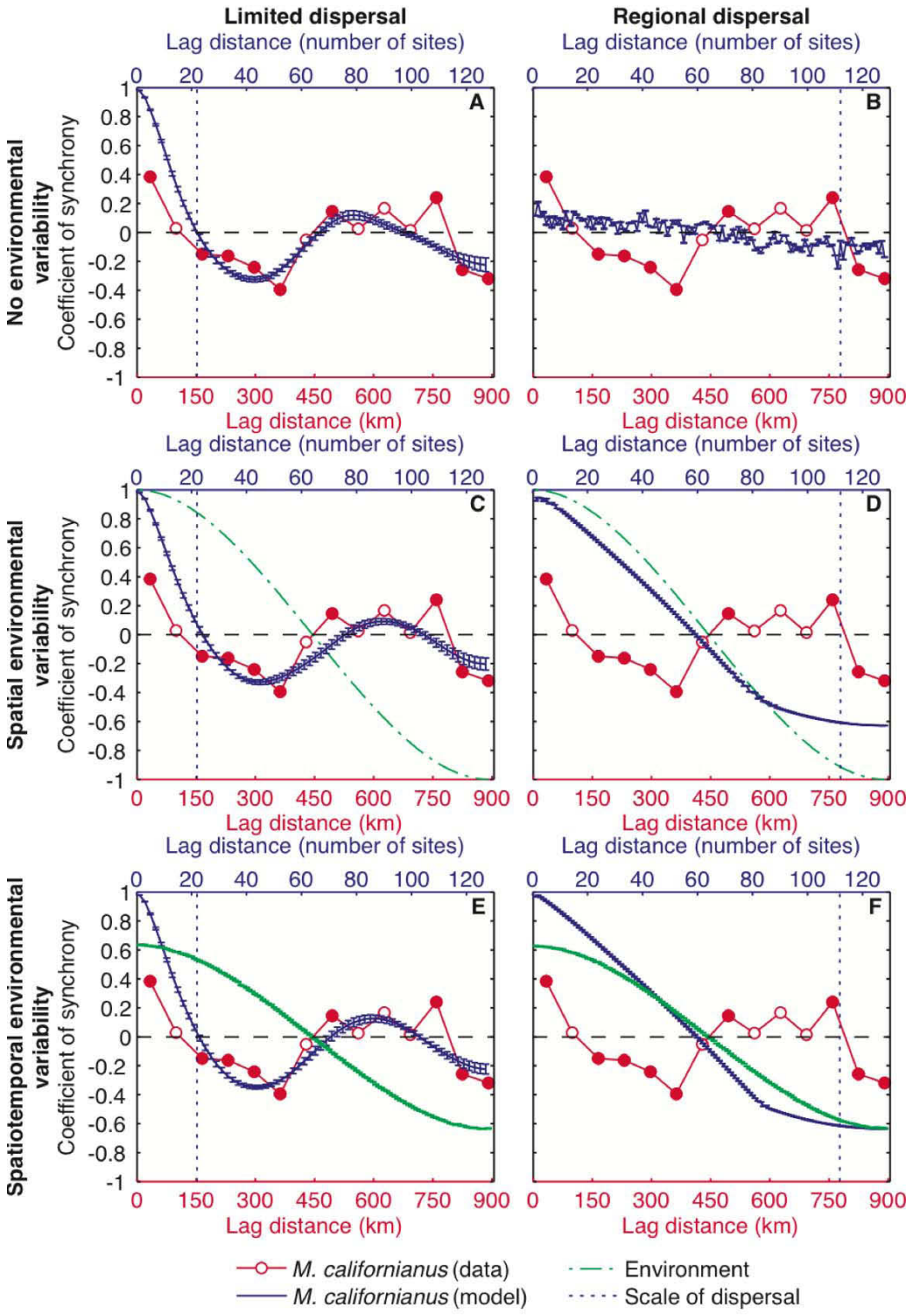
Limited dispersal
Regional dispersal
Lag distance (number of sites)
Lag distance (km)
Coefficient of synchrony
No environmental variability
Spatial environmental variability
Spatiotemporal environmental variability
A
B
C
D
E
F
M. californianus (data)
M. californianus (model)
Environment
Scale of dispersal

Figure 4

SUPPORTING INFORMATION

Data validation

We used remote sensing data to quantify sea surface temperature (SST), chlorophyll a concentration (chl-a) and upwelling currents (upwelling index) instead of *in situ* measurements because the former had greater temporal and spatial coverage. Additionally, the broad spatial extent of remote sensing data can often better reflect the spatially-integrated environmental conditions experienced by intertidal populations (1). Both the SST and chl-a data had a nominal resolution of 4 km, whereas the upwelling index had a coarser resolution of 1 degree (~111 km). Since remote sensing data are prone to errors due to cloud cover and aerosols that can influence captured irradiances, we excluded low quality data points characterized by high cloud/aerosol cover from the analysis (2). Additionally, outliers were removed from the remote sensing data series by computing the filtered mean (2) of each variable for each site:

$$\frac{\sum_{i=1}^{p}\left[\left(\overline{X}-1.5\sigma_X\right)\le X\le\left(\overline{X}+1.5\sigma_X\right)\right]}{N} \qquad (1)$$

where p represents the total number of points within 0.2 degrees (1 degree for upwelling) of the site, N is the total number of points within 1.5 standard deviations of the mean $\overline{X}$. These filtered environmental data series were then validated by using reduced major axis regression (2) to relate them to *in situ* buoy measurements (chl-a: R^2=0.42, p-value=0, n=583; SST: R^2=0.60, p-value=0, n=536).

Quantifying the relationship between *M. californianus* and the environment

In many marine species, individuals begin their lives as water-borne planktonic larvae and eventually settle onto the intertidal to become sessile adults. This bipartite lifecycle has important implications for identifying the relative influence of pre- and post-settlement processes on population dynamics and community structure. Nearshore current patterns such as coastal upwelling, which describes the offshore transport of the warm top water layer and the consequent rise of cold and nutrient-rich water to the surface, has been identified as a potentially critical process controlling recruitment in intertidal communities located along the coasts of New Zealand (3), Chile (4) and the West coast of the United States (5). Along the West coast of the United States, the pronounced spatial gradient in coastal upwelling has been linked to patterns of recruitment (5-7). Indeed, offshore transport due to coastal upwelling is weaker and less persistent north of Cape Blanco (43 °N) than it is south of Cape Blanco (5, 6). This major spatial discontinuity in coastal upwelling conditions has lead to the hypothesis that environmental conditions affecting pre-settlement processes are more likely to play an important role in adult intertidal communities south of Cape Blanco, where recruitment is environmentally-limited, than they are North of Cape Blanco, where recruitment is not environmentally-limited (5-7).

We tested this hypothesis by examining the relationship between the mean annual cover of *M. californianus* and 1-year lagged, multi-year averaged environmental conditions in each region. We chose a 1-year lag because it corresponds to the

temporal scale at which the correlation between the cover of *M. californianus* and each environmental variable is statistically significant (Fig S1). In both regions, the spatial correlation between the environment and the cover of *M. californianus* varies in time, regardless of whether the environmental conditions are averaged over two or three years (Fig S2). The spatial correlation between the growth of the mean annual *M. californianus* cover and the environment is equally variable in time for both regions. This indicates that the relationship between *M. californianus* cover and the environment is inconsistent in both regions. However, this inconsistency could be the product of the coarse division of the study system into a non-environmentally limited northern region and an environmentally-limited southern region. To test this hypothesis, we further examined this relationship by relating the 1-year lagged mean annual environmental time series to the mean annual *M. californianus* cover time series at each of the 48 sites (Fig S3). Although all environmental variables show a persistent spatial structure (Fig S3A,C,E), the sign and strength of the local correlation between the environmental time series and the *M. californianus* time series is highly variable in space (Fig S3B,D,F). Once averaged spatially, these variable local correlations lead to weak and inconsistent spatial correlations at the regional scale (Fig S2). Overall, these results indicate that the persistent latitudinal gradient seen in all environmental variables is not reflected in the cover of *M. californianus*.

Identifying the necessary conditions for the occurrence of cross-scale interactions between local fluctuations and limited dispersal

Cross-scale interactions in a predator-prey metapopulation

We have shown that local fluctuations and limited dispersal interact across spatial scales ranging from that of local ecological processes to the scale characterizing the regional distribution of abundance. Such cross-scale interactions lead to nonlinear patterns of spatial synchrony that are robust to both spatial and spatiotemporal environmental variability affecting either growth or fecundity in the discrete time successional model (Fig 4). Now, we examine the generality of this phenomenon in metapopulation models by adopting a spatially-explicit version (8, 9) of the continuous time Rosenzweig-MacArthur predator-prey model (10):

$$\frac{\mathrm{d}M_x}{\mathrm{d}t} = r_x M_x\left(1-\frac{M_x}{K}\right) - \frac{aM_xP_x}{b+aM_x} - cM_x + \frac{c}{n}\sum_{i\neq x}^{n} M_i$$
$$\frac{\mathrm{d}P_x}{\mathrm{d}t} = \frac{aM_xP_x}{b+aM_x} - P_x(m+c) + \frac{c}{n}\sum_{i\neq x}^{n} P_i \qquad (2)$$

where the prey (mussels M_x) at site x has growth rate $r_x = 0.5$, carrying capacity $K = 30$ and the predator (P_x) at site x has mortality rate $m = 0.1$, encounter rate $a = 0.2$ and half saturation constant $b = 1$. Both the predator and the prey migrate to their n nearest-neighbors with a migration rate of $c = 0.1$. We used these parameter values to illustrate the spatial dynamics of Eq. 2 and detail the generality of our results in the next sections. We assume symmetrical dispersal, equal dispersal scales for the predator and the prey, and periodic boundary conditions. All

simulations were run for 100 sites and the results were analyzed over 2000 post-transient time steps using the model selection methods described in the Model analysis section of the main text. We adopted the same spatial and spatiotemporal treatments used in the successional model. Specifically, the spatial environmental treatment consisted of varying the mussel growth rate r linearly from 0.2 to 0.8 over the entire spatial range $\left(\bar{r}=0.5\right)$. We generated the spatiotemporal environmental treatment by adding normally-distributed white noise with zero mean and variance $\sigma^2=0.2$ to the previously described spatial variation in the mussel growth rate $\left(\bar{r}=0.5\right)$. The spatial and spatiotemporal environmental treatments thus preserved the same mean mussel growth rate as the predator-prey model undergoing no environmental variability. As with the successional model, we vary dispersal and the environment to determine their relative influence on spatial synchrony patterns of mussel abundance in natural and model metapopulations.

We show that in the predator-prey model, limited dispersal is critical to the occurrence of nonlinear spatial synchrony patterns of mussel abundance that are compatible with those observed in natural populations along the West coast of the United States (Fig S4). In the absence of any environmental variability, nonlinear spatial synchrony patterns arise because of the cross-scale interaction between local mussel population fluctuations and limited dispersal (Fig S4A). These patterns are robust to both spatial (Fig S4C) and spatiotemporal (Fig S4E) environmental variability. Regional dispersal, however, prevents the occurrence of cross-scale interactions and leads to regional synchrony in the absence of environmental

variability (Fig S4B). Regional dispersal also facilitates environmental forcing in response to either spatial (Fig S4D) or spatiotemporal (Fig S4F) variability.

Hence, even though the successional model and the predator-prey model have fundamental differences in terms of their ecological structures (populations vs. communities), mathematical properties (continuous vs. discrete), dispersal mechanisms (nearest neighbor vs. dispersal kernel), connectivity rates (10% dispersal rate vs. 100% dispersal rate), perturbation types (biotic vs. abiotic) and spatial extents (256 sites vs. 100 sites), they both predict the occurrence of nonlinear spatial synchrony patterns in response to the cross-scale interaction between local fluctuations and limited dispersal.

Relation between dispersal and cross-scale interactions

We have shown that the cross-scale interaction between limited dispersal and local fluctuations yields nonlinear spatial synchrony patterns, whereas regional dispersal and environmental forcing lead to linear spatial synchrony patterns (Fig 4,S4). Hence, the linearity of spatial synchrony patterns can be used to ascertain the relative importance of cross-scale interactions and environmental forcing in natural populations. However, since the nonlinear spatial synchrony patterns are also non-stationary (Fig S7,S8), one must not rely on the specific characteristics of any single spatial synchrony pattern, but rather identify the nonlinear properties that describe a family of spatial synchrony patterns. Here, we use model selection (see Data analysis) to determine the relative importance of cross-scale interactions and environmental forcing by detecting nonlinearities in the spatial synchrony patterns of metapopulation models for a range of dispersal scales.

Our results show that in the successional and predator-prey models, nonlinear spatial synchrony patterns occur over the same limited range of dispersal scales (Fig S5A,C,E). Indeed, regardless of environmental variability, the nonlinear model is selected when the scale of dispersal is less than 10-15% of the spatial domain and systematically rejected when dispersal occurs over more than 10-15% of the spatial domain (Fig S5A,C,E). Hence, model selection methods based on linearity can be used to determine whether spatial synchrony patterns are the product of (i) the cross-scale interaction between limited dispersal and local intrinsic fluctuations or (ii) regional dispersal and environmental forcing.

Relation between local fluctuations and cross-scale interactions

We have shown that cross-scale interactions between local fluctuations and limited dispersal can occur in both the successional and the predator-prey model. Their occurrence is dependent upon the scale of dispersal, which must be limited to 3-10% of the spatial domain (Fig. S5A,C,E). Additionally, cross-scale interactions depend upon the existence of strong local fluctuations. We now demonstrate this dependence by analyzing the dynamics of the predator-prey model. Under spatially-homogeneous conditions (i.e. zero net migration and identical environmental conditions across all sites), the predator-prey metapopulation model can be analyzed as a series of uncoupled predator-prey populations. The stability of each predator-prey population can be ascertained by deriving the zero net growth isoclines (ZNGI) of the predator (M^*) and the prey (P^*):

$$P^* = \frac{r}{aK}\left[bK + M(aK - b) - aM^2\right]$$
$$M^* = \frac{mb}{a(1-m)} \qquad (3.1, 3.2)$$

The equilibrium dynamics of this predator-prey system depends on the modal shape of the prey ZNGI and where the prey and predator ZNGIs intersect. When the predator and prey ZNGIs intersect in the ascending section of the prey ZNGI $\left(\frac{\mathrm{d}P^*}{\mathrm{d}M} > 0\right)$, the equilibrium is unstable and the system undergoes stable limit cycles. When the ZNGIs intersect in the descending section of the prey ZNGI $\left(\frac{\mathrm{d}P^*}{\mathrm{d}M} < 0\right)$, the equilibrium is stable (11). We now identify the conditions under which the system transitions from stable equilibrium dynamics to stable limit cycles (i.e. the Hopf bifurcation point) by differentiating equation 3.1 and solving $\left.\frac{\mathrm{d}P^*}{\mathrm{d}M}\right|_{M=M^*} = 0$:

$$\left.\frac{\mathrm{d}P^*}{\mathrm{d}M}\right|_{M=M^*} = \frac{r}{aK}\left[(aK-b)-2a\left(\frac{mb}{a(1-m)}\right)\right] = 0 \qquad (4)$$

The sign of the derivative and the stability of the system depend upon the bracketed term in equation 4. After some algebra, it is possible to transform the bracketed term and show that the stability of the system is linked to the critical parameter K_{critical}:

$$K_{\text{critical}} = \frac{b(m+1)}{a(1-m)} \qquad (5)$$

The dynamics of the system thus directly depend on the carrying capacity *K*: when $K > K_{\text{critical}}$, the system undergoes stable limit cycles whereas when $K < K_{\text{critical}}$, the system reaches a stable equilibrium. For our particular model parameterization (b=1, a=0.2, m=0.2), $K_{\text{critical}} = 7.5$. By varying *K* across the $K_{\text{critical}} = 7.5$ threshold,

we show that cross-scale interactions, as manifested by the occurrence of compatible nonlinear spatial synchrony patterns, are directly linked to the system's transition from stable equilibrium dynamics to stable limit cycles (Fig S6).

Our results are thus robust to the specifics of our models: cross-scale interactions merely require that local populations undergo sustained fluctuations (Fig S6) and that dispersal occur over 3-10% of the spatial domain (Fig S5A,C,E).

Robustness of nonlinear spatial synchrony patterns to window size

All spatial synchrony analyses of the model data were performed over 10-time step windows in order to approximate the temporal extent of our survey data. However, our results are robust to window size. Indeed, regional dispersal never leads to nonlinear spatial synchrony patterns in either the successional or the predator-prey model, regardless of environmental variability or window size (Fig S5A,C,E). However, when dispersal is limited, the predator-prey and successional models generate nonlinear spatial synchrony patterns for a range of window sizes (Fig S5B,D,F). Hence, regardless of window size, nonlinear spatial synchrony patterns remain a signature of metapopulations experiencing limited dispersal. The robustness of spatial synchrony to window size means that the occurrence of cross-scale interactions can be detected in natural systems for which data availability is limited to short temporal scales that do not integrate many cycles of abundance fluctuations.

Dispersal mediates pattern formation in dynamical metapopulations

Dispersal is a key process that has important consequences for the regional distribution of abundance. In marine systems, dispersal has been shown to directly mediate the correlation between predator abundance and prey recruitment. Indeed, predator abundance and prey recruitment of non-dispersing predator and prey species pairs were strongly correlated, whereas no relationship existed between predator abundance and prey recruitment for dispersing predator and prey species pairs (12). Dispersal can also affect the regional distribution of abundance indirectly by interacting with local processes to modulate spatial heterogeneity and pattern formation (13-15). Here, we compare the qualitative patterns observed in the successional model time series to the quantitative spatial synchrony patterns presented in the main text in order to further clarify the role of dispersal.

When dispersal is limited and there is no environmental variability, the metapopulation mussel cover exhibits non-stationary (i.e. transient) spatial patterns (Fig S7 A) that lead to nonlinear spatial synchrony patterns characterized by different spatial scales (Fig S7B,C,D). Importantly, even though these patterns are non-stationary, the spatial range of synchrony (i.e. the lag distance at which synchrony first reaches zero) remains constant and equal to the average scale of dispersal (Fig S7B,C,D). The addition of spatiotemporal (Fig S8) environmental variability leads to the formation of spatial waves of high mussel abundance at sites with high fecundity (i.e. central sites) that slowly propagate throughout the metapopulation. However, these environmentally-mediated spatial waves do not affect the non-stationary and

nonlinear spatial synchrony patterns generated by local fluctuations and limited dispersal (Fig S8B,C,D).

Metapopulations characterized by regional dispersal and no environmental variability undergo synchronized regional fluctuations (Fig S9A) that lead to stationary and uniform patterns of spatial synchrony (Fig S9B,C,D). It is important to note that even though these metapopulations undergo strongly synchronized regional fluctuations (Fig S9A), spatial synchrony analysis shows very low levels of synchrony across the entire spatial range (Fig S9B,C,D). This is because the mussel abundance time series was detrended by removing the mean regional time series before performing spatial synchrony analysis. Hence, our spatial synchrony analysis focuses on the spatial trends of synchrony instead of the absolute strength of synchrony. The addition of spatiotemporal environmental variability (Fig S10) leads to the formation of fronts that originate from highly fecund central sites. These fronts propagate extremely rapidly across the entire metapopulation and lead to stationary and linear spatial synchrony patterns (Fig S10B,C,D).

These results thus show how dispersal modulates pattern formation in metapopulations. Furthermore, they show that spatial synchrony can be used to quantify complex spatiotemporal patterns and link them to their underlying mechanisms.

LITERATURE CITED

1. Bustamante RH & Branch GM (1996) Large scale patterns and trophic structure of Southern African rocky shores: the roles of geographic variation and wave exposure. *Journal of Biogeography* 23(3):339-351.
2. Bailey SW & Werdell PJ (2006) A multi-sensor approach for the on-orbit validation of ocean color satellite data products. *Remote Sensing of Environment* 102(1-2):12-23.

3. Menge BA, *et al.* (2003) Coastal oceanography sets the pace of rocky intertidal community dynamics. *Proceedings of the National Academy of Sciences of the United States of America* 100(21):12229-12234.
4. Navarrete SA, Wieters EA, Broitman BR, & Castilla JC (2005) Scales of benthic-pelagic coupling and the intensity of species interactions: From recruitment limitation to top-down control. *Proceedings of the National Academy of Sciences of the United States of America* 102(50):18046-18051.
5. Connolly SR & Roughgarden J (1998) A latitudinal gradient in northeast Pacific intertidal community structure: Evidence for an oceanographically based synthesis of marine community theory. *American Naturalist* 151(4):311-326.
6. Connolly SR, Menge BA, & Roughgarden J (2001) A latitudinal gradient in recruitment of intertidal invertebrates in the northeast Pacific Ocean. *Ecology* 82(7):1799-1813.
7. Connolly SR & Roughgarden J (1999) Theory of marine communities: Competition, predation, and recruitment-dependent interaction strength. *Ecological Monographs* 69(3):277-296.
8. Holland MD & Hastings A (2008) Strong effect of dispersal network structure on ecological dynamics. *Nature* 456(7223):792-794.
9. Jansen V & de Roos A (2000) The role of space in reducing predator-prey cycles. *The geometry of ecological interactions: simplifying spatial complexity*, eds Dieckmann U, Law R, & Metz JAJ (Cambridge University Press, Cambridge, U.K.), pp 183–201.
10. Rosenzweig ML & MacArthur RH (1963) Graphical Representation and Stability Conditions of Predator-Prey Interactions. *American Naturalist* 97(895):209-223.
11. May RM (1973) *Stability and Complexity in Model Ecosystems* (Princeton University Press, Princeton).
12. Wieters EA, Gaines SD, Navarrete SA, Blanchette CA, & Menge BA (2008) Scales of Dispersal and the Biogeography of Marine Predator-Prey Interactions. *The American Naturalist* 171(3):405-417.
13. Guichard F (2005) Interaction strength and extinction risk in a metacommunity. *Proceedings of the Royal Society of London B* 272:1571-1576.
14. Gouhier TC & Guichard F (2007) Local disturbance cycles and the maintenance of spatial heterogeneity across scales in marine metapopulations. *Ecology* 88(3):647-657.
15. Earn DJD, Levin SA, & Rohani P (2000) Coherence and Conservation. *Science* 290(5495):1360-1364.

FIGURE LEGENDS

Figure S1: Temporal structure of the correlation between the annual cover of *M. californianus* and the environment for all 48 sites. Spatial correlation (red circles) between the annual cover of *M. californianus* and mean annual (blue curves) (A) SST,

(B) chl-a, and (C) upwelling index across all sites as a function of lag time (number of years). The vertical dashed line indicates the 1-year lag used to correlate the cover of *M. californianus* in year *i* to the environmental conditions in year *i-1*. Full circles indicate statistical significance (α=0.05).

Figure S2: Time series of the correlation between the annual *M. californianus* cover and the multi-year average environment at 48 sites located along the West coast of the United States. The correlation between mean annual *M. californianus* cover and each 1-year lagged, (A, C, E) 2-year averaged or (B, D, F) 3-year averaged environmental variable for (A, B) all 48 sites, (C, D) sites located North of Cape Blanco (43°N) and (E, F) sites located South of Cape Blanco. The 1-year lagged, multi-year averaged environmental variables are SST (dark blue squares), (ii) chl-a (green diamonds), (iii) upwelling index (light blue triangles) and (iv) the first axis of the principal component analysis of all three environmental variables (red circles). Full circles indicate statistical significance (α=0.05).

Figure S3: The spatial structure of both the environment and the correlation between the environment and the annual *M. californianus* cover time series at 48 sites located along the West coast of the United States. (A, C, E) The spatial structure of the mean annual (A) chl-a, (C) SST and (E) upwelling index from 1999 to 2002 (dark blue circles: 1999, red squares: 2000, light blue triangles: 2001, black diamonds: 2002). The vertical dashed line depicts an upwelling index of zero. (B, D, F) The spatial structure of the correlation between the mean annual *M. californianus* cover time series and the 1-year lagged mean annual time series of (B) chl-a, (D) SST and (F) upwelling index. Blue circles indicate negative correlations and red circles indicate

positive correlations. The size of each circle is proportional to the absolute value of the correlation, with the largest circle representing a correlation of 0.95.

Figure S4: Spatial synchrony of annual mussel cover in the predator-prey model for metapopulations undergoing different environmental and dispersal treatments. (A, B) No environmental variability and either (A) limited or (B) regional dispersal. (C, D) Spatial environmental variability and either (C) limited or (D) regional dispersal. (E, F) Spatiotemporal environmental variability and either (E) limited or (F) regional dispersal. Spatial synchrony in the predator-prey model annual mussel cover is represented in blue solid curves (mean±S.E.) while that of the 1-year lagged environment is represented in green dashed curves (mean±S.E.). The spatial synchrony of the annual *M. californianus* cover from the West coast of the United States is also depicted to facilitate comparisons (red circles). The scale of dispersal is represented by the vertical dotted line. The spatial extent of the limited dispersal treatment corresponds to 6% of the domain while that of the regional dispersal treatment corresponds to 80% of the domain. Full circles indicate statistical significance (α=0.05).

Figure S5: Using model selection to detect nonlinear spatial synchrony patterns in the mussel cover time series of metapopulation models. (A, C, E) The percentage of nonlinear models selected as a function of the scale of dispersal for successional (blue) and predator-prey (red) metapopulations undergoing (A) no environmental variability, (C) spatial environmental variability or (E) spatiotemporal environmental variability. (B, D, F) The percentage of nonlinear models selected as a function of the size of the time window for successional (blue solid curve) and predator-prey (red dashed curve) metapopulations undergoing limited dispersal and (B) no

environmental variability, (D) spatial environmental variability or (F) spatiotemporal environmental variability.

Figure S6: The occurrence of nonlinear spatial synchrony patterns in the mussel cover time series of the predator-prey metapopulation model. The percentage of nonlinear spatial synchrony models selected in a predator-prey metapopulation undergoing limited dispersal (6% of the spatial domain) and no environmental variability (blue solid curve) and the minimum/maximum mussel abundance across the entire metapopulation (red circles) as a function of the critical parameter *K*. The transition from stable equilibrium dynamics to stable limit cycles occurs for $K > K_{critical} = 7.5$ and coincides with the selection of nonlinear spatial synchrony models.

Figure S7: The time series of the mussel cover from the successional model with sample spatial synchrony analyses for a metapopulation undergoing limited dispersal and no environmental variability. (A) The time series of the metapopulation mussel cover (color bar) and sample synchrony profiles (B, C, D) taken at three randomly-selected 10-time step windows indicated by the red outlines. (B, C, D) The blue solid curve indicates the spatial synchrony of the mussel cover and the blue vertical dotted line indicates the scale of dispersal.

Figure S8: The time series of the mussel cover from the successional model with sample spatial synchrony analyses for a metapopulation undergoing limited dispersal and spatiotemporal environmental variability. (A) The time series of the metapopulation mussel cover (color bar) and sample synchrony profiles (B, C, D) taken at three randomly-selected 10-time step windows indicated by the red outlines. (B, C, D) The blue solid curve indicates the spatial synchrony of the mussel cover,

the green dashed curve indicates the spatial synchrony of the environment and the blue vertical dotted line indicates the scale of dispersal.

Figure S9: The time series of the mussel cover from the successional model with sample spatial synchrony analyses for a metapopulation undergoing regional dispersal and no environmental variability. (A) The time series of the metapopulation mussel cover (color bar) and sample synchrony profiles (B, C, D) taken at three randomly-selected 10-time step windows indicated by the red outlines. (B, C, D) The blue solid curve indicates the spatial synchrony of the mussel cover and the blue vertical dotted line indicates the scale of dispersal.

Figure S10: The time series of the mussel cover from the successional model with sample spatial synchrony analyses for a metapopulation undergoing regional dispersal and spatiotemporal environmental variability. (A) The time series of the metapopulation mussel cover (color bar) and sample synchrony profiles (B, C, D) taken at three randomly-selected 10-time step windows indicated by the red outlines. (B, C, D) The blue solid curve indicates the spatial synchrony of the mussel cover, the green dashed curve indicates the spatial synchrony of the environment and the blue vertical dotted line indicates the scale of dispersal.

FIGURES

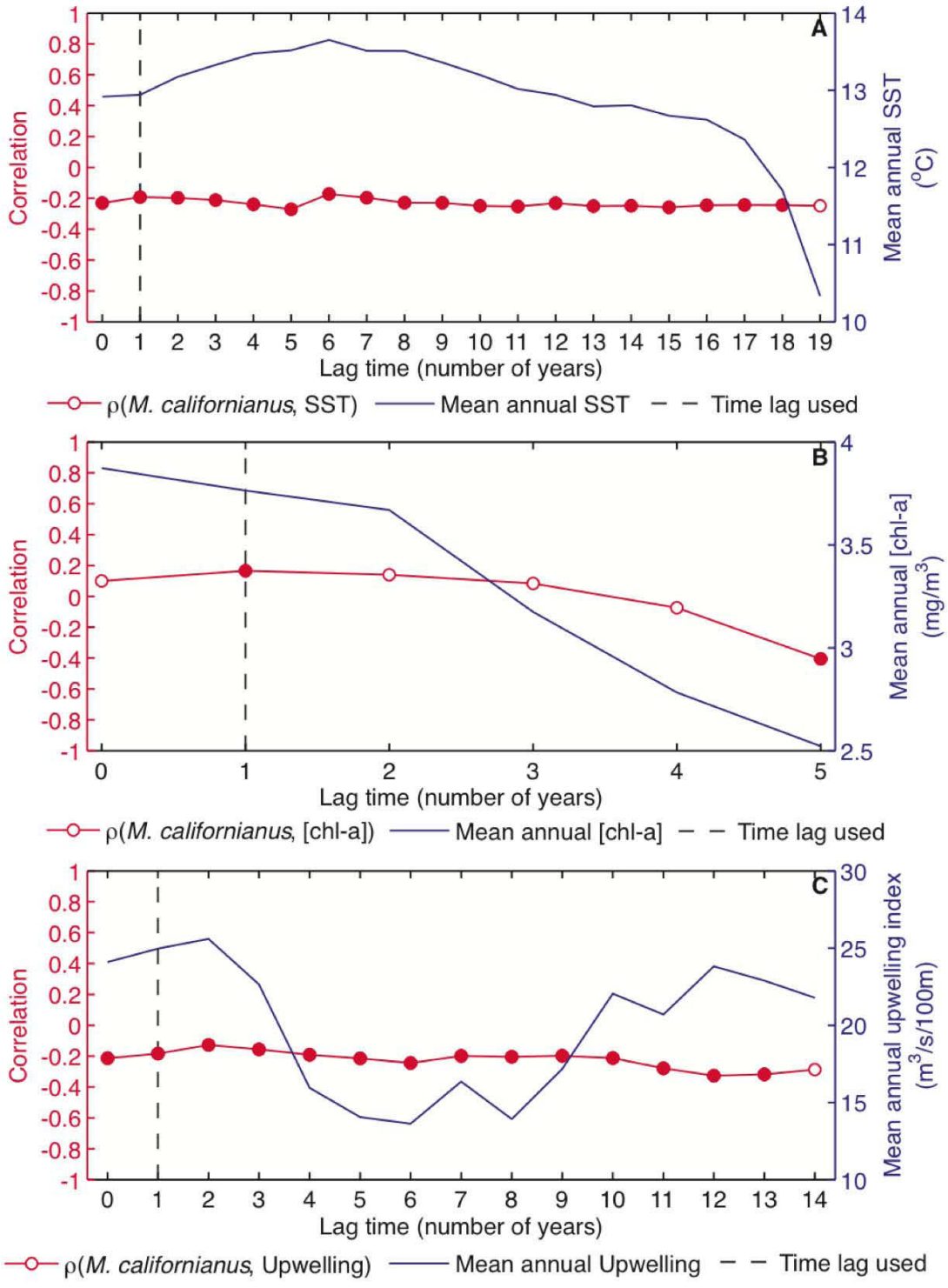

Figure S1

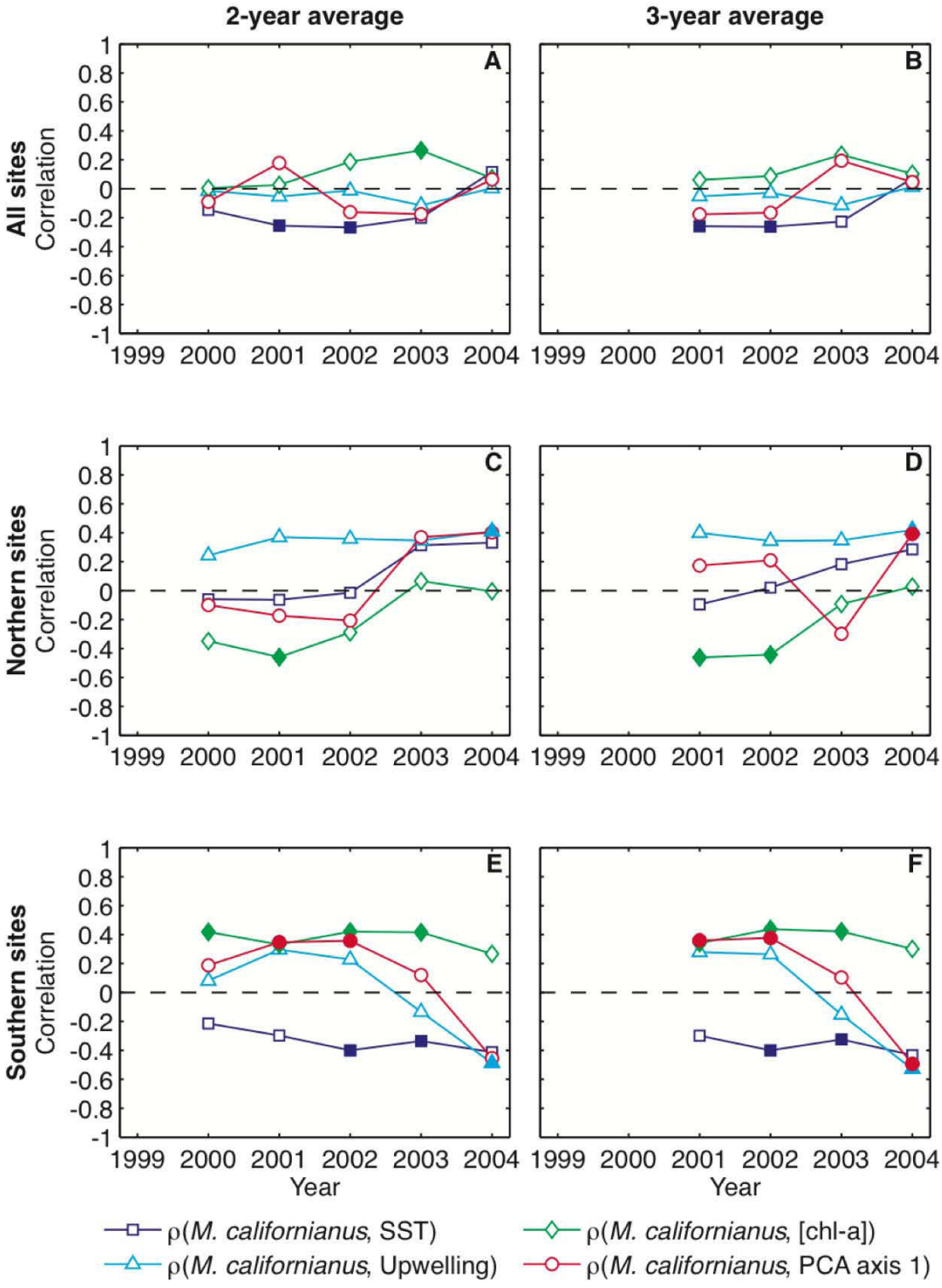
2-year average
3-year average
A
B
C
D
E
F
All sites
Northern sites
Southern sites
Correlation
1
0.8
0.6
0.4
0.2
0
-0.2
-0.4
-0.6
-0.8
-1
1999 2000 2001 2002 2003 2004
Year
ρ(M. californianus, SST)
ρ(M. californianus, [chl-a])
ρ(M. californianus, Upwelling)
ρ(M. californianus, PCA axis 1)

Figure S2

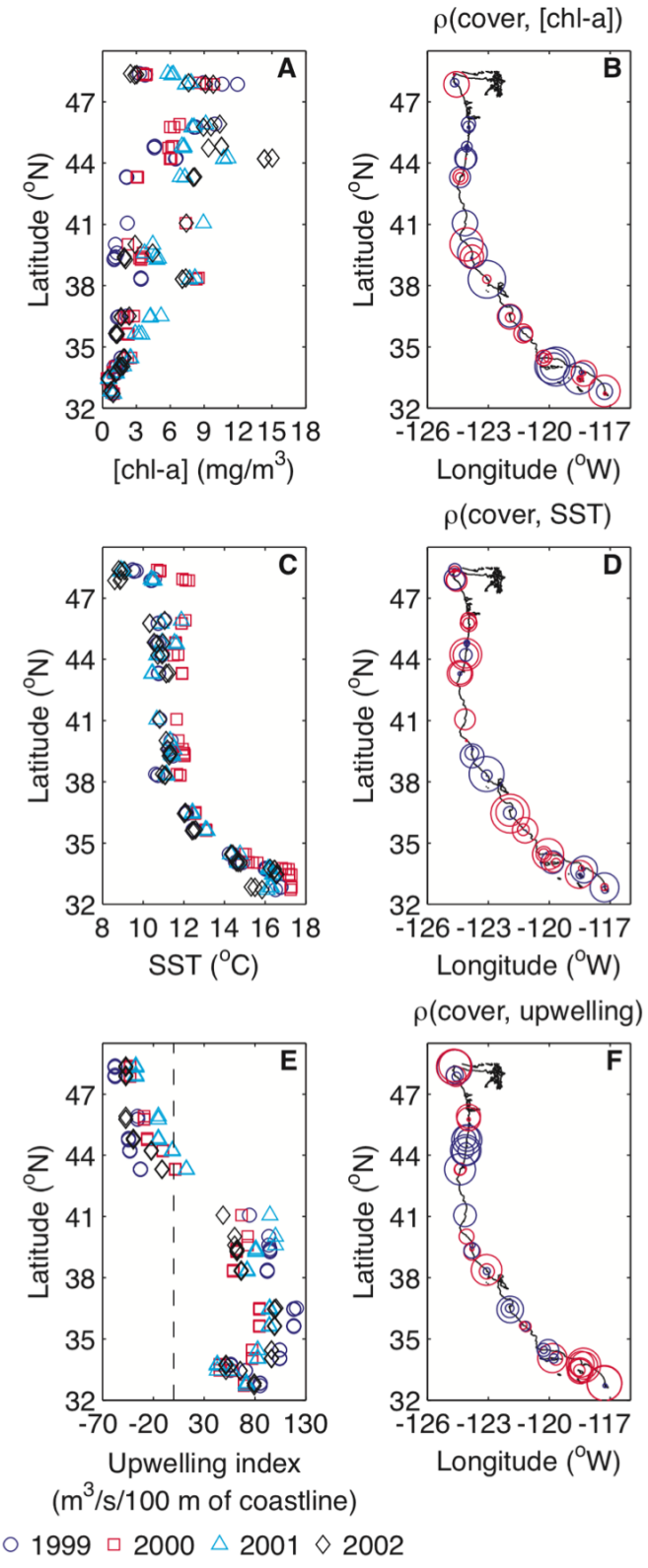
ρ(cover, [chl-a])
A
B
Latitude (°N)
47
44
41
38
35
32
0 3 6 9 12 15 18
[chl-a] (mg/m3)
-126 -123 -120 -117
Longitude (°W)
ρ(cover, SST)
C
D
8 10 12 14 16 18
SST (°C)
ρ(cover, upwelling)
E
F
-70 -20 30 80 130
Upwelling index
(m3/s/100 m of coastline)
1999 2000 2001 2002

Figure S3

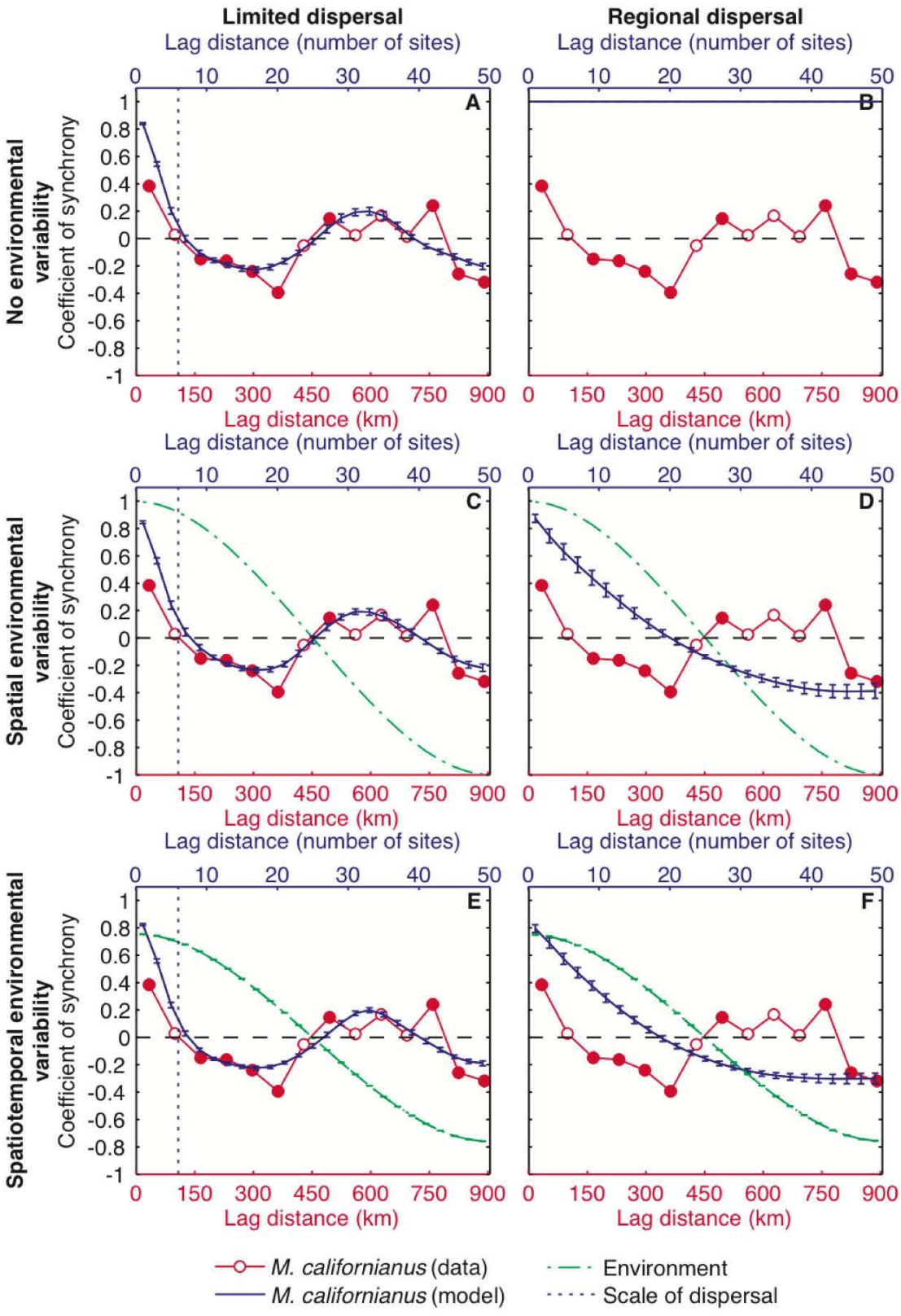
Limited dispersal
Regional dispersal
Lag distance (number of sites)
Lag distance (km)
Coefficient of synchrony
No environmental variability
Spatial environmental variability
Spatiotemporal environmental variability
A
B
C
D
E
F
M. californianus (data)
M. californianus (model)
Environment
Scale of dispersal

Figure S4

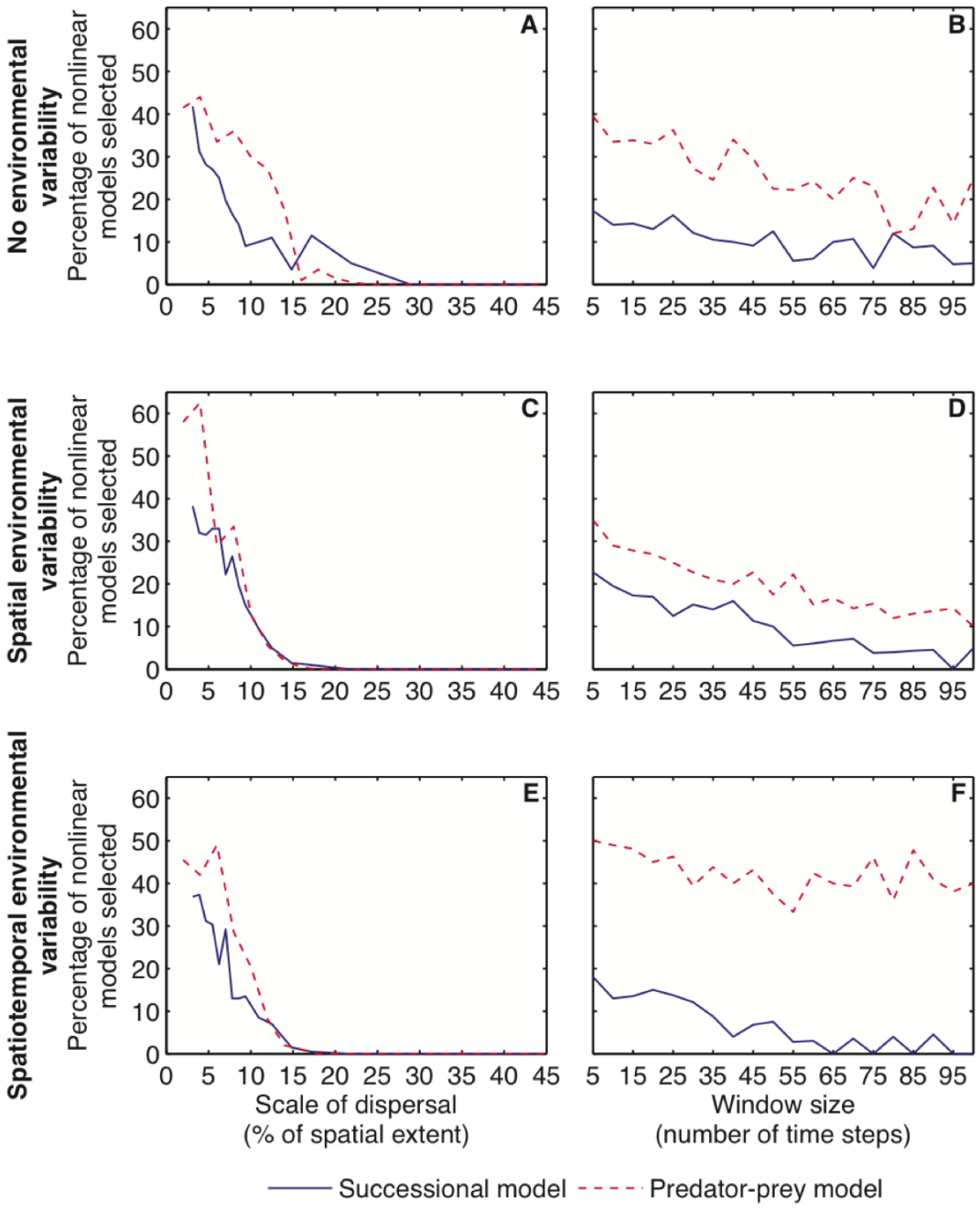
No environmental variability
Spatial environmental variability
Spatiotemporal environmental variability
Percentage of nonlinear models selected
A
B
C
D
E
F
0 5 10 15 20 25 30 35 40 45
5 15 25 35 45 55 65 75 85 95
Scale of dispersal (% of spatial extent)
Window size (number of time steps)
Successional model
Predator-prey model

Figure S5

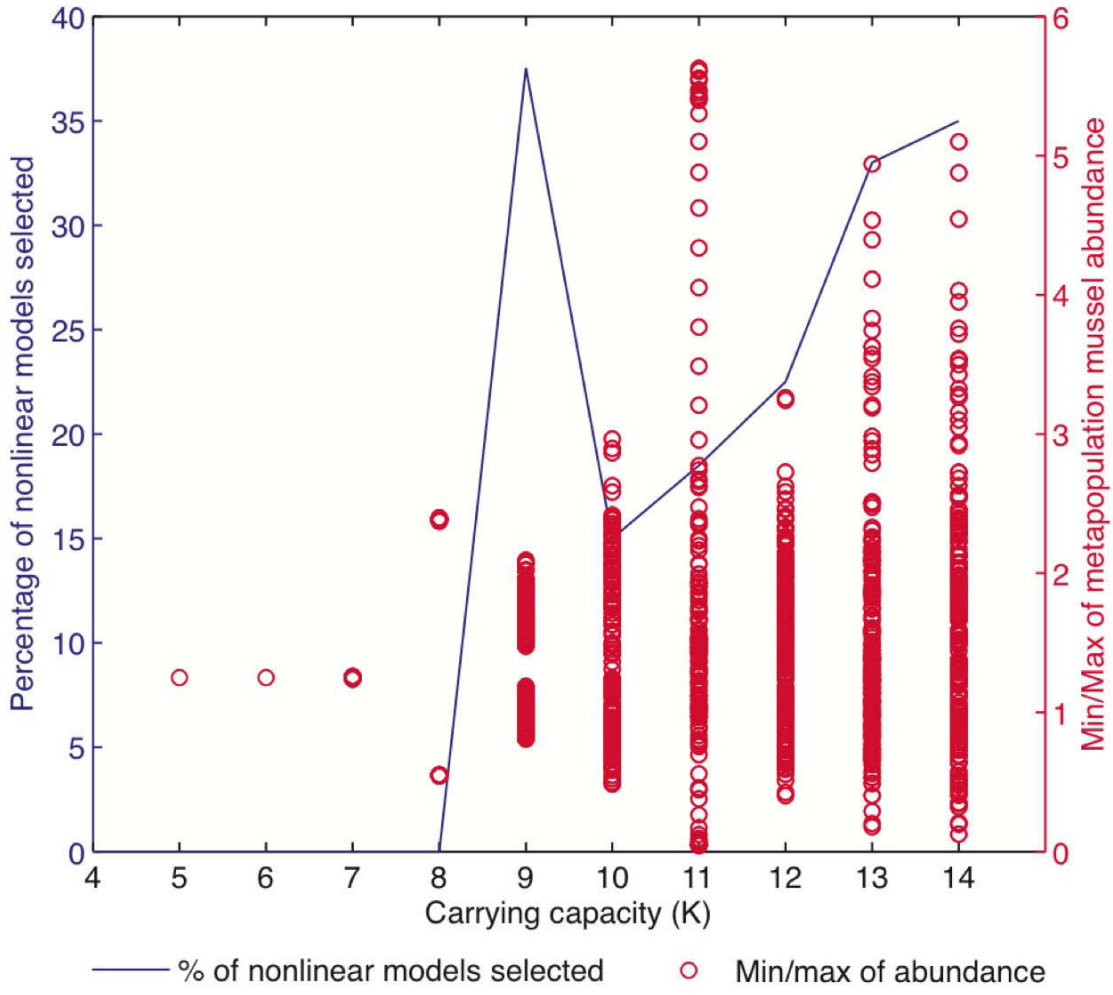
Percentage of nonlinear models selected
Min/Max of metapopulation mussel abundance
Carrying capacity (K)
% of nonlinear models selected
Min/max of abundance

Figure S6

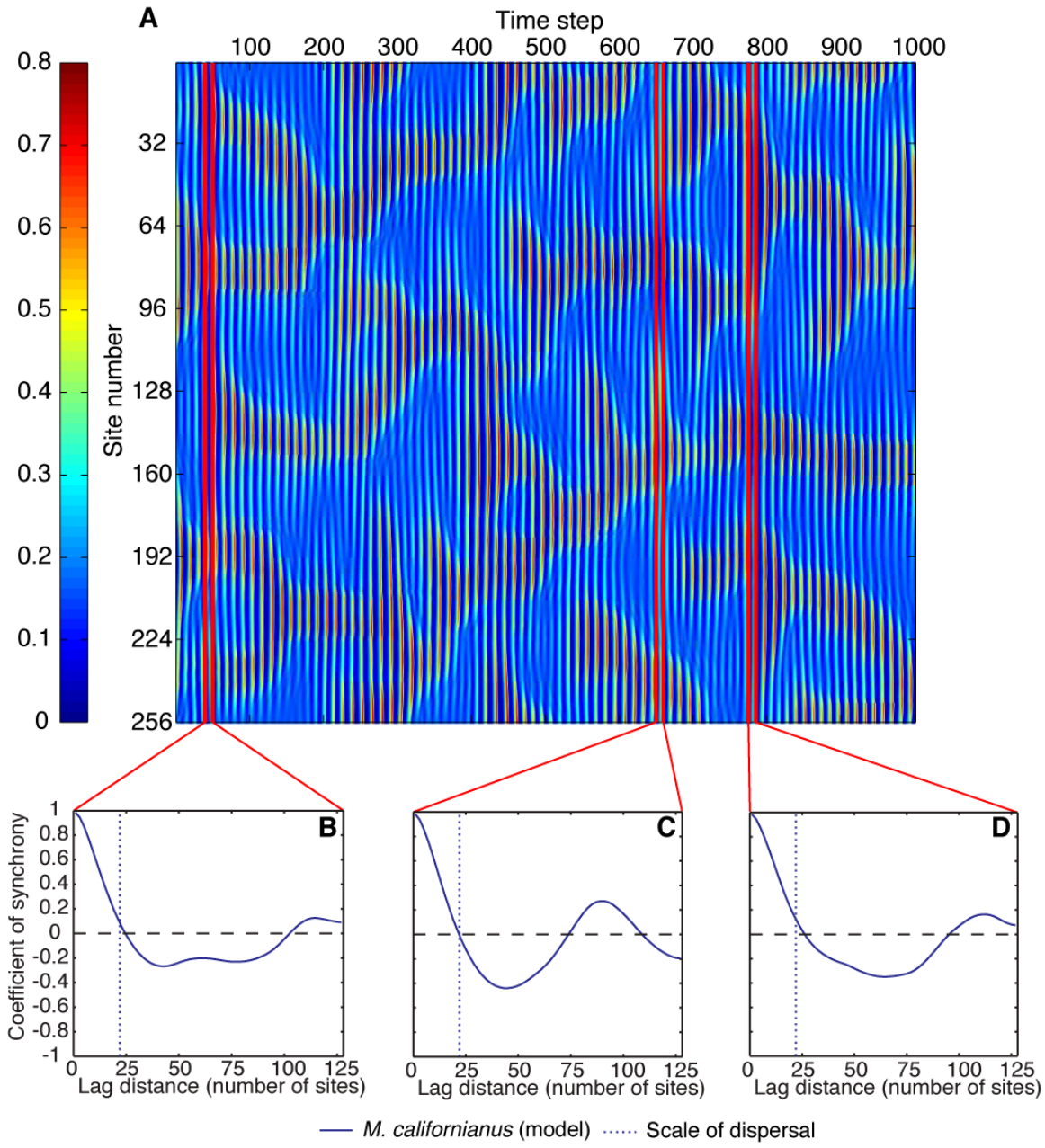
A
Time step
100 200 300 400 500 600 700 800 900 1000
Site number
32 64 96 128 160 192 224 256
0.8 0.7 0.6 0.5 0.4 0.3 0.2 0.1 0
B
C
D
Coefficient of synchrony
1 0.8 0.6 0.4 0.2 0 -0.2 -0.4 -0.6 -0.8 -1
0 25 50 75 100 125
Lag distance (number of sites)
M. californianus (model)
Scale of dispersal

Figure S7

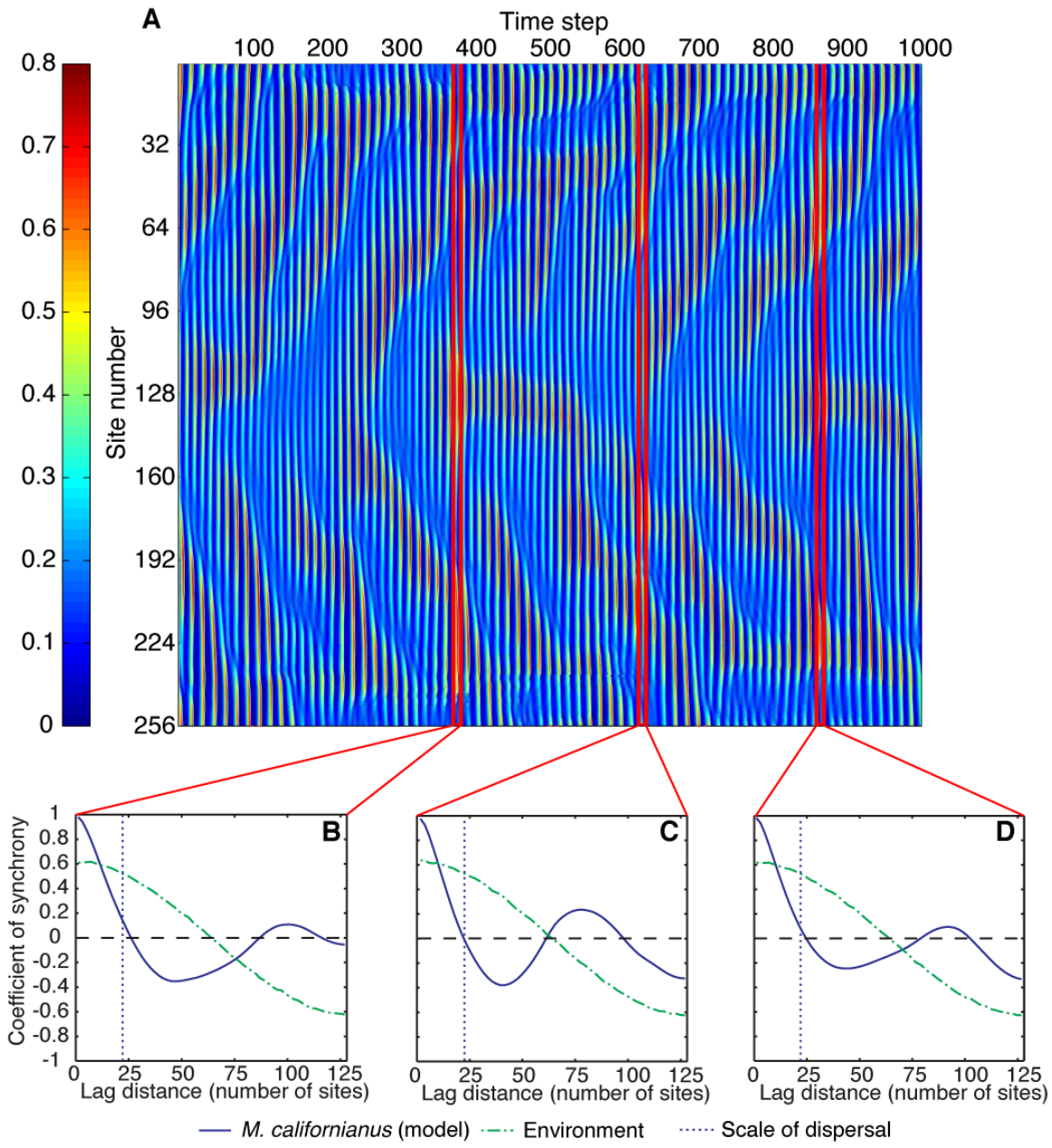
A
Time step
100 200 300 400 500 600 700 800 900 1000
Site number
32 64 96 128 160 192 224 256
0.8 0.7 0.6 0.5 0.4 0.3 0.2 0.1 0
B
C
D
Coefficient of synchrony
1 0.8 0.6 0.4 0.2 0 -0.2 -0.4 -0.6 -0.8 -1
0 25 50 75 100 125
Lag distance (number of sites)
M. californianus (model)
Environment
Scale of dispersal

Figure S8

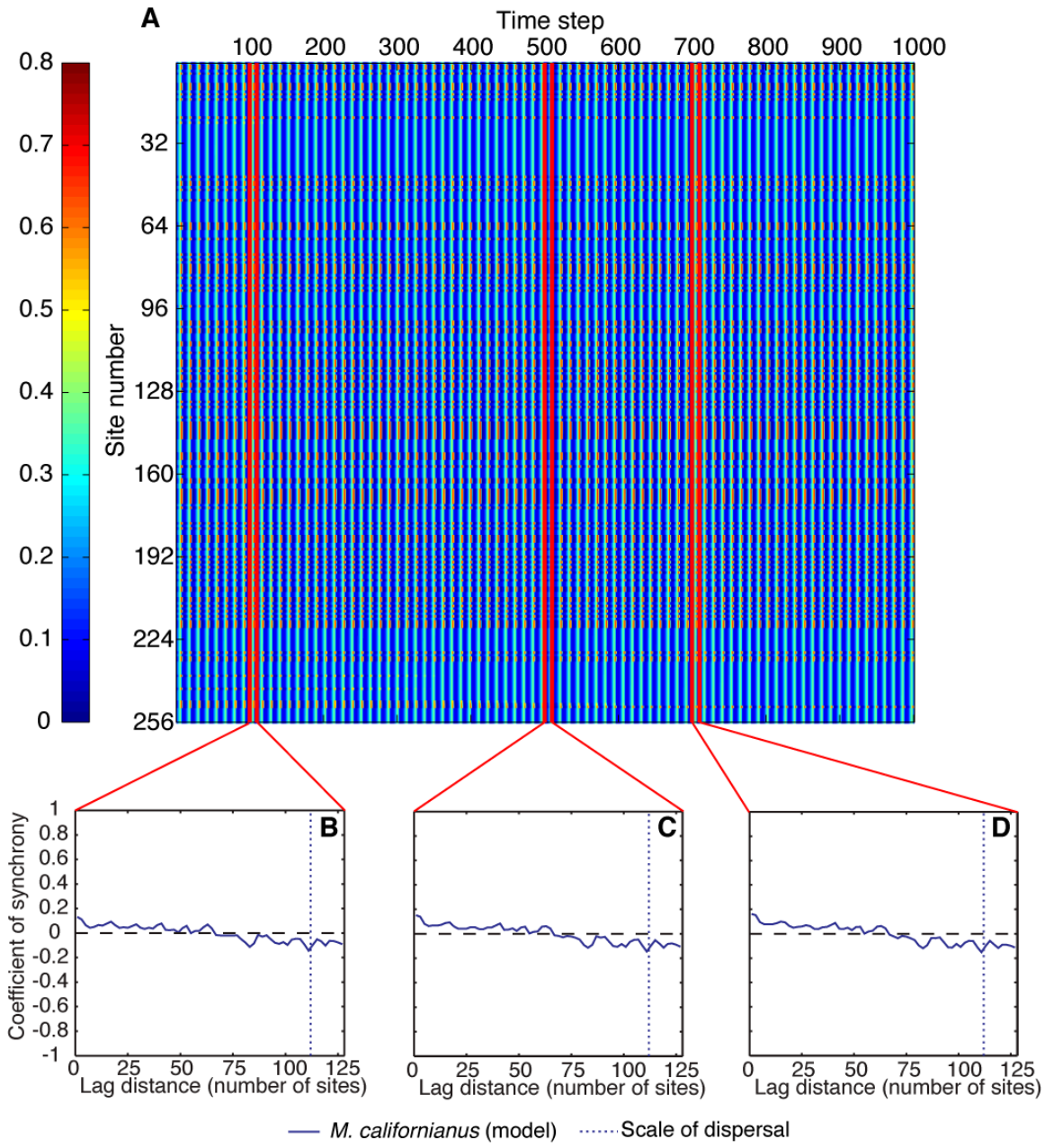
A
Time step
100 200 300 400 500 600 700 800 900 1000
Site number
32 64 96 128 160 192 224 256
0.8 0.7 0.6 0.5 0.4 0.3 0.2 0.1 0
B
C
D
Coefficient of synchrony
1 0.8 0.6 0.4 0.2 0 -0.2 -0.4 -0.6 -0.8 -1
0 25 50 75 100 125
Lag distance (number of sites)
M. californianus (model)
Scale of dispersal

Figure S9

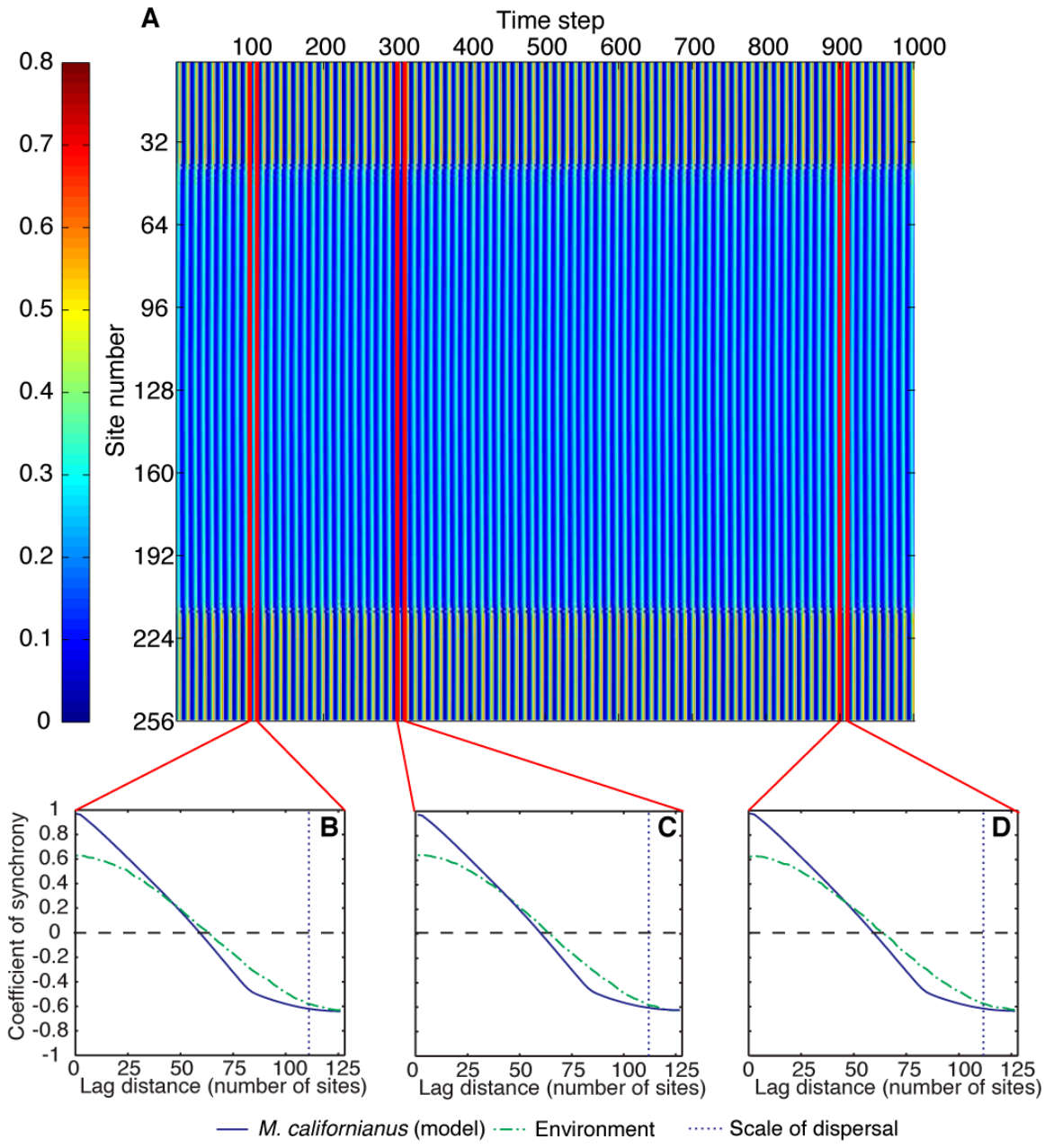
A
Time step
100 200 300 400 500 600 700 800 900 1000
0.8
0.7
0.6
0.5
0.4
0.3
0.2
0.1
0
Site number
32
64
96
128
160
192
224
256
B
C
D
Coefficient of synchrony
1
0.8
0.6
0.4
0.2
0
-0.2
-0.4
-0.6
-0.8
-1
0 25 50 75 100 125
Lag distance (number of sites)
M. californianus (model)
Environment
Scale of dispersal

Figure S10

CONNECTING STATEMENT

In the previous chapter, I developed and validated a theory of marine metapopulations that showed how local processes can interact with limited dispersal to control the regional distribution of population abundance in space and time. I now extend the theory to marine metacommunities and investigate the implications for understanding the relationship between oceanographic conditions, recruitment and adult cover in intertidal communities.

CHAPTER 2: THEORY OF DYNAMIC MARINE INTERTIDAL METACOMMUNITIES: LINKING OCEANOGRAPHY, RECRUITMENT AND ADULT ABUNDANCE

Tarik C. Gouhier [1,*], Frédéric Guichard [1] and Bruce A. Menge [2]

[*] Corresponding author: tarik.gouhier@gmail.com | Phone (514) 398-4120 | Fax: (514) 398-5069

[1] Department of Biology, McGill University, 1205 Avenue Docteur Penfield, Montreal, Quebec, H3A 1B1, Canada

[2] Department of Zoology, 3029 Cordley Hall, Oregon State University, Corvallis, OR 97331, USA

Keywords: metacommunity, dispersal, pre-settlement, post-settlement, recruitment

Status: In preparation

ABSTRACT

Patterns of (adult) population abundance and community structure reflect a combination of local and regional processes. In marine intertidal systems, early work emphasized the importance of local post-settlement processes (i.e. species interactions) whereas recent studies have focused on the role of regional pre-settlement processes (i.e. oceanographic conditions) controlling recruitment. Theory has attempted to reconcile these two perspectives by predicting that a persistent latitudinal gradient in oceanographic conditions produces a corresponding gradient in both recruitment and the strength of post-settlement processes. According to this theory, post-settlement processes corrode the relationship between oceanographic conditions and adult abundance at local scales and thus generate the observed mismatch between patterns of oceanographic conditions, recruitment and adult abundance. However, experiments have revealed no such latitudinal gradient in either the strength of post-settlement processes or their corrosive effect on the relationship between oceanographic conditions, recruitment and adult abundance.

Here, we develop and validate a theory of dynamic marine metacommunities that demonstrates that dispersal controls the relative influence of pre- and post-settlement processes on patterns of recruitment and adult abundance. In the absence of dispersal, regional pre-settlement processes generate matching spatiotemporal patterns of recruitment and adult abundance; post-settlement processes merely corrode the relationship between oceanographic conditions, recruitment and adult abundance at local scales. However, limited dispersal interacts with post-settlement processes and generates non-stationary spatiotemporal patterns of adult abundance at regional scales. This regionally constructive effect of post-settlement processes

causes an intermittent mismatch between the spatiotemporal patterns of recruitment and adult abundance, despite a strong and persistent match between oceanographic conditions and recruitment.

Hence, our work potentially resolves the relative importance of pre- and post-settlement processes in intertidal systems and in doing so, explains the relationship between the spatiotemporal patterns of oceanographic conditions, recruitment and adult abundance. Limited dispersal promotes the regionally constructive effect of post-settlement processes and leads to a mismatch between the spatiotemporal patterns of oceanographic conditions, recruitment and adult abundance. The lack of dispersal allows regional pre-settlement processes to dominate and generate matching spatiotemporal patterns of recruitment and adult abundance at regional scales.

INTRODUCTION

Ascribing natural patterns of (adult) population abundance and community structure to their causal processes is a fundamental goal of ecology. In marine systems, seminal studies identified consistencies in the spatial patterns of population abundance and community structure across rocky intertidal zones (Connell 1961a, b, Paine 1966, Connell 1970, Dayton 1971, Menge 1976, Lubchenco and Menge 1978, Paine 1984). These rather strict spatial zonation patterns were attributed to the joint effects of species interactions and the environment. That is, the distribution of species abundance was generally thought to be limited by predation (Connell 1961a, Paine 1966) in the lower intertidal and desiccation stress in the upper intertidal (Connell 1961b). Within the zone located between the lower and upper intertidal, competition

(Connell 1961a, b, Dayton 1971, Menge 1976, Paine 1984), predation (Paine 1966, Dayton 1971, Menge 1976, Lubchenco and Menge 1978) and disturbance (Dayton 1971, Sousa 1979) were believed to govern the distribution of population abundance and community structure.

However, other studies found that patterns of population abundance, community structure and species interactions were more dependent upon recruitment (Underwood 1978, Menge and Lubchenco 1981, Underwood et al. 1983, Gaines and Roughgarden 1985, Menge 1991, Underwood et al. 2000). Since many intertidal species possess a sessile adult stage and a planktonic larval stage, this perspective emphasized the importance of pre-settlement processes (i.e. regional oceanographic conditions) affecting recruitment instead of local post-settlement processes (i.e. species interactions) to explain patterns of population abundance and community structure (Underwood et al. 1983, Gaines and Roughgarden 1985).

Using the California Current Large Marine Ecosystem (CCLME) as a model system, Roughgarden et al. (1988) attempted to reconcile these conflicting findings by proposing that oceanographic processes controlling recruitment determine the relative importance of regional pre-settlement and local post-settlement processes. This theory, herein referred to as the latitudinal gradient hypothesis (Fig 1), is based on the existence of a strong and persistent latitudinal gradient in oceanographic conditions along the West coast of the United States (Roughgarden et al. 1987, Roughgarden et al. 1988, Strub and James 1988, Connolly and Roughgarden 1998, 1999, Connolly et al. 2001). Indeed, the California Current System bathing the West coast of the United States is characterized by strong equator-ward winds that generate coastal upwelling currents (Huyer 1983, Hickey 1998). These wind-driven

coastal upwelling currents cause the offshore movement of the warm, nutrient-poor surface layer of the water via Ekman transport (Mann and Lazier 2006) and its subsequent replacement by deep, cool and nutrient-rich water (Huyer 1983, Hickey 1998, Mann and Lazier 2006). This offshore transport entrains intertidal planktonic larvae into upwelling fronts (Roughgarden et al. 1988, Farrell et al. 1991, Connolly and Roughgarden 1998). When the equator-ward winds relax, the upwelling fronts move onshore and allow the larvae to settle onto the intertidal zone and metamorphose into sessile adults (Farrell et al. 1991, Connolly and Roughgarden 1998). Since (i) upwelling currents are stronger and more persistent, (ii) the upwelling season longer and (iii) the upwelling fronts farther from the shore in California than in the Pacific Northwest, these upwelling currents are more likely to limit recruitment in California than in the Pacific Northwest (Roughgarden et al. 1988, Connolly and Roughgarden 1998).

Based on theses observations, Roughgarden and Connolly (1998, 1999) used closed (no dispersal) competition and predation models to predict that pre-settlement processes controlling recruitment are more likely to govern community structure in California, where recruitment is limited, abundance is lower and species interactions are weaker (Connolly and Roughgarden 1998). In contrast, they proposed that post-settlement processes are more likely to control community structure in the Pacific Northwest, since recruitment is not limited, abundance is higher and species interactions are stronger (Connolly and Roughgarden 1998). The latitudinal gradient hypothesis thus predicts that a persistent gradient in oceanographic conditions will lead to a gradient in both the strength of post-

settlement processes and their corrosive effect on the relationship between oceanographic conditions, recruitment and adult abundance (Fig 1).

Some evidence is consistent with this hypothesis. Recruitment of mussels and a barnacle, *Balanus glandula* is dramatically higher in the northern than in the southern CCLME (Broitman et al. 2008). Phytoplankton abundance is also far greater in the northern CCLME (Barth et al. 2007). However, surveys and experiments have revealed no clear latitudinal gradient in either the strength of post-settlement processes or their corrosive effect on the relationship between oceanographic conditions, recruitment and adult abundance (Menge et al. 2004, Gouhier et al. *in press*). Spatiotemporal patterns of adult abundance do not simply reflect the latitudinal gradient observed in oceanographic conditions and recruitment (Broitman et al. 2008, Gouhier et al. *in press*). Hence, the corrosive effect of post-settlement processes is insufficient to explain the observed mismatch between oceanographic conditions, recruitment and abundance in intertidal communities along the West coast of the United States.

Recent modeling efforts indicate that local post-settlement processes such as competition and predation can interact with limited dispersal to generate complex regional patterns of population abundance in space and time (Gouhier et al. *in press*). Could this regionally constructive effect of post-settlement processes explain the observed mismatch between oceanographic conditions, recruitment and adult abundance? Here, we develop and validate a theory of marine metacommunities that incorporates both the locally corrosive and the regionally constructive effects of post-settlement processes on the relationship between oceanographic conditions, recruitment and adult abundance. In the absence of dispersal, the regionally

constructive effect of post-settlement processes is suppressed. Post-settlement processes merely corrode the matching and persistent spatiotemporal patterns of oceanographic conditions, recruitment and adult abundance. When dispersal is limited, the regionally constructive effects of post-settlement processes generate complex, non-stationary spatiotemporal patterns of adult abundance. This non-stationarity leads to an intermittent mismatch between the spatiotemporal patterns of recruitment and adult abundance, despite a strong and persistent match between oceanographic conditions and recruitment. Overall, our work highlights the importance of dispersal for understanding the relative importance of pre- and post-settlement processes for intertidal communities and their effects on the relationship between oceanographic conditions, recruitment and adult abundance.

METHODS

Data collection

Adult abundance (adult percent cover) of the mussel *M. californianus* and the barnacle *B. glandula* was quantified annually from 1999 to 2004 at 48 sites located along the West coast of the United States and stretching from southern California to northern Washington (from 32.7 °N to 48.4 °N) (Schoch et al. 2006). For each site, the cover of *M. californianus* and *B. glandula* was surveyed in 10 randomly placed 0.25 m^2 quadrats for each of three 50 m transects located within the mid-intertidal zone. The cover of *M. californianus* and *B. glandula* was averaged across all 10 replicate quadrats and all three transects in order to obtain an estimate of the mean annual cover for each species and site.

We measured annual larval recruitment of barnacles and mussels from 1997 to 2005 at 30 sites along the West coast of the United States using standard procedures that have been described in detail elsewhere (Menge 1992, Menge et al. 1999, Broitman et al. 2008). Briefly, mussel recruitment rates were quantified using standardized plastic mesh collectors and barnacle recruitment rates were quantified using 10x10 cm plexiglass or PVC plates covered with "safety-walk" tape (e.g. Farrell et al. 1991). These materials were used because they emulate the characteristics of the preferred settlement substrata for barnacle and mussel larvae (Broitman et al. 2008). Recruits from 5-8 replicates were counted in the laboratory and standardized to the number of individuals per plate (100 cm^2) for barnacles and the number of individuals per collector (~100 cm^3) for mussels. Recruitment was measured on a monthly basis and the results were subsequently averaged to provide annual estimates of barnacle and mussel recruitment rates for each site.

Mean annual sea surface temperature (SST, in °C), chlorophyll-a concentration (chl-a, in mg/m^3) and upwelling index (in $m^3/s/100$ m of coastline) data from 1997 to 2005 occurring within a 0.2 degree radius (1 degree radius for upwelling) seaward of each of the 48 adult abundance sites and 30 recruitment sites were obtained respectively from the Advanced Very High Resolution Radiometer (AVHRR; NOAA), the Sea-viewing Wide Field-of-view Sensor (SeaWiFS; NASA) and sea level pressure maps (Pacific Fisheries Environmental Laboratory). We used remote sensing data to quantify sea surface temperature (SST), chlorophyll-a concentration (chl-a) and upwelling currents (upwelling index) instead of *in situ* measurements because the former had greater temporal and spatial coverage. Additionally, the broad spatial extent of remote sensing data may better reflect the

spatially-integrated environmental conditions experienced by intertidal populations (Bustamante and Branch 1996). Both the SST and chl-a data had a nominal resolution of 4 km, whereas the upwelling index had a coarser resolution of 1 degree (~111 km). Since remote sensing data are prone to errors due to cloud cover and aerosols that can influence captured irradiances, we excluded low quality data points characterized by high cloud/aerosol cover from the analysis (Bailey and Werdell 2006). Additionally, outliers were removed from the remote sensing data series by computing the filtered mean (Bailey and Werdell 2006) of each variable for each site:

$$\frac{\sum_{i=1}^{p}\left[\left(\overline{X}-1.5\sigma_X\right)\leq X\leq\left(\overline{X}+1.5\sigma_X\right)\right]}{N} \qquad (1)$$

where p represents the total number of points within 0.2 degrees (1 degree for upwelling) of the site, N is the total number of points within 1.5 standard deviations of the mean $\overline{X}$. These filtered environmental data series were then validated by using reduced major axis regression (Bailey and Werdell 2006) to relate them to *in situ* buoy measurements (chl-a: R^2=0.42, p-value<10^{-4}, n=583; SST: R^2=0.60, p-value=0, n=536).

The metacommunity model

The metacommunity model describes disturbance-recovery dynamics in a network of (strictly) competitive communities that are connected by dispersal (Guichard 2005). Within communities, the successional dynamics observed in natural intertidal systems (Paine and Levin 1981, Paine 1984) are represented as a mean-field implementation of a spatial process affecting the proportional abundance of (i) the

subdominant barnacle (A_1), (ii) the dominant mussel (A_2), (iii) the wave disturbance (W) and (iv) the empty substrate (S) (Guichard et al. 2003). A maximum fraction $\alpha_0 = 1$ of the proportional abundance of the dominant mussel species (A_2) can be displaced by wave disturbances (W). A proportion $(1-\delta_0)$ of disturbances displace mussels through a density-dependent contact process with aggregation (Moore neighborhood, $q = 8$), while a proportion $\delta_0 = 10^{-3}$ of disturbances is density-independent. This disturbance dynamic is based on the assumption that wave disturbances destroy the byssal thread attachments of mussels around the edges of disturbed areas, thus making them temporarily more susceptible to further disturbance (Denny 1987, Guichard et al. 2003). Hence, newly disturbed areas allow the local propagation of wave disturbances to adjacent mussel beds. Once the disturbance has propagated away from the newly disturbed area, the area transitions from the 'wave disturbed' state to the 'empty substrate' state. Since our metacommunity model assumes a strict competitive hierarchy, mussels (A_2) are able to colonize a maximum fraction $\alpha_2 = 0.65$ of the proportional abundance of both the empty substrate (S) and barnacles (A_1), whereas barnacles are only able to colonize a maximum fraction $\alpha_2 = 0.65$ of the proportional abundance of the empty substrate. For both mussels and barnacles, a proportion $\delta_2 = 0.1$ of colonization occurs through a density-independent process while the remaining colonization is density-dependent $(1-\delta_2)$. Mussel and barnacle colonization also depends on the production and recruitment of larvae. Within communities x, larval production of barnacles (A_1) and mussels (A_2) is a function of the local proportional abundance

of adults $A_{i,x}$ and fecundity f_x $\left(\overline{f} = 3.85\right)$. The recruitment rate of barnacles and mussels is described by a Poisson process (Caswell and Etter 1999) $R_{i,x}^t = 1 - e^{-\beta_{i,x}^t}$ where $\beta_{i,x}^t$ integrates (i) the total number of larvae produced and retained in communities x at time t and (ii) the total number of larvae produced in other communities y and dispersed to communities x at time t. The dynamics of the model are represented by the following integro-difference equation system for communities x in a metacommunity consisting of $n = 256$ communities:

$$
\begin{aligned}
W_x^{t+1} &= \alpha_0 A_{2,x}^t \left(\delta_0 + \left(1-\delta_0\right)\left(1-\left(1-W_x^t\right)^q\right)\right) \\
S_x^{t+1} &= W_x^t + S_x^t - \alpha_2\left(A_{1,x}^t\left(1-\delta_2\right)+\delta_2\right)R_{1,x}^t S_x^t - \alpha_2\left(A_{2,x}^t\left(1-\delta_2\right)+\delta_2\right)R_{2,x}^t S_x^t \\
A_{1,x}^{t+1} &= A_{1,x}^t + \alpha_2\left(A_{1,x}^t\left(1-\delta_2\right)+\delta_2\right)R_{1,x}^t S_x^t - \alpha_2\left(A_{2,x}^t\left(1-\delta_2\right)+\delta_2\right)R_{2,x}^t A_{1,x}^t \\
A_{2,x}^{t+1} &= 1 - W_x^t - A_{1,x}^t - S_x^t
\end{aligned}
$$

with:

$$
\begin{aligned}
R_{i,x}^t &= 1 - e^{\beta_{i,x}^t} \\
\beta_{i,x}^t &= A_{i,x}^t f_x\left(1-d\right) + \int A_{i,y}^t f_y \, dD\left(\left|x-y\right|\right)\mathrm{d}y \\
D(\left|x-y\right|) &= \frac{3\left|x-y\right|^2}{2} e^{-\left|x-y\right|^3} \\
x &= u\left(\frac{2}{n}\mathbf{L} - 1\right) \\
\mathbf{L} &= \left[0,...,n-1\right]
\end{aligned}
$$

where D is the dispersal kernel of barnacles and mussels resulting from larval transport at a constant speed and with a time-dependent settlement rate (double Weibull distribution (Neubert et al. 1995)), d represents the proportion of larvae

being dispersed, u represents the scale of dispersal and **L** represents a zero-based vector of community locations.

We used a 'no dispersal' and a 'limited dispersal' treatment in order to untangle the locally corrosive and regionally constructive effects of post-settlement processes on the spatiotemporal relationship between the environment, recruitment and adult abundance. Under the 'limited dispersal' treatment, all larvae disperse to neighboring communities (i.e $d = 1,\ u = 10$: mean dispersal distance represents 8.6% of the spatial domain), whereas all larvae are retained locally under the 'no dispersal' treatment (i.e. $d = 0$). All metacommunity model simulations were performed for 256 sites with periodic boundary conditions and the results were analyzed over 2000 post-transient time steps. Although our model focused on disturbance-recovery dynamics, predator-prey dynamics generate similar results (Gouhier et al. *in press*).

Environmental variability has a significant impact on the productivity of intertidal populations (Menge 1992, Menge et al. 1997, Leslie et al. 2005). We implement this effect by varying mussel and barnacle fecundity in order to emulate the spatiotemporal properties of the environmental conditions observed along the West coast of the United States. Specifically, we implement the observed latitudinal environmental gradient (Fig 1,S2,S3) by varying mussel and barnacle fecundity f linearly from 0.2 to 7.5 over the entire spatial range $\left(\overline{f} = 3.85\right)$ and adding normally-distributed white noise with zero mean and variance $\sigma^2 = 1$.

Data and model analysis

We applied the same analyses to both the survey and the model data. We used the correlation coefficient to assess the spatial and temporal properties of the relationship between mean annual environmental conditions and both mean annual recruitment and mean annual adult abundance. We evaluated the correlation between the environment and both recruitment and adult abundance for a number of different time lags in order to determine the temporal scale at which the relationship was the strongest (Fig S1, Gouhier et al. *in press*). Based on these results, we used a 1-year time lag for the adult abundance correlation analysis and no time lag for the recruitment correlation analysis. The statistical significance of the correlations was determined by using a one-tailed test $(\alpha = 0.05)$ on 1,000 Monte Carlo randomizations (Fortin and Dale 2005, Manly 2006).

We used spatial synchrony analysis in order to describe the spatiotemporal patterns in the environmental, recruitment and adult abundance data. Prior to conducting spatial synchrony analysis, all variables were detrended by subtracting the global mean time series from each site's time series in order to remove any bias caused by common large-scale trends (Koenig 1999). The distances between all pairs of sites were then computed and used to group the detrended time series data into equally-spaced, 41 km-wide distance bins. The coefficient of synchrony for each bin was calculated by computing the correlation coefficient between the time series of all pairs of sites within the bin. The extent of the spatial synchrony analysis was restricted to half of the spatial domain in order to avoid large discrepancies in the number of pairs of sites within each bin (Fortin and Dale 2005). Statistical

significance was determined by using a one-tailed test $(\alpha = 0.05)$ on 10,000 Monte Carlo randomizations (Fortin and Dale 2005). Specifically, for each bin, the p-value was calculated by shuffling the data pairs within the bin 10,000 times, computing the coefficient of synchrony for each randomization and then calculating the proportion of randomizations with a coefficient of synchrony greater than or equal to that obtained with the original data. For the model data, we performed spatial synchrony analysis on 10-time step windows in order to approximate the temporal extent of our survey data. However, our results are robust to window size (Gouhier et al. *in press*). We present the mean and 95% confidence intervals obtained across all 10-time steps windows in order to investigate the persistence of spatial synchrony patterns in time.

RESULTS

The effects of the latitudinal environmental gradient on patterns of recruitment and adult abundance: the corrosive effect of post-settlement processes

We test the effect of the latitudinal environmental gradient (Fig 1, A2, A3) on recruitment patterns by assessing the strength of the spatial relationship across all years between the environment and recruitment. As predicted by the latitudinal gradient hypothesis, the spatial correlation across all sites between mean annual recruitment values and mean annual environmental variables is significant for both mussel and barnacle species (table 1). This significant spatial correlation is largely driven by southern sites where recruitment is environmentally-limited and the spatial correlation is strongest (table 1). Since recruitment in northern sites is not

environmentally limited, the spatial correlation between the environment and recruitment is generally weaker (table 1). The latitudinal environmental gradient is so strong and persistent (Fig 1A, A2, A3) that the (time) lagged spatial correlation between mean annual recruitment and mean annual environmental conditions remains consistently significant over time lags ranging from 0 to 20 years. This is because temporal variability in mean annual recruitment and mean annual environmental conditions is much weaker than the spatial variability imposed by the persistent latitudinal gradient (Fig A2, A3). Consistent with the latitudinal gradient hypothesis, this persistent spatial correlation between environmental conditions and recruitment occurs for southern (environmentally-limited) sites but not northern sites (Fig A1). These spatial patterns in the relationship between the environment and recruitment are predicted by metacommunity models experiencing latitudinal gradients in environmental conditions and either no or limited dispersal (table 1).

For the survey and the model data, the spatial correlation between the environment and adult abundance—whether performed across all, northern or southern sites—is inconsistent and weak compared to the correlation between the environment and recruitment (table 1 vs. table 2). This corrosion of the effect of the environment on adult abundance is likely the result of post-settlement processes that, according to the latitudinal gradient hypothesis, should be more prominent in northern sites than in southern sites (Fig 1). However, there is no clear and consistent difference between northern and southern sites in terms of the strength of the spatial correlation between the environment and adult abundance (table 2). This suggests that the strong and persistent latitudinal gradient in the environment is able to generate a similar latitudinal gradient in recruitment, but that its effect on adult

abundance is largely lost (Menge et al. 2004, Broitman et al. 2008, Menge et al. 2009, Gouhier et al. *in press*).

Analyzing the dynamics of the relationship between mean annual environmental conditions and mean annual recruitment or adult abundance reveals similar patterns in both the survey (Fig 2) and the model data (Fig 3). The spatial correlation between the environment and recruitment is relatively strong and consistent in time for all sites and southern sites (Fig 2A-B, E-F; Fig 3A-B, E-F), but not for northern sites (Fig 2C-D; Fig 3C-D). However, the spatial correlation between the environment and adult abundance is weak and inconsistent in time (Fig 2, 3), regardless of the temporal lag used or the number of years over which the environmental conditions are averaged (Gouhier et al. *in press*). These types of fluctuations in the strength and sign of the correlation between the environment and adult abundance are predicted by metacommunity models with either limited or no dispersal (Fig 3). Indeed, although the correlation between the environment and recruitment is consistent and strong, post-settlement disturbance-recovery processes induce fluctuations in the abundance of mussel and barnacle populations that corrode the correlation between the environment and the adult abundance (Fig 3; Gouhier et al. *in press*). Hence, although the latitudinal environmental gradient hypothesis accurately predicts spatial patterns of recruitment in intertidal communities, post-settlement processes limit its ability to predict adult population dynamics. This corrosive effect of post-settlement processes is evident in metacommunities with either low or no dispersal. We now focus on the implications of the regionally constructive effect of post-settlement processes for spatiotemporal patterns of recruitment and adult abundance in marine metacommunities.

Understanding spatiotemporal patterns of adult abundance and recruitment: the constructive effect of post-settlement processes

So far, we have demonstrated that the localized corrosive effect of post-settlement processes can lead to a weak and inconsistent spatial correlation between the environment and adult abundance in the survey data (Fig 2) and the metacommunity models with limited or no dispersal (Fig 3). However, post-settlement processes can also interact with limited dispersal to generate complex regional patterns of adult abundance (Gouhier et al. *in press*). This constructive effect of post-settlement processes at the regional scale leads to irregular fluctuations in the spatial correlation between the environment and adult abundance (Gouhier et al. *in press*; Fig 3B, D, F). Importantly, this constructive effect is more prevalent in mussels than in barnacles since the former experience post-settlement processes (i.e. disturbance-recovery dynamics) directly, whereas the latter experience these processes indirectly via competition (Fig 3B, D, F). The constructive effect is also more prevalent in northern sites (no environmentally-limited recruitment) than in southern sites (environmentally-limited recruitment) due to the effect of the latitudinal environmental gradient on recruitment (Fig 3D, F).

When we analyze the survey data across the entire spatial range using spatial synchrony, we see that all environmental variables undergo a quasi-linear decay in synchrony with lag distance, going from synchrony at small lag distances to no synchrony or asynchrony at large lag distances (see full circles indicating significant values in Fig 4A, B). A similar linear decay in spatial synchrony is observed in the

recruitment of *B. glandula* and *M. californianus* (Fig 4C). However, the spatial synchrony patterns in the adult abundance of *B. glandula* and *M. californianus* show a more complex nonlinear pattern, oscillating between synchrony and asynchrony with increasing lag distance (Fig 4D). This nonlinear pattern of spatial synchrony is a signature of the constructive effect of post-settlement processes and limited dispersal (Gouhier et al. *in press*). We now apply spatial synchrony analysis to our metacommunity models in order to understand the cause of these divergent patterns of recruitment and adult abundance.

In metacommunities with no dispersal, spatial synchrony patterns of adult abundance and recruitment undergo the same qualitative linear decay as the environment, albeit (quantitatively) dampened by the corrosive effect of post-settlement processes (Fig 5A, C). As previously discussed, this localized corrosive effect of post-settlement processes is more prominent in spatial synchrony patterns of mussel recruitment and adult abundance than in those of barnacles (Fig 5A vs. 5C). It thus appears that the localized corrosive effect of post-settlement processes alone is not enough to generate the nonlinear patterns of spatial synchrony observed in natural intertidal metacommunities. In metacommunities with limited dispersal, spatial synchrony patterns of recruitment undergo the same linear decay as the environment (Fig 5B, D). However, spatial synchrony patterns of adult abundance are non-stationary and nonlinear, oscillating from synchrony to asynchrony and back to synchrony with increasing lag distance (Fig 5B, D). These non-stationary and nonlinear patterns of synchrony are caused by the constructive effect of post-settlement processes and limited dispersal (Gouhier et al. *in press*); they are more prominent in mussels experiencing post-settlement processes directly than in

barnacles experiencing them indirectly via competition (Fig 5B vs. 5D). Hence, these results predict that spatiotemporal recruitment patterns need not translate into corresponding spatiotemporal patterns of adult abundance because of the locally corrosive and regionally constructive effects of post-settlement processes.

DISCUSSION

We have developed a theory of marine metacommunities that suggests that dispersal controls the relative importance of pre- and post-settlement processes for patterns of recruitment and adult abundance in space and time. In the absence of dispersal, pre-settlement processes generate persistent and matching regional patterns of oceanographic conditions, recruitment and abundance. Post-settlement processes merely corrode (without compromising) the relationship between oceanographic conditions, recruitment and abundance at local scales. When dispersal is limiting, the regionally constructive effect of post-settlement processes generates a transient mismatch between the complex and non-stationary patterns of adult abundance and the persistent and matching patterns of oceanographic conditions and recruitment. Our theory emphasizes the dynamical consequences of post-settlement processes instead of the static regional differences in pre-settlement processes to explain patterns of adult abundance and recruitment in space and time, and their relationship with oceanographic conditions. We now discuss the applicability and implications of this theory for understanding patterns of recruitment and adult abundance in intertidal systems around the world.

The relationship between patterns of recruitment and adult abundance

Recent studies have found remarkable similarities in the shape (linear decay with lag distance) and the scale of spatiotemporal patterns of recruitment between Chile and the West coast of the United States (Lagos et al. 2007, Broitman et al. 2008, Lagos et al. 2008, Navarrete et al. 2008). These patterns of recruitment were shown to be associated with oceanographic conditions (Navarrete et al. 2005, Lagos et al. 2007, Lagos et al. 2008). Using variance partitioning methods, Lagos et al. (2008) showed that the spatial patterns of recruitment were mainly attributable to spatially-structured environmental variation and space, but not the environment alone. This is consistent with our finding that the spatial correlation between the environment and recruitment is consistently strong and significant across different time lags (Fig A1): the spatial correlation between the environment and recruitment is predicted to reflect the strong spatial gradient in the environment and not the weak temporal variation in the environment itself.

Metacommunity models with either limited or no dispersal predict patterns of recruitment whose spatial and temporal properties match those of recruitment patterns observed along the West coast of the United States (Fig 4, 5) and Chile (Lagos et al. 2007, Lagos et al. 2008). Furthermore, metacommunity models predict the same strong match between the spatiotemporal patterns of the environment and those of recruitment, regardless of dispersal (Fig 5). Hence, we suggest that patterns of recruitment alone cannot be used to determine whether intertidal systems are governed by regional differences in pre-settlement processes or the regionally

constructive effects of post-settlement processes and limited dispersal. Instead, one must compare patterns of recruitment and adult abundance. Indeed, a match between the spatiotemporal patterns of recruitment and adult abundance indicates that intertidal systems are governed by regional differences in pre-settlement processes (Fig 5); a mismatch between patterns of recruitment and adult abundance underscores the importance of the regionally constructive effects of post-settlement processes and dispersal.

Applying our theory to intertidal systems around the world

Our theory predicts that dispersal controls the relative importance of pre- and post-settlement processes for patterns of recruitment and adult abundance. In the absence of dispersal, persistent regional differences in oceanographic conditions generate matching patterns of recruitment and adult abundance. When dispersal is limited, the regionally constructive effect of post-settlement processes generates a transient mismatch between patterns of recruitment and adult abundance despite the persistent match between patterns of oceanographic conditions and recruitment. We now evaluate the applicability of our theory to well-studied intertidal systems along the West coast of the United States, Chile and New Zealand. In all three of these systems, persistent regional differences in oceanographic conditions (i.e. discontinuities) controlling larval supply have been used to explain patterns of recruitment, population adult abundance and community structure (Roughgarden et al. 1988, Menge et al. 2003, Navarrete et al. 2005).

Along the West coast of the United States, strong and persistent upwelling currents limit recruitment in California, whereas weak and intermittent upwelling

currents lead to large pulses of recruitment in the Pacific Northwest (Roughgarden et al. 1988, Connolly and Roughgarden 1998, 1999, Connolly et al. 2001, Broitman et al. 2008). These regional differences in upwelling conditions were hypothesized to generate systematic differences in the strength of species interactions and the relative importance of regional pre-settlement and local post-settlement processes (Roughgarden et al. 1988, Connolly and Roughgarden 1998, 1999, Connolly et al. 2001). However, these predictions were largely refuted (Menge et al. 2004). Here, we have shown that despite strong regional differences in upwelling currents, local post-settlement processes interact with limited dispersal to generate the observed mismatch between patterns of recruitment and adult abundance. Hence, we suggest that in this system, the regionally constructive effect of post-settlement processes and limited dispersal rather than the persistent regional differences in pre-settlement processes explains patterns of recruitment and adult abundance in space and time.

On the West coast of New Zealand, intermittent periods of upwelling bring cold, nutrient rich water to the surface and move planktonic larvae offshore (Menge et al. 2003). During relaxation events, these nutrients and larvae return to the shore and generate large pulses of larval and nutrient supply for intertidal communities (Menge et al. 2003). However, since upwelling currents are almost nonexistent along the East coast of New Zealand, the surface water layer is devoid of the nutrients that normally subsidize larvae and this leads to low larval supply (Menge et al. 2003). These persistent differences in oceanographic conditions between the East coast and the West coast of New Zealand lead to striking differences in the relative influence of pre- and post-settlement processes and species interactions on community structure (Menge et al. 2003). Indeed, larval recruitment, growth and species

interactions are stronger on the West coast than they are on the East coast (Menge et al. 2003). These findings are consistent with the notion that regional oceanographic processes determine the relative importance of pre- and post-settlement processes by controlling the supply of larvae (Roughgarden et al. 1988, Connolly and Roughgarden 1998, 1999, Connolly et al. 2001) and nutrients (Menge 1992, Menge et al. 2003). How can these findings be reconciled with our theory? In this case, the regional differences in oceanographic conditions affect two different coasts with divergent circulation patterns (Menge et al. 2003). Hence, there is probably little to no dispersal occurring between intertidal communities located on the East and West coasts of New Zealand. In the absence of dispersal, our theory predicts that pre-settlement processes will generate persistent and matching patterns of recruitment and adult abundance. Hence, these observations are compatible with our predictions.

The final case study, Chile, presents a much more formidable challenge to our theory. Indeed, oceanographic conditions along the coast of Chile essentially mirror those observed along the West coast of the United States (Navarrete et al. 2005, Navarrete et al. 2008): persistent upwelling currents limit recruitment in the northern region whereas frequent relaxation events allow large supplies of recruits in the southern region (Navarrete et al. 2005). These environmentally-mediated differences in the supply of larvae lead to weak species interactions in the north and strong species interactions in the south (Navarrete et al. 2005), as predicted by the latitudinal gradient hypothesis. It is possible that the strong discontinuity in oceanographic circulation that separates the northern and southern regions (Navarrete et al. 2005) effectively limits dispersal among regions, and thus prevents

the regionally-constructive effect of post-settlement processes observed along the West coast of the United Stats.

This hypothesis can be tested by comparing levels of connectivity across discontinuities along the West coast of the United States and Chile. Along the West coast of the United States, recent work has demonstrated the existence of genetic clines, but not isolation by distance, in the barnacle *Balanus glandula* (Sotka et al. 2004, Sotka and Palumbi 2006). Hence, regional differences in oceanographic circulation patterns limit but do not prevent connectivity between sites from different regions along the West coast of the United States. Similar work on connectivity across oceanographic discontinuities in Chile would provide the information necessary to validate our claims.

Conclusion

Our theory of marine metacommunities emphasizes the importance of determining levels of connectivity among communities along environmental gradients and discontinuities in order to determine the relative influence of pre- and post-settlement processes on the regional distribution of recruitment and adult abundance. Such information could be used to validate our theory and explain the relationship between oceanographic conditions, recruitment and adult abundance in intertidal ecosystems.

ACKNOWLEDGEMENTS

We acknowledge the granting agencies that made this research possible. T.C.G. was supported by a McGill Majors fellowship and F.G. was supported by a grant from the James S. McDonnell foundation.

LITERATURE CITED

Bailey, S. W. and P. J. Werdell. 2006. A multi-sensor approach for the on-orbit validation of ocean color satellite data products. Remote Sensing of Environment **102**:12-23.

Barth, J. A., B. A. Menge, J. Lubchenco, F. Chan, J. M. Bane, A. R. Kirincich, M. A. McManus, K. J. Nielsen, S. D. Pierce, and L. Washburn. 2007. Delayed upwelling alters nearshore coastal ocean ecosystems in the northern California current. PNAS **104**:3719-3724.

Broitman, B. R., C. A. Blanchette, B. A. Menge, J. Lubchenco, C. Krenz, M. Foley, P. T. Raimondi, D. Lohse, and S. D. Gaines. 2008. Spatial and temporal patterns of invertebrate recruitment along the west coast of the United States. Ecological Monographs **78**:403-421.

Bustamante, R. H. and G. M. Branch. 1996. Large scale patterns and trophic structure of Southern African rocky shores: the roles of geographic variation and wave exposure. Journal of Biogeography **23**:339-351.

Caswell, H. and R. Etter. 1999. Cellular automaton models for competition in patchy environments: Facilitation, inhibition, and tolerance. Bulletin of Mathematical Biology **61**:625-649.

Connell, J. H. 1961a. Effects of Competition, Predation by Thais Lapillus, and Other Factors on Natural Populations of Barnacle Balanus Balanoides. Ecological Monographs **31**:61-104.

Connell, J. H. 1961b. The Influence of Interspecific Competition and Other Factors on Distribution of Barnacle Chthamalus Stellatus. Ecology **42**:710-723.

Connell, J. H. 1970. A Predator-Prey System in Marine Intertidal Region .1. Balanus-Glandula and Several Predatory Species of Thais. Ecological Monographs **40**:49-78.

Connolly, S. R., B. A. Menge, and J. Roughgarden. 2001. A latitudinal gradient in recruitment of intertidal invertebrates in the northeast Pacific Ocean. Ecology **82**:1799-1813.

Connolly, S. R. and J. Roughgarden. 1998. A latitudinal gradient in northeast Pacific intertidal community structure: Evidence for an oceanographically based synthesis of marine community theory. American Naturalist **151**:311-326.

Connolly, S. R. and J. Roughgarden. 1999. Theory of marine communities: Competition, predation, and recruitment-dependent interaction strength. Ecological Monographs **69**:277-296.

Dayton, P. K. 1971. Competition, Disturbance, and Community Organization - Provision and Subsequent Utilization of Space in a Rocky Intertidal Community. Ecological Monographs **41**:351-389.

Denny, M. W. 1987. Lift as a mechanism of patch initiation in mussel beds. Journal of Experimental Marine Biology and Ecology **113**:231-245.

Farrell, T. M., D. Bracher, and J. Roughgarden. 1991. Cross-Shelf Transport Causes Recruitment to Intertidal Populations in Central California. Limnology and Oceanography **36**:279-288.

Fortin, M. and M. Dale. 2005. Spatial Analysis: A Guide for Ecologists. Cambridge University Press.

Gaines, S. and J. Roughgarden. 1985. Larval Settlement Rate - a Leading Determinant of Structure in an Ecological Community of the Marine Intertidal Zone. Proceedings of the National Academy of Sciences of the United States of America **82**:3707-3711.

Gouhier, T. C., F. Guichard, and B. A. Menge. *in press*. Ecological processes can synchronize marine population dynamics over continental scales. Proceedings of the National Academy of Sciences.

Guichard, F. 2005. Interaction strength and extinction risk in a metacommunity. Proceedings of the Royal Society of London B **272**:1571-1576.

Guichard, F., P. M. Halpin, G. W. Allison, J. Lubchenco, and B. A. Menge. 2003. Mussel disturbance dynamics: signatures of oceanographic forcing from local interactions. The American Naturalist **161**:889-904.

Hickey, B. M. 1998. Coastal oceanography of western North America from the tip of Baja California to Vancouver Island. Pages 345-393 *in* A. R. Robinson and K. H. Brink, editors. The Sea, The Global Coastal Ocean. John Wiley & Sons, New York.

Huyer, A. 1983. Coastal Upwelling in the California Current System. Progress in Oceanography **12**:259-284.

Koenig, W. D. 1999. Spatial autocorrelation of ecological phenomena. Trends in Ecology & Evolution **14**:22-26.

Lagos, N. A., J. C. Castilla, and B. R. Broitman. 2008. Spatial environmental correlates of intertidal recruitment: A test using barnacles in northern Chile. Ecological Monographs **78**:245-261.

Lagos, N. A., F. J. Tapia, S. A. Navarrete, and J. C. Castilla. 2007. Spatial synchrony in the recruitment of intertidal invertebrates along the coast of central Chile. Marine Ecology-Progress Series **350**:29-39.

Leslie, H. M., E. N. Breck, F. Chan, J. Lubchenco, and B. A. Menge. 2005. Barnacle reproductive hotspots linked to nearshore ocean conditions. Proceedings of the National Academy of Sciences of the United States of America **102**:10534-10539.

Lubchenco, J. and B. A. Menge. 1978. Community Development and Persistence in a Low Rocky Intertidal Zone. Ecological Monographs **48**:67-94.

Manly, B. 2006. Randomization, bootstrap and Monte Carlo methods in biology. Third edition. Chapman & Hall.

Mann, K. and J. Lazier. 2006. Dynamics of marine ecosystems: biological-physical interactions in the oceans. Blackwell Publishing.

Menge, B. A. 1976. Organization of New-England Rocky Intertidal Community - Role of Predation, Competition, and Environmental Heterogeneity. Ecological Monographs **46**:355-393.

Menge, B. A. 1991. Relative Importance of Recruitment and Other Causes of Variation in Rocky Intertidal Community Structure. Journal of Experimental Marine Biology and Ecology **146**:69-100.

Menge, B. A. 1992. Community Regulation - under What Conditions Are Bottom-up Factors Important on Rocky Shores. Ecology **73**:755-765.

Menge, B. A., C. Blanchette, P. Raimondi, T. Freidenburg, S. Gaines, J. Lubchenco, D. Lohse, G. Hudson, M. Foley, and J. Pamplin. 2004. Species interaction strength: Testing model predictions along an upwelling gradient. Ecological Monographs **74**:663-684.

Menge, B. A., F. Chan, K. J. Nielsen, E. D. Lorenzo, and J. Lubchenco. 2009. Climatic variation alters supply-side ecology: impact of climate patterns on phytoplankton and mussel recruitment. Ecological Monographs **79**:379-395.

Menge, B. A., B. A. Daley, J. Lubchenco, E. Sanford, E. Dahlhoff, P. M. Halpin, G. Hudson, and J. L. Burnaford. 1999. Top-down and bottom-up regulation of New Zealand rocky intertidal communities. Ecological Monographs **69**:297-330.

Menge, B. A., B. A. Daley, P. A. Wheeler, and P. T. Strub. 1997. Rocky intertidal oceanography: An association between community structure and nearshore phytoplankton concentration. Limnology and Oceanography **42**:57-66.

Menge, B. A. and J. Lubchenco. 1981. Community Organization in Temperate and Tropical Rocky Intertidal Habitats: Prey Refuges in Relation to Consumer Pressure-Gradients. Ecological Monographs **51**:429-450.

Menge, B. A., J. Lubchenco, M. E. S. Bracken, F. Chan, M. M. Foley, T. L. Freidenburg, S. D. Gaines, G. Hudson, C. Krenz, H. Leslie, D. N. L. Menge, R. Russell, and M. S. Webster. 2003. Coastal oceanography sets the pace of rocky intertidal community dynamics. Proceedings of the National Academy of Sciences of the United States of America **100**:12229-12234.

Navarrete, S. A., B. R. Broitman, and B. A. Menge. 2008. Interhemispheric comparison of recruitment to intertidal communities: Pattern persistence and scales of variation. Ecology **89**:1308-1322.

Navarrete, S. A., E. A. Wieters, B. R. Broitman, and J. C. Castilla. 2005. Scales of benthic-pelagic coupling and the intensity of species interactions: From recruitment limitation to top-down control. Proceedings of the National Academy of Sciences of the United States of America **102**:18046-18051.

Neubert, M. G., M. Kot, and M. A. Lewis. 1995. Dispersal and Pattern-Formation in a Discrete-Time Predator-Prey Model. Theoretical Population Biology **48**:7-43.

Paine, R. T. 1966. Food Web Complexity and Species Diversity. American Naturalist **100**:65-75.

Paine, R. T. 1984. Ecological Determinism in the Competition for Space. Ecology **65**:1339-1348.

Paine, R. T. and S. A. Levin. 1981. Inter-Tidal Landscapes - Disturbance and the Dynamics of Pattern. Ecological Monographs **51**:145-178.

Roughgarden, J., S. Gaines, and H. Possingham. 1988. Recruitment Dynamics in Complex Life-Cycles. Science **241**:1460-1466.

Roughgarden, J., S. D. Gaines, and S. W. Pacala. 1987. Supply-side ecology: the role of physical transport processes. Blackwell Scientific Publications, London.

Schoch, G. C., B. A. Menge, G. Allison, M. Kavanaugh, S. A. Thompson, and S. A. Wood. 2006. Fifteen degrees of separation: Latitudinal gradients of rocky intertidal biota along the California Current. Limnology and Oceanography **51**:2564-2585.

Sotka, E. E. and S. R. Palumbi. 2006. The use of genetic clines to estimate dispersal distances of marine larvae. Ecology **87**:1094-1103.

Sotka, E. E., J. P. Wares, J. A. Barth, R. K. Grosberg, and S. R. Palumbi. 2004. Strong genetic clines and geographical variation in gene flow in the rocky intertidal barnacle Balanus glandula. Molecular Ecology **13**:2143-2156.

Sousa, W. P. 1979. Disturbance in Marine Intertidal Boulder Fields: the Non-Equilibrium Maintenance of Species-Diversity. Ecology **60**:1225-1239.
Strub, P. T. and C. James. 1988. Atmospheric Conditions During the Spring and Fall Transitions in the Coastal Ocean Off Western United States. J. Geophys. Res. **93**:15561-15584.
Underwood, A. J. 1978. Refutation of Critical Tidal Levels as Determinants of Structure of Inter-Tidal Communities on British Shores. Journal of Experimental Marine Biology and Ecology **33**:261-276.
Underwood, A. J., M. G. Chapman, and S. D. Connell. 2000. Observations in ecology: you can't make progress on processes without understanding the patterns. Journal of Experimental Marine Biology and Ecology **250**:97-115.
Underwood, A. J., E. J. Denley, and M. J. Moran. 1983. Experimental Analyses of the Structure and Dynamics of Mid-Shore Rocky Intertidal Communities in New-South-Wales. Oecologia **56**:202-219.

FIGURE LEGENDS

Figure 1: The latitudinal gradient hypothesis holds that a latitudinal gradient in the strength of offshore coastal upwelling currents (A) leads to a corresponding gradient in the relative influence of pre- and post-settlement processes (B) on the dynamics of adult abundance and recruitment for intertidal species that undergo pelagic larval dispersal (C, D). (A) The latitudinal gradient in the strength of mean annual offshore transport caused by coastal upwelling currents is highly significant (red linear regression line: $p=0$, $R^2=0.66$, $n=248$) and persistent in time (colors code for different years): offshore transport north of Cape of Blanco (horizontal dashed line) is weak and sometimes negative (i.e. net onshore transport) whereas offshore transport south of Cape Blanco is strong and persistent. (B) Weak offshore transport north of Cape Blanco does not limit recruitment in northern intertidal populations (red open circles): recruitment and adult abundance dynamics are expected to reflect post- rather than pre-settlement processes (B, C). (B) Persistent and strong offshore transport south of Cape Blanco limits recruitment in southern intertidal populations:

recruitment and adult abundance dynamics are expected to reflect pre- rather than post-settlement processes (B, D). The data plotted in panels C and D are simulated and used to illustrate the predictions of the latitudinal gradient hypothesis.

Figure 2: The dynamics of the spatial correlation between mean annual recruitment (circles) or adult abundance (triangles) and mean annual environmental conditions across all sites (A, B), northern sites (C, D) and southern sites (E, F) for intertidal metacommunities along the West coast of the United States. The correlation between mean annual recruitment or adult abundance and mean annual [chl-a] (green), SST (dark blue) and upwelling index (red) were calculated for the barnacle *B. glandula* (A, C, E) and the mussel *M. californianus* (B, D, F). Full circles or triangles indicate statistical significance based on 1000 permutations ($p < 0.05$).

Figure 3: The dynamics of the spatial correlation between mean annual recruitment (circles) or adult abundance (triangles) and mean annual environmental conditions across all sites (A, B), northern sites (C, D) and southern sites (E, F) for model metacommunities with either no dispersal (A, C, E) or limited dispersal (B, D, F). Blue and red lines represent respectively barnacle and mussel species. Full circles indicate statistical significance based on 1000 permutations ($p < 0.05$).

Figure 4: Spatial synchrony of mean annual environmental conditions (A) and mean annual recruitment (C) along the West coast of the United States from 1998 to 2004 across all sites. Spatial synchrony of mean annual environmental conditions (B) and mean annual adult abundance (D) along the West coast of the United States from 2000 to 2003 across all sites. The recruitment and population abundance datasets have different spatial and temporal extents and are thus presented in separate panels. Full circles indicate statistical significance based on 10,000 permutations ($p < 0.05$).

Figure 5: Spatial synchrony of mean annual environmental conditions (green), recruitment (blue) and adult abundance (red) for mussels (C, D) and barnacles (A, B) in model metacommunities with either no dispersal (A, C) or limited dispersal (B, D). The spatial synchrony patterns plotted represent the mean spatial synchrony (±95% confidence interval) observed across all 10-time step windows. The blue vertical dashed line represents the scale of dispersal.

TABLES AND FIGURES

Table 1: Correlation coefficient between mean annual recruitment and mean annual environmental conditions.

		Survey data			Metacommunity model	
	Region	ρ(recruitment, [chl-a])	ρ(recruitment, SST)	ρ(recruitment, upwelling)	No dispersal ρ(recruitment, environment)	Limited dispersal ρ(recruitment, environment)
B. glandula (barnacle)	All sites	**0.45**	**-0.39**	**-0.59**	**0.50**	**0.66**
	Northern sites	**0.32**	0.03	0.01	**0.22**	**0.23**
	Southern sites	**0.43**	**-0.49**	**-0.24**	**0.79**	**0.59**
M. californianus (mussel)	All sites	**0.41**	**-0.30**	**-0.36**	**0.51**	**0.56**
	Northern sites	**0.33**	-0.12	**0.29**	**0.29**	**0.20**
	Southern sites	**0.41**	**-0.36**	**-0.25**	**0.46**	**0.48**

Note: Statistically significant correlations are represented in bold and based on 1000 permutations (p-value < 0.05)

Table 2: Correlation coefficient between mean annual adult abundance and mean annual 1-year lagged environmental conditions.

		Survey data			Metacommunity model	
	Region	ρ(abundance, [chl-a])	ρ(abundance, SST)	ρ(abundance, upwelling)	No dispersal ρ(abundance, environment)	Limited dispersal ρ(abundance, environment)
B. glandula (barnacle)	All sites	**0.28**	0	**-0.22**	**-0.49**	**-0.53**
	Northern sites	**0.33**	0.09	**0.27**	**-0.17**	**-0.11**
	Southern sites	-0.09	**0.29**	-0.02	**-0.14**	**-0.39**
M. californianus (mussel)	All sites	0.12	**-0.19**	**-0.18**	**0.32**	**0.17**
	Northern sites	**-0.22**	**0.22**	0.14	**0.08**	**0.02**
	Southern sites	**0.27**	**-0.25**	0.01	**0.27**	**0.14**

Note: Statistically significant correlations are represented in bold and based on 1000 permutations (p-value < 0.05)

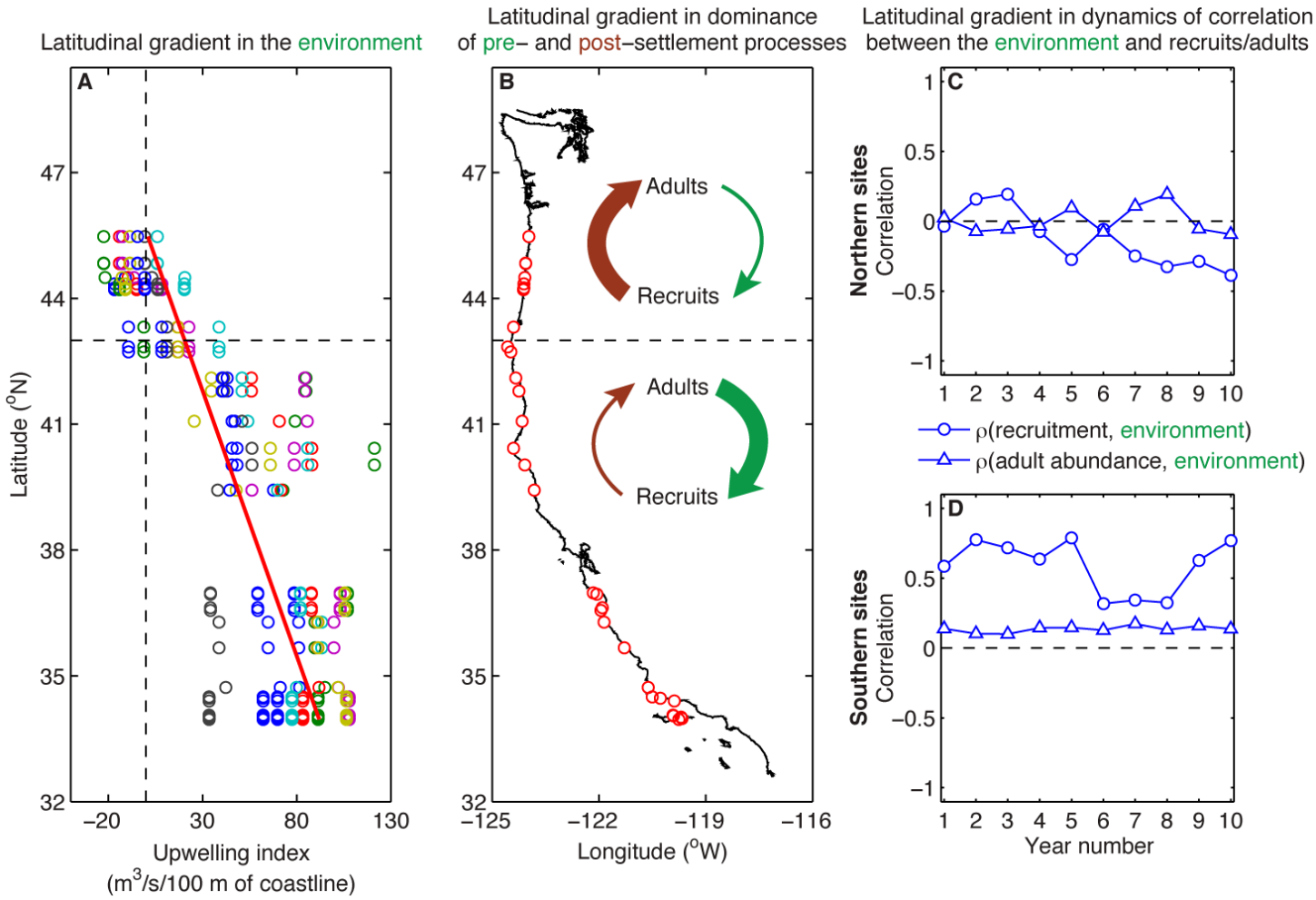
Latitudinal gradient in the environment
Latitudinal gradient in dominance of pre– and post–settlement processes
Latitudinal gradient in dynamics of correlation between the environment and recruits/adults
A
B
C
D
Latitude (°N)
Upwelling index (m³/s/100 m of coastline)
Longitude (°W)
Adults
Recruits
Adults
Recruits
Northern sites Correlation
Southern sites Correlation
ρ(recruitment, environment)
ρ(adult abundance, environment)
Year number

Figure 1

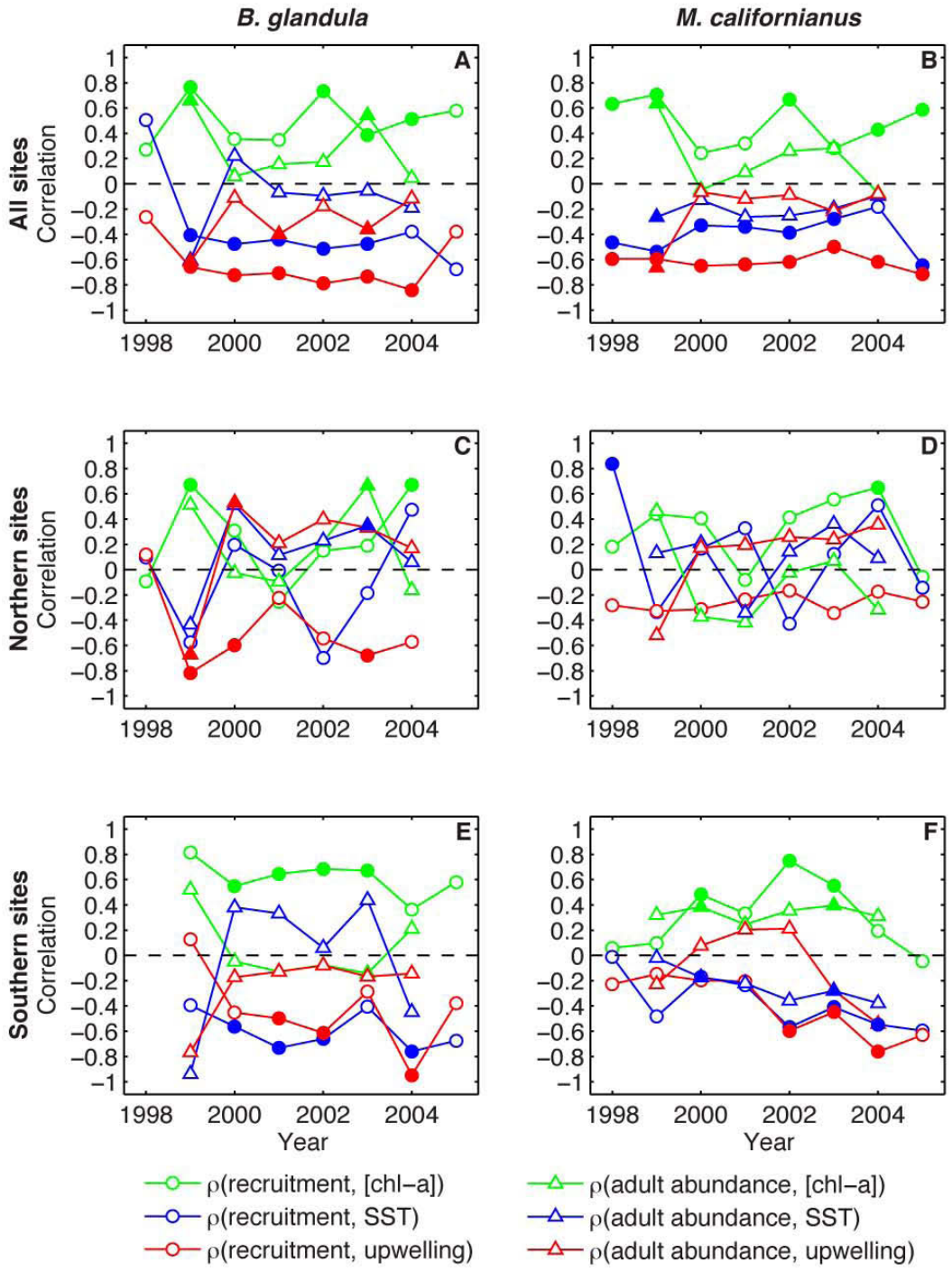
B. glandula
M. californianus
A
B
C
D
E
F
All sites
Northern sites
Southern sites
Correlation
1
0.8
0.6
0.4
0.2
0
−0.2
−0.4
−0.6
−0.8
−1
1998
2000
2002
2004
Year
ρ(recruitment, [chl−a])
ρ(recruitment, SST)
ρ(recruitment, upwelling)
ρ(adult abundance, [chl−a])
ρ(adult abundance, SST)
ρ(adult abundance, upwelling)

Figure 2

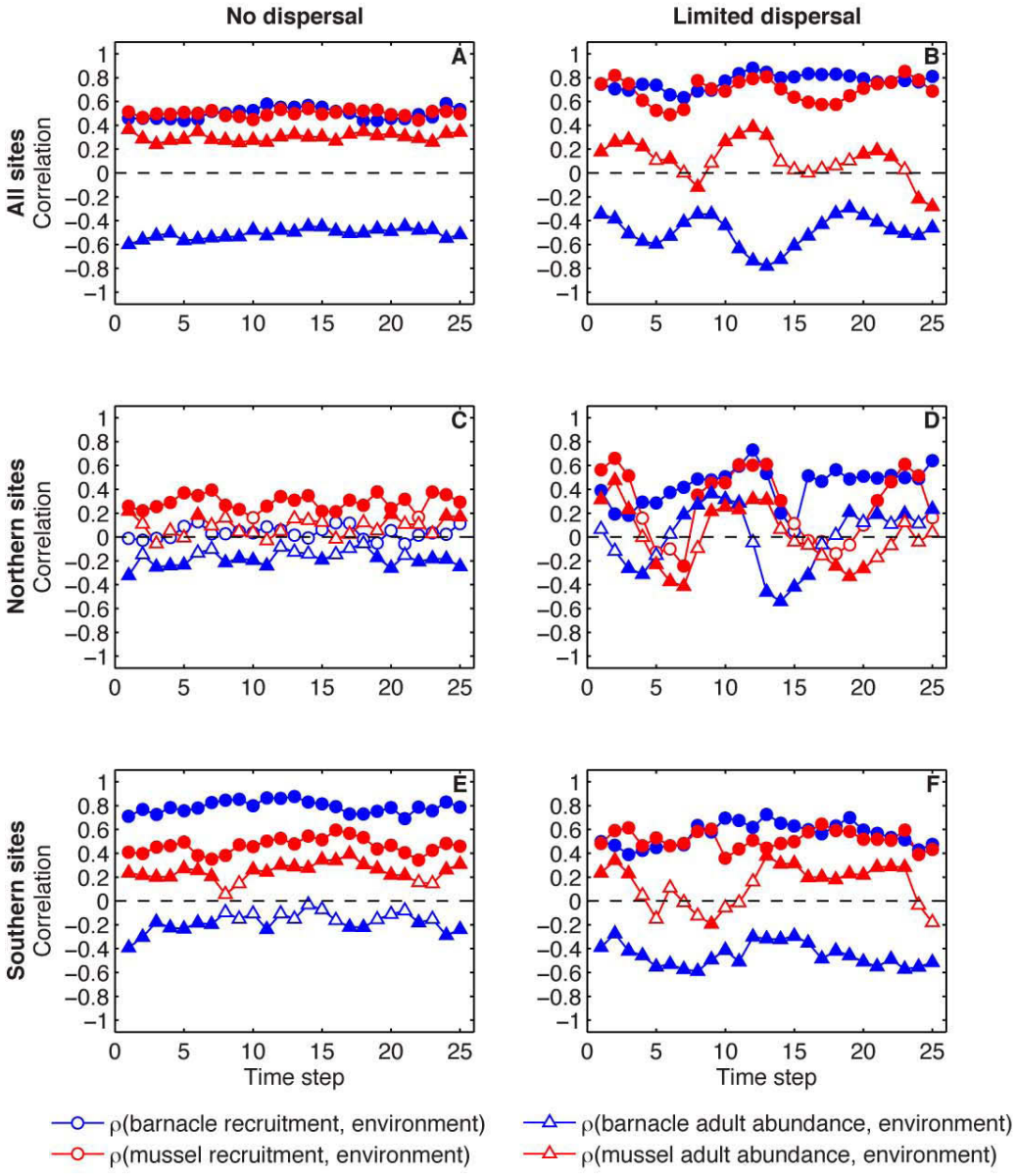
No dispersal
Limited dispersal
All sites
Correlation
Northern sites
Correlation
Southern sites
Correlation
A
B
C
D
E
F
Time step
Time step
ρ(barnacle recruitment, environment)
ρ(mussel recruitment, environment)
ρ(barnacle adult abundance, environment)
ρ(mussel adult abundance, environment)

Figure 3

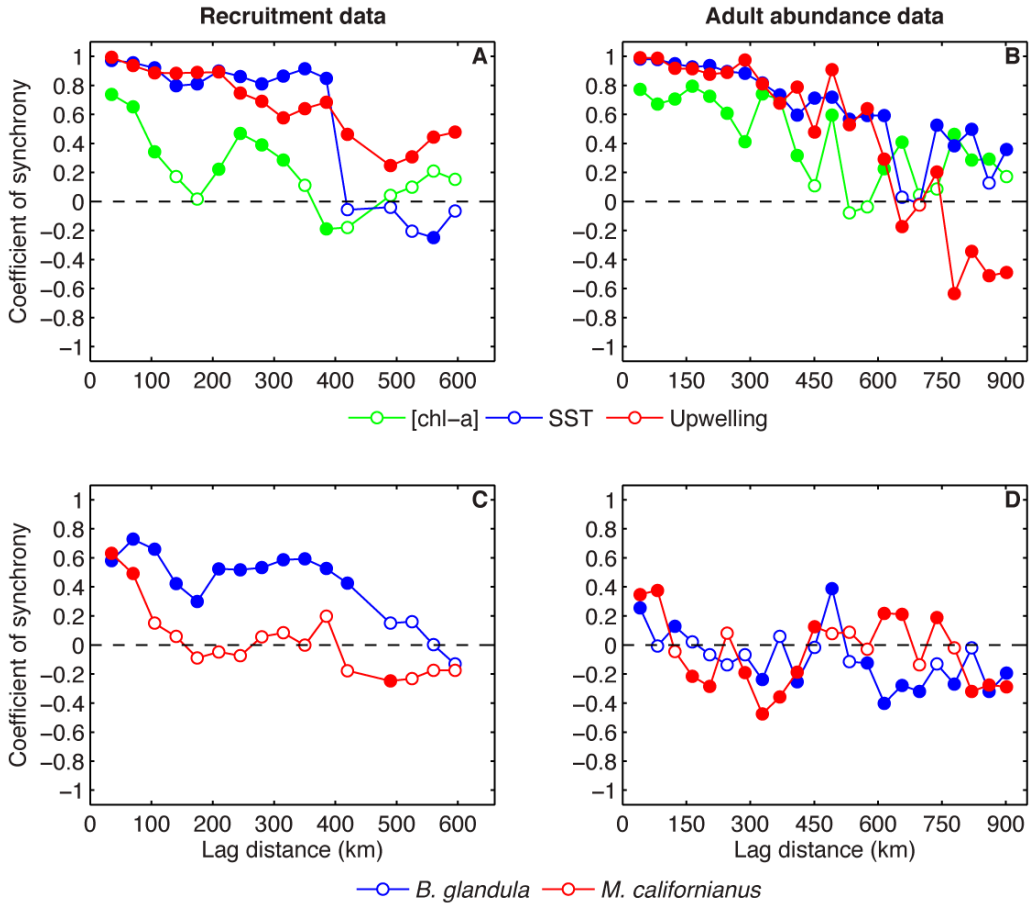
Recruitment data
Adult abundance data
A
B
C
D
Coefficient of synchrony
Lag distance (km)
[chl–a]
SST
Upwelling
B. glandula
M. californianus

Figure 4

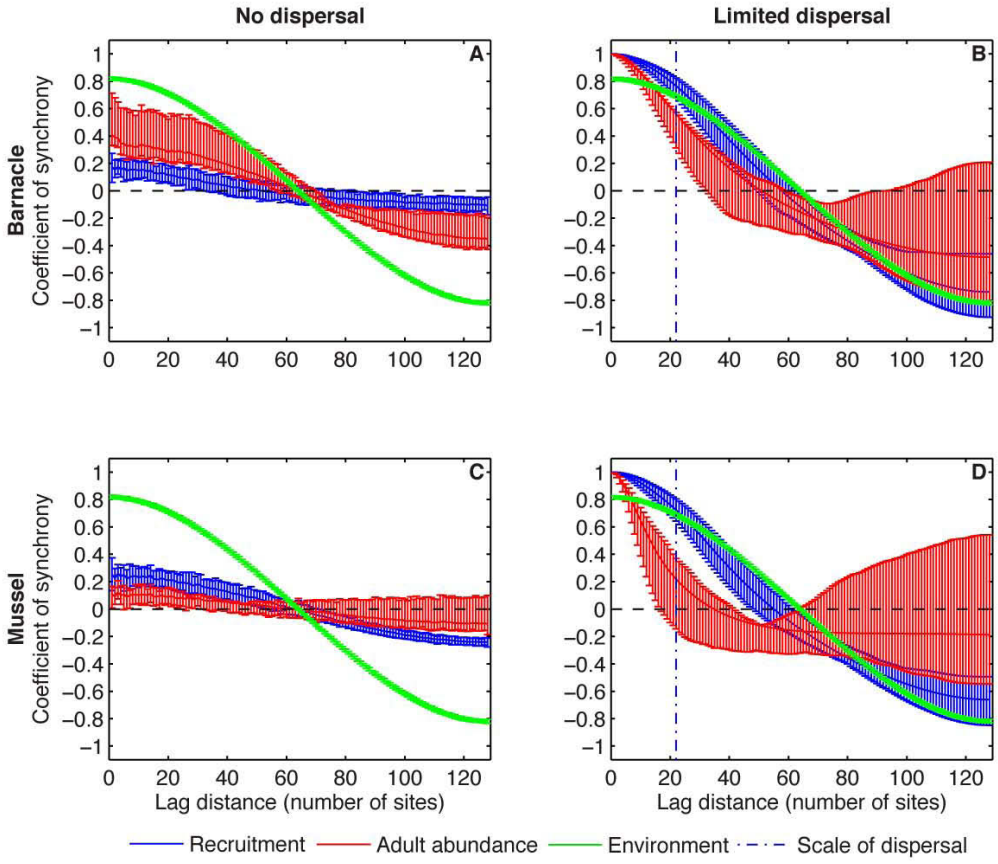
No dispersal
Limited dispersal
A
B
C
D
Barnacle
Mussel
Coefficient of synchrony
Lag distance (number of sites)
Recruitment
Adult abundance
Environment
Scale of dispersal

Figure 5

APPENDIX A

SPATIAL AND TEMPORAL PATTERNS OF RECRUITMENT IN INTERTIDAL METACOMMUNITIES ALONG THE WEST COAST OF THE UNITED STATES

FIGURE LEGENDS

Figure A1: The dynamics of the spatial correlation between mean annual recruitment and mean annual environmental conditions at different time lags from 1998 to 2004 across all sites (A-C), northern sites (D-F) and southern sites (G-I) for intertidal metacommunities along the West coast of the United States. Correlations at time lag time *t* represent the relationship between the mean annual recruitment in year *i* and the mean environmental conditions observed during year *i-t*. Full circles indicate statistical significance based on 1000 permutations ($p < 0.05$).

Figure A2: The mean annual environmental conditions (A, C, E) and the local temporal correlation between mean annual recruitment and mean annual environmental conditions (B, D, F) for *B. glandula* populations along the West coast of the United Sates. (A, C, E) Open circles represent mean annual environmental conditions at each site from 1998 to 2004 and the red lines represent the linear regression between each environmental variable and the latitude. (B, D, F) Positive and negative correlations are represented respectively in red and blue open circles. Circle size is proportional to correlation strength (maximum circle size corresponds to a correlation of 0.94). The horizontal dashed line represents the location of Cape Blanco (43°N).

Figure A3: Mean annual environmental conditions (A, C, E) and local temporal correlation between mean annual recruitment and mean annual environmental conditions (B, D, F) for *M. californianus* populations along the West coast of the United Sates. (A, C, E) Open circles represent mean annual environmental conditions at each site from 1998 to 2004 and the red lines represent the linear regression between each environmental variable and the latitude. (B, D, F) Positive and negative correlations are represented respectively in red and blue open circles. Circle size is proportional to correlation strength (maximum circle size corresponds to a correlation of 0.94). The horizontal dashed line represents the location of Cape Blanco (43°N).

FIGURES

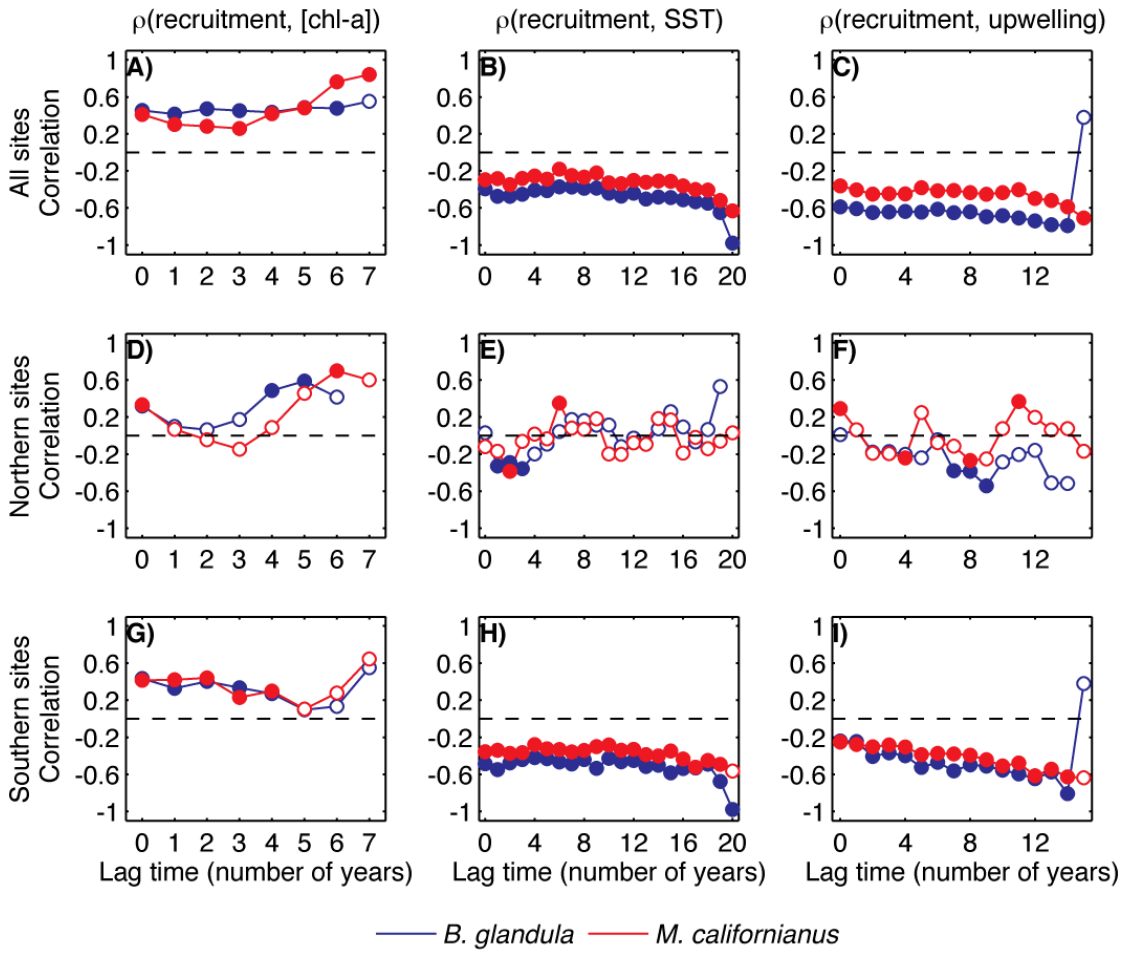

Figure A1

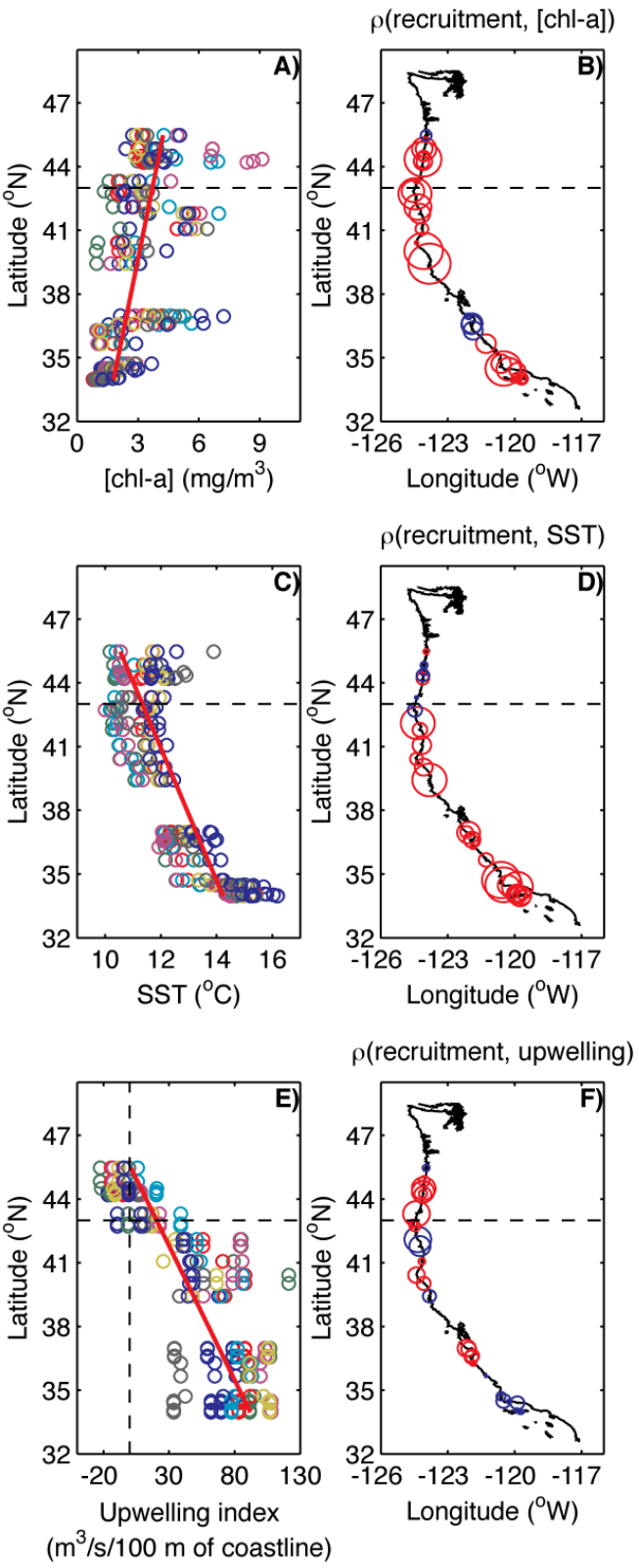
ρ(recruitment, [chl-a])
A)
B)
Latitude (°N)
47
44
41
38
35
32
0 3 6 9
[chl-a] (mg/m3)
-126 -123 -120 -117
Longitude (°W)
ρ(recruitment, SST)
C)
D)
10 12 14 16
SST (°C)
ρ(recruitment, upwelling)
E)
F)
-20 30 80 130
Upwelling index
(m3/s/100 m of coastline)

Figure A2

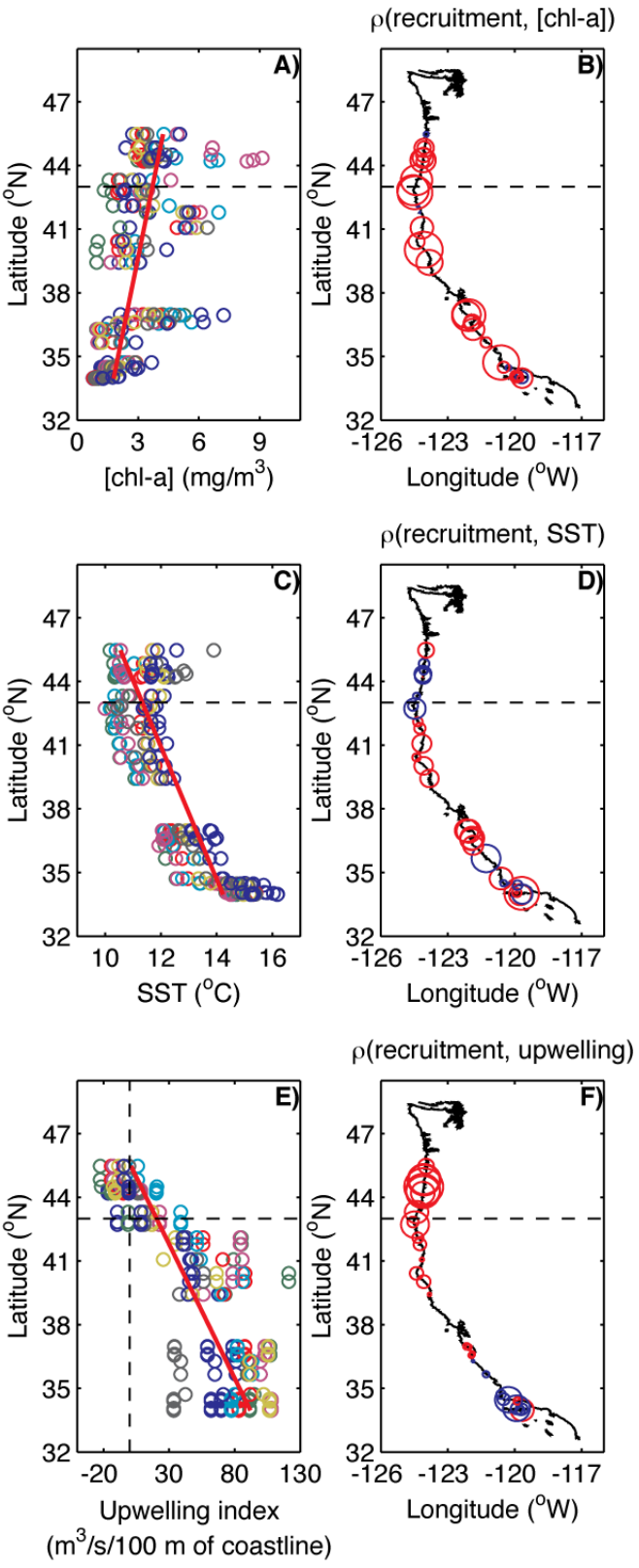
ρ(recruitment, [chl-a])
A)
B)
Latitude (°N)
47
44
41
38
35
32
0 3 6 9
[chl-a] (mg/m3)
-126 -123 -120 -117
Longitude (°W)
ρ(recruitment, SST)
C)
D)
10 12 14 16
SST (°C)
ρ(recruitment, upwelling)
E)
F)
-20 30 80 130
Upwelling index
(m3/s/100 m of coastline)

Figure A3

CONNECTING STATEMENT

In the previous chapters, I developed and validated a theory of marine intertidal systems that showed that local processes interact with limited dispersal and generate patterns of population abundance and connectivity at regional scales. I now investigate the implications of these regional patterns of connectivity for the implementation of marine reserve networks.

CHAPTER 3: DESIGNING EFFECTIVE MARINE RESERVE NETWORKS FOR DYNAMIC METAPOPULATIONS

Tarik C. Gouhier [1,*] and Frédéric Guichard [1]

[*] Corresponding author: tarik.gouhier@mail.mcgill.ca | Phone (514) 398-4120 | Fax: (514) 398-5069

[1] Department of Biology, McGill University, 1205 Avenue Docteur Penfield, Montreal, Quebec, H3A 1B1, Canada

Keywords: marine reserves, metapopulation, dispersal, connectivity

Status: In preparation

ABSTRACT

The proliferation of efficient and destructive fishing practices has promoted the depletion of commercial stocks around the world and caused significant collateral damage to marine habitats and non-commercial species. Recent work has shown that networks of marine reserves can serve both conservation and fishery management goals by protecting marine habitats and communities from collateral damage, and promoting the abundance of commercial species within reserves and in neighboring exploited areas. Theory predicts that marine reserves should be separated by the scale of dispersal of the target species in order to maintain connectivity among reserves. However, current theoretical models do not account for population dynamics and their ability to interact with dispersal to generate patterns of population abundance and connectivity at spatial scales that are much larger than the scale of dispersal.

Here, we use a dynamic metapopulation model to extend existing theory and show that the optimal spatial configuration of reserve networks depends on the rate of dispersal. Low rates of dispersal prevent the occurrence of patterns of population abundance and connectivity at large spatial scales. Under this scenario, the optimal size and spacing of marine reserves is the scale of dispersal. However, high rates of dispersal promote patterns of population abundance and connectivity at spatial scales that are larger than the scale of dispersal. In this case, using the scale of dispersal as the size and spacing of reserves reduces mean abundance, whereas using the scale of natural patterns of population abundance maximizes mean abundance. Additionally, we show that shifting the location of reserves in time reduces the performance gap

between suboptimal and optimal reserve networks, and thus provides a novel way of dealing with uncertainty about connectivity among marine populations.

Our approach emphasizes the importance of accounting for patterns of population abundance and connectivity imposed by the interaction between population dynamics and dispersal when designing marine reserve networks. Marine reserve networks that maintain these patterns maximize mean abundance and persistence in both protected and unprotected areas, and thus simultaneously satisfy conservation and fishery goals.

INTRODUCTION

Fisheries around the globe are collapsing under the weight of overexploitation (Botsford et al. 1997, Pauly et al. 1998, Pauly et al. 2002, Worm et al. 2006). Continuous socioeconomic pressure and technological advances have caused the serial depletion of commercial species and a progressive reduction in the mean trophic level of exploited marine stocks (Pauly et al. 1998, Pauly et al. 2002). The intensive and often destructive nature of large-scale commercial fishing practices has also inflicted significant collateral damage to non-commercial species and marine habitats (Botsford et al. 1997, Pauly et al. 2002, Carr et al. 2003). Marine reserves—areas protected from all destructive and extractive activities—can play an important role in reversing some of the harm caused by unsustainable fisheries (Allison et al. 1998, Halpern 2003, Lubchenco et al. 2003, Lester et al. 2009).

Recent reviews have shown that marine reserves protect marine habitats and increase the biomass, abundance, species richness and size of organisms within reserves (Halpern 2003, Lester et al. 2009). Additionally, the spillover of adults and

larvae from reserves into neighboring exploited areas can significantly improve fishery yields (Roberts et al. 2001, Gell and Roberts 2003). Indeed, theory has shown that managing fisheries via marine reserves produces yields that are equivalent to those obtained under traditional effort-based techniques (Hastings and Botsford 1999, Botsford et al. 2003). Hence, marine reserves can both protect endangered communities within and promote the growth of exploitable stocks beyond their borders.

The appeal of using marine reserves to serve both conservation and fishery goals has spurred much research into their optimal configuration (Hastings and Botsford 1999, Botsford et al. 2001, Hastings and Botsford 2003). Theory predicts that networks of marine reserves are better than single reserves of equivalent size because networks can buffer against catastrophes and variability in both environmental and oceanographic conditions (Allison et al. 1998, Allison et al. 2003, Gaines et al. 2003, Lubchenco et al. 2003). However, this buffer against extrinsic variability comes at a cost: the effectiveness of reserve networks is critically dependent upon the size and spacing of individual reserves (Botsford et al. 2001, Gaines et al. 2003, Hastings and Botsford 2003). The current consensus is that marine reserves should be separated by the scale of dispersal of the target species in order to maintain connectivity among reserves (Botsford et al. 2001, Botsford et al. 2003, Gerber et al. 2003, Shanks et al. 2003, Sale et al. 2005, Halpern et al. 2006). The optimal size of individual marine reserves then depends on the primary objective of reserve networks (Hastings and Botsford 2003). Reserve networks designed primarily to manage fisheries should be comprised of small reserves in order to maximize spillover into exploited areas, whereas reserve networks designed

to meet conservation targets should be comprised of large reserves that minimize spillover (Hastings and Botsford 2003, Sale et al. 2005).

However, these guidelines for optimal reserve configurations were derived using equilibrium models that largely ignore population fluctuations caused by natural disturbance-recovery (Paine and Levin 1981, Guichard et al. 2003, Guichard et al. 2004, Gouhier and Guichard 2007, Guichard and Steenweg 2008, Gouhier et al. *in press*) or predator-prey dynamics (Paine 1966, Jansen and de Roos 2000, Gouhier et al. *in press*). These population fluctuations are particularly germane to marine reserve design because they can interact with dispersal to generate complex patterns of population abundance in space and time that promote connectivity among populations over spatial scales that are larger than the scale of dispersal (Jansen and de Roos 2000, Guichard 2005, Gouhier et al. *in press*). Hence, using the scale of dispersal to build reserve networks for such systems could significantly diminish connectivity among reserves and thus potentially reduce mean population abundance and persistence.

Here, we extend existing theory by incorporating population fluctuations into a dynamic metapopulation model. We show that the optimal spatial configuration of reserve network depends on the maintenance of natural patterns of population abundance and connectivity between reserves. When low rates of dispersal prevent the occurrence of patterns of population abundance and connectivity at large spatial scales, the optimal size and spacing of reserves is the scale of dispersal. However, when high rates of dispersal promote patterns of population abundance and connectivity at spatial scales that are larger than the scale of dispersal, the optimal

size and spacing of reserves is the scale of patterns imposed by the interaction between population dynamics and dispersal.

METHODS

The model

We use a simple metapopulation model based on the bipartite life cycle commonly found in marine invertebrate species to investigate the effectiveness of marine reserves. Like previous frameworks, our model assumes that populations consist of sessile adults (in this case, mussels) whose planktonic larvae disperse to neighboring populations (Botsford et al. 2001, Botsford et al. 2003, Guichard et al. 2004, Guichard 2005). Within populations, the successional dynamic observed in natural intertidal systems (Paine and Levin 1981, Paine 1984) is represented as a mean-field implementation of a spatial process affecting the proportional abundance of (i) the dominant mussel (m), (ii) the wave disturbance (w) and (iii) the empty substrate (s) (Fig. 1A; Guichard et al. 2003). A maximum fraction $\alpha_0 = 1$ of the proportional abundance of the dominant mussel species (m) can be displaced by wave disturbances (w). A proportion $(1-\delta_0)$ of the disturbance displaces mussels through a density-dependent contact process with aggregation (Moore neighborhood, $q = 8$), while a proportion $\delta_0 = 10^{-3}$ of the disturbance is density-independent. This disturbance dynamic is based on the assumption that wave disturbances destroy the byssal thread attachments of mussels around the edges of disturbed areas, thus making them temporarily more susceptible to further disturbance (Denny 1987, Guichard et al. 2003). Hence, newly disturbed areas allow

the local propagation of wave disturbances to adjacent mussel beds. Once the disturbance has propagated away from the newly disturbed area, the area transitions from the 'wave disturbed' state to the 'empty substrate' state. Similarly to disturbance, a maximum fraction $\alpha_2 = 1$ of the empty substrate (s) can be colonized by mussels. A proportion $\delta_2 = 0.1$ of colonization occurs through a density-independent process, while the remaining colonization is density-dependent $(1-\delta_2)$. Mussel colonization also depends on the production and recruitment of larvae (Fig 1B). Within populations x, larval production is a function of local mussel proportional abundance (m_x) and fecundity f_x $(\bar{f} = 3.75)$. The recruitment rate C_x^t is described by a Poisson process (Caswell and Etter 1999) $C_x^t = 1 - e^{-\beta_x^t}$, where β_x^t integrates (i) the total number of larvae produced and retained in populations x at time t and (ii) the total number of larvae produced in other populations y and dispersed to populations x at time t (Fig 1B). The dynamics of the model are represented by the following integro-difference equation system for populations x in a metapopulation consisting of $n = 256$ populations:

$$\begin{aligned} w_x^{t+1} &= \alpha_0 m_x^t \left(\delta_0 + (1-\delta_0)\left(1-\left(1-w_x^t\right)^q\right)\right) \\ s_x^{t+1} &= w_x^t + s_x^t - \alpha_2 C_x^t s_x^t \left(\delta_2 + m_x^t (1-\delta_2)\right) \\ m_x^{t+1} &= 1 - w_x^t - s_x^t \end{aligned} \qquad (1)$$

with:

$$
\begin{aligned}
C_x^t &= 1 - e^{\beta_x^t} \\
\beta_x^t &= m_x^t f_x (1-d) + \int m_y^t f_y \, dD(|x-y|) \mathrm{d}y \\
D(|x-y|) &= \frac{3|x-y|^2}{2} e^{-|x-y|^3} \\
x &= u\left(\frac{2}{n}\mathbf{L} - 1\right) \\
\mathbf{L} &= [0,...,n-1]
\end{aligned}
\qquad (2)
$$

where D is the mussel dispersal kernel resulting from larval transport at a constant speed and with a time-dependent settlement rate (double Weibull distribution, Fig. 1B; see Neubert et al. (1995)), d represents the proportion of larvae being dispersed, u represents the scale of dispersal and **L** represents a zero-based vector of population locations. The mean scale of dispersal was kept constant at 8.6% of the spatial extent for all simulations by setting $u = 10$. We applied periodic boundary conditions to the model and simulated the dynamics for 256 coastal populations. The model has been shown to produce complex dynamical patterns for a broad range of parameter values that control both local and regional dynamics (Guichard 2005, Guichard and Steenweg 2008, Gouhier et al. *in press*). Here, we use parameter values that generate irregular abundance cycles within populations and complex spatiotemporal patterns of abundance at the regional scale to assess the effectiveness of marine reserve networks for dynamic metapopulations. The predictions of the model have been validated in natural intertidal systems along the West coast of the United States (Gouhier et al. *in press*).

Implementing marine reserve networks

We follow existing frameworks (Botsford et al. 2001, Botsford et al. 2003) and model marine reserve networks by varying larval production (i.e. fecundity) spatially (Fig 1C). Although previous studies have used a square wave to describe the spatial variation in larval production (Botsford et al. 2001, Botsford et al. 2003), we use a sinusoidal function to simulate a more gradual change in fecundity across space (Fig 1C). However, both the traditional square wave and the sinusoidal function yield qualitatively similar results. The amplitude λ of the sinusoidal function controls the difference in fecundity between the center of marine reserves and the center of unprotected areas, whereas the frequency φ of the sinusoidal function controls the size and the spacing of marine reserves (Fig 1C). Implementing marine reserves in a metapopulation of N populations thus yields fecundity $f(p)$ for population p along the coastline:

$$f(p) = \lambda \cdot \sin\left(2\pi\varphi \frac{p}{N}\right) + \bar{f} \qquad (3)$$

where λ and φ are respectively the amplitude and the frequency of the sinusoidal function and $\bar{f} = 3.75$ is the global mean fecundity. Since the frequency φ of the sinusoidal function controls both the spacing and the size of reserves (i.e. φ = size of individual reserves = distance between reserves), these parameters cannot be manipulated independently. Nevertheless, our results are robust to more traditional marine reserve implementations in which the spacing and the size of reserves remain unlinked (Botsford et al. 2001). We keep the total protected area in our simulations constant at 50% of the coastline, a value that falls within the range

(20-70%) advocated by both theoretical (Game et al. 2009) and applied (Airame et al. 2003, Gell and Roberts 2003) studies.

We chose to implement marine reserves without assuming that they would boost global mean fecundity. Hence, for all of our simulations, the global mean fecundity was kept constant $\left(\bar{f} = 3.75\right)$: marine reserve networks merely change the spatial distribution of fecundity without affecting its global mean. Our study thus describes the worst case scenario whereby marine reserves do not reduce exploitation overall but displace it beyond their boundaries (Ewers and Rodrigues 2008): increased fecundity in protected areas is offset by a concomitant decrease of fecundity in unprotected areas. However, our results also apply when this assumption is relaxed and marine reserves boost global mean fecundity.

We evaluated the effectiveness of four main types of marine reserve networks for metapopulations with either low $\left(d = 0.4\right)$ or high $\left(d = 1.0\right)$ rates of dispersal. We first tested a null marine reserve network by which protected sites were allocated randomly. The second type of reserve network consisted of protecting the most abundant sites based on a snapshot of the entire metapopulation at time step $t = 1000$. For the third type of reserve network, we used the scale of dispersal as the size and spacing of marine reserves. The final type of reserve network consisted of using the scale of patchiness as the size and spacing of marine reserves. Since marine reserve implementations vary from partially- to fully- protected reserve areas (Lester et al. 2009), we evaluated each of our four types of reserve networks for a range of protection levels by varying the amplitude λ of the sinusoidal function describing the spatial variation in fecundity f such that $0 < \lambda \leq \bar{f}$. This allowed us to assess

the performance of fully-protected ($\lambda = \bar{f}$: difference in fecundity of 100% between protected and unprotected areas) and partially-protected reserves ($0 < \lambda < \bar{f}$: difference in fecundity of <100% between protected and unprotected areas).

Additionally, we tested the effect of alternating the location of protected and unprotected areas in time by systematically shifting the phase of the sinusoidal function describing the spatial distribution of fecundity at each τ^{th} time step for fully-protected reserves ($\lambda = \bar{f}$). These dynamic shifts were performed for a series of different periods τ such that:

$$f(p,t,\tau) = \bar{f} \cdot \sin\left(2\pi\varphi\frac{p}{N} + \theta_\tau\right) + \bar{f} \qquad (4)$$

where $f(p,t,\tau)$ is the fecundity of population p at time t, $\bar{f} = 3.75$ is the mean fecundity, φ is the frequency of the sinusoidal function, $N = 256$ is the total number of populations and $\theta_\tau = \left\lfloor \frac{t}{\tau} \right\rfloor \pi$ defines the phase shift undergone by the spatial distribution of fecundity $f(p,t,\tau)$ for each period τ. These dynamic shifts in the location of protected areas were applied to marine reserves whose size and spacing were based on (i) the scale of dispersal and (ii) the scale of patchiness. All simulations were run for a total of 3000 time steps: from time step 0 to 1000 without reserves and from time step 1001 to 3000 with reserves. The analyses were conducted over the last 1000 time steps in order to avoid transient dynamics.

Model analysis

Measuring the temporal and spatial scales of patterns

We applied the autocorrelation function (ACF) to the mussel abundance in order to (i) quantify naturally-occurring patterns in the absence of marine reserves and (ii) assess the impact of marine reserves on pattern formation in metapopulations consisting of $N = 256$ populations. The ACF measures the correlation c_k of a given variable (here, mussel abundance m) between pairs of populations as a function of the lag distance k that separates them (Fortin and Dale 2005):

$$c_k = \frac{\frac{1}{N}\sum_{i=1}^{N-k}(m_i - \bar{m})(m_{i+k} - \bar{m})}{\frac{1}{N}\sum_{i=1}^{N}(m_i - \bar{m})^2} \qquad \text{for } k = 0,1,2,...,K \qquad (5)$$

Here, we apply the ACF in space and time to quantify the spatial and temporal patterns in the metapopulation model. For each marine reserve design we used the spatial range $k|_{c_k=0}$, defined as the spatial lag at which the ACF first reaches zero (Fig 1F), to quantify the scale of patchiness in the metapopulation (Fortin and Dale 2005). Specifically, for each of the 1000 post-transient time steps t, the ACF was applied across the entire metapopulation to calculate the spatial range $k|^{t}_{c_k=0}$. The average across those 1000 time steps was then defined as the scale of patchiness.

We also used the ACF to measure the temporal patterns in the metapopulation. To quantify the residence time of abundance cycles within populations (i.e. local cycles), we applied the ACF to each population across 1000 time steps and calculated the temporal range, which is analogous to the spatial range

and defined as the temporal lag at which the ACF first reaches zero. We then averaged the temporal range across all populations to quantify the residence time of local cycles. This provided us with a measure of the average duration or residence time of local abundance cycles.

We also used the temporal ACF to measure the return time of local cycles by determining the non-zero temporal lag $k\big|^{k\neq 0}_{c_k=\max(c_k)}$ at which the ACF reaches a maximum. Finally, we used the spatial ACF to quantify the return time of regional patterns. This was accomplished by applying the ACF and measuring the spatial range $k\big|^{t}_{c_k=0}$ for each post-transient time step t. The non-zero time lag T that minimized the mean absolute difference in spatial range Δ_T was used as the return time of regional patterns:

$$\Delta_T = \frac{1}{N}\sum_{t=1}^{N}\left| k\big|^{t}_{c_k=0} - k\big|^{t+T}_{c_k=0} \right| \qquad \text{for } T = 1,2,3,...,K \qquad (6)$$

The effect of marine reserves on synchrony and extinction risk

Kendall's coefficient of concordance was used as a measure of synchrony among populations. Kendall's coefficient of concordance is a nonparametric statistic that quantifies the association between multiple ranked variables with values that range from 0 to 1 (Zar 1999). It is commonly used to measure the level of agreement among several rankings and, as such, has been suggested as the most effective method for determining synchrony among multiple data series (Buonaccorsi et al. 2001). The calculation was performed by first ranking (R_i) the abundance time

series of each population. Kendall's coefficient of concordance (Φ) was then calculated as (Zar 1999):

$$\Phi = \frac{\sum R_i^2 - \frac{\left(\sum R_i\right)^2}{n}}{\frac{S^2\left(n^3 - n\right) - S\sum \tau}{12}} \qquad (7)$$

where $S = 256$ represents the total number of populations, $n = 1000$ represents the total number of post-transient time steps, and $\sum \tau$ is an adjustment for tied ranks within each population such that for t_i ties in the i^{th} group of ties and j groups of tied ranks:

$$\sum \tau = \sum_{i=1}^{j} (t_i^3 - t_i) \qquad (8)$$

We also quantified the effect of marine reserve networks on metapopulation persistence by measuring the probability of extinction of the entire metapopulation in response to a global disturbance, which we defined as normally-distributed white noise with zero mean and variance 0.7 (Earn et al. 2000). The global disturbance was applied to the abundance of each population at each time step and the probability of extinction was calculated by determining the proportion of time steps for which all populations saw their abundance reach zero.

RESULTS

The relevance of naturally-occurring patterns for designing marine reserve networks

The cost of ignoring patterns

Marine reserve networks based on the protection of random sites or the protection of the most abundant sites (at a given time *t*) ignore naturally-occurring patterns of population abundance in space and time. In doing so, they impose spatial patterns of variation in fecundity that have deleterious effects on metapopulations with either low or high rates of dispersal (Fig 2). The deleterious effects of these marine reserve networks depend on the rate of dispersal. Indeed, dispersal acts as a low-pass filter on fecundity for all dispersed larvae (Roughgarden 1974). Hence, only marine reserve networks that alter fecundity at spatial scales that are larger than or equal to the scale of dispersal will have an effect on the dispersed larvae.

When the rate of dispersal is low (d=0.4), locally retained larvae are not filtered by the low-pass dispersal filter and thus respond to the spatial variation in fecundity induced by marine reserve networks (Fig 2A,C,E,G). In this case, marine reserve networks based on the protection of random or the most abundant sites reduce the scale of patchiness, promote extinction risk and reduce global mean abundance (Fig 2A,E,G). The strength of these effects increases with the level of protection within reserves (Fig 2 A,C,E,G). Since the rate of dispersal is low, synchrony remains low and largely impervious to the implementation of marine reserve networks (Fig 2C).

When the rate of dispersal is high (d=1.0), all larval production is filtered by dispersal (Roughgarden 1974). Hence, only variation in fecundity at spatial scales that are larger than that of dispersal will affect metapopulations. Since marine reserve networks based on the random allocation of protected sites lead to spatial variation in fecundity at spatial scales that are much smaller than that of dispersal, they have no discernable effect on the metapopulation (Fig 2B,D,F,H). For marine reserve networks based on the protection of the most abundant sites, increasing the level of protection within reserves reduces global mean abundance and increases extinction risk without affecting the scale of patchiness or synchrony (Fig 2B,D,F,H).

Using patterns to optimize the spatial configuration of marine reserve networks

We have shown that ignoring natural patterns of population abundance when implementing marine reserve networks can lead to counterproductive results. We now show that the optimal spatial scale of marine reserve networks depends on the rate of dispersal and its effect on patterns of population abundance. Low dispersal rates limit patterns of population abundance and connectivity at large spatial scales (Fig 1D-F, compare the scale of patchiness in Fig 2A vs. 2B, Fig B1), and thus promote the scale of dispersal as the optimal spatial scale for marine reserve networks (Fig 2,3). However, high dispersal rates generate regional patterns of population abundance (Fig 1E-F, Fig 2A vs. 2B, Fig B2) and thus promote the scale of patchiness as the optimal spatial scale for marine reserve networks (Fig 2,3).

Indeed, when the rate of dispersal is low (d=0.4), increasing the level of protection within reserves leads to an increase in global mean abundance and a reduction in extinction risk for marine reserve networks based on the scale of

dispersal (Fig 2E,G). Synchrony and the scale of patchiness remain unchanged (Fig 2A,C). When the level of protection within reserves is maximal, the scale of dispersal is the optimal spatial scale for the size and spacing of marine reserves (Fig 3A,C,E,G). Indeed, using the scale of dispersal to implement marine reserve networks maximizes global mean abundance, mean abundance in both protected sites and unprotected sites and minimizes extinction risk (Fig 3C,E,G). However, for marine reserve networks based on the scale of patchiness, increasing the level of protection of marine reserves reduces global mean abundance and promotes extinction risk (Fig 2E,G).

Conversely, when the dispersal rate is high (d=1.0), increasing the level of protection within reserves reduces global mean abundance and increases extinction risk for marine reserve networks based on the scale of dispersal (Fig 2F,H). Additionally, marine reserve networks based on the scale of dispersal destroy naturally-occurring patterns by inducing synchrony (Fig 2B,D). When marine reserve networks are based on the scale of patchiness, increasing the level of protection within reserves increases global mean abundance and reduces extinction risk without affecting the scale of patchiness or synchrony (Fig 2B,D,F,H). When the level of protection within reserves is maximal, the scale of patchiness is the optimal spatial scale for the size and spacing of marine reserves (Fig 3D,F,H). Indeed, using the scale of patchiness to implement marine reserve networks maximizes global mean abundance, mean abundance in both protected sites and unprotected sites, and minimizes extinction risk (Fig 3D,F,H).

Righting the wrongs: the restorative properties of dynamic marine reserve networks

We now investigate the effect of alternating the location of protected and unprotected sites in time on the effectiveness of marine reserve networks based on the scale of dispersal or the scale of patchiness. When the rate of dispersal is low (d=0.4), dynamically alternating the location of protected and unprotected sites at temporal scales that are larger than the return time of local abundance cycles (i.e. 11-40 time steps) promotes global mean abundance and reduces extinction risk without affecting the scale of patchiness or synchrony for marine reserve networks based on the scale of dispersal or the scale of patchiness (Fig 4A,C,E,G). Global mean abundance for reserve networks based on the scale of patchiness and those based on the scale of dispersal are equivalent for dynamic reserves at temporal scales ~11-40 time steps (table A1).

When the rate of dispersal is high (d=1.0), dynamic reserve networks based on the scale of dispersal perform much better than their static counterparts (Fig 4B,D,F,H; Fig B1A,C). Dynamically alternating the location of protected and unprotected sites at temporal scales that fall between the residence time and the return time of local abundance cycles (i.e. 5-11 time steps) leads to a large increase in global mean abundance and a consequent decrease in extinction risk (Fig 4F,H, table A2). This phenomenon is analogous to the effect of dispersal as a low-pass filter on spatial variation in fecundity. Here, dispersal 'smoothes' the variation in fecundity in space and time as long as the spatial distribution of fecundity is dynamically shifted at temporal scales that are smaller than the return time of local abundance cycles (Fig

B1C). Hence, by frequently shifting the spatial distribution of reserves, dynamic designs counteract the deleterious effects of static reserve networks by preventing the onset of synchrony and resurrecting natural patterns (Fig 4B,D; Fig B1A,C). When reserve networks are based on the scale of patchiness, dynamic shifts occurring at temporal scales that are smaller than the return time of regional patterns decrease global mean abundance (Fig 4H). Only when dynamic shifts occur at temporal scales that are larger than the return time of regional patterns does global mean abundance increase (Fig 4H; Fig B1B,D; table A2). These results show that dynamic marine reserve networks can benefit metapopulations regardless of the rate of dispersal by (i) counteracting the deleterious effects associated with the implementation of static reserve networks based on the wrong spatial scales and (ii) improving the performance of static reserve networks based on the optimal spatial scales (table A1-2).

Additionally, we show that the effectiveness of static and dynamic reserve networks can be explained by understanding the interaction between population dynamics and dispersal, and its effect on spatial patterns of population abundance, recruitment and connectivity (Appendix C).

DISCUSSION

Our work extends existing theory by showing that reserve networks must account for natural patterns of population abundance and connectivity generated by the interaction between dispersal and population dynamics. Marine reserve networks that embrace these natural patterns maximize abundance and persistence in both protected and unprotected areas, and thus simultaneously fulfill conservation and

fishery management goals. Additionally, we show that dynamic marine reserve networks can mitigate the risks associated with selecting the wrong spatial configuration, thus extending the applicability of reserve networks to marine systems for which connectivity remains either poorly documented or completely unknown.

Designing optimal marine reserve networks

Current theory suggests that marine reserve networks should maintain connectivity among reserves by using the scale of dispersal of the target species as the distance between reserves (Botsford et al. 2001, Botsford et al. 2003, Gerber et al. 2003, Halpern et al. 2006). However, this assumes that the scale of dispersal and the scale of connectivity are one and the same. This assumption is correct for equilibrium metapopulations, but not necessarily correct for nonequilibrium metapopulations. Indeed, successional (Guichard et al. 2004, Guichard 2005, Gouhier and Guichard 2007, Gouhier et al. *in press*) and predator-prey (Jansen and de Roos 2000, Gouhier et al. *in press*) dynamics can induce strong population fluctuations in nonequilibrium metapopulations. These fluctuations can interact with dispersal to generate patterns of population abundance and connectivity at spatial scales that are much larger than the scale of dispersal (Jansen and de Roos 2000, Guichard et al. 2004, Guichard 2005, Gouhier et al. *in press*).

We show that in such nonequilibrium metapopulations, the rate of dispersal controls the scale of patchiness and connectivity. When low rates of dispersal limit patterns of population abundance and connectivity, the optimal size and spacing of marine reserves is the scale of dispersal. When high rates of dispersal promote patterns of population abundance and connectivity over scales that are much larger

than the scale of dispersal, using the scale of dispersal as the size and spacing of marine reserves reduces mean population abundance and persistence. However, using the scale of patchiness imposed by natural patterns as the size and spacing of marine reserves maximizes mean population abundance and persistence. These results highlight the importance of using the scale of connectivity, which may or may not be the same as the scale of dispersal, in order to design effective marine reserve networks. Reserve networks that account for natural patterns of population abundance and connectivity facilitate the recruitment of larvae into populations undergoing favorable conditions and thus maximize overall productivity, persistence and abundance. Recruitment subsidies from (optimally) protected sites maximize abundance in unprotected sites and thus allow these reserve networks to (optimally) satisfy both conservation and fishery goals.

Managing uncertainty in marine systems by using dynamic reserve networks

Uncertainty exerts a strong influence on the design and effectiveness of marine reserves (Allison et al. 1998, Allison et al. 2003, Botsford et al. 2003, Halpern et al. 2006). Periodic catastrophes (Allison et al. 2003), variable oceanographic currents (Gaines et al. 2003) and environmental change (Allison et al. 1998) favor the development of reserve networks instead of single reserves of the same size. The spatial redundancy afforded by reserve networks provides a natural protection against localized catastrophes (Allison et al. 2003) and reduces, to a certain extent, the impact of regional oceanographic and environmental variability (Gaines et al. 2003). However, the effectiveness of reserve networks is highly dependent upon

their spatial configuration (Botsford et al. 2001, Gaines et al. 2003). Indeed, as we have shown (Fig 2-4, Appendix C), the effectiveness of marine reserve networks depends on their ability to maintain connectivity among individual marine reserves. However, connectivity and dispersal are poorly understood in marine systems and subject to considerable oceanographic and environmental variability (Botsford et al. 2001, Botsford et al. 2003, Grantham et al. 2003, Halpern et al. 2006). Hence, the performance of marine reserve networks is highly susceptible to uncertainty about the rates and scales of dispersal and connectivity (Botsford et al. 2001, Botsford et al. 2003).

The simplest way of dealing with this source of uncertainty is to increase the size of individual marine reserves by a predetermined insurance factor (Allison et al. 2003). Larger reserves are more likely to be self-sufficient and thus less dependent upon the uncertain arrival of subsidies from neighboring reserves. However, making reserves larger reduces spillover into neighboring exploited areas and thus limits the potential of reserve networks to fulfill fishery management goals (Hastings and Botsford 2003, Sale et al. 2005). Uncertainty about connectivity and dispersal can also be built into models of marine reserve networks in order to determine the optimal spatial configuration under different scenarios (Halpern et al. 2006). Here, we show that dynamic reserve networks can provide an alternative method for dealing with uncertain patterns of connectivity among reserves.

Dynamic reserves are being increasingly championed because they can (1) track dynamic resources, (2) prevent diminishing returns by shifting protection from recovered sites to vulnerable sites, and (3) allow access to resources accrued within recovered sites (Game et al. 2009). Here, we show that shifting the location of

protected and unprotected sites can significantly reduce the performance gap between reserve networks that are based on the true scale of connectivity and those that are not. Indeed, dynamic reserve networks are able to track the spatiotemporal patterns of abundance generated by the interaction between population fluctuations and dispersal, even if reserve networks are based on the wrong spatial scale of connectivity. Hence, dynamic reserves can limit the risks associated with implementing marine reserve networks when patterns of connectivity are uncertain or unknown.

However, the success of dynamic reserves is dependent upon the temporal scale at which the protection of sites is shifted. Recent theory has shown that dynamic reserve networks can increase herbivore density in coral reef systems as long as the temporal shifts in the location of reserves occur at the proper temporal scale (Game et al. 2009). Indeed, reserves must be maintained long enough to allow sites to fully recover (Gerber et al. 2003, Claudet et al. 2008), but not so long as to result in diminished returns (Game et al. 2009). Here, we show that in dynamic metapopulations, the optimal temporal scale for switching the location of reserves depends on the temporal scale of population fluctuations. When the location of reserves is shifted at the proper temporal scale (between the residence time and the return time of population cycles when dispersal is low and after the return time of regional patterns when dispersal is high), dynamic reserve networks can perform better than optimal static reserve networks (table A1-2). Hence, our work demonstrates that by implementing dynamic marines, one can trade-off the need for spatial information about connectivity at the regional scale for temporal information about population abundance at the local scale.

FIGURE LEGENDS

Figure 1: Diagram of the metapopulation model and description of its dynamics. (A) Local successional dynamic within each population is based on the interplay between the propagation of wave disturbances (w) within mussel beds (m) and the subsequent recolonization of empty substrate (s) by mussels. (B) A fraction *d* of mussel larvae disperse to neighboring populations via a symmetrical dispersal kernel whose mean distance represents 8.6% of the spatial extent of the metapopulation. (C) Marine reserves (protected sites) are allocated by varying fecundity spatially using a sinusoidal function. The blue (red) sections of the curve represent sites that are designated as protected (unprotected) sites and the blue (red) filled circles indicate the center of marine reserves (unprotected areas) where fecundity is maximal (minimal). The vertical dashed line represents the mean fecundity across the metapopulation, which is kept constant at 3.75 for all simulations. (D, E) The effect of dispersal on metapopulation time series as illustrated by two extreme cases. In the absence of dispersal (D), populations fluctuate independently thereby preventing pattern formation (F). When the rate of dispersal is high (E), population fluctuations interact with dispersal to generate patchiness and abundance and connectivity at spatial scales that are larger than the scale of dispersal (F).

Figure 2: The effect of varying the level of protection within reserves on the scale of patchiness (A, B), synchrony (C, D), the probability of extinction (E, F) and global mean abundance (G, H) for metapopulations with low (d=0.4, first column) and high (d=1.0, second column) rates of dispersal. The level of protection within reserves represents the percentage difference in fecundity between protected and unprotected sites. Each curve corresponds to a different marine reserve design: random allocation

of protected sites (black), protection of the most abundant sites at the onset of the simulations (green), protection of sites separated by the scale dispersal (blue) and protection of sites separated by the scale of patchiness (red). The results represent the means and standard errors from 10 replicate simulations.

Figure 3: The effect of varying the distance between marine reserves on synchrony (A, B), the probability of extinction (C, D), global mean abundance (E, F) and the mean abundance in protected (blue) and unprotected sites (red) (G, H) for metapopulations with low (d=0.4, first column) and high (d=1.0, second column) rates of dispersal. Here, the level of protection within reserves is set to the maximum. Blue and red vertical dashed lines represent respectively the scale of dispersal and the scale of patchiness. The results represent the means and standard errors from 10 replicate simulations.

Figure 4: The effect of dynamically alternating the location of protected and unprotected areas in time on the scale of patchiness (A, B), synchrony (C, D), the probability of extinction (E, F) and global mean abundance (G, H) for metapopulations with low (d=0.4, first column) and high (d=1.0, second column) rates of dispersal. Here, the level of protection within reserves is set to the maximum. Each curve represents a different type of marine reserve design: protection of sites separated by the scale of dispersal (blue) and protection of sites separated by the scale of patchiness (red). Black, blue and red vertical dashed lines represent respectively the residence time of local cycles, the return time of local cycles and the return time of regional patterns. The horizontal green dashed lines indicate the global mean abundance from baseline simulations in which marine

reserves are allocated statically. The results represent the means and standard errors from 10 replicate simulations.

ACKNOWLEDGEMENTS

We acknowledge the granting agencies that made this research possible. T.G. was supported by a McGill Majors fellowship and F.G. was supported by a grant from the James S. McDonnell foundation.

LITERATURE CITED

Airame, S., J. E. Dugan, K. D. Lafferty, H. Leslie, D. A. McArdle, and R. R. Warner. 2003. Applying ecological criteria to marine reserve design: A case study from the California Channel Islands. Ecological Applications **13**:S170-S184.

Allison, G. W., S. D. Gaines, J. Lubchenco, and H. P. Possingham. 2003. Ensuring persistence of marine reserves: Catastrophes require adopting an insurance factor. Ecological Applications **13**:S8-S24.

Allison, G. W., J. Lubchenco, and M. H. Carr. 1998. Marine reserves are necessary but not sufficient for marine conservation. Ecological Applications **8**:S79-S92.

Botsford, L. W., J. C. Castilla, and C. H. Peterson. 1997. The Management of Fisheries and Marine Ecosystems. Science **277**:509-515.

Botsford, L. W., A. Hastings, and S. D. Gaines. 2001. Dependence of sustainability on the configuration of marine reserves and larval dispersal distance. Ecology Letters **4**:144-150.

Botsford, L. W., F. Micheli, and A. Hastings. 2003. Principles for the design of marine reserves. Ecological Applications **13**:S25-S31.

Buonaccorsi, J. P., J. S. Elkinton, S. R. Evans, and A. M. Liebhold. 2001. Measuring and testing for spatial synchrony. Ecology **82**:1668-1679.

Carr, M. H., J. E. Neigel, J. A. Estes, S. Andelman, R. R. Warner, and J. L. Largier. 2003. Comparing marine and terrestrial ecosystems: Implications for the design of coastal marine reserves. Ecological Applications **13**:S90-S107.

Caswell, H. and R. Etter. 1999. Cellular automaton models for competition in patchy environments: Facilitation, inhibition, and tolerance. Bulletin of Mathematical Biology **61**:625-649.

Claudet, J., C. W. Osenberg, L. Benedetti-Cecchi, P. Domenici, J.-A. Garcia-Charton, A. Perez-Ruzafa, F. Badalamenti, J. Bayle-Sempere, A. Brito, F. Bulleri, J.-M. Culioli, M. Dimech, J. M. Falcon, I. Guala, M. Milazzo, J. Sanchez-Meca, P. J. Somerfield, B. Stobart, F. Vandeperre, C. Valle, and S. Planes. 2008. Marine reserves: size and age do matter. Ecology Letters **11**:481-489.

Denny, M. W. 1987. Lift as a mechanism of patch initiation in mussel beds. Journal of Experimental Marine Biology and Ecology **113**:231-245.

Earn, D. J. D., S. A. Levin, and P. Rohani. 2000. Coherence and Conservation. Science **290**:1360-1364.

Ewers, R. M. and A. S. L. Rodrigues. 2008. Estimates of reserve effectiveness are confounded by leakage. Trends in Ecology & Evolution **23**:113-116.

Fortin, M. and M. Dale. 2005. Spatial Analysis: A Guide for Ecologists. Cambridge University Press.

Gaines, S. D., B. Gaylord, and J. L. Largier. 2003. Avoiding current oversights in marine reserve design. Ecological Applications **13**:S32-S46.

Game, E. T., M. Bode, E. McDonald-Madden, H. S. Grantham, and H. P. Possingham. 2009. Dynamic marine protected areas can improve the resilience of coral reef systems. Ecology Letters **12**:1336-1346.

Gell, F. R. and C. M. Roberts. 2003. Benefits beyond boundaries: the fishery effects of marine reserves. Trends in Ecology & Evolution **18**:448-455.

Gerber, L. R., L. W. Botsford, A. Hastings, H. P. Possingham, S. D. Gaines, S. R. Palumbi, and S. Andelman. 2003. Population models for marine reserve design: A retrospective and prospective synthesis. Ecological Applications **13**:S47-S64.

Gouhier, T. C. and F. Guichard. 2007. Local disturbance cycles and the maintenance of spatial heterogeneity across scales in marine metapopulations. Ecology **88**:647-657.

Gouhier, T. C., F. Guichard, and B. A. Menge. *in press*. Ecological processes can synchronize marine population dynamics over continental scales. Proceedings of the National Academy of Sciences.

Grantham, B. A., G. L. Eckert, and A. L. Shanks. 2003. Dispersal potential of marine invertebrates in diverse habitats. Ecological Applications **13**:S108-S116.

Guichard, F. 2005. Interaction strength and extinction risk in a metacommunity. Proceedings of the Royal Society of London B **272**:1571-1576.

Guichard, F., P. M. Halpin, G. W. Allison, J. Lubchenco, and B. A. Menge. 2003. Mussel disturbance dynamics: signatures of oceanographic forcing from local interactions. The American Naturalist **161**:889-904.

Guichard, F., S. A. Levin, A. Hastings, and D. Siegel. 2004. Toward a dynamic metacommunity approach to marine reserve theory. Bioscience **54**:1003-1011.

Guichard, F. and R. Steenweg. 2008. Intrinsic and extrinsic causes of spatial variability across scales in a metacommunity. Journal of Theoretical Biology **250**:113-124.

Halpern, B. S. 2003. The impact of marine reserves: Do reserves work and does reserve size matter? Ecological Applications **13**:S117-S137.

Halpern, B. S., H. M. Regan, H. P. Possingham, and M. A. McCarthy. 2006. Accounting for uncertainty in marine reserve design. Ecology Letters **9**:2-11.

Hastings, A. and L. W. Botsford. 1999. Equivalence in Yield from Marine Reserves and Traditional Fisheries Management. Science **284**:1537-1538.

Hastings, A. and L. W. Botsford. 2003. Comparing designs of marine reserves for fisheries and for biodiversity. Ecological Applications **13**:S65-S70.

Jansen, V. and A. de Roos. 2000. The role of space in reducing predator-prey cycles. Pages 183–201 *in* U. Dieckmann, R. Law, and J. A. J. Metz, editors. The geometry of ecological interactions: simplifying spatial complexity. Cambridge University Press, Cambridge, U.K.

Lester, S. E., B. S. Halpern, K. Grorud-Colvert, J. Lubchenco, B. Ruttenberg, S. Gaines, S. Airame, and R. R. Warner. 2009. Biological effects within no-take marine reserves: a global synthesis. Marine Ecology Progress Series **384**:33-46.

Lubchenco, J., S. R. Palumbi, S. D. Gaines, and S. Andelman. 2003. Plugging a hole in the ocean: The emerging science of marine reserves. Ecological Applications **13**:S3-S7.

Neubert, M. G., M. Kot, and M. A. Lewis. 1995. Dispersal and Pattern-Formation in a Discrete-Time Predator-Prey Model. Theoretical Population Biology **48**:7-43.

Paine, R. T. 1966. Food Web Complexity and Species Diversity. American Naturalist **100**:65-75.

Paine, R. T. 1984. Ecological Determinism in the Competition for Space. Ecology **65**:1339-1348.

Paine, R. T. and S. A. Levin. 1981. Inter-Tidal Landscapes - Disturbance and the Dynamics of Pattern. Ecological Monographs **51**:145-178.

Pauly, D., V. Christensen, J. Dalsgaard, R. Froese, and F. Torres, Jr. 1998. Fishing Down Marine Food Webs. Science **279**:860-863.

Pauly, D., V. Christensen, S. Guenette, T. J. Pitcher, U. R. Sumaila, C. J. Walters, R. Watson, and D. Zeller. 2002. Towards sustainability in world fisheries. Nature **418**:689-695.

Roberts, C. M., J. A. Bohnsack, F. Gell, J. P. Hawkins, and R. Goodridge. 2001. Effects of marine reserves on adjacent fisheries. Science **294**:1920-1923.

Roughgarden, J. 1974. Population-dynamics in a spatially varying environment - How population-size tracks spatial variation in carrying capacity. American Naturalist **108**:649-664.

Sale, P. F., R. K. Cowen, B. S. Danilowicz, G. P. Jones, J. P. Kritzer, K. C. Lindeman, S. Planes, N. V. C. Polunin, G. R. Russ, Y. J. Sadovy, and R. S. Steneck. 2005. Critical science gaps impede use of no-take fishery reserves. Trends in Ecology & Evolution **20**:74-80.

Shanks, A. L., B. A. Grantham, and M. H. Carr. 2003. Propagule dispersal distance and the size and spacing of marine reserves. Ecological Applications **13**:S159-S169.

Worm, B., E. B. Barbier, N. Beaumont, J. E. Duffy, C. Folke, B. S. Halpern, J. B. Jackson, H. K. Lotze, F. Micheli, S. R. Palumbi, E. Sala, K. A. Selkoe, J. J. Stachowicz, and R. Watson. 2006. Impacts of biodiversity loss on ocean ecosystem services. Science **314**:787 - 790.

Zar, J. H. 1999. Biostatistical Analysis. Fourth edition. Prentice-Hall, Inc., Upper Saddle River, NJ.

FIGURES

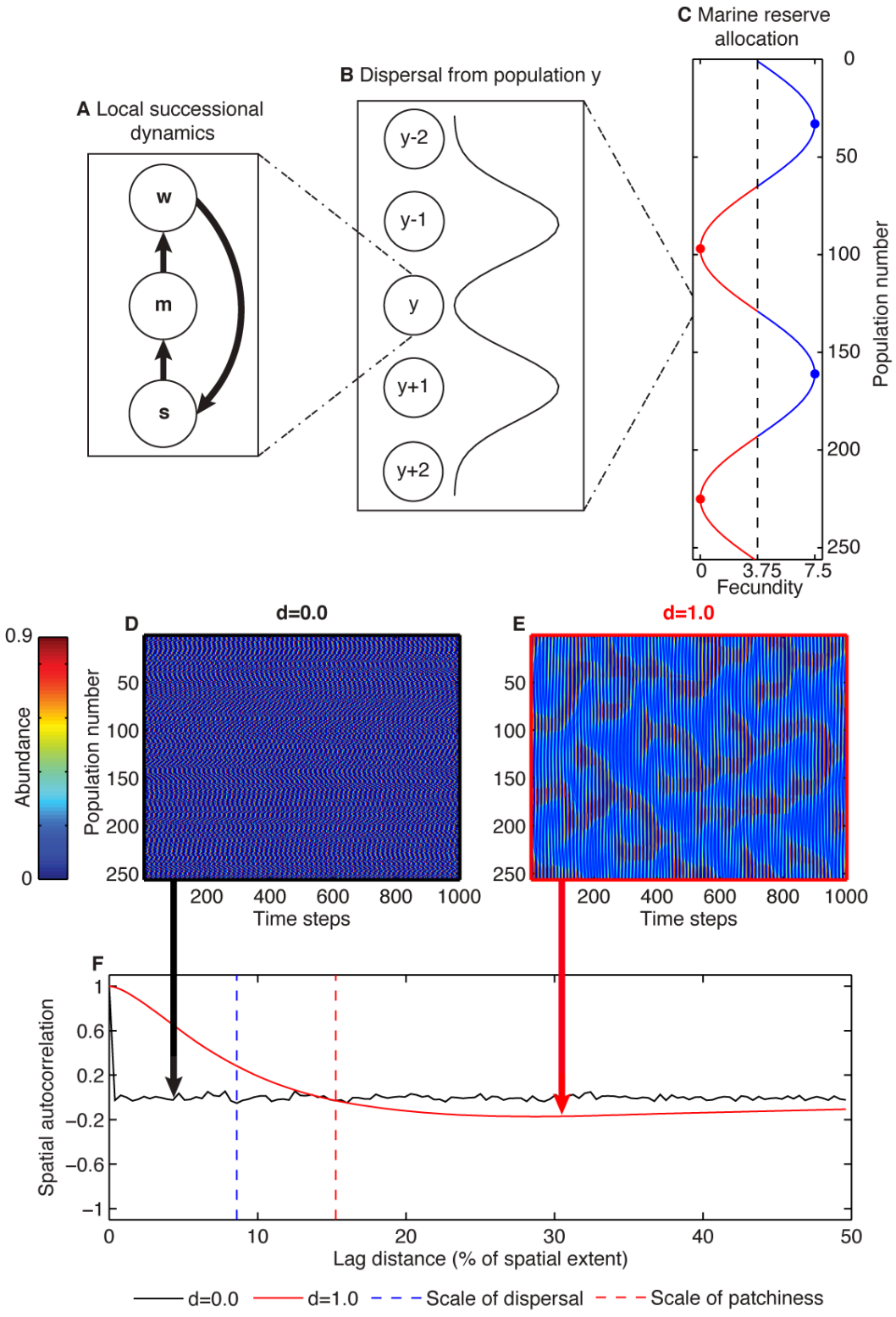

Figure 1

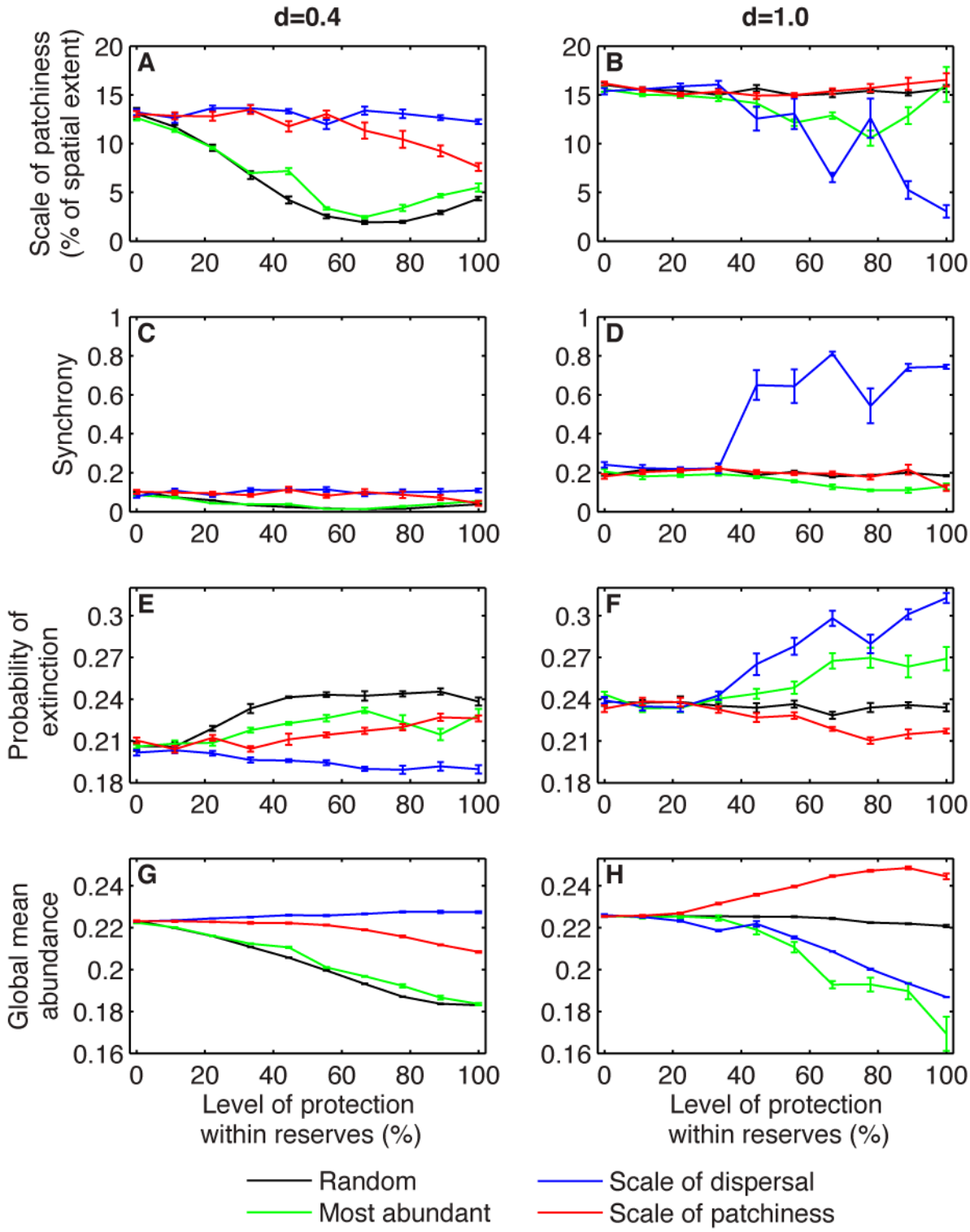
d=0.4
d=1.0
A
B
C
D
E
F
G
H
Scale of patchiness (% of spatial extent)
Synchrony
Probability of extinction
Global mean abundance
Level of protection within reserves (%)
Level of protection within reserves (%)
Random
Most abundant
Scale of dispersal
Scale of patchiness

Figure 2

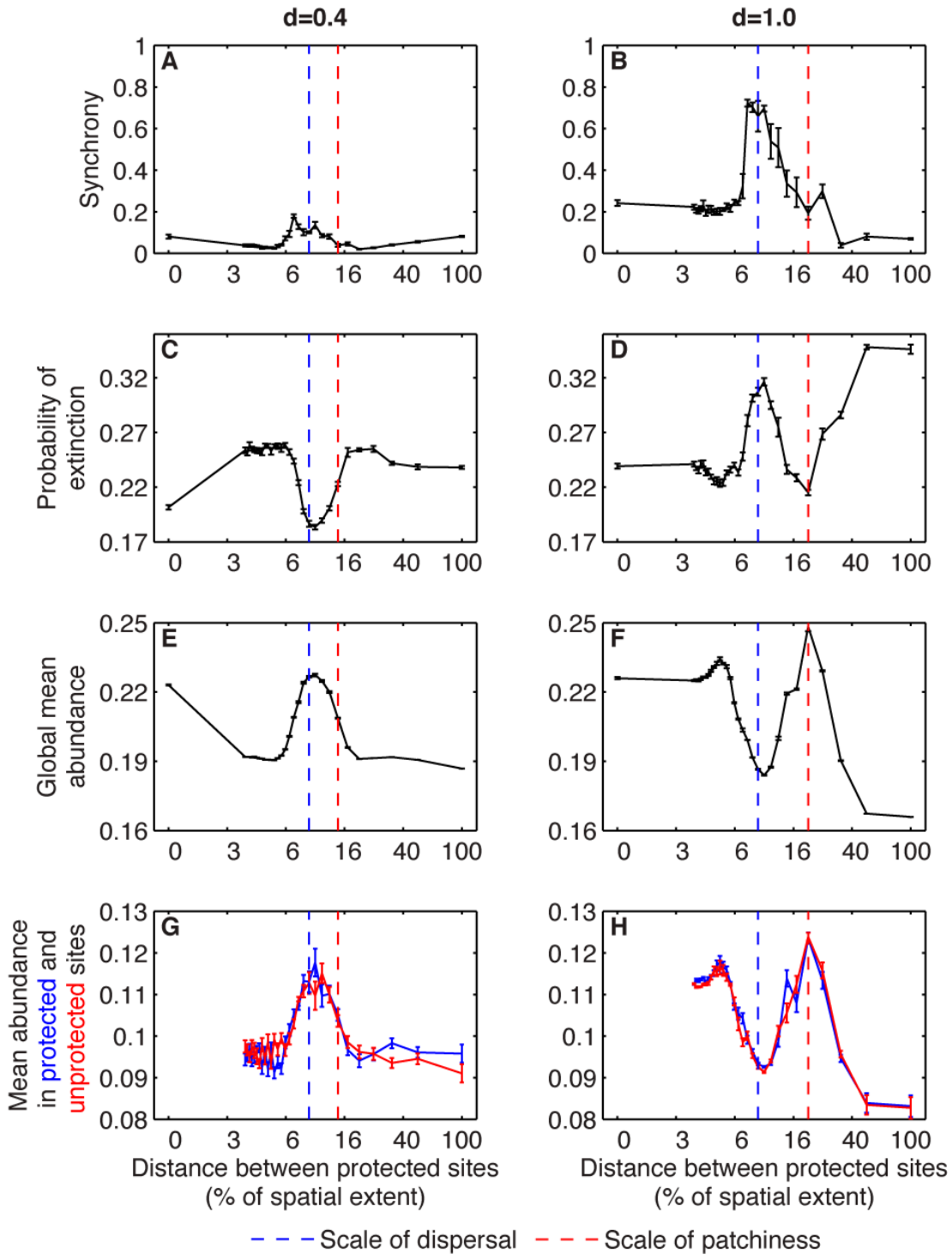
d=0.4
d=1.0
A
B
C
D
E
F
G
H
Synchrony
Probability of extinction
Global mean abundance
Mean abundance in protected and unprotected sites
Distance between protected sites (% of spatial extent)
Distance between protected sites (% of spatial extent)
Scale of dispersal
Scale of patchiness

Figure 3

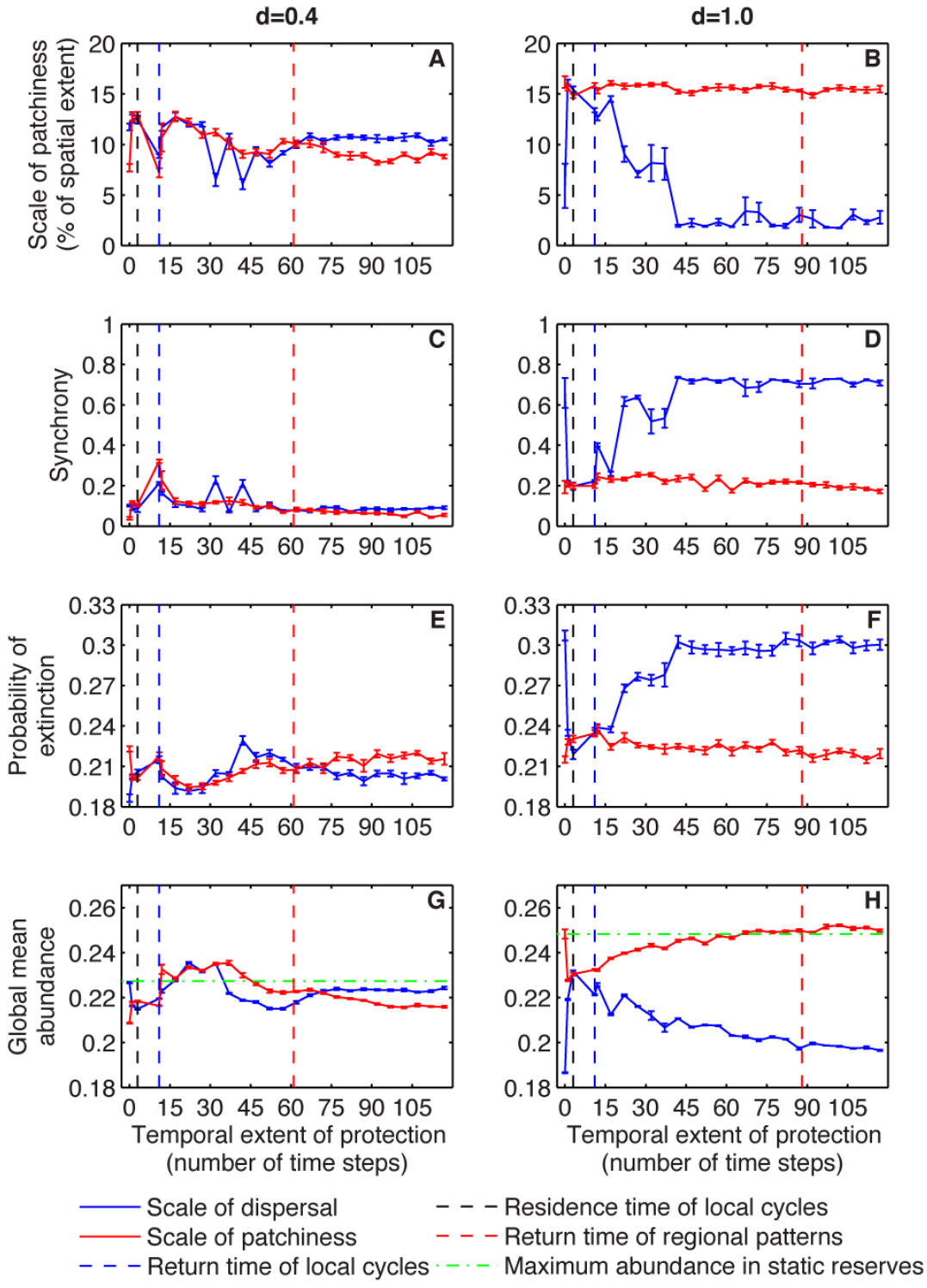
d=0.4
d=1.0
A
B
C
D
E
F
G
H
Scale of patchiness (% of spatial extent)
Synchrony
Probability of extinction
Global mean abundance
Temporal extent of protection (number of time steps)
Temporal extent of protection (number of time steps)
Scale of dispersal
Scale of patchiness
Return time of local cycles
Residence time of local cycles
Return time of regional patterns
Maximum abundance in static reserves

Figure 4

APPENDIX A

A COMPARISON OF THE PERFORMANCE OF DIFFERENT MARINE RESERVE NETWORKS

Table A1: The performance of different marine reserve designs based on their effect on global mean abundance for metapopulations with low rates of dispersal (d=0.4). The values represent percent differences in the mean global abundance between marine reserve designs described in rows and baseline marine reserve designs described in columns.

		Percentage change in mean global abundance for metapopulations with low rates of dispersal (d=0.4)				
		No reserves	Static reserves		Dynamic reserves	
			Scale of dispersal	Scale of patchiness	Scale of dispersal	Scale of patchiness
No reserves		**0**	**-**	**-**	**-**	**-**
Static reserves	Scale of dispersal	2	**0**	**-**	**-**	**-**
	Scale of patchiness	-6	-8	**0**	**-**	**-**
Dynamic reserves	Scale of dispersal	6	4	13	**0**	**-**
	Scale of patchiness	6	4	13	0	**0**

Table A2: The performance of different marine reserve designs based on their effect on global mean abundance for metapopulations with high rates of dispersal (d=1.0). The values represent percent differences in the mean global abundance between marine reserve designs described in rows and baseline marine reserve designs described in columns.

		Percentage change in mean global abundance for metapopulations with high rates of dispersal (d=1.0)				
		No reserves	Static reserves		Dynamic reserves	
			Scale of dispersal	Scale of patchiness	Scale of dispersal	Scale of patchiness
No reserves		**0**	**-**	**-**	**-**	**-**
Static reserves	Scale of dispersal	-17	**0**	**-**	**-**	**-**
	Scale of patchiness	9	31	**0**	**-**	**-**
Dynamic reserves	Scale of dispersal	3	24	-5	**0**	**-**
	Scale of patchiness	12	35	3	9	**0**

APPENDIX B

THE EFFECTS OF STATIC AND DYNAMIC MARINE RESERVE NETWORKS ON METAPOPULATION DYNAMICS

FIGURE LEGENDS

Figure B1: The effect of static and dynamic marine reserve networks on naturally occurring patterns in metapopulations with high rates of dispersal (d=1.0). Abundance time series of metapopulations subjected to static marine reserve designs that use (A) the scale of dispersal or (B) the scale of patchiness as the distance between protected sites. Abundance time series of metapopulations subjected to dynamic marine reserve designs based on (C) the scale of dispersal and the residence time of cycles (3 time steps) or (D) the scale of patchiness and the return time of regional patterns (90 time steps). All reserves were implemented at time step 200 (highlighted in red) and side plots of fecundity indicate their spatial configuration. For dynamic designs, alternating schemes are represented in red and blue.

Figure B2: The effect of static and dynamic marine reserve networks on naturally occurring patterns in metapopulations with low rates of dispersal (d=0.4). Abundance time series of metapopulations subjected to static marine reserve designs that use (A) the scale of dispersal or (B) the scale of patchiness as the distance between protected sites. Abundance time series of metapopulations subjected to dynamic marine reserve designs based on (C) the scale of dispersal and the residence time of cycles (3 time steps) or (D) the scale of patchiness and the return time of regional patterns (90 time steps). All reserves were implemented at time step 200

(highlighted in red) and side plots of fecundity indicate their spatial configuration. For dynamic designs, alternating schemes are represented in red and blue.

FIGURES

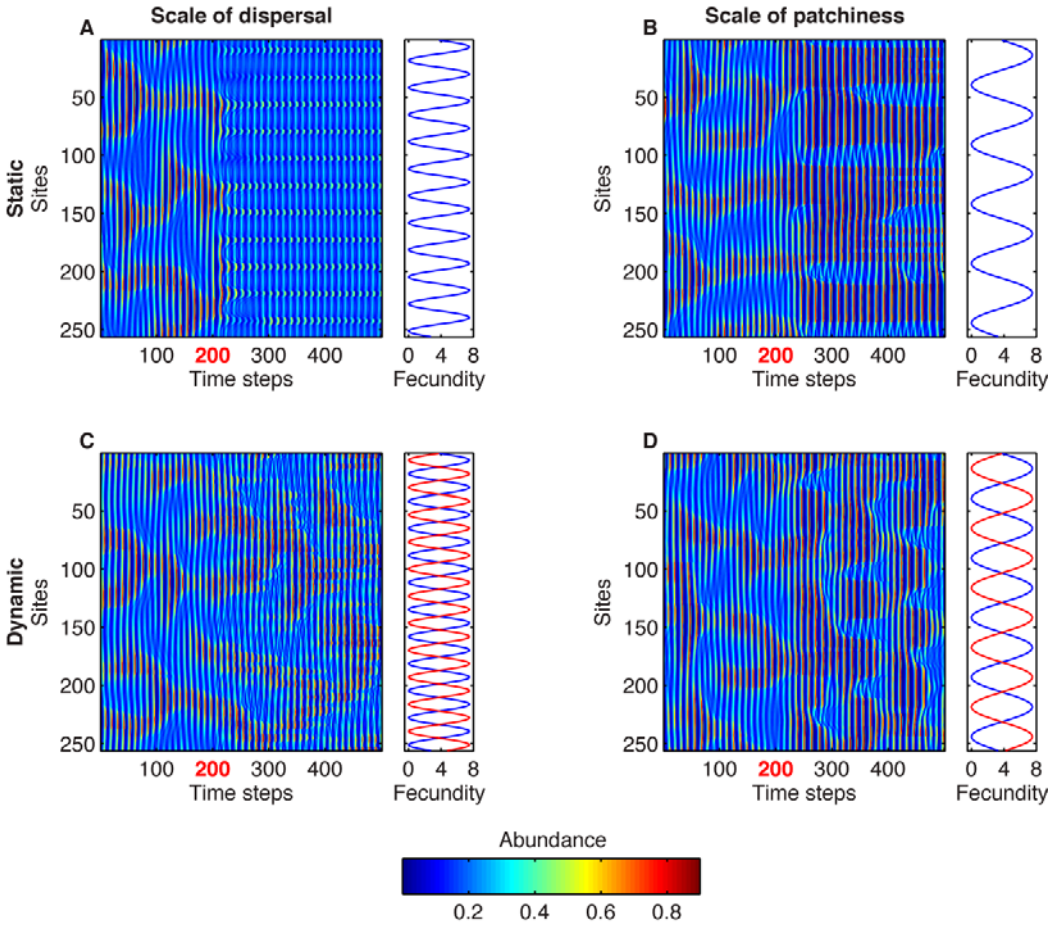

Figure B1

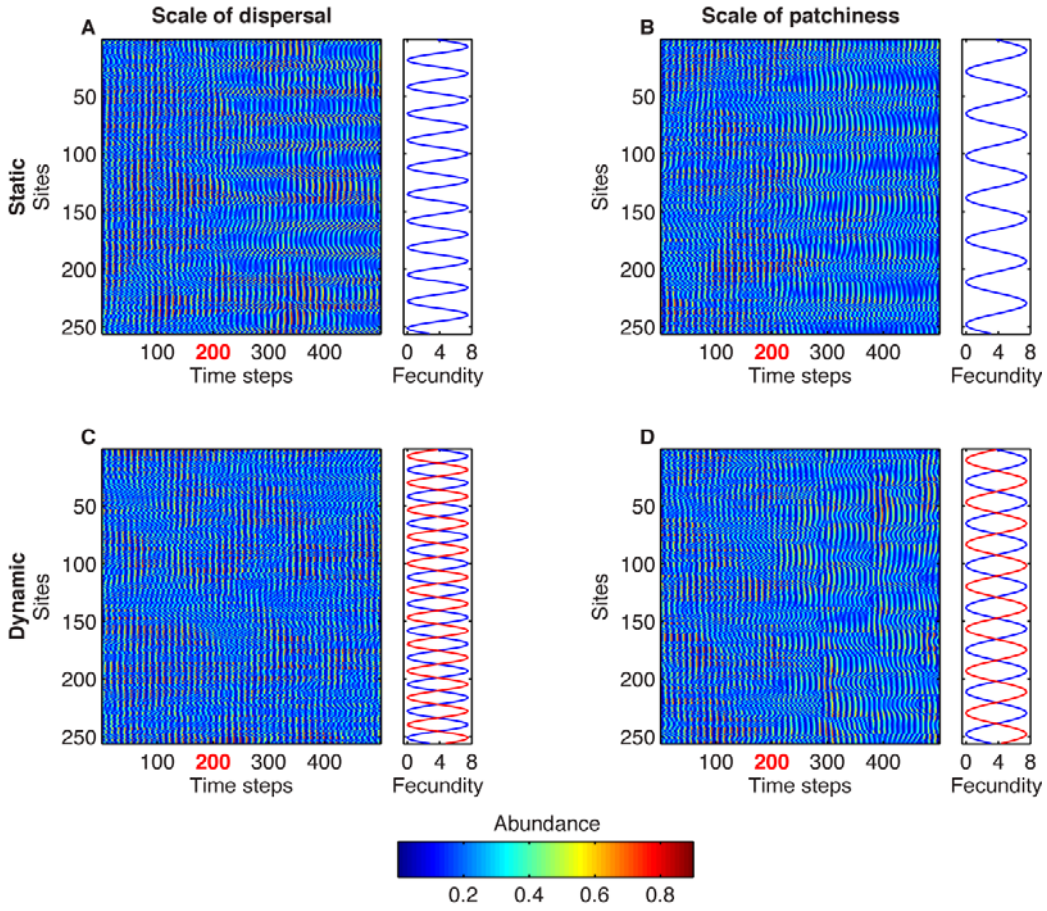
A
Scale of dispersal
B
Scale of patchiness
Static
Dynamic
Sites
50
100
150
200
250
100 200 300 400
Time steps
0 4 8
Fecundity
C
D
Abundance
0.2 0.4 0.6 0.8

Figure B2

APPENDIX C

PREDICTING THE EFFECTIVENESS OF MARINE RESERVE NETWORKS

We use a general statistical framework to understand the effects of static and dynamic marine reserve networks on dynamic metapopulations. Since all marine reserve networks considered here alter the spatial distribution (i.e. the spatial variance) of fecundity without affecting global mean fecundity, we can use Jensen's inequality as a statistical framework to interpret the effect of marine reserves on global mean abundance.

Jensen's inequality states that for decelerating nonlinear functions, the variance of the independent variable tends to depress the response variable (Ruel and Ayres 1999). Since abundance (the response variable) is a saturating function of fecundity (the independent variable), Jensen's inequality predicts that increased spatial variance in fecundity will tend to decrease mean abundance. This occurs because populations experiencing low fecundities contribute more to mean abundance than those experiencing high fecundities. It is this asymmetry between the contribution of low and high fecundity populations that leads to a net decrease in global mean abundance (Ruel and Ayres 1999).

Our simulation results have demonstrated (Figs 2-4) that the effects of Jensen's inequality are avoidable: maintaining natural patterns of population abundance and connectivity can allow the 'selective aggregation' of recruits into favorable sites. Such 'selective aggregation' can reverse the asymmetry between the contribution of low and high fecundity sites and thus increase global mean

abundance. The goal is then to determine whether the contradictions between Jensen's inequality and our simulations can be explained by a simple metric that measures 'selective aggregation'.

Here, we use three spatial metrics that measure aggregation at different life stages (Bolker 2003): (i) the spatial correlation $\rho(m,\beta)$ between abundance m and recruitment β measures the ability of recruits to arrive in populations undergoing favorable conditions; (ii) the spatial correlation $\rho(m,f)$ between abundance m and fecundity f measures the association between abundance and the location of reserves; (iii) the spatial correlation $\rho(\beta,f)$ between recruitment β and fecundity f measures the degree to which recruits are retained within reserves. All three metrics were computed for- and averaged over- 1000 post-transient time steps.

In our simulations, $\rho(m,f)$ is consistently weak and unrelated to global mean abundance because (i) dispersal naturally erodes the spatial correlation between fecundity and abundance and (ii) abundance undergoes dynamic cycles (Fig C1). $\rho(\beta,f)$ is a much stronger metric, but its strength and sign vary with both the scale of marine reserve networks and the rate of dispersal, and it is a poor predictor of global mean abundance (Fig C1). However, $\rho(m,\beta)$ shows a very strong and consistent positive relationship with global mean abundance, regardless of the rate of dispersal (Fig C1).

The correlation between abundance and recruitment (i.e. $\rho(m,\beta)$) demonstrates that the contradictions between the simulation results and Jensen's inequality occur when marine reserve networks are designed using the proper spatial

scales. Indeed, reserve networks designed using the appropriate spatial scales account for natural patterns of population abundance and connectivity, and thus promote the 'selective aggregation' of recruits into populations undergoing favorable conditions (Fig C1). This 'selective aggregation' reverses the asymmetry predicted by Jensen's inequality and allows populations undergoing favorable conditions to contribute more to the global mean abundance than those undergoing unfavorable conditions, thereby boosting global mean abundance.

LITERATURE CITED

Bolker, B. M. 2003. Combining endogenous and exogenous spatial variability in analytical population models. Theoretical Population Biology **64**:255-270.

Ruel, J. J. and M. P. Ayres. 1999. Jensen's inequality predicts effects of environmental variation. Trends in Ecology & Evolution **14**:361-366.

FIGURE LEGENDS

Figure C1: Relating the correlation between (i) abundance and recruitment $\rho(m,\beta)$, (ii) abundance and fecundity $\rho(m,f)$ and (iii) recruitment and fecundity $\rho(\beta,f)$ (A, B) to the to the global mean abundance (C, D) for different marine reserve designs applied to metapopulations with low (A, C) and high (B, D) rates of dispersal. Each colored bar represents a different type of marine reserve design: protection of sites separated by the scale dispersal (dark blue), protection of sites separated by the scale of patchiness (light blue), protection of sites separated by the scale of dispersal with dynamic shifts based on the return time of local cycles (11 time steps; dark yellow) and protection of sites separated by the scale of patchiness with dynamic shifts based on the return time of regional patterns (88 time steps; dark

red). The results represent the means and standard errors from 10 replicate simulations.

FIGURES

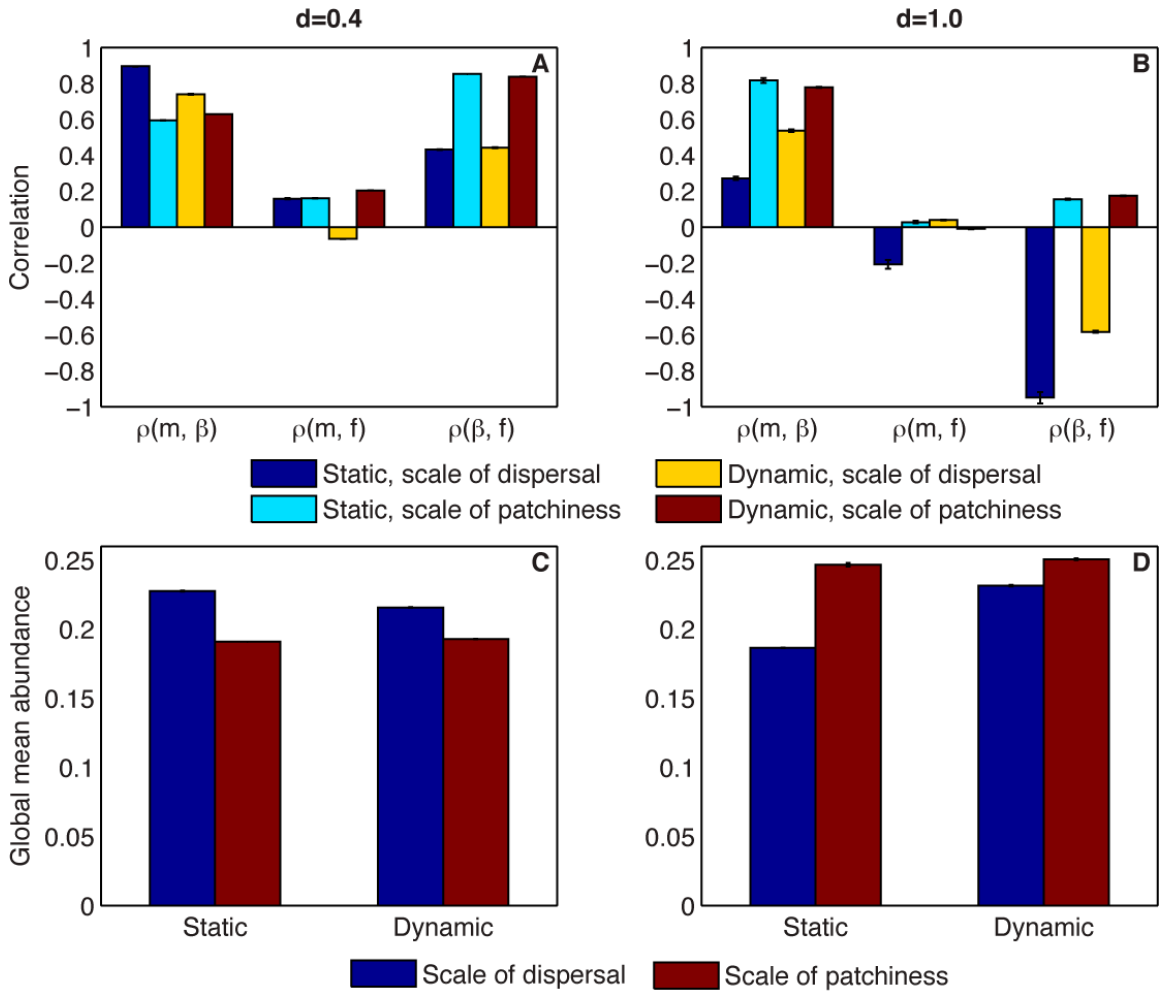

Figure C1

CONNECTING STATEMENT

In the previous chapters (chapter 1, 2), I assessed the relative importance of biotic and abiotic processes in relatively simple spatial ecological systems and determined the implications for the preservation of natural systems (chapter 3). In the next chapter, I investigate the role of biotic and abiotic processes for the maintenance of stability in more complex spatial food webs.

CHAPTER 4: SYNCHRONY AND STABILITY OF FOOD WEBS IN METACOMMUNITIES

Tarik C. Gouhier [1,*], Frédéric Guichard [1] and Andrew Gonzalez [1]

[*] Corresponding author: tarik.gouhier@mail.mcgill.ca | Phone: (514) 398-4120 | Fax: (514) 398-5069

[1] Department of Biology, McGill University, 1205 Avenue Docteur Penfield, Montreal, Quebec, H3A 1B1, Canada

Keywords: food web, stability, metacommunity, synchrony, environmental variability, compensatory dynamics

Status: published in The American Naturalist (2010) **175**: 120-156 (Feature Article)

ABSTRACT

Synchrony has fundamental but conflicting implications for the persistence and stability of food webs at local and regional scales. In a constant environment, compensatory dynamics between species can maintain food web stability, but factors that synchronize population fluctuations within and between communities are expected to be destabilizing. We studied the dynamics of a food web in a metacommunity to determine how environmental variability and dispersal affect stability by altering compensatory dynamics and average species abundance. When dispersal rate is high, weak correlated environmental fluctuations promote food web stability by reducing the amplitude of compensatory dynamics. However, when dispersal rate is low, weak environmental fluctuations reduce food web stability by inducing intraspecific synchrony across communities. Irrespective of dispersal rate, strong environmental fluctuations disrupt compensatory dynamics and decrease stability by inducing intermittent correlated fluctuations between consumers in local food webs, which reduce both total consumer abundance and predator abundance. Strong correlated environmental fluctuations lead to (i) spatially asynchronous and highly correlated local consumer dynamics when dispersal is low and (ii) spatially synchronous but intermediate local consumer correlation when dispersal is high. By controlling intraspecific synchrony, dispersal mediates the capacity of strong environmental fluctuations to disrupt compensatory dynamics at both local and metacommunity scales.

INTRODUCTION

The persistence and stability of natural populations appears improbable given the enormous diversity of species interactions and the highly variable nature of the environment. Theory both confirms (May 1973) and refutes this intuition (Allesina and Pascual 2008; Ives and Carpenter 2007), but recent surveys of the literature (Loreau et al. 2002; McCann 2000; Murdoch et al. 2003) identify a number of scale-dependent processes that can stabilize populations embedded within food webs. Natural food webs persist because these stabilizing mechanisms play out within a hierarchy of biotic and abiotic processes that operate at local to regional scales (Amarasekare 2008; DeAngelis and Waterhouse 1987; McCann et al. 2005; Polis et al. 2004; Rooney et al. 2006)

Our perception of stability depends in part on the level of organization at which it is measured. For example, increasing species richness may increase the variability of individual populations whilst reducing the aggregate variability of total abundance in the community (Ives et al. 1999; May 1973; Tilman 1999; Yachi and Loreau 1999). This hierarchical perspective is particularly valuable when the nonlinear dynamics of food webs are studied (McCann et al. 1998; Vandermeer 2006). For instance, in mean-field food web models experiencing constant environmental conditions, competition for a common resource can generate large oscillations in the consumer dynamics that can be dampened and stabilized by the presence of a generalist predator that preferentially feeds upon the dominant competitor (McCann et al. 1998). In this case, the compensatory consumer

oscillations (i.e. interspecific asynchrony) sustain and buffer the fluctuations of the generalist predator and stabilize the entire food web.

Recent research suggests that compensatory dynamics may be disrupted by environmental perturbations (both press and pulse) that can cause periods of correlated (coherent) interspecific fluctuations at one or more temporal scales (Keitt 2008; Vasseur and Fox 2007; Vasseur et al. 2005). Any process that can cause correlated species fluctuations will affect food web stability at local scales, but factors that can induce synchronous species populations across space will influence food web stability at a regional scale (Blasius et al. 1999). How then do dispersal and stochastic environmental variability correlate population (intraspecific synchrony) and community (interspecific synchrony) dynamics so that local destabilizing effects propagate up to the metacommunity scale?

Intraspecific synchrony across subpopulations is generated by three well-known processes: spatially correlated environmental variation (Moran 1953), high rates of dispersal between subpopulations, and strong interactions with mobile predators or parasites (Liebhold et al. 2004). The Moran effect and dispersal have been shown to interact to increase population synchrony (Fontaine and Gonzalez 2005). This type of synchrony is predicted to destabilize populations and increase regional extinction risk. In contrast, intraspecific asynchrony can maintain food web stability at both local and regional scales. Limited dispersal and movement of individuals over space can decouple local densities from growth and dampen local population dynamics (Briggs and Hoopes 2004). When accompanied by intraspecific asynchrony, this decoupling promotes stability at regional scales through spatial averaging (Briggs and Hoopes 2004), or by allowing high-density populations to

subsidize or rescue other populations (Blasius et al. 1999; Earn et al. 2000). Depending on the extent of dispersal, these local and regional processes can interact and have either similar or contrasting effects on food web stability (Maser et al. 2007).

Synchrony can also be observed between species within food webs. At small scales, such interspecific synchrony can be driven by environmental fluctuations (Greenman and Benton 2005; Keitt 2008; Ranta et al. 2006; Ripa and Ives 2003; Vasseur and Fox 2007) or by changes in the interaction strength of consumer species (McCann et al. 1998). These same studies predict that interspecific synchrony will destabilize local food webs (Vandermeer 2006). In contrast, Vasseur and Fox (2007) reported that synchronous responses by consumers to stochastic environmental fluctuations can promote food web stability by dampening predator and consumer oscillations. Although this effect greatly reduced interspecific asynchrony between consumers within the keystone consumer configuration (McCann et al. 1998), it did not result in correlated consumer fluctuations. Thus, how robust compensatory dynamics are to the synchronizing effects of the environment and dispersal remains an important and unresolved question (Gonzalez and Loreau, in press).

Here, we study the dynamics of a simple food web model (Maser et al. 2007; McCann et al. 1998; Vasseur and Fox 2007) embedded within a metacommunity and assess the relative importance of intra- and interspecific synchrony for stability. We show that environmental fluctuations interact with dispersal to affect food web stability through their combined influence on intra- and interspecific synchrony. In metacommunities experiencing high dispersal, weak environmental fluctuations stabilize food webs by reducing the amplitude of endogenous dynamics, whilst

strong environmental fluctuations can induce intermittent spatial and temporal patterns of correlated consumer dynamics. However, low dispersal prevents the onset of intraspecific synchrony, which allows the destabilization of population fluctuations by the environment and the emergence of spatially persistent interspecific synchrony. These results are robust to changes in the intrinsic dynamics of the food web and to the nature and temporal structure of environmental fluctuations. By controlling intraspecific synchrony, dispersal mediates the effect of strong environmental fluctuations on compensatory dynamics at both local and metacommunity scales.

METHODS

We used a spatially-explicit metacommunity implementation (Maser et al. 2007) of the mean-field food web model analyzed by McCann et al. (1998). We focused on the keystone food web configuration in which a superior (C_1) and an inferior consumer (C_2) compete for a common resource R and undergo asynchronous oscillations (i.e. compensatory dynamics) (Fig. 1A, Table 1). Coexistence in this model is maintained by the generalist predator's (P) predilection for the superior competitor (Table 1). The consumers and the predator exhibit a type-2 functional response and the resource R undergoes logistic growth**.** Although the basic model can display many dynamical behaviors, we used the same parameter values as Vasseur and Fox (2007) in order to generate stable limit cycles in the mean-field model (Table 1). We also tested the robustness of our results to alternative food web dynamics and implementations of environmental noise (see Appendix B).

Metacommunity structure

The metacommunity consists of a 256 x 256 grid of cells with periodic boundary conditions. Each cell contains a complete community described by the following difference equation system:

$$\begin{aligned}
\Delta P(x,y) &= -M_P + \frac{J_P P\left[\Omega_{PC_1} C_1 + \left(1-\Omega_{PC_1}\right)C_2\right]}{\Omega_{PC_1} C_1 + \left(1-\Omega_{PC_1}\right)C_2 + C_0} \\
\Delta C_1(x,y) &= -M_{C_1} C_1 + \frac{\Omega_{C_1 R} J_{C_1} C_1 R}{R + R_{0_1}} - \frac{\Omega_{PC_1} J_P P C_1}{\Omega_{PC_1} C_1 + \left(1-\Omega_{PC_1}\right)C_2 + C_0} \\
\Delta C_2(x,y) &= -M_{C_2} C_2 + \frac{\Omega_{C_2 R} J_{C_2} C_2 R}{R + R_{0_2}} - \frac{\left(1-\Omega_{PC_1}\right) J_P P C_2}{\Omega_{PC_1} C_1 + \left(1-\Omega_{PC_1}\right)C_2 + C_0} \\
\Delta R(x,y) &= rR\left(1-\frac{R}{K}\right) - \frac{\Omega_{C_1 R} J_{C_1} C_1 R}{R + R_{0_1}} - \frac{\Omega_{C_2 R} J_{C_2} C_2 R}{R + R_{0_2}}
\end{aligned} \qquad (1)$$

where $\Delta P(x,y)$, $\Delta C_1(x,y)$, $\Delta C_2(x,y)$ and $\Delta R(x,y)$ respectively represent the change in the abundance of predator *P*, consumer C_1, consumer C_2 and resource *R* at location (*x,y*). The model parameter descriptions and values are given in table 1.

At each time step, 256^2 focal cells are randomly selected and updated in order to approximate a continuous time process (Durrett and Levin 1994). Each focal cell *F* is updated by first iterating its own set of difference equations and then allowing all species to disperse between the focal cell and one of its eight closest neighbors. Dispersal is implemented for all species as a simple passive diffusion process defined as the product of the maximum dispersal rate *d* (hereafter termed dispersal) and the differential in abundance between the focal cell *F* and its randomly selected neighbor *N* (Maser et al. 2007; McCann et al. 2000). Specifically, the abundance of each population at time step *t+1* is:

$$A_F^{t+1} = A_F^t - d\left(A_F^t - A_N^t\right)$$
$$A_N^{t+1} = A_N^t + d\left(A_F^t - A_N^t\right) \qquad (2)$$

where A_F^t and A_F^{t+1} respectively represent the population abundances of each species at time step *t* and *t+1* in focal cell *F*. A_N^t, A_N^{t+1} are their respective homologues for the randomly selected neighbor *N*.

In order to reduce the length of transients, we initialized the metacommunity by assigning identical population abundances to all cells (R=0.9, C_1=0.5, C_2=0.5, P=0.1). However, our results are robust to both random and spatially heterogeneous initial abundances. All analyses were performed after discarding the first 1000 time steps as transients.

Environmental variability

Environmental variability was implemented as a stochastic process with strength σ_ξ and cross-correlation ρ_ξ affecting the mortality rates of consumers C_1 and C_2 (Vasseur and Fox 2007). The mortality rates of the consumers were allowed to vary in time by using two cross-correlated time series generated by the product of the Cholesky factorization of the 2x2 variance-covariance matrix *B* and a 2x*n* matrix *A* of random draws from a normal distribution (0, 1) (Vasseur and Fox 2007) (3):

$$\xi = BA = \begin{bmatrix} \sigma_\xi & \rho_\xi\sigma_\xi \\ \rho_\xi\sigma_\xi & \sigma_\xi \end{bmatrix}\begin{bmatrix} a_{11} & \dots & a_{1n} \\ a_{21} & \dots & a_{2n} \end{bmatrix} = \sigma_\xi \begin{bmatrix} a_{11} + \rho_\xi a_{21} & \dots & a_{1n} + \rho_\xi a_{2n} \\ \rho_\xi a_{11} + a_{21} & \dots & \rho_\xi a_{1n} + a_{2n} \end{bmatrix}$$

Specifically, the consumer mortality rate of all consumer populations in the metacommunity was updated at the beginning of each time step *j* so that:

$$M_{C_i}(j) = M_{C_i} e^{\xi_i(j)} \qquad (4)$$

where M_{Ci} represents the median consumer mortality rate for consumer C_i and $\xi \sim N_2(0,\Sigma)$. Hence, the environmentally-mediated mortality rates for all consumer populations varied over time but remained spatially homogeneous. Although the results presented below were all generated using environmental fluctuations with no temporal structure (i.e. white noise), our findings are robust to temporally autocorrelated environmental fluctuations (i.e. red noise, see Appendix B).

Model analysis

Food web stability

We computed food web stability at local and global scales. At the global scale, each species' metacommunity time series was determined by spatially-averaging the abundance time series across the entire metacommunity. Using these metacommunity time series, we measured each species' mean abundance μ, temporal variance σ and global stability (μ/σ). For each species, local food web stability was determined by randomly selecting 100 cells and computing the mean abundance μ_{Cell}, temporal variance σ_{Cell} and stability ($\mu_{\text{Cell}}/\sigma_{\text{Cell}}$) within each cell. Local food web stability (μ_L/σ_L) was then computed by averaging the within-cell stability ($\mu_{\text{Cell}}/\sigma_{\text{Cell}}$) across all 100 randomly selected cells. We used this method for calculating local food web stability because of its efficiency and its equivalence to the more intuitive (but costly) method of averaging the within-cell stability of all 256^2 cells in the metacommunity.

Intraspecific synchrony

Kendall's coefficient of concordance was used as an index of intraspecific synchrony among local populations. Kendall's coefficient of concordance is a nonparametric statistic that measures the association between multiple ranked variables (Zar 1999). It is commonly used to measure the level of agreement among several rankings and, as such, has been suggested as the most effective method for determining synchrony between multiple data series (Buonaccorsi et al. 2001). In order to limit simulation time, we computed intraspecific synchrony on a random subset of 100 cells instead of the entire metacommunity. Test simulations confirmed that computing intraspecific synchrony over a subset of 100 cells or the entire metacommunity yielded equivalent results. The calculation was performed by first ranking (R_i) each species' abundance time series in 100 randomly selected cells. Kendall's coefficient of concordance (W) was then calculated for each species as (Zar 1999):

$$W = \frac{\sum R_i^2 - \frac{\left(\sum R_i\right)^2}{n}}{\frac{S^2\left(n^3 - n\right) - S\sum \tau}{12}} \qquad (5)$$

where $S=100$ represents the total number of randomly selected cells, $n=1000$ represents the total number of post-transient time steps, and $\sum \tau$ is an adjustment for tied ranks within each cell such that for t_i ties in the i^{th} group of ties and j groups of tied ranks:

$$\sum \tau = \sum_{i=1}^{j} (t_i^3 - t_i) \qquad (6)$$

Global consumer correlation

The global consumer correlation was calculated by taking the cross-correlation of the metacommunity consumer time series:

$$\rho_G = \frac{1}{n\sigma_{C_1}\sigma_{C_2}} \sum_{t=1}^{n} \left(C_1(t) - \mu_{C_1}\right)\left(C_2(t) - \mu_{C_2}\right) \qquad (7)$$

where *n=1000* represents the number of time steps, and μ_{C_i} , σ_{C_i} represent respectively the mean and standard deviation of the global abundance time series of consumer C_i. $C_i(t)$ represents the global abundance of consumer C_i at time step *t*.

Determining the effect of environmental noise upon compensatory dynamics

At the local scale - To determine how correlated environmental noise affects the consumer dynamics at the local scale, we analyzed the consumer time series of 100 randomly selected cells. For each cell *j*, we split the local consumer time series into *w* 100-time step windows and computed the local consumer correlation $\rho_{L,j,w}$:

$$\rho_{L,j,w} = \frac{1}{n\sigma_{C_{1,j,w}}\sigma_{C_{2,j,w}}} \sum_{t=n(w-1)+1}^{nw+1} \left(C_{1,j,w}(t) - \mu_{C_{1,j,w}}\right)\left(C_{2,j,w}(t) - \mu_{C_{2,j,w}}\right) \qquad (8)$$

where *n=100* time steps and $\mu_{C_{i,j,w}}$, $\sigma_{C_{i,j,w}}$ represent respectively the mean and standard deviation of the local abundance time series of consumer C_i in cell *j* during time window *w*.

Within each time window *w*, the minimum $\left(\rho_{L,w}\big|_{\min}\right)$ and the maximum $\left(\rho_{L,w}\big|_{\max}\right)$ local consumer correlations were computed across all 100 cells:

$$\rho_{L,w}\big|_{\min} = \min\left\{\rho_{L,1,w}, \rho_{L,2,w}, \ldots, \rho_{L,100,w}\right\}$$
$$\rho_{L,w}\big|_{\max} = \max\left\{\rho_{L,1,w}, \rho_{L,2,w}, \ldots, \rho_{L,100,w}\right\} \qquad (9)$$

These spatial minimum and maximum consumer correlations were then averaged over all k time windows:

$$\overline{\rho_L}\big|_{\min} = \frac{1}{k}\sum_{i=1}^{k} \rho_{L,i}\big|_{\min}$$
$$\overline{\rho_L}\big|_{\max} = \frac{1}{k}\sum_{i=1}^{k} \rho_{L,i}\big|_{\max} \qquad (10)$$

The mean spatial minima/maxima of local consumer correlations $\left(\overline{\rho_L}\big|_{\min}, \overline{\rho_L}\big|_{\max}\right)$ were computed in order to assess the joint effects of environmental fluctuations and dispersal on local compensatory dynamics.

At the metacommunity scale - To determine the effect of correlated noise upon consumer dynamics at the metacommunity scale, we decomposed the global consumer time series into (1) their regular endogenous fluctuations and (2) the residuals representing the effect of correlated environmental noise. We performed this decomposition using two fitting routines: an aggressive fit based on cubic smoothing splines and a more conservative sinusoidal fit based on the dominant frequency of the consumer dynamics. We used both methods in order to ensure that our analysis was robust to the specifics of the fitting techniques.

The cubic smoothing spline routine attempts to approximate data by finding an adjustable compromise between the smoothness of the fit and its fidelity to the data. Specifically, the cubic spine s was generated for the time series of each consumer by minimizing:

$$p\sum_{i=1}^{n}\left(y_i - s\left(x_i\right)\right)^2 + \left(1-p\right)\int_{x_i}^{x_n}\left(\frac{\mathrm{d}^2 s}{\mathrm{d}x^2}\right)^2 \mathrm{d}x \qquad (11)$$

where p is a smoothness parameter set to 10^{-4} and x and y respectively represent the time steps and the consumer abundances. The fitted cubic splines were used to approximate the consumers' endogenous dynamics. The residuals r_i were then computed for each consumer i as the difference between the spline fit s_i time series and the abundance time series y_i:

$$r_i = y_i - s_i \qquad (12)$$

Additionally, a sinusoidal trend was fitted to the consumer abundance time series by using spectral analysis to determine the existence and the dominant frequency of periodic fluctuations in each consumer's time series. Nonlinear least squares analysis was then used to fit a sinusoidal model to the time series such that:

$$y = a\cos\left(\omega x\right) + b \qquad (13)$$

where y represents the predicted consumer time series, a is the fitted coefficient, ω is the consumer time series' dominant frequency, x is the time step and b is the mean of the consumer time series. The sinusoidal fit served as a conservative approximation of the consumers' endogenous dynamics because it is based solely on the dominant frequency of the consumer time series, whereas the more aggressive cubic spline fit is not constrained by a single frequency. As with the cubic splines, the residuals from the sinusoidal fit represented the effect of the correlated environmental fluctuations.

Correlation analysis was then performed using the trends and residuals from both the spline and the sinusoidal decompositions in order to determine (1) the correlation between the consumers' fitted trends (i.e. the correlation of the

endogenous consumer dynamics) and (2) the correlation of the consumer residuals. This analysis allowed us to demonstrate the effect of environmental fluctuations upon each component of the metacommunity consumer time series.

RESULTS

Food web stability in the absence of environmental fluctuations

We first investigate the effect of dispersal on food web stability in metacommunities experiencing constant environmental conditions. When dispersal is extremely low ($d < 0.001$), our stochastic approximation of the continuous-time model breaks down and leads to large changes in the mean abundance of all species (Fig. 2B). The quasi-extinctions of consumer C_2 and predator P (Fig. 2B) allow the trivial disruption of compensatory dynamics (i.e. $\rho_G > 0$; Fig. 2F). We now focus on the broad section of the dispersal gradient that remains unaffected by this artifact (i.e. $d > 0.001$).

Low dispersal ($d < 0.03$) decouples local food webs and allows them to fluctuate autonomously without disrupting local compensatory dynamics (Fig. 1B, Fig. 2, movie A1, A3A). The asynchronous fluctuations of local food webs lead to low intraspecific synchrony (Fig. 2E), low temporal variance (Fig. 2C) and high stability (Fig. 2A) for all species at the scale of the metacommunity. Here, low dispersal promotes statistical stabilization at the regional scale through the spatial averaging of uncorrelated local fluctuations (Briggs and Hoopes 2004). Additionally, low intraspecific synchrony decouples immigration and local abundance (Briggs and Hoopes 2004), which promotes stability at both local and regional scales (Fig. 2A,D).

The effect of increasing dispersal on stability is highly nonlinear as dispersal rates of $d > 0.03$ homogenize the metacommunity and lead to regional intraspecific synchrony (Fig. 2E, movie S2). The onset of regional intraspecific synchrony is associated with a large decrease in stability (Fig. 2A) that is driven primarily by an increase in the temporal variance (Fig. 2C). In contrast, global consumer correlation remains negative and unaffected by dispersal (Fig. 2F, movie S3A, S4A). Hence, in the absence of environmental fluctuations, dispersal modulates stability by controlling intraspecific synchrony without affecting compensatory dynamics. We now explore the effect of environmental fluctuations on compensatory dynamics under these two distinct dispersal regimes ($d > 0.03$ *vs.* $d < 0.03$). We use the two components of stability (i.e. temporal variance and mean abundance) to distinguish between the modulating effect of weak environmental fluctuations and the disruptive effect of strong environmental fluctuations on compensatory dynamics.

The modulating effect of weak environmental fluctuations

High dispersal – When dispersal is set to its maximum value (d=0.5), intraspecific synchrony is very high (Fig. 4A) and the metacommunity becomes approximately equivalent to the mean-field food web model (Vasseur and Fox 2007; Fig. 3A, C, E, G). Weak correlated environmental fluctuations ($0 < \sigma_\xi \leq 0.1$) are associated with increased food web stability (Fig. 3A,C,E, 4G). This increased food web stability is achieved through the mechanism documented by Vasseur and Fox (2007): weak correlated noise repeatedly jolts the entire food web into transient synchronous fluctuations that dampen the amplitude of compensatory dynamics (Fig. 4E) and thus increase stability (Fig. 4G). However, weak noise is unable to disrupt

compensatory dynamics (i.e. $\rho_G < 0$, Fig. 3G, 4A) and thus has little effect on the mean abundance of all species in the food web (Fig. 4C). Weak correlated environmental fluctuations merely add positively correlated noise to the otherwise negative correlation caused by endogenous compensatory dynamics (Fig. 3G, 4A).

Low dispersal – As shown above when the environment is constant and dispersal is low (d=0.004), intraspecific synchrony is low (Fig. 2E) and stability at the metacommunity level is high (Fig. 2A). The addition of weak environmental fluctuations ($0 < \sigma_\xi \leq 0.1$) decreases stability (Fig. 3B,D,F, 4H). This destabilization is caused by the Moran effect, which predicts that in linear systems, intraspecific synchrony among local populations should match the synchrony of the shared environment. Since the environmental fluctuations are spatially uniform (i.e. perfectly synchronized), the pure Moran effect should lead to perfect intraspecific synchrony among local populations, but this effect can be restricted by nonlinear and spatially-heterogeneous density-dependence (Engen and Saether 2005). Here, the Moran effect only leads to partial intraspecific synchrony because perfectly synchronized environmental fluctuations are unable to completely counteract the desynchronizing effect of low dispersal (Fig. 4B). Additionally, the correlation of the environment modulates the extent to which weak environmental fluctuations ($0 < \sigma_\xi \leq 0.1$) reduce stability through the Moran effect. Correlated environmental fluctuations are less destabilizing than negatively correlated environmental fluctuations because the addition of correlated environmental noise dampens compensatory dynamics whereas negatively correlated noise amplifies compensatory dynamics (Fig. 4B,F). This is the same dampening effect of correlated noise described above and by Vasseur and Fox (2007).

Here too weak noise is unable to disrupt compensatory dynamics (i.e. $\rho_G < 0$, Fig. 3H, 4B) and has little effect on the mean abundance of all species in the food web (Fig. 4D). Weak correlated environmental fluctuations merely add positively correlated noise to the endogenous compensatory dynamics (Fig. 3H, A1).

The disruptive effects of strong environmental fluctuations

Local effects – In both low and high dispersal metacommunities, strong environmental fluctuations ($\sigma_\xi \geq 0.15$) destabilize food webs (Fig. 3A-F, 4G,H) by increasing the temporal variance (Fig. 4E,F) and altering the mean abundance of all species in the metacommunity (Fig. 4C,D). Strong correlated environmental fluctuations disrupt compensatory dynamics in local food webs by inducing intermittent periods of strong positive local consumer correlation (Fig. 5A,B, movie A3,A4). During these periods of positive local consumer correlation, environmental noise inflates the abundance of the superior competitor (C_1) and the abundance of the inferior competitor (C_2) decreases due to direct competition (Fig. 5). Since the abundance of the inferior competitor decreases faster than the abundance of the superior competitor increases, both total consumer abundance and predator abundance decrease (Fig. 4C,D).

Scaling-up to the metacommunity – Dispersal controls the strength and the regional properties of environmentally-mediated disruptions of local compensatory dynamics. In metacommunities experiencing maximum dispersal (d=0.5) and environmental variability, all food webs undergo strong synchronized fluctuations (Fig. 4A). Since spatial heterogeneity in abundance is low, the disruptive effect of strong correlated environmental fluctuations is characterized by local consumer

correlation of intermediate strength that is temporally intermittent and spatially synchronized at the scale of the metacommunity: many local food webs become disrupted at the same time, yielding low spatial heterogeneity in local consumer correlation across the metacommunity (Fig. 5C, movie A4). The synchronous disruption of local compensatory dynamics (Fig. 5C) leads to gradual changes in the mean abundance of all species at the metacommunity level (Fig. 4C). Increasing the strength of environmental fluctuations ($\sigma_\xi > 0.15$) increases the frequency and the strength of these synchronous disruptions of local compensatory dynamics (Fig. 5C). The intermittent phases of strong positive and negative local consumer correlation cancel each other and lead to the emergence of low average global consumer correlation (i.e. $\rho_G \approx 0$, Fig. 3G,4A).

Low dispersal sustains low intraspecific synchrony (Fig. 2E, 4B) and dampens the fluctuations of local food webs by decoupling immigration and local abundance (Fig. 2D). By doing so, low dispersal allows strong correlated environmental fluctuations to induce periods of highly correlated local consumer fluctuations that are temporally intermittent and spatially asynchronous at the scale of the metacommunity: different local food webs become disrupted at different times, yielding high spatial heterogeneity in local consumer correlation across the metacommunity (Fig. 5C, movie A3). These asynchronous and intermittent disruptions of local compensatory dynamics lead to a further decrease of intraspecific synchrony and increased global consumer correlation (Fig. 4B). As the strength of environmental fluctuations is increased ($0.15 \leq \sigma_\xi \leq 0.25$), intermittent disruptions of local compensatory dynamics become more frequent and affect more local food webs (Fig. 5C, movie A3). The increased prevalence of strong local

disruptions leads to large changes in the mean abundance of all species due to the inflationary effect of the environment on the superior consumer (C_1) and the increased competition experienced by the inferior consumer (C_2) (Fig. 4D). As environmental fluctuations reach their maximum strength ($\sigma_\xi > 0.25$), local disruptions become widespread in the metacommunity (Fig 5C, movie A3) and lead to increased intraspecific synchrony (Fig. 4B). Additionally, these strong and asynchronous local disruptions lead to partial global interspecific synchrony (Fig. 4B). However, this partial global interspecific synchrony does not represent the loss of compensatory dynamics at the scale of the metacommunity. Instead, strong and asynchronous local disruptions register as correlated noise overlying the endogenous compensatory dynamics of the consumers at this scale (Fig. A1). As the strength of the noise is increased, these local disruptions become more frequent and lead to uncorrelated endogenous consumer dynamics (Fig. A1). Hence, correlated environmental fluctuations are unable to synchronize the endogenous consumer dynamics at the scale of the metacommunity.

DISCUSSION

We have shown how dispersal mediates the effect of the environment on food web stability at local and metacommunity scales through its own dual effect on food web dynamics. When high dispersal causes strong and synchronous food web fluctuations, weak environmental noise can stabilize food webs by dampening the amplitude of compensatory consumer fluctuations (Vasseur and Fox 2007). However, when low dispersal sustains intraspecific asynchrony and dampens the amplitude of local food web fluctuations, weak environmental noise destabilizes food

webs through the Moran effect. Although the effect of weak environmental noise on food web stability is contingent upon dispersal, strong environmental noise is consistently associated with destabilization at local and global scales. Indeed, strong environmental noise is able to disrupt compensatory dynamics and induce positive consumer correlation (i.e. interspecific synchrony) within local food webs. Dispersal, through its effect on intraspecific synchrony, controls the strength and the spatial extent of environmentally-mediated interspecific synchrony. These results are robust to alternative implementations of food web dynamics and environmental fluctuations. The interactions between dispersal and the environment have important implications for (i) the stability of food webs, (ii) the relative importance of environmental forcing and density-dependent regulation, and for (iii) the general understanding of intraspecific and interspecific synchrony in environmentally-forced metacommunities.

Food web stability: the role of space and noise

The destabilizing effect of noise on local food webs

Our measure of food web stability depends on both the variance and the mean of abundance. The effect of increasing environmental variance is to (1) increase population variance and (2) decrease mean population abundance through the nonlinear functional response of mortality to the environment. The changes in the mean abundance of all species are mediated by two distinct mechanisms that involve Jensen's inequality. Jensen's inequality states that for accelerating nonlinear functions, the variance of the independent variable tends to elevate the response variable (Ruel and Ayres 1999). Since environmental fluctuations are implemented using the

exponential function, increases in the variance of the noise (independent variable) will elevate mean consumer mortality (response variable). This increased consumer mortality causes declines in total consumer abundance and mean predator abundance at the metacommunity level (i.e. Fig 4C,D). The second mechanism involves the inflationary effect of the environmental fluctuations (Gonzalez and Holt 2002; Holt et al. 2003). Strong correlated environmental fluctuations disrupt compensatory dynamics in local food webs by inducing intermittent periods of strong positive consumer correlation. During these periods of positive local consumer correlation, environmental noise drives outbreak dynamics that inflate the abundance of the superior competitor (C_1) and the abundance of the inferior competitor (C_2) decreases due to direct competition. Since the abundance of the inferior competitor decreases faster than the abundance of the superior competitor increases, both total consumer abundance and predator abundance decrease. The distinction between these two mechanisms is particularly evident when dispersal is low. Indeed, mean abundances respond more strongly and rapidly to strong correlated environmental fluctuations than they do to strong negatively correlated environmental fluctuations. How the disruption of local compensatory dynamics by the environment affects the stability of the metacommunity depends on the rate of dispersal and its effect on intraspecific synchrony.

The stabilizing effect of space

Three mechanisms can stabilize spatially heterogeneous predator-prey and parasitoid-host systems (Briggs and Hoopes 2004): (1) The averaging of spatially heterogeneous local dynamics increases global stability (i.e. 'statistical stabilization');

(2) nonlinear spatial averaging can stabilize (or destabilize) local systems when spatially heterogeneous densities are combined with nonlinear responses to density. The final mechanism (3) involves the decoupling of local abundance and immigration (Cuddington and Yodzis 2000). This decoupling leads to a negative correlation between immigration and local abundance that dampens local fluctuations by (i) promoting growth when local abundance is low and (ii) limiting growth when local abundance is high (Briggs and Hoopes 2004). The negative correlation between abundance and immigration promotes stability at both local and global scales. These mechanisms have been used to explain the stabilizing effect of dispersal on enriched trophic metacommunities (Maser et al. 2007). These same mechanisms also operate in our metacommunities when environmental conditions are constant.

In our metacommunity model, intraspecific synchrony and stability exhibit a sharp nonlinear response to changes in dispersal. This nonlinear response leads to two distinct regimes characterized by either (i) low dispersal, intraspecific asynchrony and high stability or (ii) high dispersal, intraspecific synchrony and low stability. This threshold response of synchrony is a general property of locally coupled and self-sustained oscillators and is due to the fact that the dispersal rate controls a phase transition from asynchronous to synchronous fluctuations (Marodi et al. 2002). More specifically, regional asynchrony is maintained by the dynamic instability of synchrony between locally interacting food webs. Once dispersal is high enough to stabilize local synchrony, it necessarily translates into regional intraspecific synchrony, which prevents intermediate levels of local and regional synchrony. However, intraspecific synchrony can respond more gradually to changes in global

(Pikovsky et al. 2002) or irregular (Holland and Hastings 2008) dispersal. For instance, Holland and Hastings (2008) showed that in spatial predator-prey networks, progressively randomizing the local neighborhood of each patch leads to a gradual decrease in regional intraspecific synchrony. Hence, altering either the strength or the spatial structure of dispersal can stabilize spatially-extended systems by decreasing regional intraspecific synchrony.

Space and noise interact to govern food web stability at local and metacommunity scales

Environmental noise can have a strong effect on the stability of food webs. In mean-field systems and in metacommunities experiencing high dispersal, weak correlated environmental noise can promote food web stability by dampening the amplitude of compensatory dynamics (Vasseur and Fox 2007). However, weak correlated environmental noise does not disrupt compensatory dynamics, as global consumer correlation remains negative. In metacommunities experiencing low dispersal, the net effect of weak environmental fluctuations is to destabilize food webs by inducing partial intraspecific synchrony via the Moran effect (Moran 1953). By increasing intraspecific synchrony, the Moran effect reduces spatial heterogeneity and thus limits the effectiveness of spatial stabilization via (i) 'statistical stabilization' or (ii) the decoupling of local abundance and immigration. Hence, weak correlated noise can either stabilize food webs by dampening the amplitude of compensatory dynamics when high dispersal induces intraspecific synchrony, or promote destabilization via the Moran effect when dispersal is low.

Strong environmental noise consistently destabilizes metacommunities by disrupting compensatory dynamics and inducing positive consumer correlation within local food webs. We show how this disruption strongly depends on the amplitude of local consumer fluctuations, which links disruption (i.e. interspecific synchrony) to the effect of dispersal on intraspecific synchrony. Low dispersal dampens local food web fluctuations and sustains intraspecific asynchrony. Within this context, strong correlated environmental noise causes strong consumer correlation in local food webs across the metacommunity. As the strength of the noise is further increased, the spatial average registers as partial interspecific synchrony at the metacommunity scale (Fig. 4B). In contrast, high dispersal induces spatially synchronous food web fluctuations that limit the ability of weak environmental fluctuations to disrupt compensatory dynamics. At the metacommunity scale, as the variance of the environment increases, global consumer correlation increases from negative to zero (Fig. 4A): the intermittent phases of strong positive and negative consumer correlation at the local scale cancel each other and average global consumer correlation approaches zero. This result suggests the counterintuitive appearance of independent consumer fluctuations at the metacommunity scale despite the strong intermittent phases of positive and negative consumer correlation at the local scale (Fig. 5).

Metacommunity stability under strong environmental noise: compensation versus interspecific synchrony

The relative importance of density-dependent regulation and density-independent limitation is a long standing debate in ecology (see review by Coulson et al. 2004).

Here, we show that in environmentally forced metacommunities, the relative importance of regulation and limitation varies in space and time and affects food web stability. As described above, strong correlated environmental noise leads to intermittent disruptions of compensatory dynamics within local food webs. These environmentally-mediated disruptions occur when the local abundance of the consumers—and thus the strength of density-dependent competition—is low. It is during these periods of weak density-dependent regulation that correlated environmental noise induces interspecific synchrony between consumers within local food webs. Communities experiencing the joints effects of strong regulation and strong environmental noise may thus alternate between periods of compensatory dynamics driven by regulation and periods of interspecific synchrony driven by correlated environmental noise. The alternation of compensatory dynamics and interspecific synchrony in metacommunities experiencing both environmental forcing and strong competition suggests that interspecific synchrony cannot be used to exclude the presence of competition or compensatory dynamics in natural systems (Houlahan et al. 2007; Ranta et al. 2008).

Explaining patterns of synchrony in environmentally-forced metacommunities

Recent work has shown how to disentangle the synchronizing effects of dispersal and the environment in simple metapopulation and predator-prey models (Grenfell et al. 1998; Lande et al. 1999; Liebhold et al. 2004). Here, we show that patterns of intra and interspecific synchrony in more complex food webs are generated by the strong interaction between dispersal and the environment.

When dispersal is low, weak correlated environmental fluctuations induce partial intraspecific synchrony through the Moran effect. However, we found that fully correlated environmental variability of intermediate strength can reduce intraspecific synchrony under low dispersal (Fig. 4B). Environmental fluctuations generate intermittent disruptions of local compensatory dynamics (Fig. 5A) that are characterized by periods of high consumer correlation with outbreak dynamics. Intraspecific synchrony declines because these distinct dynamic regimes are asynchronous across space (Fig. 4B, 5C). This phenomenon cannot be explained by recent ecological theories predicting the non-additive but positive effects of dispersal and environmental stochasticity on intraspecific synchrony (Colombo et al. 2008; Lande et al. 1999). Indeed, the reduction of intraspecific synchrony in response to increased environmental variance is due to the complex interplay between dispersal, the environment and local compensatory dynamics.

At the community level, we see an increase in interspecific synchrony whilst intraspecific synchrony declines. Recent work has argued that since dispersal cannot synchronize different species, interspecific synchrony could be used as a signature of the synchronizing effect of the environment (Cattadori et al. 2000; Cheal et al. 2007). We have shown this to be the case in metacommunities experiencing strong correlated environmental noise and low dispersal but not high dispersal (Fig. 4A vs. 4B). Hence, although dispersal cannot directly induce interspecific synchrony, it can have a strong indirect effect on the strength and the spatiotemporal properties of interspecific synchrony.

Several of our predictions can be tested via experiments in the laboratory (Benton et al. 2001; Fontaine and Gonzalez 2005) and field (e.g. Downing et al.

2008). For instance, Fontaine and Gonzalez (2005) showed how dispersal and environmental variability could induce synchrony in an aquatic predator-prey microcosm. By adding an alternative prey and controlling the strength of fully correlated environmental fluctuations (e.g. temperature), one could determine whether the level of dispersal mediates the degree to which the environment disrupts local compensatory dynamics, and whether these effects are synchronized in space: (i) does low dispersal lead to strong but asynchronous disruptions, and (ii) does high dispersal lead to weak but synchronous disruptions?

Caveats and limitations

Our results are robust to chaotic food web dynamics and to the temporal structure of the environment (see Appendix B). However, we also assumed spatially uniform environmental conditions and nearest-neighbor (vs. random) dispersal. Theory and experiments show that even locally correlated environmental noise or random dispersal can induce regional synchrony in populations undergoing stable limit cycles (Bjornstad 2000; Bjornstad et al. 1999). Hence, intraspecific synchrony—a key phenomenon in our findings—is not expected to depend on our simplifying assumption of spatially uniform (i.e. perfectly synchronized) environment noise or our implementation of local dispersal. We used a simple keystone food web module to identify and describe the joint effects of dispersal and environmental variability on food web stability. However, real food webs are much more speciose, and the extension of our findings to more complex food web networks warrants additional attention. Still, the simple keystone module is a useful starting point because it is a

very common motif in natural systems (Milo et al. 2002; Williams and Martinez 2000).

Conclusion

We have shown that the metacommunity concept is critical for understanding how dispersal, environmental variability and compensatory dynamics interact to control the stability of food webs. Interspecific asynchrony emerging from compensatory food web interactions has been proposed as a solution to the complexity-stability paradox and has been demonstrated in simplified, well-mixed food web models experiencing constant environments (McCann et al. 1998). We suggest that food web stability at both local and regional scales is more generally governed by the interaction between compensatory dynamics, dispersal and the environment. These results further suggest a synergy between two components of environmental change: habitat fragmentation and climate change. Low dispersal, due to declining habitat connectivity, and changing patterns of environmental variability (variance and autocorrelation) may act in concert to destabilize food web dynamics.

ACKNOWLEGEMENTS

We thank Jeremy Fox and one anonymous reviewer for their thoughtful comments and suggestions that improved both the analysis and the text. We also acknowledge the granting agencies that made this research possible. T.G. was supported by a McGill Majors fellowship. F.G. was supported by grants from the James S. McDonnell foundation. A.G. was supported by grants from the Natural Sciences and Engineering Research Council of Canada, and the Canada Research Chair Program.

FG and AG are supported by a team grant from Fonds Quebecois de la Recherche sur la Nature et les Technologies (FQRNT).

LITERATURE CITED

Allesina, S., and M. Pascual. 2008. Network structure, predator–prey modules, and stability in large food webs. Theoretical Ecology 1:55-64.

Amarasekare, P. 2008. Spatial Dynamics of Foodwebs. Annual Review of Ecology, Evolution, and Systematics 39:479-500.

Benton, T. G., C. T. Lapsley, and A. P. Beckerman. 2001. Population synchrony and environmental variation: an experimental demonstration. Ecology Letters 4:236-243.

Bjornstad, O. N. 2000. Cycles and synchrony: two historical 'experiments' and one experience. Journal of Animal Ecology 69:869-873.

Bjornstad, O. N., R. A. Ims, and X. Lambin. 1999. Spatial population dynamics: analyzing patterns and processes of population synchrony. Trends in Ecology & Evolution 14:427-432.

Blasius, B., A. Huppert, and L. Stone. 1999. Complex dynamics and phase synchronization in spatially extended ecological systems. Nature 399:354-359.

Briggs, C. J., and M. F. Hoopes. 2004. Stabilizing effects in spatial parasitoid-host and predator-prey models: a review. Theoretical Population Biology 65:299-315.

Buonaccorsi, J. P., J. S. Elkinton, S. R. Evans, and A. M. Liebhold. 2001. Measuring and testing for spatial synchrony. Ecology 82:1668-1679.

Cattadori, I. M., S. Merler, and P. J. Hudson. 2000. Searching for mechanisms of synchrony in spatially structured gamebird populations. Journal of Animal Ecology 69:620-638.

Cheal, A. J., S. Delean, H. Sweatman, and A. A. Thompson. 2007. Spatial synchrony in coral reef fish populations and the influence of climate. Ecology 88:158-169.

Colombo, A., F. Dercole, and S. Rinaldi. 2008. Remarks on Metacommunity Synchronization with Application to Prey-Predator Systems. The American Naturalist 171:430-442.

Coulson, T., P. Rohani, and M. Pascual. 2004. Skeletons, noise and population growth: the end of an old debate? Trends in Ecology & Evolution 19:359-364.

Cuddington, K. M., and P. Yodzis. 2000. Diffusion-limited predator-prey dynamics in euclidean environments: An allometric individual-based model. Theoretical Population Biology 58:259-278.

DeAngelis, D. L., and J. C. Waterhouse. 1987. Equilibrium and Nonequilibrium Concepts in Ecological Models. Ecological Monographs 57:1-21.

Downing, A. L., B. L. Brown, E. M. Perrin, T. H. Keitt, and M. A. Leibold. 2008. Environmental Fluctuations Induce Scale-Dependent Compensation and Increase Stability in Plankton Ecosystems. Ecology 89:3204-3214.

Durrett, R., and S. Levin. 1994. The Importance of Being Discrete (and Spatial). Theoretical Population Biology 46:363-394.

Earn, D. J. D., S. A. Levin, and P. Rohani. 2000. Coherence and Conservation. Science 290:1360-1364.

Engen, S., and B. E. Saether. 2005. Generalizations of the Moran effect explaining spatial synchrony in population fluctuations. American Naturalist 166:603-612.

Fontaine, C., and A. Gonzalez. 2005. Population synchrony induced by resource fluctuations and dispersal in an aquatic microcosm. Ecology 86:1463-1471.

Gonzalez, A., and R. D. Holt. 2002. The inflationary effects of environmental fluctuations in source-sink systems. Proceedings of the National Academy of Sciences of the United States of America 99:14872-14877.

Gonzalez, A., and M. Loreau. (in press). The causes and consequences of compensatory dynamics in ecological communities. Annual Review of Ecology, Evolution, and Systematics.

Greenman, J. V., and T. G. Benton. 2005. The impact of environmental fluctuations on structured discrete time population models: Resonance, synchrony and threshold behaviour. Theoretical Population Biology 68:217-235.

Grenfell, B. T., K. Wilson, B. F. Finkenstadt, T. N. Coulson, S. Murray, S. D. Albon, J. M. Pemberton et al. 1998. Noise and determinism in synchronized sheep dynamics. Nature 394:674-677.

Holland, M. D., and A. Hastings. 2008. Strong effect of dispersal network structure on ecological dynamics. Nature 456:792-794.

Holt, R. D., M. Barfield, and A. Gonzalez. 2003. Impacts of environmental variability in open populations and communities: "inflation" in sink environments. Theoretical Population Biology 64:315-330.

Houlahan, J. E., D. J. Currie, K. Cottenie, G. S. Cumming, S. K. M. Ernest, C. S. Findlay, S. D. Fuhlendorf et al. 2007. Compensatory dynamics are rare in natural ecological communities. Proceedings of the National Academy of Sciences 104:3273-3277.

Ives, A. R., and S. R. Carpenter. 2007. Stability and Diversity of Ecosystems. Science 317:58-62.

Ives, A. R., K. Gross, and J. L. Klug. 1999. Stability and variability in competitive communities. Science 286:542-544.

Keitt, T. H. 2008. Coherent ecological dynamics induced by large-scale disturbance. Nature 454:331-334.

Lande, R., S. Engen, and B. E. Saether. 1999. Spatial scale of population synchrony: Environmental correlation versus dispersal and density regulation. American Naturalist 154:271-281.

Liebhold, A., W. D. Koenig, and O. N. Bjornstad. 2004. Spatial synchrony in population dynamics. Annual Review of Ecology Evolution and Systematics 35:467-490.

Loreau, M., A. L. Downing, M. C. Emmerson, A. Gonzalez, J. Hughes, P. Inchausti, J. Joshi et al. 2002. A new look at the relationship between diversity and stability, Pages 79–91 *in* M. Loreau, S. Naeem, and P. Inchausti, eds. Biodiversity and Ecosystem Functioning: Synthesis and Perspectives. Oxford, United Kingdom, Oxford University Press.

Marodi, M., F. d'Ovidio, and T. Vicsek. 2002. Synchronization of oscillators with long range interaction: Phase transition and anomalous finite size effects. Physical Review E 66:1-8.

Maser, G. L., F. Guichard, and K. S. McCann. 2007. Weak trophic interactions and the balance of enriched metacommunities. Journal of Theoretical Biology 247:337-345.

May, R. M. 1973, Stability and Complexity in Model Ecosystems. Princeton, Princeton University Press.

McCann, K., A. Hastings, S. Harrison, and W. Wilson. 2000. Population outbreaks in a discrete world. Theoretical Population Biology 57:97-108.

McCann, K., A. Hastings, and G. R. Huxel. 1998. Weak trophic interactions and the balance of nature. Nature 395:794-798.

McCann, K. S. 2000. The diversity-stability debate. Nature 405:228-233.

McCann, K. S., J. B. Rasmussen, and J. Umbanhowar. 2005. The dynamics of spatially coupled food webs. Ecology Letters 8:513-523.

Milo, R., S. Shen-Orr, S. Itzkovitz, N. Kashtan, D. Chklovskii, and U. Alon. 2002. Network motifs: Simple building blocks of complex networks. Science 298:824-827.

Moran, P. A. P. 1953. The Statistical Analysis of the Canadian Lynx Cycle .2. Synchronization and Meteorology. Australian Journal of Zoology 1:291-298.

Murdoch, W. W., C. J. Briggs, and R. M. Nisbet. 2003, Consumer-resource Dynamics. Princeton, New Jersey, Princeton University Press.

Pikovsky, A., M. Rosenblum, and J. Kurths. 2002, Synchronization: a Universal Concept in Nonlinear Science. Cambridge, United Kingdom, Cambridge University Press.

Polis, G. A., M. E. Power, and G. R. Huxel. 2004, Food Webs at the Landscape Level. Chicago, Illinois, University Of Chicago Press.

Ranta, E., V. Kaitala, M. S. Fowler, J. Laakso, L. Ruokolainen, and R. B. O'Hara. 2008. Detecting compensatory dynamics in competitive communities under environmental forcing. Oikos 117:1907-1911.

Ranta, E., V. Kaitala, and P. Lundberg. 2006, Ecology of Populations. Cambridge, United Kingdom, Cambridge University Press.

Ripa, J., and A. R. Ives. 2003. Food web dynamics in correlated and autocorrelated environments. Theoretical Population Biology 64:369-384.

Rooney, N., K. McCann, G. Gellner, and J. C. Moore. 2006. Structural asymmetry and the stability of diverse food webs. Nature 442:265-269.

Ruel, J. J., and M. P. Ayres. 1999. Jensen's inequality predicts effects of environmental variation. Trends in Ecology & Evolution 14:361-366.

Tilman, D. 1999. The Ecological Consequences of Changes in Biodiversity: A Search for General Principles. Ecology 80:1455-1474.

Vandermeer, J. 2006. Oscillating populations and biodiversity maintenance. Bioscience 56:967-975.

Vasseur, D. A., and J. W. Fox. 2007. Environmental fluctuations can stabilize food web dynamics by increasing synchrony. Ecology Letters 10:1066-1074.

Vasseur, D. A., U. Gaedke, and K. S. McCann. 2005. A seasonal alternation of coherent and compensatory dynamics occurs in phytoplankton. Oikos 110:507-514.

Williams, R. J., and N. D. Martinez. 2000. Simple rules yield complex food webs. Nature 404:180-183.
Yachi, S., and M. Loreau. 1999. Biodiversity and ecosystem productivity in a fluctuating environment: The insurance hypothesis. Proceedings of the National Academy of Sciences of the United States of America 96:1463-1468.
Zar, J. H. 1999, Biostatistical Analysis. Upper Saddle River, NJ., Prentice-Hall, Inc.

TABLE AND FIGURE LEGENDS

Table 1: Model parameters and their values (Vasseur and Fox 2007)

Figure 1: Metacommunity model diagram. (A) The metacommunity is comprised of 256^2 cells, each of which contains a diamond shaped food web whose dynamics are governed by a discrete version of the differential equation system introduced by McCann *et al.* (1998). The preference coefficients Ω_{ij} are used to adjust the interaction strength between successive trophic levels. Here, a competitively-superior consumer C_1 $\left(\Omega_{C_1R}=1\right)$ and a competitively-inferior consumer C_2 $\left(\Omega_{C_2R}=0.98\right)$ compete for a common resource *R*. The predator *P* preferentially consumes the superior competitor C_1 $\left(\Omega_{PC_1}=0.92\right)$ thus allowing stable coexistence. Dispersal occurs between a focal cell *F* and a single randomly selected cell *N* located within the Moore neighborhood (i.e. 8 nearest neighbors). Dispersal between the focal cell *F* and its randomly selected neighbor *N* is implemented as the product of the maximum dispersal rate *d* and the population abundance differential between *F* and *N*. At each update, all species in the focal cell *F* disperse to the same randomly selected neighboring cell *N*. (B) Representative time series of two neighboring cells *F* and *N* and a distant cell *K* when the environment is constant and dispersal is limited

(d=0.004). These sample cell time series highlight how low dispersal induces spatial heterogeneity and dampened dynamics within the metacommunity.

Figure 2: The effect of dispersal on (A) global stability (μ / σ), (B) global mean abundance (μ), (C) global temporal variance (σ), (D) local stability (μ_L / σ_L), (E) intraspecific synchrony and (F) global consumer correlation (ρ_G) in metacommunities experiencing constant environmental conditions. Results represent means from 10 replicate simulations.

Figure 3: The effect of environmental fluctuations on (A, B) global stability (μ / σ) for predator P, (C, D) consumer C_1, (E, F) consumer C_2 and (G, H) global consumer correlation (ρ_G) for metacommunities with high (d=0.5, first column) and low (d=0.004, second column) dispersal. All results represent means from 10 replicate simulations.

Figure 4: The effect of positively correlated ($\rho_\xi = 1$) and negatively correlated ($\rho_\xi = -1$) environmental fluctuations on (A, B) intraspecific synchrony and global consumer correlation (ρ_G), (C, D) global temporal variance (σ), (E, F) global mean abundance (μ) and (G, H) global stability (μ / σ) for metacommunities with high (d=0.5, first column) and low (d=0.004, second column) dispersal. The grey horizontal dashed lines indicate zero consumer correlation. Results represent means from 10 replicate simulations.

Figure 5: The effect of positively correlated ($\rho_\xi = 1$) environmental fluctuations on the local consumer dynamics of metacommunities experiencing low and high dispersal. (A) The effect of disruptive environmental fluctuations ($\sigma_\xi = 0.25$) on the local consumer dynamics obtained from a single random cell within a

metacommunity experiencing low dispersal. (B) The effect of disruptive environmental fluctuations ($\sigma_\xi = 0.45$) on the local consumer dynamics obtained from a single random cell within a metacommunity experiencing high dispersal. The vertical dashed lines delineate sample 100 time step windows over which local consumer correlation is either negative ($\rho_L < 0$; blue dashed lines) or positive ($\rho_L > 0$; red dashed lines). (C) The mean spatial minimum and maximum local consumer correlations in metacommunities experiencing low (blue) and high (red) dispersal as a function of the strength of correlated environmental fluctuations ($\rho_\xi = 1$). The spatial minimum and maximum local consumer correlations were obtained by splitting the local consumer abundance time series of 100 randomly selected cells into 100-time step windows. Within each time window, the local consumer correlation was calculated for each cell and the minimum and maximum consumer correlations across all cells were determined. These spatial minimum and maximum local consumer correlations were then averaged across all time windows and over 10 replicate simulations (error bars represent standard error; see text for details). The grey horizontal dashed line indicates zero consumer correlation.

TABLES AND FIGURES

Table 1: Model parameters and their values (Vasseur and Fox 2007)

Parameter	Description	Value
r	Resource intrinsic growth rate	1.0
K	Resource carrying capacity	1.0
J_{C_1}	Consumer C_1 ingestion rate	0.8036
J_{C_2}	Consumer C_2 ingestion rate	0.7
J_P	Predator ingestion rate	0.4
M_{C_1}	Medial consumer C_1 mortality rate	0.4
M_{C_2}	Medial consumer C_2 mortality rate	0.2
M_P	Predator mortality rate	0.08
R_{0_1}	Half saturation constant	0.16129
R_{0_2}	Half saturation constant	0.9
C_0	Half saturation constant	0.5
Ω_{PC_1}	Preference coefficient	0.92
Ω_{C_1R}	Preference coefficient	1.0
Ω_{C_2R}	Preference coefficient	0.98

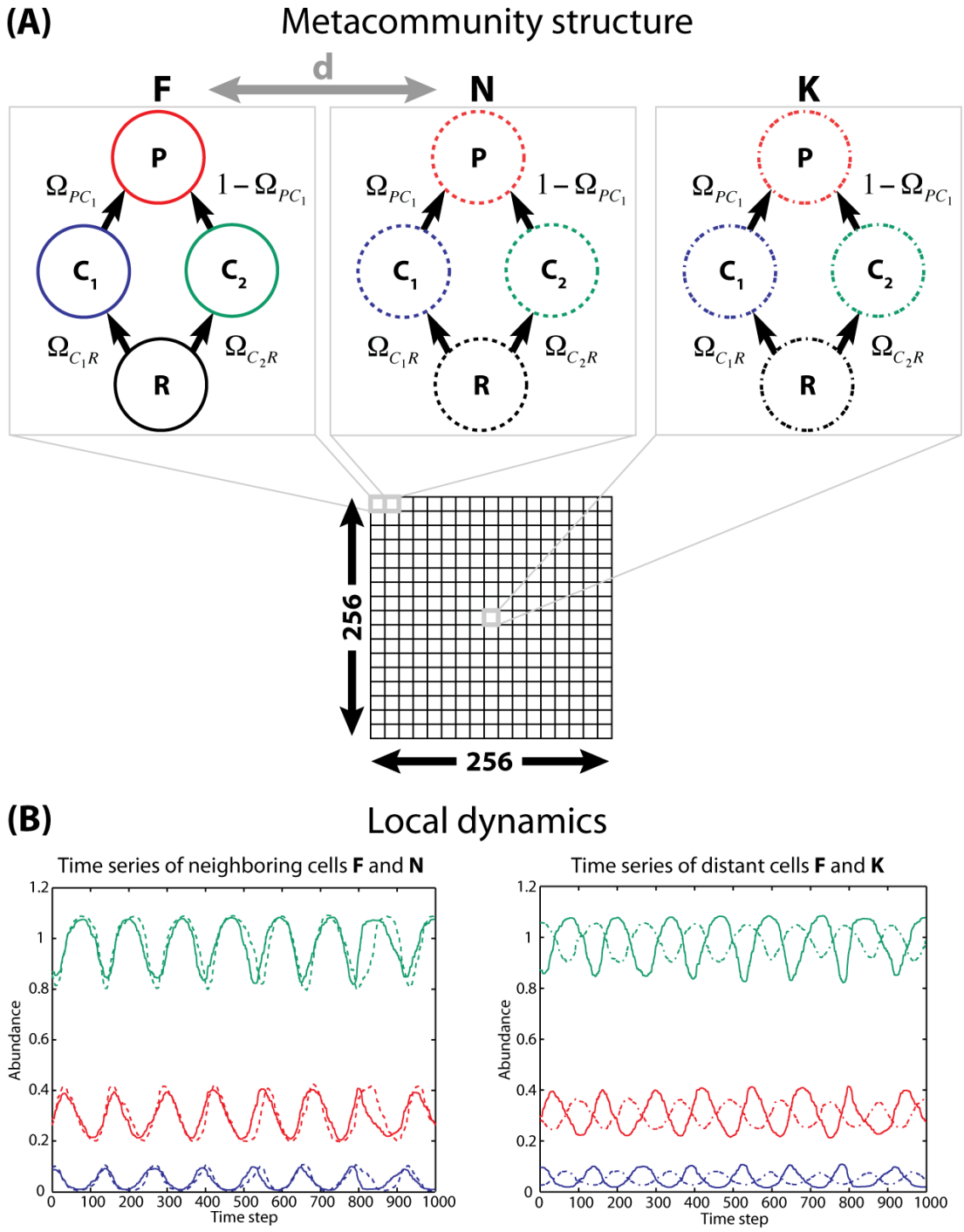
(A)
Metacommunity structure
d
F
N
K
P
C1
C2
R
Ω_{PC_1}
$1-\Omega_{PC_1}$
Ω_{C_1R}
Ω_{C_2R}
256
256
(B)
Local dynamics
Time series of neighboring cells F and N
Time series of distant cells F and K
Abundance
Time step
0
0.2
0.4
0.6
0.8
1
1.2
0
100
200
300
400
500
600
700
800
900
1000

Figure 1

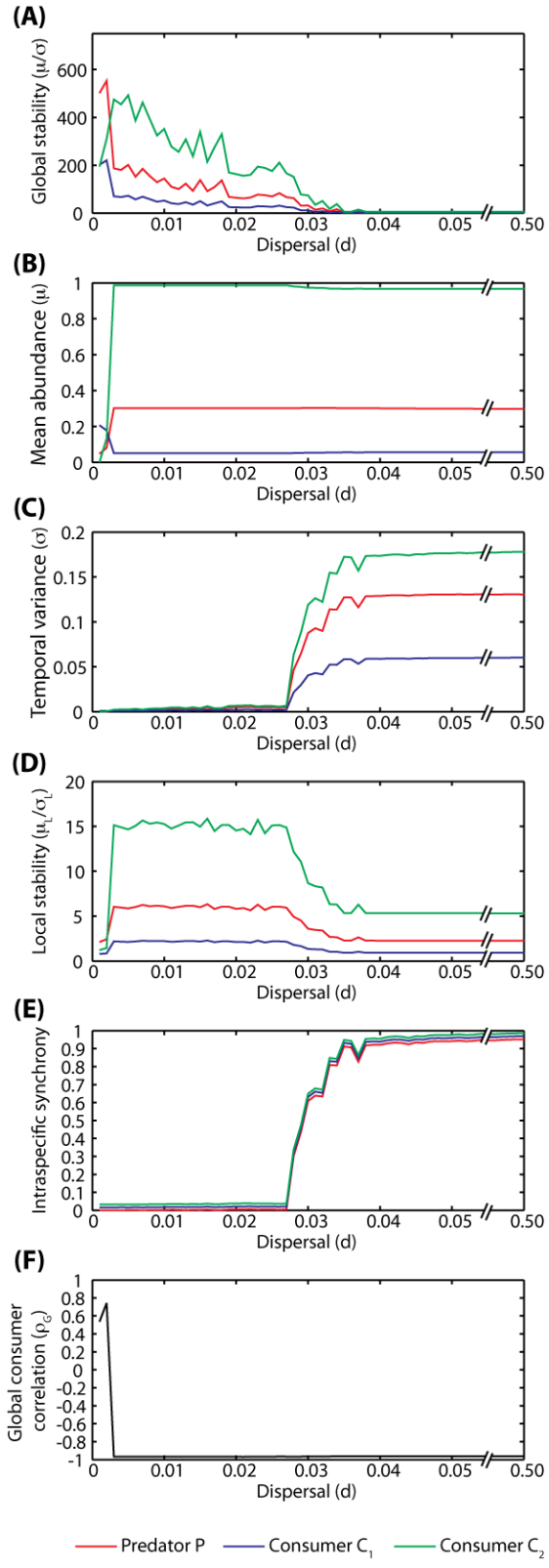
(A)
Global stability (μ/σ)
600
400
200
0
0 0.01 0.02 0.03 0.04 0.05 0.50
Dispersal (d)
(B)
Mean abundance (μ)
1
0.8
0.6
0.4
0.2
0
0 0.01 0.02 0.03 0.04 0.05 0.50
Dispersal (d)
(C)
Temporal variance (σ)
0.2
0.15
0.1
0.05
0
0 0.01 0.02 0.03 0.04 0.05 0.50
Dispersal (d)
(D)
Local stability (μL/σL)
20
15
10
5
0
0 0.01 0.02 0.03 0.04 0.05 0.50
Dispersal (d)
(E)
Intraspecific synchrony
1
0.9
0.8
0.7
0.6
0.5
0.4
0.3
0.2
0.1
0
0 0.01 0.02 0.03 0.04 0.05 0.50
Dispersal (d)
(F)
Global consumer correlation (ρc)
1
0.8
0.6
0.4
0.2
0
-0.2
-0.4
-0.6
-0.8
-1
0 0.01 0.02 0.03 0.04 0.05 0.50
Dispersal (d)
Predator P
Consumer C1
Consumer C2

Figure 2

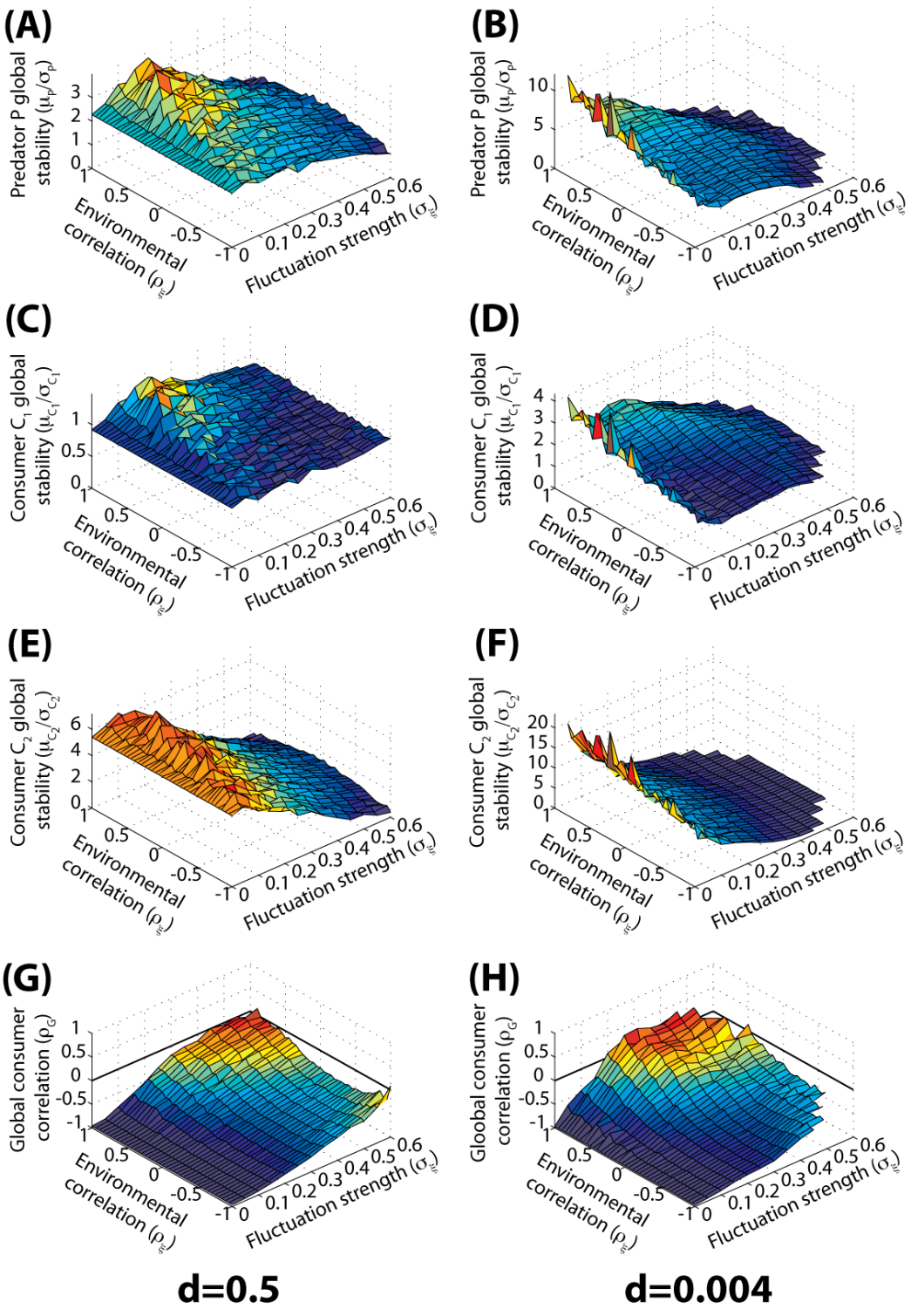
(A)
Predator P global stability (μ_P/σ_P)
(B)
Predator P global stability (μ_P/σ_P)
(C)
Consumer C_1 global stability (μ_{C_1}/σ_{C_1})
(D)
Consumer C_1 global stability (μ_{C_1}/σ_{C_1})
(E)
Consumer C_2 global stability (μ_{C_2}/σ_{C_2})
(F)
Consumer C_2 global stability (μ_{C_2}/σ_{C_2})
(G)
Global consumer correlation (ρ_G)
(H)
Gloobal consumer correlation (ρ_G)
Environmental correlation (ρ_E)
Fluctuation strength (σ_E)
d=0.5
d=0.004

Figure 3

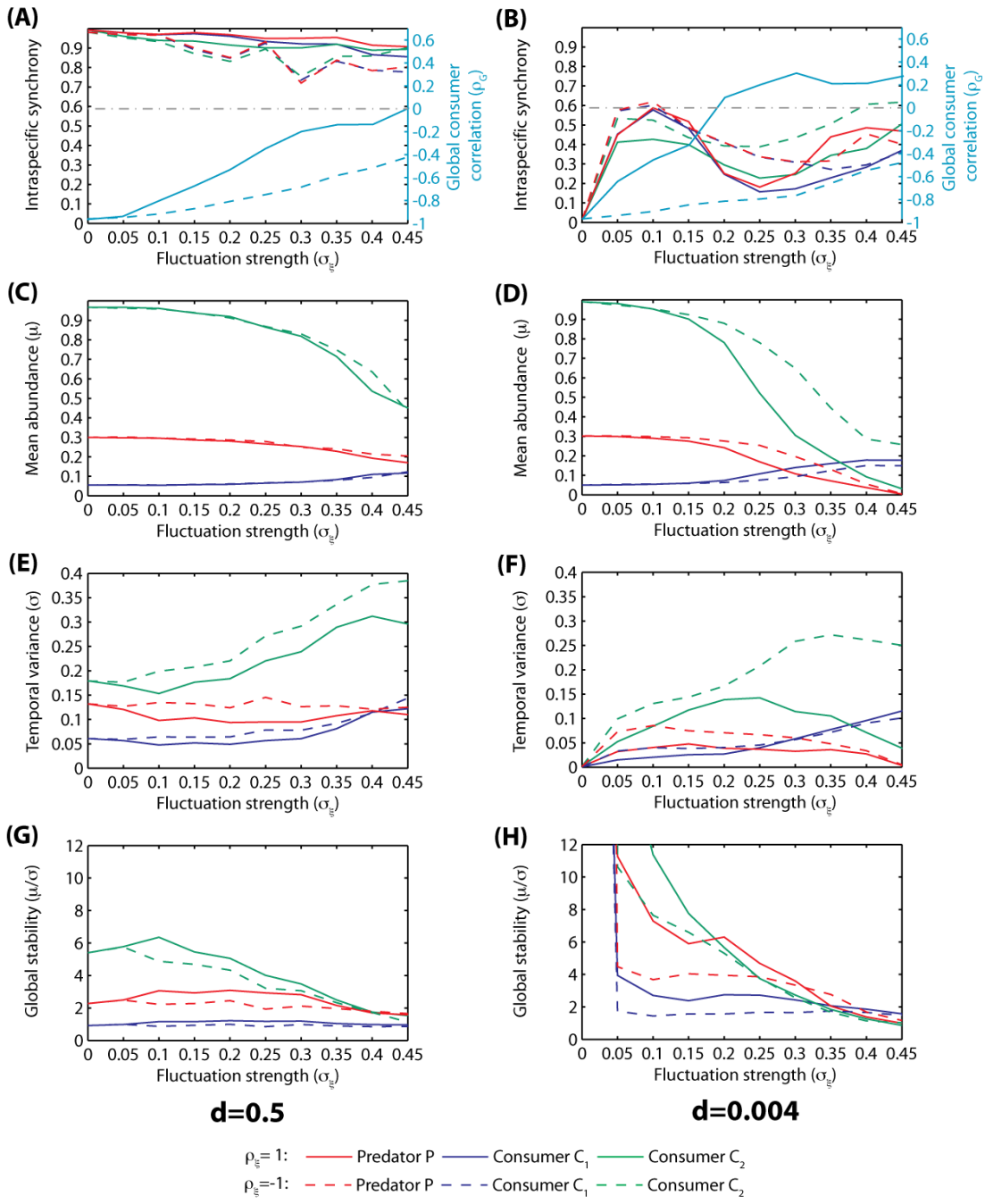
(A)
(B)
(C)
(D)
(E)
(F)
(G)
(H)
Intraspecific synchrony
Global consumer correlation (ρ_C)
Mean abundance (μ)
Temporal variance (σ)
Global stability (μ/σ)
Fluctuation strength (σ_ξ)
d=0.5
d=0.004
ρ_ξ= 1: Predator P Consumer C_1 Consumer C_2
ρ_ξ=-1: Predator P Consumer C_1 Consumer C_2

Figure 4

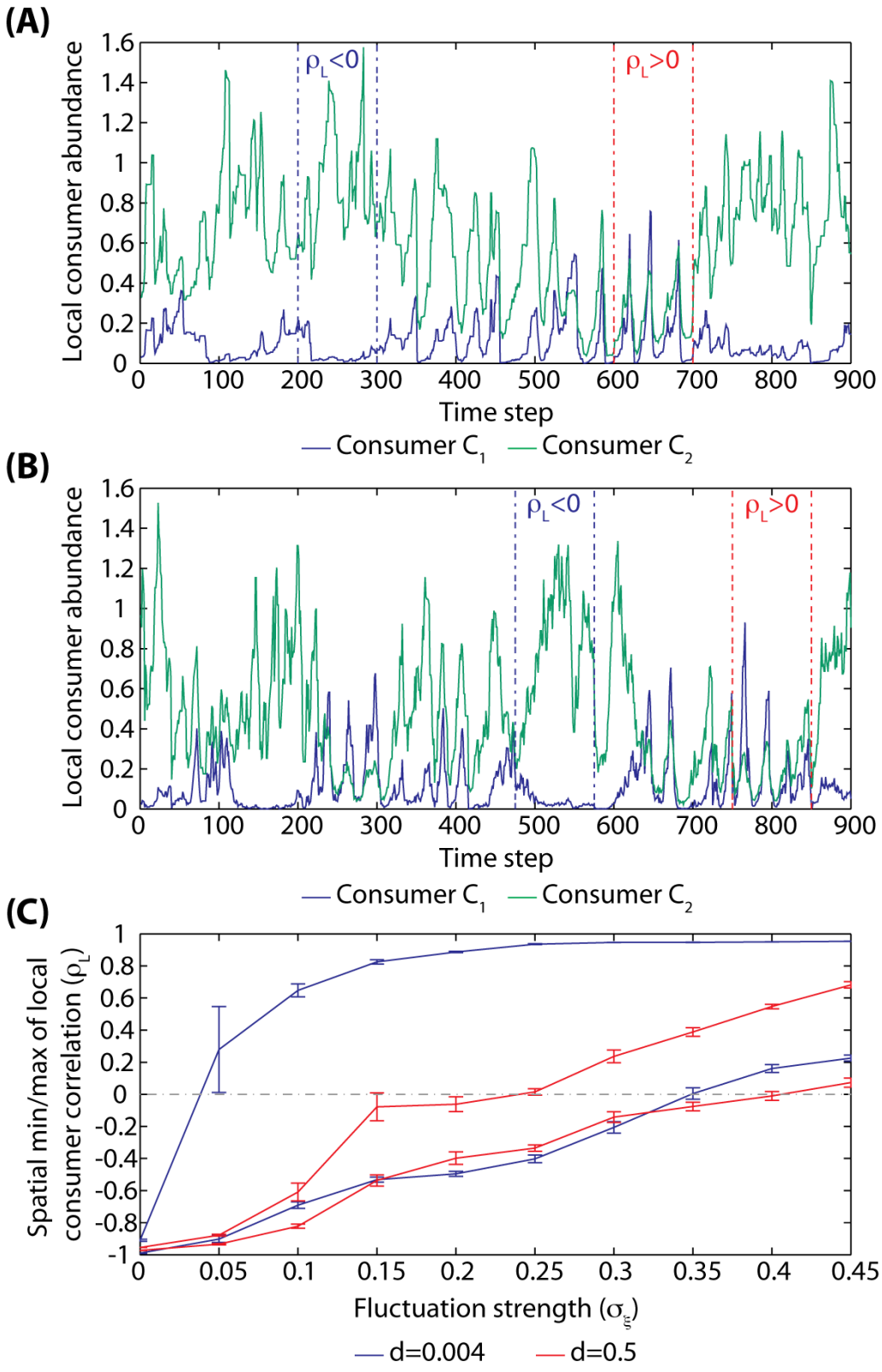
(A)
Local consumer abundance
ρL<0
ρL>0
Time step
Consumer C1
Consumer C2
(B)
Local consumer abundance
ρL<0
ρL>0
Time step
Consumer C1
Consumer C2
(C)
Spatial min/max of local consumer correlation (ρL)
Fluctuation strength (σξ)
d=0.004
d=0.5

Figure 5

APPENDIX A

THE EFFECTS OF ENVIRONMENTAL NOISE AND DISPERSAL ON LOCAL AND REGIONAL METACOMMUNITY DYNAMICS

FIGURE LEGENDS

Figure A1: The effect of fully correlated environmental fluctuations on the different components of the global consumer dynamics in metacommunities experiencing low dispersal (d=0.004). (A) The global consumer time series were decomposed into their endogenous dynamics and their residuals using two different methods: the aggressive (B) cubic splines and a more conservative (C) fitted cosine function (see methods for details regarding this decomposition). Here, an example of this decomposition is provided using both methods ($\sigma_\xi = 0.15$). (B) The effect of environmental fluctuation strength on the correlation between (i) the endogenous components of the global consumer dynamics (blue) and (ii) their residuals (red) using fitted cubic splines. (C) The effect of environmental fluctuation strength on the correlation between (i) the endogenous components of the global consumer dynamics (blue) and (ii) their residuals (red) using fitted cosine functions.

Movie A1-A, -B, -C: The abundance time series of (A) predator P, (B) consumer C_1 and (C) consumer C_2 in a metacommunity with low dispersal (d=0.004) and constant environmental conditions. Low dispersal leads to spatial heterogeneity in the abundance of all species in the food web. The movie files were encoded using the H.264/MPEG-4 AVC codec.

Movie A2-A, -B, -C: The abundance time series of (A) predator *P*, (B) consumer C_1 and (C) consumer C_2 in a metacommunity with high dispersal (d=0.5) and constant environmental conditions. Very low levels of dispersal ($d > 0.03$) are enough to bring about the onset of regionally synchronized oscillations for each species in the food web. The movie files were encoded using the H.264/MPEG-4 AVC codec.

Movie A3-A, -B, -C: Local consumer correlation for metacommunities with low dispersal (d=0.004) experiencing (A) constant environmental conditions, (B) mildly disruptive $\left(\sigma_\xi = 0.2\right)$ or (C) strongly disruptive $\left(\sigma_\xi = 0.3\right)$ correlated environmental fluctuations. The local consumer correlation was computed over 100-time step windows for each cell in the lattice. (A) Low dispersal allows the abundance of local food webs to fluctuate autonomously without affecting the strength of compensatory dynamics (consistent negative local consumer correlation). (B) Weak disruptive environmental fluctuations $\left(\sigma_\xi = 0.2\right)$ lead to the intermittent and asynchronous disruption of compensatory dynamics within a few local food webs (periods of positive local consumer correlation). The rare and fleeting nature of these asynchronous disruptive events leads to very weak interspecific synchrony at the regional scale and only marginal changes in the mean abundance of all species across the metacommunity. (C) When environmental fluctuations are strong $\left(\sigma_\xi > 0.2\right)$, the disruption of compensatory dynamics becomes more pervasive (i.e. more local food webs exhibit periods of positive consumer correlation). This disruption allows the emergence of partial regional interspecific synchrony and leads to large changes in the mean abundance of all species across the metacommunity. The movie files were encoded using the H.264/MPEG-4 AVC codec.

Movie A4-A, -B, -C: Local consumer correlation for metacommunities with high dispersal (d=0.5) experiencing (A) constant environmental conditions, (B) mildly disruptive $\left(\sigma_\xi = 0.2\right)$ or (C) strongly disruptive $\left(\sigma_\xi = 0.3\right)$ correlated environmental fluctuations. The local consumer correlation was computed over 100-time step windows for each cell in the lattice. (A) In the absence of environmental variability, local compensatory dynamics remain consistent in space and time (consistent negative local consumer correlation). (B) Weakly disruptive environmental fluctuations $\left(\sigma_\xi = 0.2\right)$ lead to the intermittent and synchronous disruption of compensatory dynamics within all local food webs (periods of positive local consumer correlation across the entire metacommunity). The rare and fleeting nature of these synchronous disruptive events leads to a very weak increase in the consumer correlation at the regional scale and only marginal changes in the mean abundance of all species across the metacommunity. (C) When environmental fluctuations are strong $\left(\sigma_\xi > 0.2\right)$, the synchronous disruption of compensatory dynamics across all local food webs becomes more persistent (more frequent periods of positive local consumer correlation across the entire metacommunity). This disruption allows the emergence of consumer independence at the regional scale and leads to large changes in the mean abundance of all species across the metacommunity. The movie files were encoded using the H.264/MPEG-4 AVC codec.

FIGURES

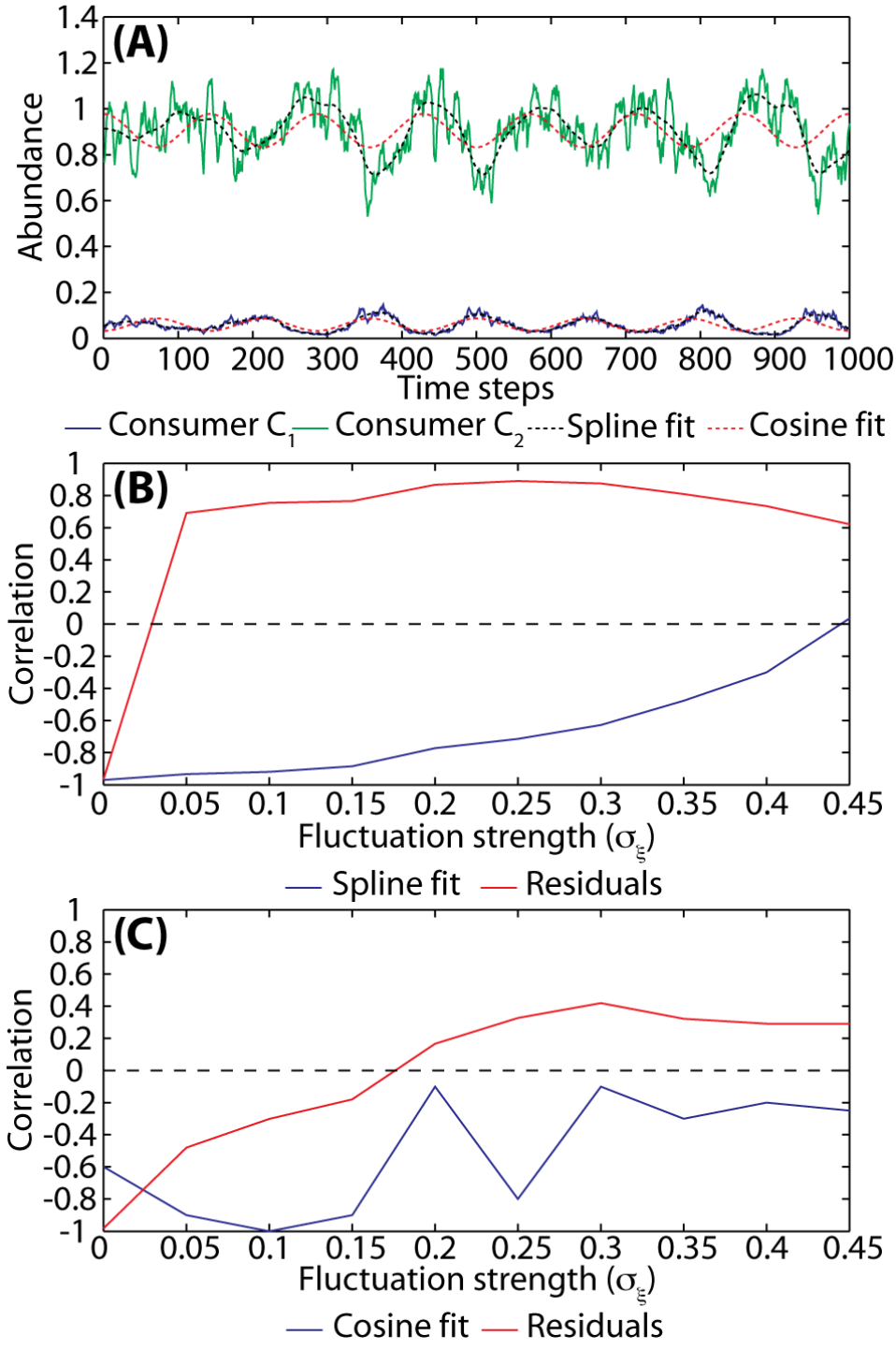

Figure A1

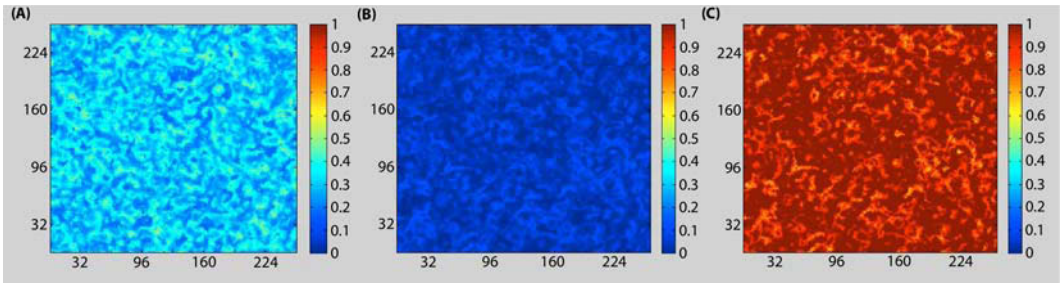

Movie A1

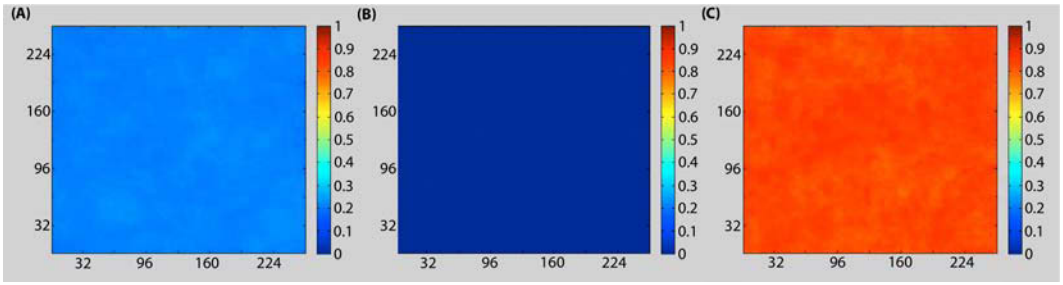

Movie A2

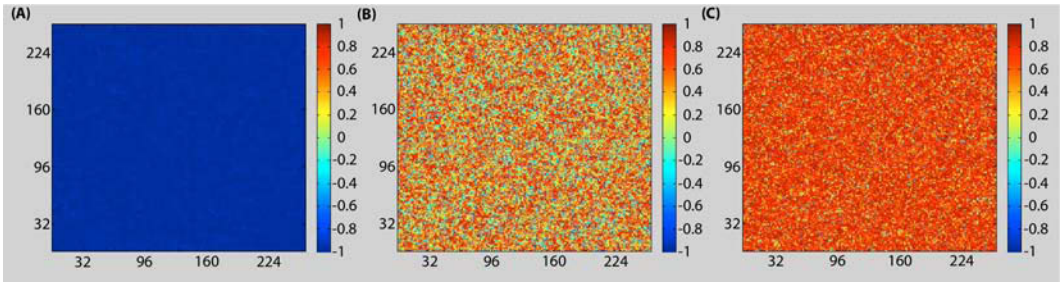

Movie A3

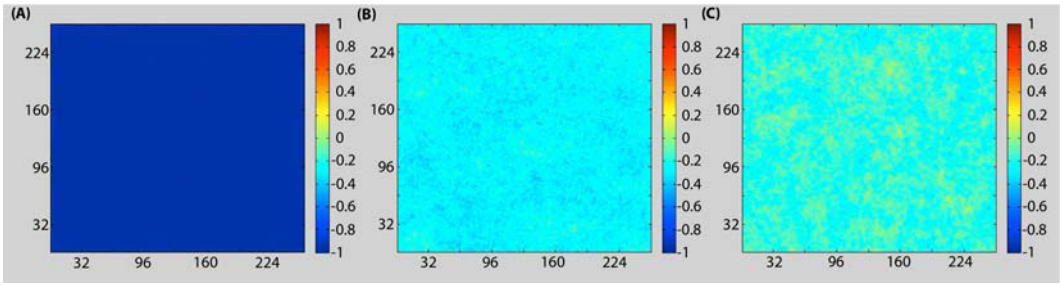

Movie A4

APPENDIX B

ASSESSING THE ROBUSTNESS OF OUR RESULTS TO DIFFERENT IMPLEMENTATIONS OF THE METACOMMUNITY MODEL

We have shown that the effect of environmental fluctuations on food webs stability can be understood by decomposing stability into its temporal variance and mean abundance components. Weak environmental fluctuations can promote stability by dampening but not disrupting compensatory dynamics. Strong environmental fluctuations reduce food web stability by (1) adding more stochastic noise to local food webs and, in the case of correlated noise, (2) disrupting local compensatory dynamics. The local properties and regional consequences of these environmentally-mediated disruptions depend on dispersal and its effect on intraspecific synchrony. By decoupling immigration and local abundance and thereby dampening local food web fluctuations, low dispersal leads to strong and spatially asynchronous local disruptions that generate large changes in the mean abundance of all species. However, by inducing strong synchronized food web fluctuations, high dispersal limits the disruptive effect of strong environmental fluctuations. Indeed, when dispersal is high, strong environmental fluctuations cause spatially synchronized local disruptions that generate small changes in the mean abundance of all species. Hence, by controlling intraspecific synchrony, dispersal mediates the disruptive effect of strong correlated environmental fluctuations on food web stability. In order to assess the generality of these findings, we now explore their robustness to (1) chaotic food

web dynamics and (2) alternative implementations of environmental variability. All model parameter values remain unchanged unless specified otherwise (see table 1).

Chaotic food web dynamics

We increased the predator's preference for consumer C_1 $\left(\Omega_{PC_1} = 0.99\right)$ in order to generate chaotic dynamics in the well-mixed metacommunity (Vasseur and Fox 2007). In the absence of environmental variability, food webs undergoing chaotic dynamics (Fig. B1) or stable limit cycles (Fig. 2) respond similarly to changes in dispersal. When dispersal is extremely low ($d < 0.005$), our stochastic approximation of the continuous-time model fails. This failure leads to the quasi-extinctions of consumer C_2 and predator P, along with the trivial loss of compensatory dynamics (i.e. $\rho_G > 0$; Fig. B1E). Low dispersal ($0.005 < d < 0.04$) promotes stability (Fig. B1A) by reducing intraspecific synchrony (Fig. B1D) without affecting compensatory dynamics (i.e. $\rho_G < 0$, Fig. B1E). Increasing dispersal beyond its threshold value ($d > 0.04$) homogenizes the metacommunity (Fig. B1D). This homogenization reduces food web stability (Fig. B1A) without affecting compensatory dynamics (Fig. B1E).

When dispersal is high (d=0.5), weak environmental fluctuations ($0 < \sigma_\xi \leq 0.1$) stabilize the entire food web (Fig. Appendix B2A,C,E, B3G) by reducing intraspecific synchrony (Fig. B3A). Correlated environmental fluctuations are more stabilizing than their negatively correlated counterparts (Fig. B3G) because in addition to reducing intraspecific synchrony, they also dampen (but do not disrupt) compensatory dynamics (Fig. B3A,E). Strong environmental fluctuations ($\sigma_\xi > 0.1$) reduce food web stability (Fig. B3G,H) by (1) adding more stochastic noise to local

food webs (Fig. B3E,F) and, in the case of correlated environmental fluctuations, (2) disrupting local compensatory dynamics (Fig. B3A,B). The properties of these environmentally-mediated disruptions of local compensatory dynamics depend on dispersal and its effect on intraspecific synchrony. Low dispersal limits intraspecific synchrony (Fig. B3B) and leads to strong and spatially asynchronous local disruptions that generate large changes in the mean abundance of all species (Fig. B3D). High dispersal increases intraspecific synchrony (Fig. B3A) and leads to spatially synchronous local disruptions of intermediate strength that generate small changes in the mean abundance of all species (Fig. B3C). Hence, the results we outlined for food webs undergoing stable limit cycles also apply to food webs undergoing chaotic dynamics.

Alternative implementations of environmental variability

Environmental variability as temporally autocorrelated noise affecting consumer mortality

We first explore how the temporal structure of environmental fluctuations affects our main results by using autocorrelated environmental fluctuations for each consumer. Specifically, we generated environmental time series with the desired fluctuation strength, cross-correlation and autocorrelation by using the 'phase partnering' method described by Vasseur (2007):

$$\xi_i(t) = \sum_{f=1}^{n/2} \frac{1}{f^{\gamma/2}} \sin\left(\frac{2\pi f t}{n} + \theta_i(f)\right) \qquad (1)$$

where $\xi_i(t)$ is the environmental time series of consumer *i, n* is the length of the time series, γ determines the relationship between power and frequency f, t is time and $\theta_i(f)$ is a uniform deviate in the interval [0, 2π). The desired cross-correlation between the two environmental time series was achieved by partnering the uniform phase deviates of the consumers (Vasseur 2007):

$$\theta_2(f) = \theta_1 + \cos^{-1}\left(\rho_\xi\right) \qquad (2)$$

The cross-correlated environmental time series were then scaled to the requisite fluctuation strength σ_ξ:

$$\xi_i(t) = \sigma_\xi \frac{\xi_i(t)}{\sigma_i} \qquad (3)$$

where σ_i represents the standard deviation of the environmental time series $\xi_i(t)$ of consumer *i* prior to any scaling. The scaled environmental time series $\xi_i(t)$ were then incorporated into the consumer mortality rates. The mortality rate of consumer *i* at time *t* was:

$$M_{Ci}(t) = M_{Ci} \cdot e^{\xi_i(t)} \qquad (4)$$

where M_{Ci} represents the medial consumer mortality rate of consumer *i* (table 1). Since most environmental variables show some degree of autocorrelation (Vasseur 2007), we tested the robustness of our findings to autocorrelated environmental noise (i.e. red noise, $\gamma = 0.8$).

In metacommunities experiencing high dispersal, weak environmental fluctuations ($\sigma_\xi \leq 0.15$) promote stability (Fig. B4A,C,E, B5G) by dampening the amplitude of compensatory dynamics (Fig. B4G, B5A,E). As before, strong environmental fluctuations ($\sigma_\xi > 0.15$) reduce food web stability (Fig. B4) by (1)

adding more stochastic noise to local food webs (Fig. B5E,F) and, in the case of correlated noise, (2) disrupting local compensatory dynamics (Fig. B4G,H, B5A,B). In addition to these two mechanisms, strong negatively correlated environmental fluctuations can also destabilize food webs by amplifying compensatory dynamics (Fig. B5C-H). However, this novel effect does not change our main findings: it merely highlights the fact that strong environmental fluctuations can destabilize food webs by either amplifying or disrupting local compensatory dynamics (Fig. B4G,H, B5A,B). As before, by controlling intraspecific synchrony, dispersal mediates the strength of this disruptive effect and its consequences for the stability of food webs (Fig. B5A,B).

Environmental variability as additive demographic noise

We now determine the robustness of our main findings to the nature of environmental fluctuations by implementing environmental variability as demographic noise affecting the consumer population growth rates (Vasseur and Fox 2007). Under this scenario, the growth rate of consumer C_i in cell (x,y) at time t becomes:

$$\Delta C_i(x,y,t) = \Delta C_i(x,y,t) + \xi_i(t) \qquad (5)$$

where $\xi_i(t)$ is spatially-uniform, normally-distributed white noise with zero mean. We varied the strength (σ_ξ) and cross-correlation (ρ_ξ) of demographic noise in order to assess the robustness of our results.

This implementation of environmental variability has two fundamental implications. First, since demographic noise is not filtered by the exponential function, it can add both positive and negative values to the abundance of

consumers and thus lead to rapid destabilization (Fig. B6,B7). Second, demographic noise is additive and thus largely independent of local abundances. It can thus be interpreted as an allochthonous source or sink of consumers, depending on the sign of the noise. Since the demographic noise has zero-mean, positive noise will balance negative noise in time. However, since abundances are bounded by zero at the low end but remain unbounded at the high end, balanced zero-mean noise will lead to an unbalanced (net positive) allochthonous effect and an increase in total consumer abundance. This imbalance increases with the strength of demographic noise and leads to increased predator *P* abundance (Fig. B7C,D).

Negatively correlated noise will tend to amplify the overall allochthonous imbalance because at each time step, adding positive noise to the abundance of one consumer will add negative noise to the abundance of the other consumer. Since abundances are zero-bounded, negatively correlated noise will lead to a net increase in total consumer abundance at each time step. Hence, in addition to the imbalance between allochthonous inputs and outputs over time, negative noise also generates an instantaneous imbalance between allochthonous inputs and outputs. These accrued imbalances increase with demographic noise and lead to the monotonic increase of predator *P* abundance (Fig. B7C,D). By providing large allochthonous inputs of consumers, strong negatively correlated noise increases predator mean abundance and stability (Fig. B7G).

However, this allochthonous effect does not change our main results. Indeed, when dispersal is high, weak correlated noise ($\sigma_\xi \leq 0.01$) stabilizes food webs by dampening (but not disrupting) compensatory dynamics (Fig. B6A,C,E,G, B7E,G). Strong noise ($\sigma_\xi > 0.01$) reduces food web stability (Fig. B6, B7G,H) by (1) adding

more stochastic noise to local food webs and (Fig. B7E,F), in the case of correlated noise, (2) disrupting local compensatory dynamics (Fig. B7A,B). The properties of these noise-induced disruptions of local compensatory dynamics depend on dispersal and its effect on intraspecific synchrony. Low dispersal limits intraspecific synchrony (Fig. B7B) and leads to strong and spatially asynchronous local disruptions, whereas high dispersal increases intraspecific synchrony (Fig. B7A) and leads to spatially synchronous local disruptions of intermediate strength (Fig. B7C). As noise is increased ($\sigma_\xi > 0.02$), the allochthonous effect overwhelms local food web dynamics and the sign of the global consumer correlation largely reflects the sign of the demographic noise (Fig. B6G,H, B7A,B).

Hence, our results are robust to both the nature (i.e. filtered noise affecting mortality or additive noise affecting demography) and the temporal structure (white noise vs. red noise) of environmental fluctuations.

LITERATURE CITED

Vasseur, D. A. 2007. Environmental colour intensifies the Moran effect when population dynamics are spatially heterogeneous. Oikos 116:1726-1736.

Vasseur, D. A., and J. W. Fox. 2007. Environmental fluctuations can stabilize food web dynamics by increasing synchrony. Ecology Letters 10:1066-1074.

FIGURE LEGENDS

Figure B1: The effect of dispersal on (A) global stability (μ/σ), (B) global mean abundance (μ), (C) global temporal variance (σ), (D) intraspecific synchrony and (E) global consumer correlation (ρ_G) in metacommunities experiencing constant

environmental conditions and chaotic dynamics. All results represent means from 10 replicate simulations.

Figure B2: The effect of environmental fluctuations on (A, B) global stability (μ/σ) for predator *P*, (C, D) consumer C_1, (E, F) consumer C_2 and (G, H) global consumer correlation (ρ_G) for metacommunities experiencing chaotic dynamics and either high (d=0.5, first column) or low (d=0.005, second column) dispersal. All results represent means from 10 replicate simulations.

Figure B3: The effect of positively correlated ($\rho_\xi = 1$) and negatively correlated ($\rho_\xi = -1$) environmental fluctuations on (A, B) intraspecific synchrony and global consumer correlation (ρ_G), (C, D) global temporal variance (σ), (E, F) global mean abundance (μ) and (G, H) global stability (μ/σ) for metacommunities experiencing chaotic dynamics and either high (d=0.5 first column) or low (d=0.005, second column) dispersal. The grey horizontal dashed line indicates zero consumer correlation. All results represent means from 10 replicate simulations.

Figure B4: The effect of autocorrelated $(\gamma = 0.8)$ environmental fluctuations on (A, B) global stability (μ/σ) for predator *P*, (C, D) consumer C_1, (E, F) consumer C_2 and (G, H) global consumer correlation (ρ_G) for metacommunities with high (d=0.5, first column) and low (d=0.004, second column) dispersal. All results represent means from 10 replicate simulations.

Figure B5: The effect of positively cross-correlated ($\rho_\xi = 1$) and negatively cross-correlated ($\rho_\xi = -1$) autocorrelated $(\gamma = 0.8)$ environmental fluctuations on (A, B) intraspecific synchrony and global consumer correlation (ρ_G), (C, D) global temporal variance (σ), (E, F) global mean abundance (μ) and (G, H) global stability

(μ/σ) for metacommunities with high (d=0.5, first column) and low (d=0.004, second column) dispersal. The grey horizontal dashed line indicates zero consumer correlation. Results represent means from 10 replicate simulations.

Figure B6: The effect of additive demographic noise on (A, B) global stability (μ/σ) for predator P, (C, D) consumer C_1, (E, F) consumer C_2 and (G, H) global consumer correlation (ρ_G) for metacommunities with high (d=0.5, first column) and low (d=0.004, second column) dispersal. All results represent means from 10 replicate simulations.

Figure B7: The effect of positively correlated ($\rho_\xi = 1$) and negatively correlated ($\rho_\xi = -1$) environmental fluctuations on (A, B) intraspecific synchrony and global consumer correlation (ρ_G), (C, D) global temporal variance (σ), (E, F) global mean abundance (μ) and (G, H) global stability (μ/σ) for metacommunities with high (d=0.5, first column) and low (d=0.004, second column) dispersal. The grey horizontal dashed line indicates zero consumer correlation. All results represent means from 10 replicate simulations.

FIGURES

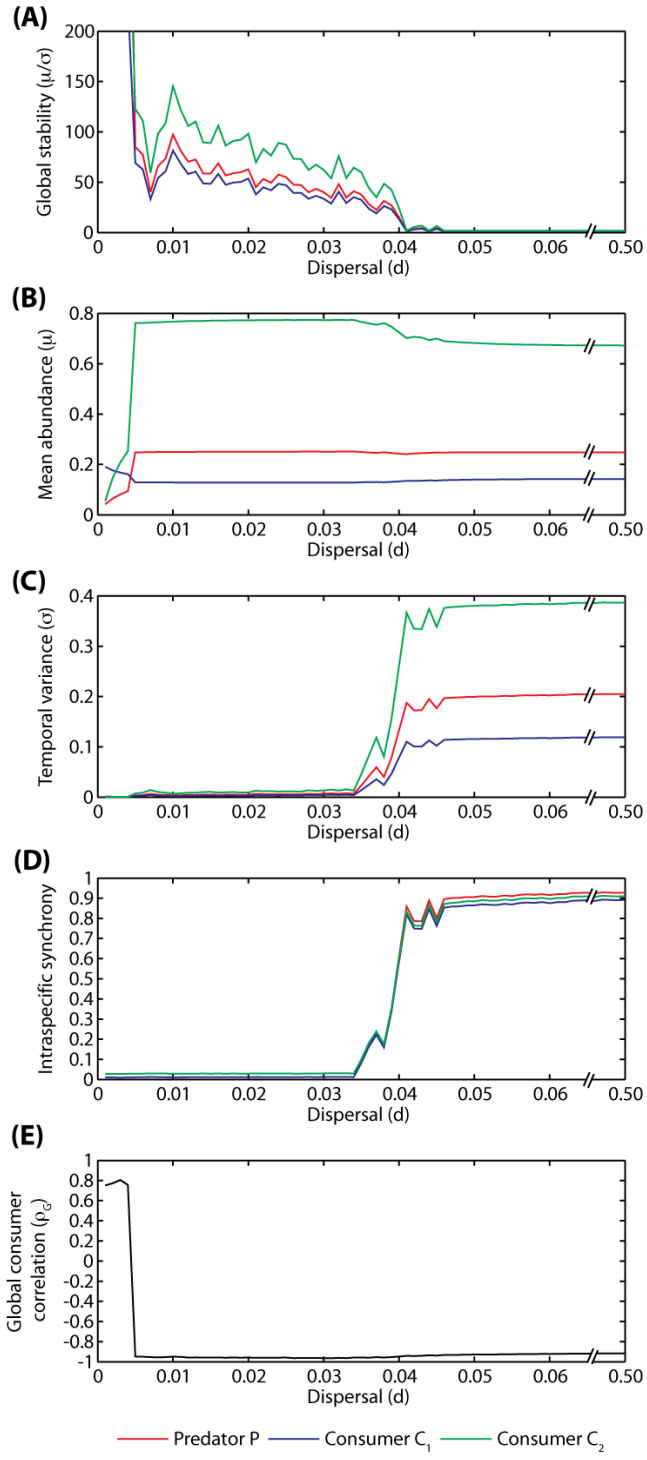

Figure B1

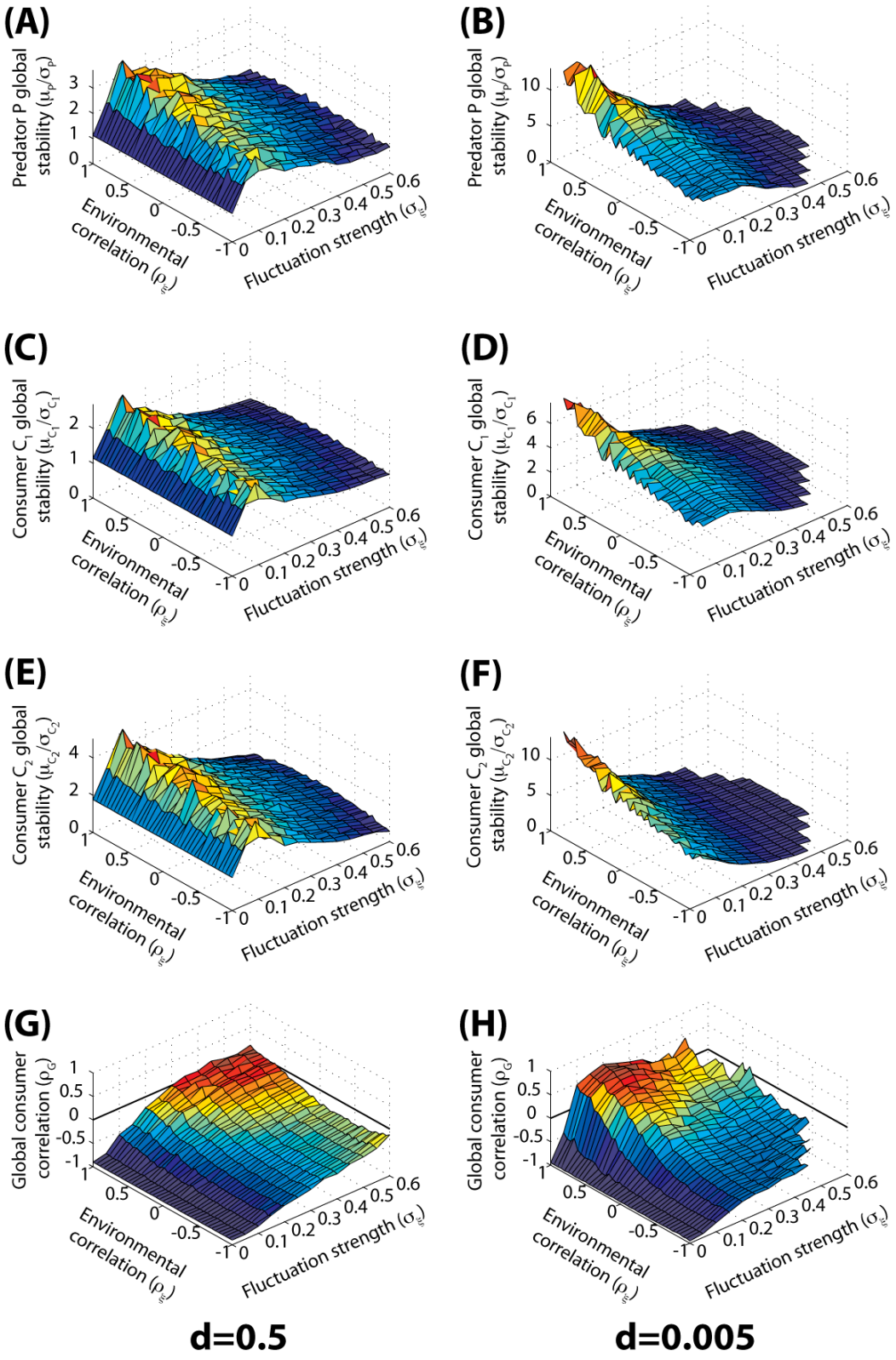
(A)
Predator P global stability (μ_p/σ_p)
(B)
Predator P global stability (μ_p/σ_p)
(C)
Consumer C_1 global stability (μ_{C_1}/σ_{C_1})
(D)
Consumer C_1 global stability (μ_{C_1}/σ_{C_1})
(E)
Consumer C_2 global stability (μ_{C_2}/σ_{C_2})
(F)
Consumer C_2 global stability (μ_{C_2}/σ_{C_2})
(G)
Global consumer correlation (ρ_G)
(H)
Global consumer correlation (ρ_G)
Environmental correlation (ρ_E)
Fluctuation strength (σ_E)
d=0.5
d=0.005

Figure B2

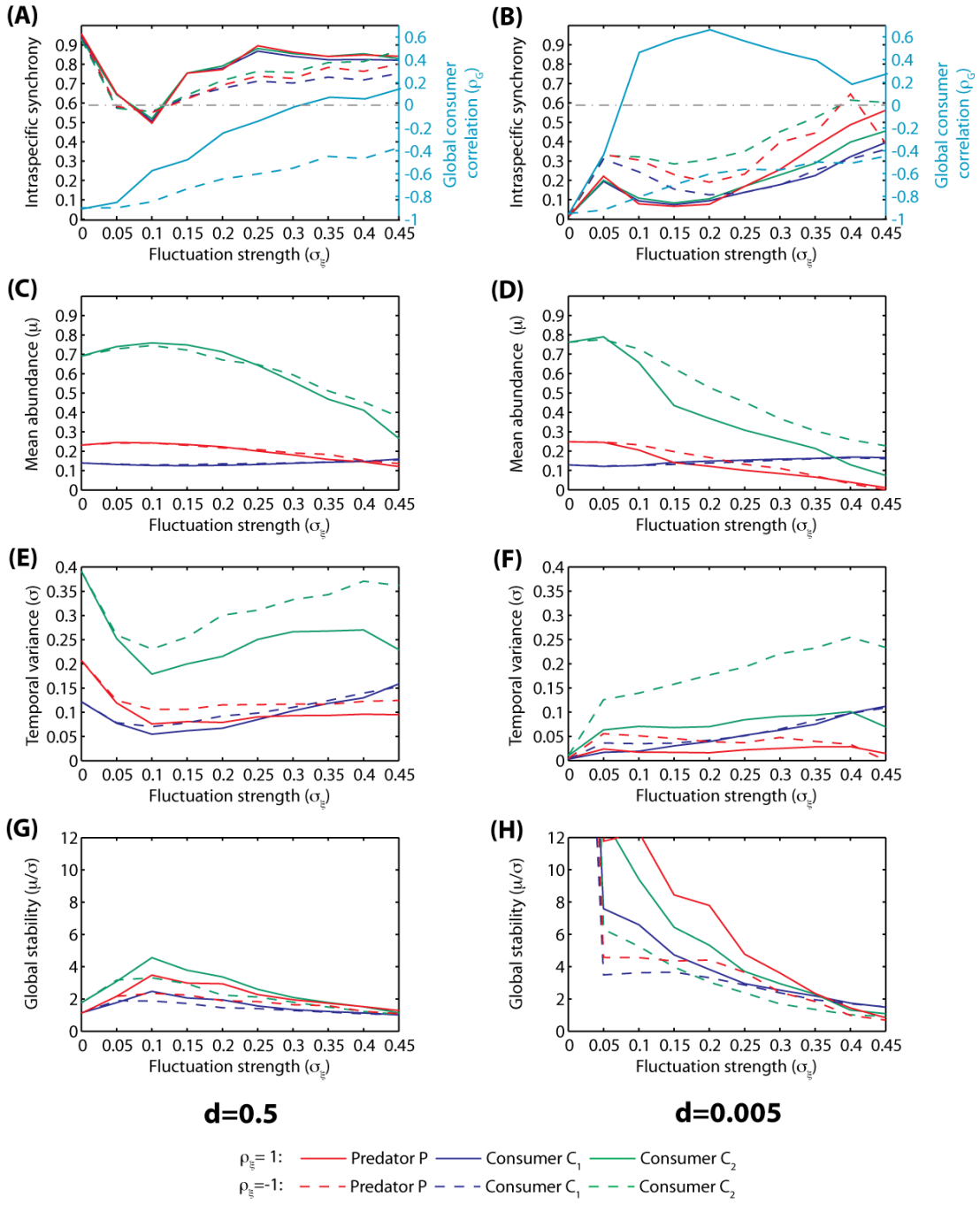
(A)
(B)
(C)
(D)
(E)
(F)
(G)
(H)
Intraspecific synchrony
Global consumer correlation (ρ_G)
Mean abundance (μ)
Temporal variance (σ)
Global stability (μ/σ)
Fluctuation strength (σ_ξ)
d=0.5
d=0.005
ρ_ξ= 1: Predator P Consumer C_1 Consumer C_2
ρ_ξ=-1: Predator P Consumer C_1 Consumer C_2

Figure B3

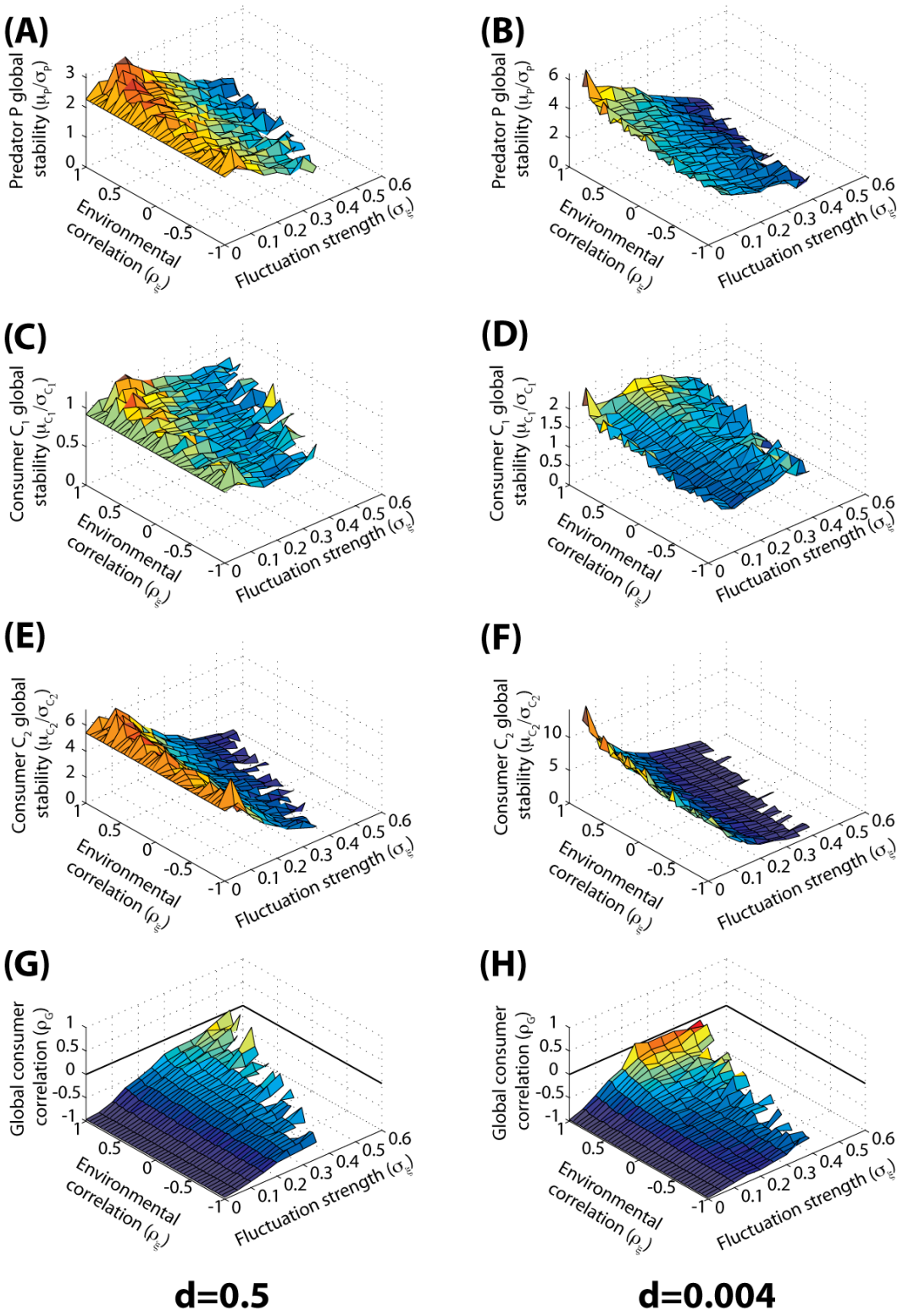
(A)
Predator P global stability (μ_P/σ_P)
(B)
Predator P global stability (μ_P/σ_P)
(C)
Consumer C_1 global stability (μ_{C_1}/σ_{C_1})
(D)
Consumer C_1 global stability (μ_{C_1}/σ_{C_1})
(E)
Consumer C_2 global stability (μ_{C_2}/σ_{C_2})
(F)
Consumer C_2 global stability (μ_{C_2}/σ_{C_2})
(G)
Global consumer correlation (ρ_G)
(H)
Global consumer correlation (ρ_G)
Environmental correlation (ρ_E)
Fluctuation strength (σ_E)
d=0.5
d=0.004

Figure B4

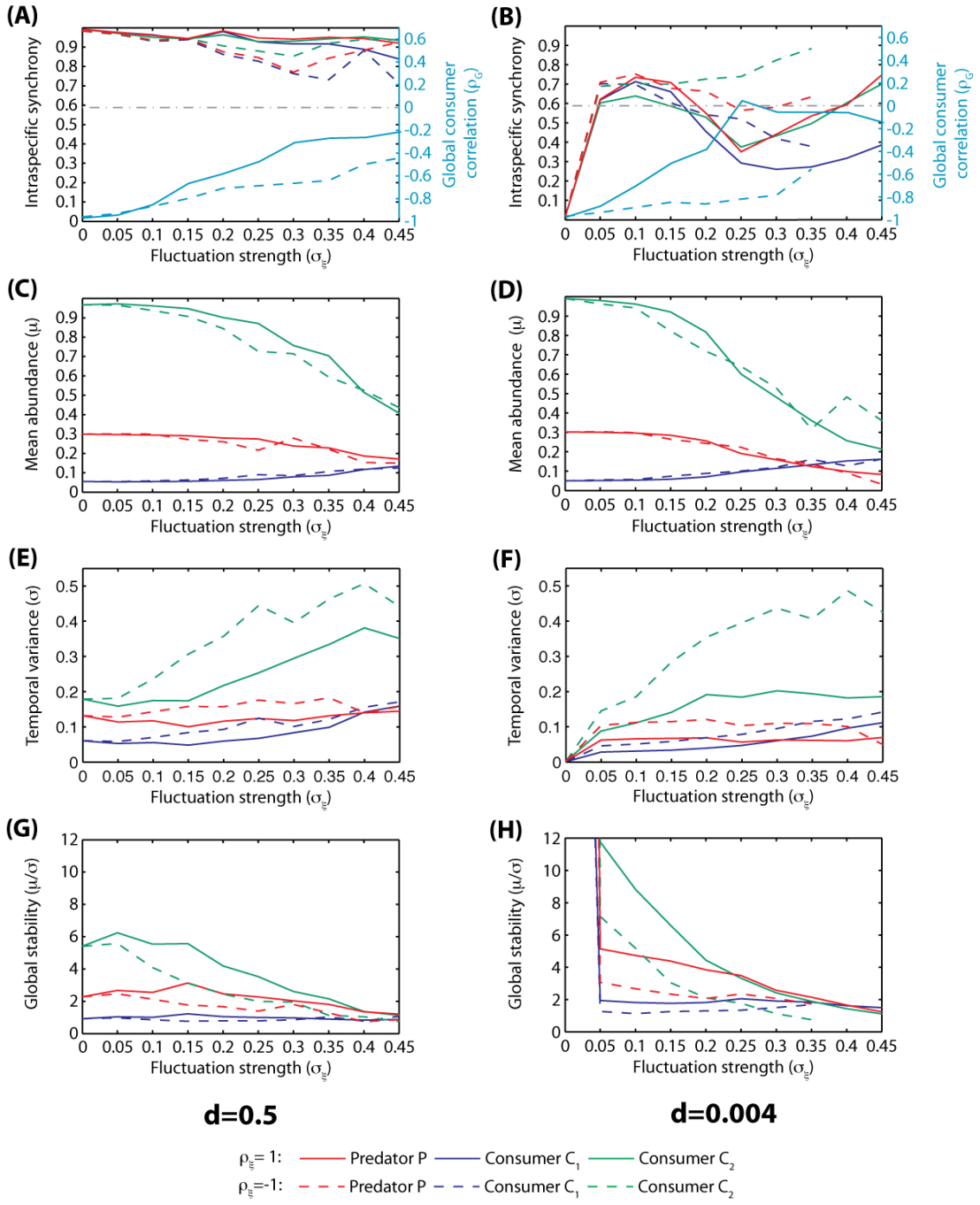
(A)
(B)
(C)
(D)
(E)
(F)
(G)
(H)
Intraspecific synchrony
Global consumer correlation (ρ_G)
Mean abundance (μ)
Temporal variance (σ)
Global stability (μ/σ)
Fluctuation strength (σ_ξ)
d=0.5
d=0.004
ρ_ξ= 1: Predator P Consumer C_1 Consumer C_2
ρ_ξ=-1: Predator P Consumer C_1 Consumer C_2

Figure B5

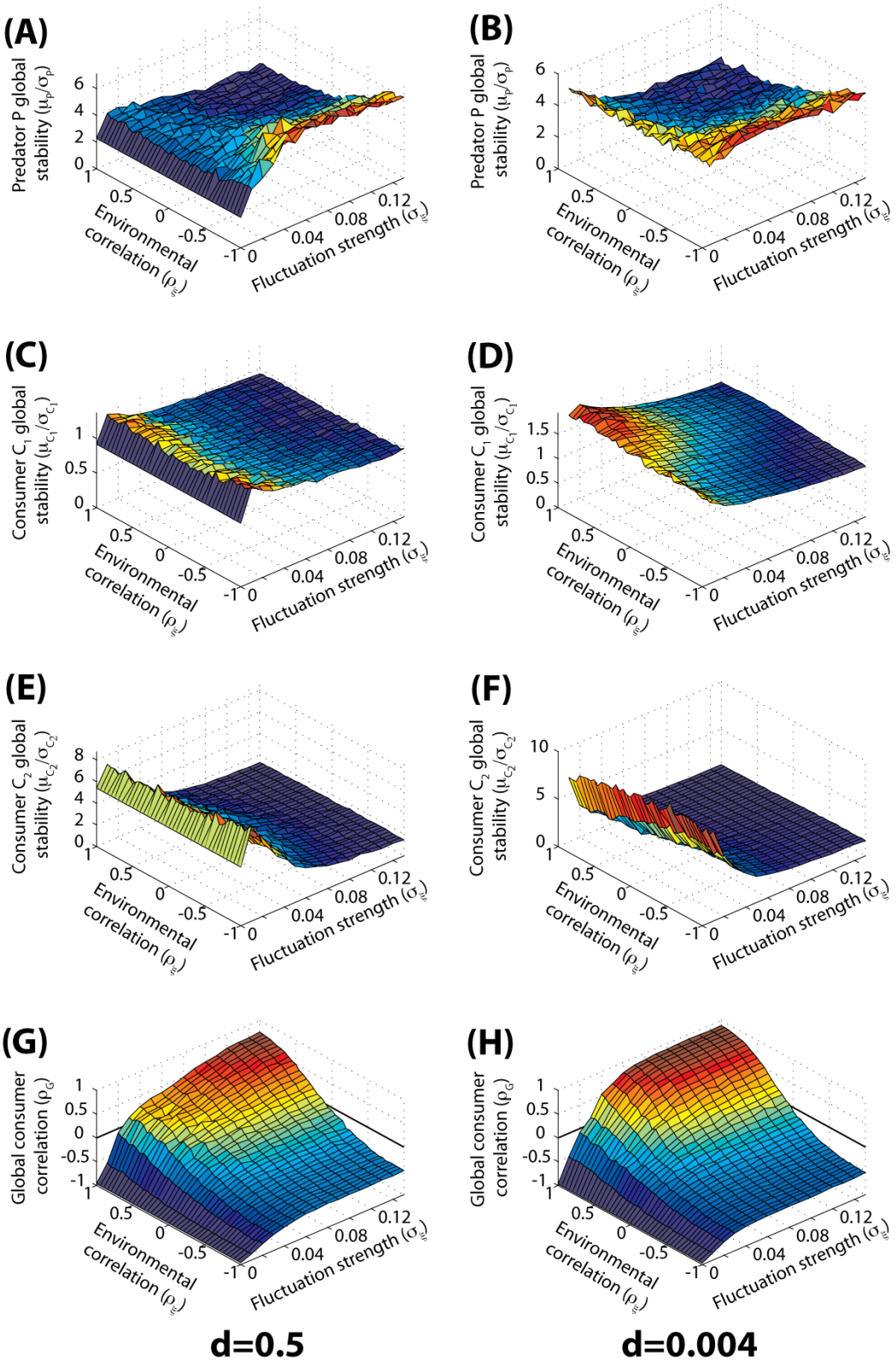
(A)
Predator P global stability (μ_P/σ_P)
(B)
Predator P global stability (μ_P/σ_P)
(C)
Consumer C_1 global stability (μ_{C_1}/σ_{C_1})
(D)
Consumer C_1 global stability (μ_{C_1}/σ_{C_1})
(E)
Consumer C_2 global stability (μ_{C_2}/σ_{C_2})
(F)
Consumer C_2 global stability (μ_{C_2}/σ_{C_2})
(G)
Global consumer correlation (ρ_G)
(H)
Global consumer correlation (ρ_G)
Environmental correlation (ρ_E)
Fluctuation strength (σ_E)
d=0.5
d=0.004

Figure B6

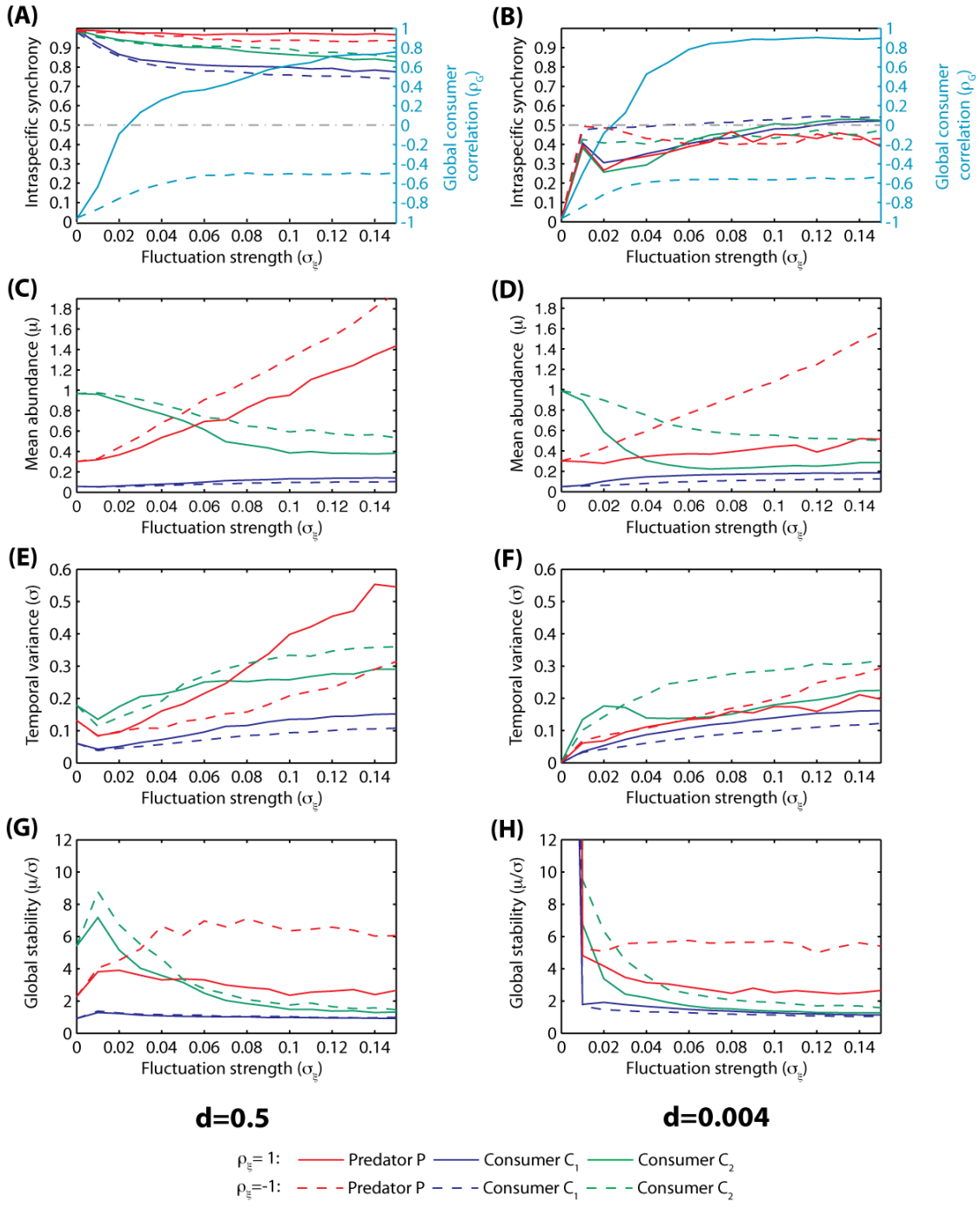
(A)
(B)
(C)
(D)
(E)
(F)
(G)
(H)
Intraspecific synchrony
Global consumer correlation (ρ_G)
Mean abundance (μ)
Temporal variance (σ)
Global stability (μ/σ)
Fluctuation strength (σ_ξ)
d=0.5
d=0.004
ρ_ξ= 1: Predator P Consumer C_1 Consumer C_2
ρ_ξ=-1: Predator P Consumer C_1 Consumer C_2

Figure B7

SUMMARY AND CONCLUSION

I have combined a series of dynamical models with large datasets to develop and validate a theory of marine metacommunities that emphasizes the importance of dispersal for determining the relative influence of local biotic and regional abiotic processes on the regional distribution of population abundance and community structure (chapter 1, 2). I have shown that the current theory (Connolly and Roughgarden 1998, 1999) advocating the importance of regional abiotic processes operates only in the absence of dispersal among populations. However, along the West coast of the United States, limited dispersal interacts with local biotic processes to control regional patterns of abundance and recruitment in mussel and barnacle communities (chapter 1, 2).

These cross-scale interactions between local processes and dispersal emphasize the limits of the scale-dependent approach, which advocates a match between the scale of patterns and their causal processes (Turner et al. 2001, Willis and Whittaker 2002, Pearson and Dawson 2003). Indeed, this scale-dependent approach is currently being used by climate envelope models that attempt to predict the effects of global climate change on the distribution of population abundance (Pearson and Dawson 2003, Elith et al. 2006). This approach consists of mapping current distributions of population abundance to current climate conditions and then shifting the distributions according to various global climate change scenarios (Pearson and Dawson 2003, Elith et al. 2006). However, this approach has been heavily criticized for its lack of integration of species interactions and dispersal when predicting the distribution of population abundance (Davis et al. 1998a, Davis et al. 1998b, Suttle et al. 2007). The results from chapters 1 and 2 emphasize the

limitations of this approach. Indeed, I have shown that the distribution of population abundance is dynamic, governed by the interaction between dispersal and local biotic processes and largely unrelated to the environment. Hence, in such systems, climate envelope model predictions are likely to fail to predict the effects of global climate change. Hence, chapters 1 and 2 emphasize the ability of processes to scale-up and generate patterns at much larger spatial scales (Levin 1992).

Based on the validated theory developed in chapters 1 and 2, I investigated the consequences of the interaction between local processes and limited dispersal for the design of marine reserve networks (chapter 3). I showed that current reserve design theory, predicated on the use of the scale of dispersal as the distance between reserves (Botsford et al. 2001, Botsford et al. 2003, Gerber et al. 2003, Shanks et al. 2003, Sale et al. 2005, Halpern et al. 2006), is optimal only when the rate of dispersal is low and thereby limits the scale of connectivity to the scale of dispersal (chapter 3). However, when the rate of dispersal is high, the interaction between dispersal and local biotic processes leads to patterns of connectivity at spatial scales that are much larger than that of dispersal. In such cases, reserve networks based on the scale of dispersal reduce mean abundance and persistence, whereas reserve networks based on the scale of connectivity maximize mean abundance and persistence (chapter 3). This works reiterates the importance of quantifying and maintaining connectivity in marine systems and highlights the distinction between the scale of dispersal and the scale of connectivity. Future work should assess the robustness of these predictions to more realistic patterns of dispersal by coupling these dynamic metapopulation models to ocean circulation models (Gaines et al. 2003, Pfeiffer-Herbert et al. 2007). Future efforts should also assess the effects of species interactions such as

competition and predation on the robustness of these predictions (Baskett et al. 2007).

Finally, in chapter 4, I showed that in more complex spatial food webs, the relative importance of biotic regulation and abiotic limitation depends on the rate of dispersal and varies in time (Gouhier et al. 2010). Low rates of dispersal dampen biotically-induced fluctuations among food webs and promote environmental destabilization, whereas high rates of dispersal promote biotically-induced fluctuations among food webs and mitigate environmental destabilization (Gouhier et al. 2010). Importantly, the relative influence of biotic regulation and abiotic limitation changes in time: food webs shift from periods of biotic regulation to periods of abiotic limitation. These emergent dynamic shifts between abiotic limitation and biotic regulation highlight the importance of including stochastic noise (a common feature in natural systems) into deterministic models in order to detect potential synergistic interactions (Grenfell et al. 1998, Coulson et al. 2004).

So, what can we conclude about the relative importance of abiotic limitation and biotic regulation in ecological systems? Predictably, the answer is that it depends. Chapters 1 and 2 have shown that in marine systems, although regional abiotic processes largely control recruitment patterns, biotic processes can control the distribution of population abundance, and chapter 3 has investigated the consequences of this for marine reserve design. Chapter 4 has demonstrated that more complex ecological may be governed by the joint effects of abiotic limitation and biotic regulation.

Importantly, the results outlined in chapters 1-3 should be applicable to any marine or terrestrial system that features sustained local population fluctuations and

limited dispersal (chapters 1-2). Hence, the properties of spatial synchrony should be able to elucidate the relative importance of biotic and abiotic processes for a range of spatial ecological systems. The generality of these results and their applicability to a broad range of ecological systems have critical implications for understanding the factors that control the spatiotemporal distribution of population abundance in natural systems and for predicting their response to global climate change. Indeed, the ability of cross-scale interactions between local biotic processes and limited dispersal to control the dynamic distribution of population abundance at the continental scale emphasizes the importance of adopting a broader perspective that encompasses biotic and abiotic factors occurring across different spatial scales to understand and protect natural systems.

Overall, by adopting a rigorous comparative approach and systematically using dispersal as a treatment in my dynamical models, I have been able to compare competing theories and predict the conditions under which one is likely to prevail over the other. In doing so, I have attempted to strike a conciliatory tone and build bridges between competing theoretical towers.

LITERATURE CITED

Baskett, M. L., F. Micheli, and S. Levin. 2007. Designing marine reserves for interacting species: Insights from theory. Biological Conservation **137**:163-179.

Botsford, L. W., A. Hastings, and S. D. Gaines. 2001. Dependence of sustainability on the configuration of marine reserves and larval dispersal distance. Ecology Letters **4**:144-150.

Botsford, L. W., F. Micheli, and A. Hastings. 2003. Principles for the design of marine reserves. Ecological Applications **13**:S25-S31.

Connolly, S. R. and J. Roughgarden. 1998. A latitudinal gradient in northeast Pacific intertidal community structure: Evidence for an oceanographically based synthesis of marine community theory. American Naturalist **151**:311-326.

Connolly, S. R. and J. Roughgarden. 1999. Theory of marine communities: Competition, predation, and recruitment-dependent interaction strength. Ecological Monographs **69**:277-296.

Coulson, T., P. Rohani, and M. Pascual. 2004. Skeletons, noise and population growth: the end of an old debate? Trends in Ecology & Evolution **19**:359-364.

Davis, A. J., L. S. Jenkinson, J. H. Lawton, B. Shorrocks, and S. Wood. 1998a. Making mistakes when predicting shifts in species range in response to global warming. Nature **391**:783-786.

Davis, A. J., J. H. Lawton, B. Shorrocks, and L. S. Jenkinson. 1998b. Individualistic species responses invalidate simple physiological models of community dynamics under global environmental change. Journal of Animal Ecology **67**:600-612.

Elith, J., C. H. Graham, R. P. Anderson, M. Dudik, S. Ferrier, A. Guisan, R. J. Hijmans, F. Huettmann, J. R. Leathwick, A. Lehmann, J. Li, L. G. Lohmann, B. A. Loiselle, G. Manion, C. Moritz, M. Nakamura, Y. Nakazawa, J. M. Overton, A. T. Peterson, S. J. Phillips, K. Richardson, R. Scachetti-Pereira, R. E. Schapire, J. Soberon, S. Williams, M. S. Wisz, and N. E. Zimmermann. 2006. Novel methods improve prediction of species' distributions from occurrence data. Ecography **29**:129-151.

Gaines, S. D., B. Gaylord, and J. L. Largier. 2003. Avoiding current oversights in marine reserve design. Ecological Applications **13**:S32-S46.

Gerber, L. R., L. W. Botsford, A. Hastings, H. P. Possingham, S. D. Gaines, S. R. Palumbi, and S. Andelman. 2003. Population models for marine reserve design: A retrospective and prospective synthesis. Ecological Applications **13**:S47-S64.

Gouhier, T. C., F. Guichard, and A. Gonzalez. 2010. Synchrony and Stability of Food Webs in Metacommunities. The American Naturalist **175**:E16-E34.

Grenfell, B. T., K. Wilson, B. F. Finkenstadt, T. N. Coulson, S. Murray, S. D. Albon, J. M. Pemberton, T. H. Clutton-Brock, and M. J. Crawley. 1998. Noise and determinism in synchronized sheep dynamics. Nature **394**:674-677.

Halpern, B. S., H. M. Regan, H. P. Possingham, and M. A. McCarthy. 2006. Accounting for uncertainty in marine reserve design. Ecology Letters **9**:2-11.

Levin, S. A. 1992. The Problem of Pattern and Scale in Ecology. Ecology **73**:1943-1967.

Pearson, R. G. and T. P. Dawson. 2003. Predicting the impacts of climate change on the distribution of species: are bioclimate envelope models useful? Global Ecology and Biogeography **12**:361-371.

Pfeiffer-Herbert, A. S., M. A. McManus, P. T. Raimondi, Y. Chao, and F. Chai. 2007. Dispersal of barnacle larvae along the central California coast: A modeling study. Limnology and Oceanography **52**:1559-1569.

Sale, P. F., R. K. Cowen, B. S. Danilowicz, G. P. Jones, J. P. Kritzer, K. C. Lindeman, S. Planes, N. V. C. Polunin, G. R. Russ, Y. J. Sadovy, and R. S. Steneck. 2005. Critical science gaps impede use of no-take fishery reserves. Trends in Ecology & Evolution **20**:74-80.

Shanks, A. L., B. A. Grantham, and M. H. Carr. 2003. Propagule dispersal distance and the size and spacing of marine reserves. Ecological Applications **13**:S159-S169.

Suttle, K. B., M. A. Thomsen, and M. E. Power. 2007. Species Interactions Reverse Grassland Responses to Changing Climate. Science **315**:640-642.

Turner, M., R. Gardner, and R. O'Neill. 2001. Landscape ecology in theory and practice: pattern and process. Springer-Verlag, New York.

Willis, K. J. and R. J. Whittaker. 2002. Ecology - Species diversity - Scale matters. Science **295**:1245-1248.